

**IMPROVEMENT OF PERFORMANCE OF
A COHESIVE SUBGRADE MODIFIED
WITH TYRE SCRAP FOR FLEXIBLE
PAVEMENT**

Thesis submitted by

SUJOY SARKAR

DOCTOR OF PHILOSOPHY IN ENGINEERING

CIVIL ENGINEERING DEPARTMENT

FACULTY COUNCIL OF ENGINEERING & TECHNOLOGY

JADAVPUR UNIVERSITY

KOLKATA-700032, INDIA

2024

1. Title of the Thesis:

**IMPROVEMENT OF PERFORMANCE OF A COHESIVE
SUBGRADE MODIFIED WITH TYRE SCRAP FOR FLEXIBLE
PAVEMENT**

2. Name, Designation and Institution of the Supervisors:

(1) Prof. (Dr.) Sumit Kumar Biswas,
Associate Professor,
Department of Civil Engineering,
Jadavpur University,
Kolkata-700032, India.

(2) Prof. (Dr.) Saibal Chakraborty,
Head of the Department,
Civil Engineering Dept.
Jnan Chandra Ghosh Polytechnic
Govt. of West Bengal
Kolkata-700023, India.

3. List of Journal Publications:

- (i) Sujoy Sarkar, Sumit Kumar Biswas and Saibal Chakraborty (2024)
“Assessment of Deflection and In-Situ California Bearing Ratio (CBR)
of Clayey Subgrade of Flexible Pavement Reinforced with Waste Tyre
Scrap Material”. SSRG International Journal of Civil Engineering, Vol-
11, Issue 1,18-31 (ISSN: 2348-8352).
- (ii) Sujoy Sarkar, Sumit Kumar Biswas and Saibal Chakraborty (2024)
“Deflection and Elastic Modulus Assessment of Subgrade in Flexible
Pavement Mixed with Waste Tire Scrap Material”. Engineering,
Technology & Applied Science Research, Vol-14, No 2,13208-13215
(E ISSN: 1792-8036).

4. List of Presentations in National/International Conferences/Workshops:

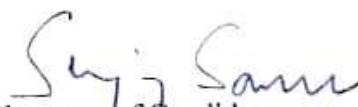
- (i) Sujoy Sarkar, Saibal Chakraborty and Sumit Kumar Biswas (2023)
“Improvement of CBR of Cohesive Soil Subgrade with
Shredded Tyre Scrap”. National Seminar on Geotechnics-Recent
Advancement in Research and Practice (GEO RARP), 4th -5th August
2023, Organised by Kolkata Chapter of Indian Geotechnical Society.

STATEMENT OF ORIGINALITY

I, Sujoy Sarkar, registered on 24.04.2017 do hereby declare that this thesis entitled "**Improvement of Performance of a Cohesive Subgrade Modified with Tyre Scrap for Flexible Pavement**" contains literature survey and original research work done by the undersigned candidate as part of Doctoral studies.

All information in this thesis have been obtained and presented in accordance with existing academic rules and ethical conduct. I declare that, as required by these rules and conduct, I have fully cited and referred all materials and results that are not original to this work.

I also declare that I have checked this thesis as per the "Policy on Anti Plagiarism, Jadavpur University, 2019", and the level of similarity as checked by iThenticate software is 7%.

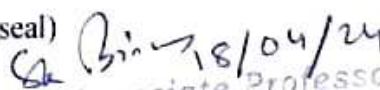

Signature of Candidate:

Date: 18/04/2024


Certified by Supervisor(s):

(Signature with date, seal)

1.


Associate Professor
Department of Civil Engineering
Jadavpur University
Kolkata-700 032

2.


18-04-2024
Dr. Saibal Chakraborty
Head, Civil Engineering Department
Jnan Chandra Ghosh Polytechnic
Department of Technical Education,
Training & Skill development
Govt. of West Bengal

CERTIFICATE FROM THE SUPERVISOR(S)

This is to certify that the thesis entitled “**Improvement of Performance of a Cohesive Subgrade Modified with Tyre Scrap for Flexible Pavement**” submitted by **Shri Sujoy Sarkar**, who got his name registered on 24.04.2017 for the award of Ph.D. (Engineering) degree of Jadavpur University is absolutely based upon his own work under the supervision of **Prof. (Dr.) Sumit Kumar Biswas**, Associate Professor, Department of Civil Engineering, Jadavpur University & **Prof. (Dr.) Saibal Chakraborty**, Head of the Department, Civil Engineering Dept. Jnan Chandra Ghosh Polytechnic, Govt. of West Bengal, and that neither his thesis nor any part of the thesis has been submitted for any degree/diploma or any other academic award anywhere before.

1. Sumit K. Biswas 18/04/24

Signature of the Supervisor
and date with Office Seal

Associate Professor
Department of Civil Engineering
Jadavpur University
Kolkata-700 032

2. Saibal 18-04-2024

Signature of the Supervisor
and date with Office Seal

Dr. Saibal Chakraborty
Head, Civil Engineering Department
Jnan Chandra Ghosh Polytechnic
Department of Technical Education,
Training & Skill development
Govt. of West Bengal

ACKNOWLEDGEMENT

It is with great pleasure and a profound sense of privilege that I express my heartfelt gratitude to my research supervisors, Prof. Sumit Kumar Biswas and Prof. Saibal Chakraborty. Their unwavering inspiration and support were pivotal to the completion of this thesis. I am deeply grateful for their patience, detailed and constructive feedback, continuous encouragement, and invaluable guidance throughout my research journey.

I would like to offer thanks to Prof. Partha Bhattacharya (Present HOD, Civil Engineering Department) of Civil Engineering Department, Jadavpur University for his valuable support and cooperation in my research work.

I would like to express my gratitude to Prof. Sankar Chakraborty, Prof. Ramendu Bikas Sahu, Prof. Santosh Kumar Das, and Prof. Narayan Roy of Civil Engineering Department, Jadavpur University for their insightful suggestions and valuable advice. I am thankful to Prof. Gokul Chandra Mondal, Prof. Partha Pratim Biswas, and Prof. Manoj Kumar Sahis of Construction Engineering Department, Jadavpur University for their invaluable support and cooperation in my research endeavors.

I also wish to express my immense gratitude to all my professors, laboratory staff, and research colleagues of Civil Engineering Department, Jadavpur University for their constant encouragement and cooperation.

I would like to convey my immense gratitude to Mr. Arun Nath, the former Executive Engineer of South 24 Parganas, PWD, Government of West Bengal, for giving me permission to conduct fieldwork on a PWD road under his jurisdiction

I am very much grateful to Mr. Arijit Ghosh of Alfresco Construction Services, Kolkata, for his immense support for providing field test equipment and proper guidance to perform each step methodically.

I would like to extend my sincere thanks to Mr. Rupesh Thakur and Sahil Thakur of Dhela Baba Enterprise, Naihati for their diligent efforts in support of fieldwork.

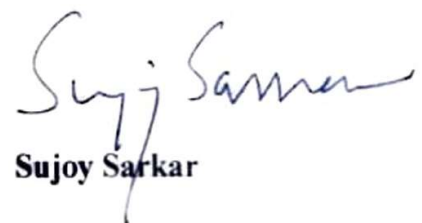
I would like to thank my colleagues of Sircon Engineering Services Pvt. Ltd. Kolkata, Nilkamal Santra, Susovan Tunga, Gopal Pradhan, Swapnasish Das, Sanjay Sarkar, Bubai Karmakar, Balaram Das, Subol das for their unwavering assistance, support, and encouragement throughout the duration of my work.

I would like to express my gratitude to my niece, Srijita Saha, for her continuous encouragement and support throughout my entire thesis work

Furthermore, I am immensely grateful to Mr. Rajesh Nandi, Faculty of the Civil Engineering Department, Narula Institute of Technology, Kolkata, for his unwavering encouragement and support during times of need.

I am deeply grateful to my parents for their unwavering love and support throughout my life. They have stood by me through every high and low, sharing in my joys and comforting me in moments of frustration. Their boundless love and understanding have been instrumental in my success.

Place: Jadavpur University



Sujoy Sarkar

DEDICATED TO
MY BELOVED PARENTS

ABSTRACT

The present investigation has been done to examine the performance of a cohesive subgrade mixed with shredded tyre scrap. A road named Jibantala-Taldi Road in South 24 Parganas District, West Bengal, measuring 12.45 km in length and 5.50 m in width, has been selected for this study. This road falls under the jurisdiction of the Public Works Department (PWD), Government of West Bengal.

Soil samples have been collected from the road site to determine the fundamental soil properties, while scrap tyres have been obtained from a local car garage in Jadavpur, Kolkata, West Bengal. The study involves conducting appropriate tests to observe changes in soil strength after mixing different sizes of scrap tyre (10mmX10mm, 15mmX15mm, 20mmX20mm, 25mmX25mm, 30mmX30mm) with soil at varying percentages ranging from 5% to 30% to identify the maximum improvement achievable. Various laboratory tests have been performed to assess critical soil properties, including: a) Grain size distribution b) Atterberg Limits c) Modified Proctor compaction test d) California Bearing Ratio (CBR) test. Soil-tyre mixtures have been prepared by combining road subgrade soil with shredded tyre scrap based on dry weight proportions. The soil-to-tyre ratios explored were 100:0, 95:5, 90:10, 85:15, 80:20, 75:25, and 70:30. To fulfill the objective of the study, two standard test methods have been conducted for soil-tyre mixtures: a) Modified Proctor test b) CBR test. Optimal results have been achieved with a 10% inclusion of 15mm x 15mm tyre scrap, enhancing the soaked CBR value by 164%, from an initial 3.36 to 8.90. In addition, a comprehensive traffic study, including an axle load test, have been carried out on the road to collect necessary data. The analysis of flexible pavement design considered two types of subgrade soil: normal soil and soil mixed with tyre scrap. This analysis followed the guidelines specified in IRC:37-2018 and considered two CBR values: one for normal soil and another for soil with tyre scrap. These findings guided the redesign of the pavement structure using IIT PAVE software, ultimately reducing the pavement thickness by 90mm and suggesting a more sustainable approach with scrap tyre materials.

Moreover, the construction of a new 30.0m road section incorporating these modifications allowed for in-field testing with Dynamic Cone Penetrometer (DCP) and Falling Weight Deflectometer (FWD). A FWD study has been conducted on a selected segment of the Jibantala-Taldi Road, including the newly constructed pavement with a subgrade modified using scrap tyres. Deflection measurements have been taken at various

intervals from the load cell, including 0 mm, 300 mm, 600 mm, 900 mm, 1200 mm, 1500 mm, and 1800 mm. These measurements have been used to calculate deflection bowl parameters, such as the Lower Layer Index (LLI), to assess subgrade deflection. The enhanced subgrade displayed a notable increase in stiffness and load-bearing capacity, evidenced by a 141% increase in the in-situ CBR value and a significant reduction in vertical deflections. The tests revealed a notable increase in subgrade stiffness and load-bearing capacity. These indices are instrumental in predicting the structural performance of in-service pavement layers and identifying homogeneous sections for condition assessment. Elastic modulus values have been determined and compared for both pavement types, following the guidelines outlined in IRC:115-2014. PLAXIS 3D Dynamic Finite Element (FE) modelling of the FWD test has been conducted to create an approximate simplified numerical model and use experimental data to validate the findings. A regression analysis, supported by MINITAB statistical software, demonstrated strong correlations ($R^2 = 0.84$, Adjusted $R^2 = 0.8163$) between the modified CBR and variables such as scrap tyre size, percentage, and existing pavement thickness.

This analysis confirms the effectiveness of the scrap tyre admixture in enhancing subgrade strength, offering a sustainable solution to improve road durability and performance. This approach provides valuable insights into the effective reuse of scrap tyre in civil engineering, highlighting its benefits for enhancing road durability and performance while advocating for environmentally friendly construction practices.

Keywords: *California Bearing Ratio (CBR); subgrade; Tyre Scrap; Falling Weight Deflectometer (FWD); Deflection; Elastic modulus*

INDEX

ACKNOWLEDGEMENT	V
ABSTRACT	VIII
INDEX	X
LIST OF TABLES	XIV
LIST OF FIGURES	XVII
LIST OF ABBREVIATIONS	XXIII
LIST OF SYMBOLS	XXV
CHAPTER 1 INTRODUCTION	1
1.1 BACKGROUND	1
1.2 THE PRESENT STUDY	4
1.3 ORGANIZATION OF THE THESIS	5
CHAPTER 2 LITERATURE REVIEW	6
2.1 OVERVIEW	6
2.2 REVIEW OF PAST WORKS	6
2.2.1 Soil Property Improvement by Scrap Tyre Incorporation	6
2.2.2 Pavement Design and Traffic Studies	27
2.2.3 Falling Weight Deflectometer (FWD) Test	32
2.2.4 Simulation of FWD Test by Finite Element Method (FEM)	45
2.3 SUMMARY	49
2.4 MOTIVATION	50
CHAPTER 3	52
OBJECTIVE AND SCOPE	52
3.1 OVERVIEW	52
3.2 OBJECTIVE	52
3.3 SCOPE OF WORK	52
3.3.1 Laboratory Tests	54
3.3.2 Field Study	55
3.3.3 Numerical Work	55
3.3.4 Regression Analysis	56
CHAPTER 4 METHODOLOGY	57
4.1 OVERVIEW	57
4.2 LABORATORY TESTING AND MECHANISM	57
4.2.1 Grain Size Analysis	58
4.2.2 Atterberg Limits	58
4.2.2.1 Liquid Limit	58
4.2.2.2 Plastic Limit	58
4.2.3 Water Content	59
4.2.4 Specific Gravity	59

4.2.5 Unconsolidated Undrained (UU) test	59
4.2.6 Modified Proctor Compaction Test	59
4.2.7 California Bearing Ratio (CBR)	59
4.3 FIELD STUDIES	60
4.3.1 Traffic Study	60
4.3.1.1 Traffic Census	60
4.3.1.2 Axle Load Survey	63
4.3.2 Dynamic Cone Penetration Test (DCPT)	65
4.3.2.1 Setup of Dynamic Cone Penetrometer (DCP)	65
4.3.2.2 DCPT mechanism	66
4.3.2.3 Preparation of DCPT outcome data	67
4.3.2.4 Relationship between Penetration Index (PI) and CBR Values	68
4.3.3 Falling Weight Deflectometer (FWD) Test	70
4.3.3.1 FWD deflection testing points & measurement:	72
4.3.3.2 Analysis of data	73
4.4 NUMERICAL WORK	77
4.4.1 Pavement Design and Analysis by IIT PAVE Software	78
4.4.2 Finite Element Analysis by PLAXIS 3D	79
4.4.2.1 Model Setup in PLAXIS 3D:	79
4.4.2.2 Loading Conditions:	80
4.4.2.3 Analysis and Calculation:	80
4.4.2.4 Correlation with FWD Data:	80
4.4.2.5 Interpretation and Validation:	80
4.4.2.6 Adjustments and Iterations:	81
4.5 FLOWCHART OF THE STEPS:	81
4.6 SUMMARY:	82
CHAPTER 5 LABORATORY TESTS	83
5.1 OVERVIEW	83
5.2 TEST PROGRAM FOR SOIL	84
5.3 TEST PROGRAMME FOR SCRAP TYRE MIX SOIL	85
5.4 LABORATORY TEST RESULTS	86
5.4.1 Test Results for Original Soil	86
5.4.2 Evaluation of Design CBR And Soil Sample Collection for Tests on Soil Tyre Mix	91
5.4.3 Property Of Scrap Tyre Material Used in This Study	92
5.4.4 Test Results for Shredded Tyre Scrap Mixed Soil	93
5.4.4.1 Collection and preparation of soil samples for tyre scrap mixing	93
5.5 SUMMARY	105
CHAPTER 6 FIELD TESTS AND ASSOCIATED STUDY	106
6.1 OVERVIEW	106
6.2 TRAFFIC STUDY AND PAVEMENT DESIGN	106
6.2.1 Traffic Census	106
6.2.2 Axle Load Survey	110
6.2.3 Pavement Design	111
6.2.3.1 Determination of pavement thickness by IITPAVE using original soil as subgrade	112

6.2.3.2 Determination of pavement thickness by IITPAVE using shredded tyre scrap mixed soil as subgrade	119
6.3 STRUCTURAL PERFORMANCE ASSESSMENT STUDY OF SUBGRADE	122
6.3.1 Pavement Preparation for Scrap Tyre-Modified Subgrade	123
6.3.1.1 Preparation of subgrade	124
6.3.1.2 Preparation of Base and Subbase	127
6.3.2 FWD Study on Pavement	131
6.3.2.1 Locations of FWD Test	131
6.3.2.2 Details of FWD equipment	132
6.3.2.3 Testing procedure & frequency	133
6.3.2.4 Testing Equipment:	134
6.3.2.5 Pavement composition details:	134
6.3.2.6 CBR determination for FWD	135
6.3.2.7 FWD test on existing pavement and tyre scrap modified pavement	143
6.3.2.8 Back Calculation of Layer Modulus (KGPBACK) for both type of pavement	146
6.3.2.9 Determination of corrected back calculated moduli (MPa)	151
6.3.2.10 Deflection and Elastic Modulus of Subgrade	153
6.4 SUMMARY	154
CHAPTER 7 PLAXIS MODELLING	156
7.1 OVERVIEW	156
7.2 PLAXIS 3D ANALYSIS ON MODEL PAVEMENT:	156
7.2.1 Input Parameters for PLAXIS Modelling	159
7.2.2 Output from PLAXIS 3D Analysis	159
7.2.2.1 Vertical Deflections from PLAXIS:	160
7.3 RESULTS OF FWD SIMULATION FROM PLAXIS ANALYSIS.	161
7.4 COMPARISON OF THE RESULTS OBTAINED FROM FWD TEST AND FWD SIMULATION IN PLAXIS 3D:	162
7.5 SUMMARY	164
CHAPTER 8 REGRESSION ANALYSIS	165
8.1 OVERVIEW	165
8.2 GENERAL:	165
8.3 TERMINOLOGY USED:	166
8.3.1 R^2 , Adjusted R^2 and Mean Squared Error (MSE), F Value and t-Value:	166
8.4 REGRESSION MODEL:	167
8.4.1 Results Obtained from Regression Model:	167
8.5 SUMMARY	170
CHAPTER 9 DISCUSSION	172
9.1 OVERVIEW	172
9.2 LABORATORY TEST RESULTS	172
9.2.1 Modified Proctor and CBR Test Results	172
9.3 FIELD TEST RESULTS	175
9.3.1 Traffic Study	175

9.3.2 Dynamic Cone Penetration Test (DCPT) Result	176
9.3.3 FWD Oriented Result	177
9.3.3.1 Subgrade deflection	177
9.3.4 Elastic Modulus (E_s) of Subgrade	179
9.4 NUMERICAL RESULTS	180
9.5 EFFECT OF SCRAP TYRE ON SUBGRADE	182
9.5.1 Discussion on Impact of Thickness of Pavement	182
9.5.2 Discussion on Impact of Subgrade Strain (ϵ_v)	182
9.6 IMPACT OF COSTS ON MODIFIED PAVEMENT CONSTRUCTION	184
9.7 SUMMARY	186
CHAPTER 10 SUMMARY AND CONCLUSIONS	187
10.1 SUMMARY	187
10.2 CONCLUSIONS	188
10.3 CONTRIBUTION OF PRESENT INVESTIGATION TO THE EXISTING KNOWHOW IN LITERATURE	189
10.4 LIMITATION AND SCOPE OF THE FURTHER RESEARCH	191
10.4.1 Limitations of the Study	191
10.4.2 Scope of Future Research	191
REFERENCES:	193
ANNEXURE- I	200
ANNEXURE- II	202
ANNEXURE- III	204
ANNEXURE- IV	207
ANNEXURE- V	215
ANNEXURE- VI	225

LIST OF TABLES

Table 2.1: Variation in CBR Test Results of BC Soil with Varying Proportions of Shredded Tyre. (After Tabasum et al. 2023)	7
Table 2.2: Characteristics of materials (After Amin et al.2023)	7
Table 2.3: Analysis of Normal Stress and shear stress (After Amin et al.2023).....	8
Table 2.4: CBR values for different samples (After Juliana et al. 2020).....	10
Table 2.5: Shear Strength Characteristics of soil mixed with rubber particles. (After Bai et al. 2020)	11
Table 2.6: Outcomes from the conducted soaked CBR test. (Munnoli et al.2014)	24
Table 2.7: Horizontal tensile strains (After Kumar and Kumar 2020).....	29
Table 2.8: Vertical compressive strains (After Kumar and Kumar 2020).....	29
Table 2.9: Summary of Average Deflection (After Alam 2020)	34
Table 2.10: DCP measurement for sample 1 within the research zone.....	38
Table 2.11: Cement (2–4% CEM I) stabilized RAP testing results (After Skels et al.2017). 40	
Table 2.12: Assumed input values for generating the dataset in the pavement system model using KENLAYER. (After Adigopula 2021)	47
Table 4.1: Test programme for soil and soil tyre scrap mix.....	58
Table 4.2: Correlations between CBR and PI (After Harison 1987 and Gabr et al. 2000)....	69
Table 4.3: Correlations between CBR and PI	70
Table 5.1: Test program for soil	85
Table 5.2: Test program for tyre scrap mix soil	85
Table 5.3: Laboratory test results on road soil with respect to chainage	88
Table 5.4: Properties of scrap tyre	92

Table 5.5: Property of mixed soil formed by collecting soil from different chainages of 3.00Km, 6.00Km, 7.00Km, 11.00Km, 12.00Km, and 12.45Km. (Atterberg Limits, Bulk Density, Moisture Content and Grain Size Analysis)	93
Table 5.6: Property of mixed soil formed by collecting soil from different chainages of 3.00Km, 6.00Km, 7.00Km, 11.00Km, 12.00Km, and 12.45Km. (Modified Proctor, Unconsolidated Undrained (UU) and Laboratory CBR (%))	94
Table 5.7: Laboratory test results for soil- shredded tyre scrap mix.....	96
Table 5.8: UU and Bulk Density of soil mixed with tyre scrap of size 15mm x 15mm at a percentage of 10%.....	104
Table 6.1: Summary of Traffic census	108
Table 6.2: Summary of Axle load test results	111
Table 6.3: Input Parameters for design traffic calculation of Jibantala-Taldi Road.....	113
Table 6.4: Input parameters for the analysis of pavement performance criteria for normal soil and scrap tyre modified soil.....	115
Table 6.5: Trial pavement thickness analysis for normal soil subgrade by IITPAVE.....	118
Table 6.6: Trial pavement thickness analysis for tyre scrap modified soil subgrade by IITPAVE.....	121
Table 6.7: Soil and scrap tyre requirements for each layer.....	126
Table 6.8: Test points and Chainages.....	132
Table 6.9: Crust thickness for both the pavements	135
Table 6.10: CBR Test points and chainage	135
Table 6.11: Summary of DCPT test results.....	138
Table 6.12: Modified Proctor and CBR test results for existing and modified subgrade soil	140
Table 6.13: Comparison table between field and laboratory CBR	142
Table 6.14: FWD test points and chainage	143

Table 6.15: Summary of average deflection (For Existing pavement)	144
Table 6.16: Summary of average deflection (for modified subgrade)	145
Table 6.17: Input parameters for KGPBACK software analysis	147
Table 6.18: Back calculated moduli for pavement layers	150
Table 6.19: Corrected Back Calculated moduli for bituminous layer of pavements	151
Table 6.20: Corrected Back Calculated moduli for granular ($E_{\text{gran_win}}$) and subgrade ($E_{\text{sub_win}}$) layers of pavement	152
Table 6.21: LLI for Subgrade Layer in both pavement types	154
Table 6.22: Average Elastic Moduli (E_s) for Subgrade Layer in both pavement types	154
Table 7.1: Parameters used for finite element analyses of normal soil subgrade pavement	159
Table 7.2: Parameters used for finite element analyses of scrap tyre modified subgrade pavement	159
Table 7.3: vertical deflection data, obtained from FE analysis	161
Table 7.4: Vertical deflection data, obtained from FWD test and FE analysis for normal soil subgrade pavement	162
Table 7.5: Vertical deflection data, obtained from FWD test and FE analysis for tyre modified soil subgrade pavement	163
Table 8.1: Regression model summary (Analysis of variance)	168
Table 8.2: Regression model summary (Coefficients)	168
Table 8.3: Model summary	168
Table 9.1: Different layer pavement thickness for normal and tyre scrap mixed soil	182
Table 9.2: Quantity and cost analysis of flexible pavement for normal and tyre scrap modified subgrade	185
Table 9.3: Thickness and costs analysis of flexible pavement for normal and tyre scrap modified subgrade	186

LIST OF FIGURES

Fig. 2.1: Approach utilized for formulating empirical equations. (After Adigopula 2021).....	9
Fig. 2.2: $p - \epsilon - c$ - curves (η is proportion). (After Bai et al. 2020).....	12
Fig. 2.3: Field CBR setup (After Dhorajiya et al 2019).....	14
Fig. 2.4: Angle of internal friction with the rubber waste content.....	15
Fig. 2.5: Cohesion with the rubber waste content.....	15
Fig. 2.6: Cohesion with waste tyre rubber. (After Akshatha et al 2018).....	16
Fig. 2.7: Soaked CBR with different-sized tyre rubber. (After Akshatha et al 2018).....	17
Fig. 2.8: Effect of tyre chips on CBR improvement of sand mixtures (After Al-Nemi 2018)	18
Fig. 2.9: CBR Value of Soil-Tyre Mixture (10mm×20mm) (After Singh and Sonthwal 2016)	21
Fig. 2.10: Alteration in the effect of admixture influence factor (AIF) on CBR values due to the inclusion of Crumb Rubber Powder (CRP).	22
Fig. 2.11: Comparative analysis of CBR values (After Teja and Siddhartha 2015)	23
Fig. 2.12: Soil Profile for Sample 1	38
Fig. 2.13: Location of research sections along the road A7 Riga—Bauska—Lithuanian border and designed pavement structure. (After Skels et al.2017)	39
Fig.2.14: FWD measurement and t distribution for the studied four road A7 sections (After Skels et al.2017).....	39
Fig. 2.15: Configuration design of a standard FWD, placement of the loading plate, geophones, and the recorded deflection basin. (After Nega et al. 2016)	41
Fig. 2.16: The nonlinear analysis identified dynamic deflection basins at various locations for Project 5 (After Nega et al. 2016)	42
Fig. 2.17: Field DCP-CBR relationship (merged data) (After Sahoo and Reddy,2009).....	44

Fig. 2.18: Dynatest 3031 assessment involving (a) a 20 kg drop weight and (b) a 15 kg drop weight. (After Adigopula 2021).....	46
Fig.2.19: Approach employed in formulating empirical equations. (After Adigopula 2021).....	47
Fig. 3.1: Sample stretch of Jibantala-Taldi Road.....	53
Fig. 4.1: Schematic diagram of the DCPT instrument.....	66
Fig. 4.2: DCP test before and after hammer drooping effect.....	67
Fig. 4.3: Typical DCP test result.....	68
Fig. 4.4: Typical representation of FWD operation.	71
Fig. 4.5: Curvature zones of a deflection bowl (After Horak,2008).....	72
Fig. 4.6: Back calculation process (After Singh et al.,2019).....	75
Fig. 4.7 : Flowchart of steps.....	81
Fig. 5.1: Sample collection chainages on the road.....	83
Fig. 5.2: Soil sample collection from Jibantala-Taldi Road.....	84
Fig. 5.3: Sample tyre scrap of size 15mm X 15mm.....	85
Fig. 5.4(A) and (B): Laboratory sample preparation and data collection.	86
Fig. 5.5: Particle size distribution curve.....	89
Fig. 5.6: Modified Proctor Compaction Curve for existing road subgrade between chainages 0.100 Km and 12.450 Km.....	89
Fig. 5.7: Load vs. Penetration curve for existing road subgrade between 0.100 km and 6.000 km in unsoaked condition.....	90
Fig. 5.8: Load vs. Penetration curve for existing road subgrade between 0.100 km and 6.000 km in soaked condition.....	90
Fig. 5.9: Load vs. Penetration curve for existing road subgrade between 7.000 km and 12.450 km in unsoaked condition.....	91
Fig. 5.10: Load vs. Penetration curve for existing road subgrade between 7.000 km and 12.450 km in soaked condition.....	91

Fig. 5.11: Design CBR curve	92
Fig. 5.12: Particle size distribution curve for mix soil.....	94
Fig. 5.13: Modified Proctor Compaction Curve for mix soil	95
Fig. 5.14: Load vs. Penetration Curve for mix soil.....	95
Fig. 5.15: Modified Proctor Compaction Curve for Original Soil mixed with Various Percentages of 10 mm x 10 mm tyre Scrap	97
Fig. 5.16: Modified Proctor Compaction Curve for original soil mixed with Various Percentages of 15 mm x 15 mm tyre Scrap	97
Fig. 5.17: Modified Proctor Compaction curve for original soil mixed with various Percentages of 20 mm x 20 mm tyre Scrap	98
Fig. 5.18: Modified Proctor Compaction curve for original Soil mixed with various Percentages of 25 mm x 25 mm tyre Scrap	98
Fig. 5.19: Modified Proctor Compaction curve for original Soil mixed with various Percentages of 30 mm x 30 mm tyre Scrap	99
Fig. 5.20: Load vs. Penetration Curve for Original Soil Mixed with Different Percentages of 10 mm x 10 mm tyre scrap, in unsoaked condition	99
Fig. 5.21: Load vs. Penetration Curve for Original Soil Mixed with Different Percentages of 10 mm x 10 mm tyre scrap, in soaked condition	100
Fig. 5.22: Load vs. Penetration Curve for Original Soil Mixed with Different Percentages of 15 mm x 15mm tyre scrap, in unsoaked condition	100
Fig. 5.23: Load vs. Penetration Curve for Original Soil Mixed with Different Percentages of 15 mm x 15mm tyre scrap, in soaked condition.	101
Fig. 5.24: Load vs. Penetration Curve for Original Soil Mixed with Different Percentages of 20 mm x 20mm tyre scrap, in unsoaked condition	101
Fig. 5.25: Load vs. Penetration Curve for Original Soil Mixed with Different Percentages of 20 mm x 20mm tyre scrap, in soaked condition	102

Fig. 5.26: Load vs. Penetration Curve for Original Soil Mixed with Different Percentages of 25 mm x 25mm tyre scrap, in unsoaked condition	102
Fig. 5.27: Load vs. Penetration Curve for Original Soil Mixed with Different Percentages of 25 mm x 25mm tyre scrap, in soaked condition	103
Fig. 5.28: Load vs. Penetration Curve for Original Soil Mixed with Different Percentages of 30 mm x 30mm tyre scrap, in unsoaked condition	103
Fig. 5.29: Load vs. Penetration Curve for Original Soil Mixed with Different Percentages of 30 mm x 30mm tyre scrap, in soaked condition	104
Fig. 6.1: Vehicle distribution chart as per PCU	109
Fig. 6.2: Vehicle distribution chart as per ADT	109
Fig. 6.3: Axle load test	110
Fig. 6.4: Axle load test data collection.....	110
Fig. 6.5: Trial pavement thickness for 5% CBR. (After IRC 37:2018)	117
Fig. 6.6: Typical input window of IITPAVE analysis for normal soil subgrade.....	117
Fig. 6.7: Typical output window of IITPAVE analysis for normal soil subgrade.....	118
Fig. 6.8: Typical Cross Section of pavement for original Soil Subgrade of CBR 3.36	119
Fig. 6.9: Trial pavement thickness for 9% CBR. (After IRC 37:2018)	120
Fig. 6.10: Typical input window of IITPAVE analysis for tyre scrap modified soil subgrade.	120
Fig. 6.11: Typical output window of IITPAVE analysis for tyre scrap modified soil subgrade	121
Fig. 6.12: Typical Cross Section of pavement for scrap tyre modified subgrade of CBR 8.90	122
Fig. 6.13: Site before model pavement preparation.....	123
Fig. 6.14: Scrap tyre mixing with subgrade soil	125
Fig. 6.15: Preparation of subgrade	126

Fig. 6.16: Preparation of subbase layer.....	128
Fig. 6.17: Preparation of surface layer.....	129
Fig. 6.18: Finished pavement under FWD study	130
Fig. 6.19: GEOTRAN FWD operation under process.....	131
Fig. 6.20: DCPT operation on subgrade	138
Fig. 6.21: DCPT Test Result Graph for existing subgrade at Chainage 3.0×10^3 m.....	139
Fig. 6.22: DCPT Test Result Graph for modified subgrade at Chainage 0.00m.	139
Fig. 6.23: Variation in modified proctor for different pavements.....	141
Fig. 6.24: Variation in CBR for different pavements.....	141
Fig. 6.25: FWD deflection recording on Jibantala -Taldi Road.....	144
Fig. 6.26: FWD deflection recording on scrap tyre modified subgrade pavement.....	145
Fig. 6.27: Deflection data collected for the subgrades.....	146
Fig. 6.28: Sample Input window of KGPBACK for existing pavement	148
Fig. 6.29: Sample output window of KGPBACK for existing pavement.....	148
Fig. 6.30: Sample Input window of KGPBACK for modified pavement.....	149
Fig. 6.31: Sample Output window of KGPBACK for modified pavement.....	149
Fig. 6.32: Back calculated moduli chart for both the pavements.....	150
Fig. 6.33: Corrected back calculated Moduli chart for both the pavements	152
Fig. 7.1: The model of FWD test pulse load.....	157
Fig. 7.2: FE model of flexible pavement with meshing.....	158
Fig. 7.3: Vertical deformation on the pavement surface and at layer boundaries as a function of dynamic time for normal soil.....	160
Fig. 7.4: Vertical deformation on the pavement surface and at layer boundaries as a function of dynamic time for scrap tyre modified soil.....	161
Fig. 7.5: Comparison of vertical deflection bowl for normal soil subgrade pavement and scrap tyre modified soil subgrade pavement.....	162

Fig. 7.6: Deflection bowl comparison, obtained from FWD test and FE analysis for existing pavement.....	163
Fig. 7.7: Deflection bowl comparison, obtained from FWD test and FE analysis for modified pavement.....	164
Fig. 8.1: Residual analysis of prediction of stabilized CBR.....	169
Fig. 8.2: Validation plot of stabilized CBR.....	170
Fig. 9.1: Variations in Optimum moisture content (OMC) test results with respect to road chainage	172
Fig. 9.2: Variations in Maximum dry density (MDD) test results, with respect to road chainage	173
Fig. 9.3: Variations in CBR test results, with respect to existing road chainage	173
Fig. 9.4: Variation in Optimum moisture content (OMC) test results for soil mixed with different sizes of shredded tyre scrap of different percentages.....	174
Fig. 9.5: Variation in Maximum dry density (MDD) test results for soil mixed with different sizes of shredded tyre scrap of different percentages	174
Fig. 9.6: Variation in soaked CBR test results for soil mixed with different sizes of shredded tyre scrap of different percentages	175
Fig. 9.7: Comparison bar chart between Laboratory CBR and In-situ CBR.....	176
Fig. 9.8: Deflection variation in subgrade for both the pavements.....	178
Fig. 9.9: Corrected back calculated Moduli chart for both the pavements	179
Fig. 9.10: Vertical deformation for both pavements as a function of dynamic time at the layer borders and on the pavement surface.....	180
Fig. 9.11: Comparison of vertical deflection bowl for both the pavements.....	181
Fig. 9.12: Pavement Section Showing the Locations of Critical Strains. (IRC 37:2018)....	183
Fig. 9.13: Comparison chart between ϵ_{cvc} VS. ϵ_{mvc}	184

LIST OF ABBREVIATIONS

AADT	Annual Average Daily Traffic
AIF	Admixture Influence Factor
ADT	Average Daily Traffic
ATCC	Auto Traffic Counter and Classifier
ANOVA	Analysis of Variance
BC	Bituminous Concrete
BCI	Base Curvature Index
BD	Base Damage Index
Ch.	Chainage
CBR	California Bearing Ratio
CSTC	Contents of Scrap Tyre Crumbs
CR	Crumb Rubber
CRP	Crumb Rubber Powder
CTSB	Cement Treated Sub-base
CVPD	Commercial Vehicle Per Day
DBM	Dense Bituminous Macadam
DBP	Deflection Basin Parameter
DCPT	Dynamic Cone Penetration Test
DCP	Dynamic Cone Penetrometer
DF	Design Factor
EGL	Existing Ground Level
EIRR	Economic Internal Rate of Return
ENPV	Economic Net Present Value
ESAL	Equivalent Standard Axle Load
FE	Finite Element
FEM	Finite Element Method
FWD	Falling Weight Deflectometer
GGBS	Ground Granulated Blast Furnace Slag
GSB	Granular Sub Base
GS	Government Standard
HMA	Hot Mix Asphalt

IRC	Indian Road Congress
IRI	International Roughness Index
LCV	Light Commercial Vehicle
LL	Liquid Limit
LLI	Lower Layer Index
MAV	Multi Axle Vehicle
MDD	Maximum Dry Density
MSA	Million Standard Axle
MSE	Mean Squared Error
MLI	Middle Layer Index
NH	National Highway
NGT	National Green Tribunal
NDT	Non-Destructive Testing
NL	Non lateritic
ODD	Optimal Dry Density
OMC	Optimum Moisture Content
PCU	Passenger Car Unit
PI	Plasticity Index
PL	Plastic Limit
PMS	Pavement Management Systems
PWD	Public Works Department
RAP	Reclaimed Asphalt Pavement
RC	Reference Chainage
SCI	Surface Curvature Index
SH	State Highway
STCR	Scrap Tyre Crumb Rubber
UU	Unconsolidated Undrained
UCS	Unconfined Compression Strength
VDF	Vehicle Damage Factor
WMM	Wet Mix Macadam
WPSA	Waste Paper Sludge Ash
WTR	Waste Tyre Rubber

LIST OF SYMBOLS

3D	Three Dimensional
A	Initial traffic (CPVD) in the year of completion of construction
C	Adjustment Factor
c	Cohesion
D	Lane distribution factor
E_{eps}	Elastic Modulus of existing subgrade
E_{eq}	Equivalent Modulus of Elasticity
E_{gran_sum}	Granular layer modulus in summer (MPa)
E_{gran_win}	Granular layer modulus in winter (MPa)
E_{mps}	Elastic Modulus of modified subgrade
E_{sub_mon}	Subgrade modulus in monsoon (MPa)
E_{sub_sum}	Subgrade modulus in summer (MPa)
E_{sub_win}	Subgrade modulus in winter (MPa)
E_s	Elastic Modulus of subgrade
E_{T1}	Back-calculated modulus (MPa) at temperature T1 (°C)
E_{T2}	Back-calculated modulus (MPa) at temperature T2 (°C)
e	Residuals
F	Vehicle damage factor (VDF)
LLI_{mps}	Average LLI for modified subgrade
LLI_{eps}	Average LLI for existing subgrade
M_{Rm}	Resilient modulus (MPa) of the bituminous mix used in the bottom Bituminous layer
n	Design period (years)
N_f	Fatigue life of bituminous layer
N_R	Subgrade rutting life
P	Count of commercial vehicles per day as per the previous record
r	Annual inflation rate of commercial vehicles in decimal
R^2	coefficient of regression
V_a	Percent volume of air void in the mix used in the bottom bituminous layer
V_{be}	Percent volume of effective bitumen in the mix used in the bottom bituminous layer

V	Volume
W_s	Weight of solid
W_w	Weight of water
w	Moisture content (%)
x	Difference in the number of years between the last record and the year of termination of construction
Y	Dependent variable
\hat{Y}	Response of the fitted model
X_k	k^{th} independent variable,
b_k	Estimate of k^{th} population regression coefficient
Y_b	Bulk Density

LATIN

β_k	Regression coefficient of k^{th} population
ΔBC	Blow counts corresponding to penetration depth.
ΔD_p	penetration depth
ε_{cvc}	Calculated vertical compressive strain at the top of the subgrade
ε_{mvc}	Maximum vertical compressive strain at the top of the subgrade.
ε_t	Horizontal tensile strain at the bottom of the bituminous layer,
ε_v	Vertical compressive strain at the top of the subgrade.
λ	Temperature Correction Factor
\emptyset	Angle of Internal Friction

UNIT

Km	Kilo meter
kN	Kilo Newton
KPa	Kilo Pascal
MPa	Mega Pascal
m	Meter

CHAPTER 1

INTRODUCTION

1.1 BACKGROUND

In the recent trend related to environmental impact, disposal of vehicle-generated scrap tyres has become a major landmark. From the manufacturing point of view, those tyres are generated from petroleum products and which can't be recycled or dissolved into nature. With the consequence of population growth and simultaneous increase in vehicle numbers, the accumulation of solid waste material in the form of scrap tyres needs a healthy assessment of reuse. In the Union Budget 2021, Indian government announced the Vehicle Scrappage Policy 2021. On March 18, 2021, the Honourable Minister for Road Transport and Highways, India, Nitin Gadkari, provided extensive insights about the scheme. This policy is designed to identify vehicles, that are unfit for the roads and will lead to the scrapping of old and unfit vehicles, which are causing pollution and harming the environment. The policy varies for different types of vehicles on Indian roads. It mandates a fitness test for commercial vehicles after 15 years, and if found unfit, they are proposed to be scrapped. Government vehicles over 15 years old will be scrapped starting from April 2022, with more than nine lakhs targeted for scrapping by January 2023. Private vehicles will be de-registered after 20 years if they are unfit or if their registration is not renewed, and higher re-registration fees will apply after 15 years. All vehicles must undergo regular fitness tests, as vehicles over 15 years old tend to pollute more. This policy not only reduces pollution but also provides other benefits, such as enabling the recycling of materials like steel, plastic, tyres, and other metals. Therefore, it is clear that the significant volume of scrap tyres generated from vehicles poses a considerable environmental challenge to the nation.

On September 19, 2019, the National Green Tribunal (NGT), in a case concerning the inadequate management of End-of-Life Tyres/Waste Tyres (ELTs), instructed the Central Pollution Control Board (CPCB) to develop a comprehensive waste management plan specifically for waste tyres and their recycling. This directive came in light of the significant challenges posed by tyre waste in India. India faces a critical issue with tyre waste management, as highlighted by data presented in the NGT case. Every day, the country discards approximately 275,000 tyres, yet lacks a comprehensive plan to effectively handle this waste. Compounding the problem, India also imports about 3 million waste tyres annually for recycling purposes. This situation, underscored by the NGT's directive, highlights the urgent need for a structured and effective approach to tyre waste management. The quantity of automobiles globally has markedly risen over recent years, leading to a significant uptick in the buildup of disposed tyres and inner tubes. Multiple studies predict that the worldwide volume of scrap vehicles is poised to reach up to 2 billion by 2030, consequently generating a significant volume of waste tyres (Dargay et al., 2007). Due to their non-degradable nature and unfavourable size for storage, these waste tyres have contributed significantly to the diminishing available disposal space for solid waste, making them a substantial contributor to the solid waste crisis. According to Tahami et al. (2019), annually, one billion tyres reach the end of their lifespan, with only about half undergoing recycling while the remainder ends up in landfills. F.D.B. de Sousa (2017) noted that the accumulation of large volumes of scrap tyres, emphasises the environmental risks if not managed properly. Often, these tyres are disposed of uncontrolledly, exacerbating the rapid depletion of waste disposal sites and leading to severe environmental issues. However, emerging research in geotechnical engineering offers many potential benefits of recycling waste tyres. In light of escalating environmental concerns, the proper management of scrap tyres generated by vehicles has emerged as a critical issue. When these tyres are disposed of in landfills, they exhibit limited decomposition and tend to linger near the surface, posing risks such as fire hazards, air

pollution, particulate matter, unpleasant odours, visual eyesores, and the release of harmful contaminants like fumes, aromatic polycyclic hydrocarbons, dioxins, furans and nitrogen oxides (Rokade, 2012). Alternatively, incinerating these tyres results in the production of toxic gases. In terms of production, these tyres are made from materials derived from petroleum and cannot be recycled or undergo natural biodegradation. As the population grows and the quantity of vehicles grows simultaneously, solid waste, including tyres that are thrown away, accumulates and it becomes necessary to figure out whether or not they may be repurposed. Studies have shown that using waste tyres in geotechnical engineering applications is beneficial because of their robust resistance to ageing, high tensile strength, durability, and toughness (Mashiri et al., 2018). Consequently, geotechnical engineers have been actively exploring ways to reuse discarded tyres. Several investigations conducted over the past three decades have examined the use of waste tyre material as an additional reinforcing agent. These investigations have consistently shown that the incorporation of scrap tyre material can significantly enhance the performance and cost-effectiveness of various construction projects, including road subgrades, highway embankments, and retaining wall backfills. Non-biodegradable waste materials such as tyres and plastics present substantial challenges to both human life and the environment. The exploration of alternative applications, particularly in the field of construction, offers a promising avenue for addressing these issues.

Pavements are vital for the efficient transportation of passengers, freight, and other community services. A flexible pavement, as a load-bearing structure, comprises layers of various granular materials over a soil subgrade. The durability of pavement hinges on multiple factors, such as the strength of the subgrade soil, material quality, layer thickness, environmental conditions, and traffic characterization. To ensure the structural integrity and load-bearing capacity or the overall pavement performance, subgrade plays an important role in distributing loads effectively onto the subsoil, reducing the strain on the layers of pavement and possibly increasing pavement life. Waste tyres, possessing unique attributes like

lightweight, insulation properties, water resistance, durability, and compressibility, can be effectively employed in improving the performance of road subgrades. Taking those factors into account, waste tyres have been successfully employed to reinforce soft soil subgrade in road construction. India boasts one of the world's most extensive road networks, but the rapid escalation in traffic has rendered existing roads structurally inadequate. Conventional design and construction practices have proven insufficient in meeting construction standards. In response, researchers have sought alternatives, including unconventional materials and innovative design methodologies. Waste tyre products have played a pivotal role in aiding designers in resolving various engineering challenges. The present study has been taken up considering those aspects and it is detailed hereunder.

1.2 THE PRESENT STUDY

Based on these considerations, the study aims to investigate the potential for reusing tyre scraps in the subgrade layer of pavements. The foundation layer under the pavement is known as the subgrade, and using scrap tyres in this context could be a form of recycling that contributes to both waste management and potentially improved engineering properties of the road. To establish the guidelines and scope, and to investigate the findings, an adequate literature review has been conducted. Based on this literature, the scope and target of the current research work have been obtained.

1.3 ORGANIZATION OF THE THESIS

The thesis has been organized into ten (10) different chapters in the following order: -

Chapter 1: Introduction presents the background and brief description of the present study.

Chapter 2: Literature Review describes in brief the works of the past research in chronological order. The works have been divided into four different types in different subsections of the chapter namely- soil property improvement through the incorporation of scrap tyres, pavement design and traffic studies, Falling weight Deflectometer (FWD) test, Simulation of FWD test by Finite element method (FEM)

Chapter 3: Objective and scope of work covers the objectives and scope of the present research.

Chapter 4: Methodology describes the methodology used for the study, including existing subgrade clayey soil and tyre scrap, along with their properties.

Chapter 5: Laboratory study depicts the experimental results and provides interpretations of the test results.

Chapter 6: Field Tests and Associated Study focuses on traffic studies and pavement design. The chapter introduces a field study that includes pavement preparation, Dynamic Cone Penetration Test (DCPT), and FWD Test.

Chapter 7: PLAXIS Modelling aims to simulate the FWD test and obtain deflection bowls.

Chapter 8: Regression Analysis establishes correlations between laboratory tests and field test results.

Chapter 9: Discussion presents observations and analyses of the results of all field tests and laboratory tests.

Chapter 10: Conclusions summarizes the present study and draws conclusions from it, while also suggesting some guidelines for further research.

CHAPTER 2

LITERATURE REVIEW

2.1 OVERVIEW

The behaviour of soil has been researched in detail during the previous few decades, with various researchers focusing on improvements achieved through the incorporation of different-sized scrap tyre materials in different proportions. These investigations have encompassed experimental studies as well as numerical and analytical approaches. However, most of these studies have concentrated on soil improvement through the addition of various sizes and quantities of tyres. This chapter aims to provide a comprehensive analysis of the existing literature about these research topics. Subsequent sections will offer a sequential summary of research concerning the use of shredded tyre scraps for soil stabilization, highlighting key developments in recent years. Furthermore, this chapter will address the rationale behind the current investigation, as derived from the insights gathered from the literature review

2.2 REVIEW OF PAST WORKS

The past works have been divided into four different parts

2.2.1 Soil Property Improvement by Scrap Tyre Incorporation

Tabasum et al. (2023) studied the use of tyre shreds to improve the bearing capacity of black cotton (BC) soil, a cost-effective approach gaining attention in geotechnical engineering. BC soil, common in tropical regions like India, has properties such as a 34% liquid limit (LL) and a 50% free swell index. The study used shredded rubber tyres from a factory near Ayyappa Gudi Centre in Nellore, mixed with BC soil in varying proportions. The mixture was then tested, with Table 2.1 presenting the California Bearing Ratio (CBR) results for the different tyre scrap blends.

Table 2.1: Variation in CBR Test Results of BC Soil with Varying Proportions of Shredded Tyre. (After Tabasum et al. 2023)

Sl. No.	Mix proportions	CBR Values(2.5mm penetration(%))	CBR Values(5.0mm penetration(%))
1.0	BC soil	3.57	2.91
2.0	BC soil +4% shredded	5.17	4.77
3.0	BC soil +6% shredded	7.96	8.49
4.0	BC soil +8% shredded	9.55	8.89
5.0	BC soil +10% shredded	8.95	7.83

Key findings of the study were:

- Adding shredded rubber to BC soil increased the CBR value up to 8%; beyond this, the benefits decreased.
- The reduction in benefits at higher percentages may be due to the lightweight nature of the tyre waste.
- As the rubber content increased, both moisture content and dry density of the soil decreased.

Amin et al. (2023) explored the application of tyre chips and sand as a substitute geo-material in civil engineering, focusing on shear strength through direct shear and triaxial tests. A sustainable method of material reuse was demonstrated by the creative use of scrap tyre rubber in civil engineering practices, making the mixture suitable for construction. Tables 2.2 and 2.3 in the document detailed the analysis of material properties and Characteristics of shear stress and normal stress, in that order.

Table 2.2: Characteristics of materials (After Amin et al.2023)

Cc (curvature coefficient)	.045
Cu (Uniformity coefficient)	1.388
D60, D30, D10	0.25, 0.24, and 0.18 mm
Unified Soil Classification System (USCS)	Poorly Graded (SP)
Specific Gravity of sand	2.65
Specific Gravity of tire chips	1.02

These tables were instrumental in understanding the fundamental properties of the tyre chip-sand mixtures and their implications in civil construction.

Table 2.3: Analysis of Normal Stress and shear stress (After Amin et al.2023)

0% TC	Normal stress (kPa)	Shear stress (kPa)
	50	38
	100	70
	150	100
20% TC	50	45
	100	78
	150	110
30% TC	50	51
	100	84
	150	118
40% TC	50	47.5
	100	80
	150	112

Ibrahim et al. (2022) investigated improving non-lateritic (NL) soils, which often fail to meet construction standards due to their variability. They collected NL soil samples from Dungulbi, Bauchi State, and stabilized them using scrap tyre crumb rubber (STCR) at concentrations of 1% to 5%, with STCR particle sizes ranging from 0.212 mm to 4.75 mm. The study involved compaction tests at three energy levels and CBR assessments. Results showed a reduction in Optimum Moisture Content (OMC) and Maximum Dry Density (MDD) with increasing STCR content. CBR values improved up to 3% STCR replacement, then declined. ANOVA and multiple linear regression were used to compare predicted and experimental values, revealing that 3% STCR content provided adequate strength for embankments and road layers. The soil was classified as A-2-7(0) and GW, with low plasticity. The study concluded that STCR can enhance non-lateritic soil stability, offering valuable insights for future stabilization projects.

Johns et al. (2022) investigated the utilization of tyre crumb waste as a material for the subgrade in flexible pavement construction, highlighting environmental and engineering benefits. The study used soil mixed with crumb tyres from light motor vehicles, passed through a 2.36mm sieve, and evaluated for CBR and compressive strength. Results showed

that adding crumb tyres to soil could enhance the CBR value, indicating improved subgrade strength and potential for reduced pavement thickness. The optimal moisture content for compaction was determined to be 16%, with the highest CBR value observed at 9.49% for a 5mm penetration. This study addressed waste tyre management challenges and provided support for the innovative application of recycled tyre materials in pavement subgrades, providing a sustainable substitute for conventional building techniques.

Mangi and Sarki (2021) aimed to enhance subgrade soil's load-bearing capacity using discarded tyre aggregates. CBR tests were conducted on the original subgrade soil and blends containing 5%, 15%, and 30% tyre aggregates. The subgrade soil MDD was 1636 kg/m³ at 21.26% moisture content. The initial soil exhibited a CBR value of 3.90%. The study showcased tyre-derived aggregate's positive impact, enhancing CBR values. As seen in Fig. 2.1, CBR improvements of 5.1%, 10%, and 28.7% were obtained by replacing subgrade soil with different percentages of tyre aggregates.

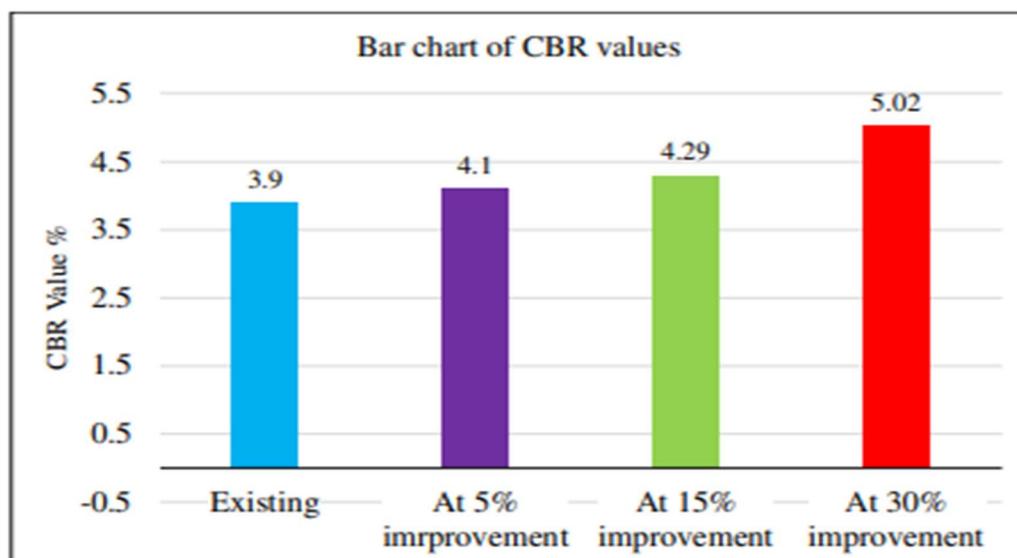


Fig. 2.1: Approach utilized for formulating empirical equations. (After Adigopula 2021)

Key conclusions from the investigation:

- Standard proctor tests showed peak dry density of clayey soil at 1636 kg/m³ with 21.26% optimum moisture, compared to the original 26.5%.

- Initial soil's subgrade bearing pressure of 3.90% under 5 mm penetration gained stiffness and lessened penetration with tyre aggregates. At 5 mm penetration, the CBR value increased to 4.1% with a 5% replacement of the tyre aggregate.
- Adding 15% tyre aggregates enhanced the CBR value of the upgraded subgrade to 4.29% at 5 mm penetration. And the addition of 30% tyre aggregates resulted in a significant rise in the CBR value to 5.02% at a penetration depth of 5 mm.
- The study highlighted that incorporating tyre aggregates into subgrade soil significantly improved pavement performance and load-bearing capacity.

Juliana et al. (2020) investigated soil stabilization using crumb rubber, a lightweight material with high shear strength, to modify subgrade soil properties. This method offered benefits like addressing improper tyre disposal and reducing pollution. In Seberang Perai Tengah, Penang, soil from a landslide site nearer Mengkuang Dam was used to evaluate the efficacy of soil stabilized with different percentages of crumb rubber (CR) (2%, 4%, 6%, and 8%). Laboratory tests were conducted to identify the optimal CR percentage meeting Public Works Department Malaysia (JKR) standards of subgrade. The findings showed that every combination (M2 through M5) complied with JKR's subgrade (CBR > 5%) criterion. The 4% CR combination (M3) produced the highest CBR values, thus recommending it for subgrade stabilization as shown in Table 2.4. The influence of CR on subgrade soil's geotechnical properties was scrutinized. The presence of CR led to increased CBR values, with 4% CR showing the most significant improvement for both conditions. This concentration fulfilled JKR's minimum CBR requirement.

Table 2.4: CBR values for different samples (After Juliana et al. 2020)

Mixture	Percentage Mixture (%)		Average CBR Value (%)	
	Soil	Crumb Rubber (CR)	Unsoaked	Soaked (4 days)
M1 (control sample)	100	0	5.62	3.40
M2	98	2	17.12	14.07
M3	96	4	36.09	30.14
M4	94	6	29.70	24.51
M5	92	8	21.90	18.98

The study concluded that 4% crumb rubber effectively enhanced subgrade soil strength. Furthermore, its use as a soil stabilizer could decrease road construction costs, and address waste tyre disposal and pollution issues. However, further investigations were advised:

1. For reliable determination of the ideal CR content, experiment with smaller increments of CR percentages.
2. Examine shredded, chips and powdered rubber to assess their impact on soil properties.
3. Explore combining CR with other additives, such as Portland Cement, to bolster soil strength, particularly under soaked conditions.

Bai et al. (2020) explored the results of combining rubber particles made from used tyres with various soil types, including fly ash, sand, clay, loess, and expansive soil. Recent advancements in soil modification techniques had led to the innovative use of scrap tyre rubber particles. This review, explored the multifaceted impact of rubber particles on various soil types, highlighting significant improvements in soil mechanics and sustainability. In sandy soils, rubber particles enhanced cohesion and internal friction angle, with optimal effects observed at specific rubber content levels as shown in Table 2.5.

Table 2.5: Shear Strength Characteristics of soil mixed with rubber particles. (After Bai et al. 2020)

Proportion/%	Cohesion/kPa	Internal friction angle/(°)
0	7.5	36.02
10	14.7	42.27
20	18.9	38.34
30	18.2	34.42
40	15	31.95
50	12.4	27.4

Moreover, Fig.2.2 illustrated the stress-strain relationships in these mixtures, underlining the rubber content's influence on soil behaviour.

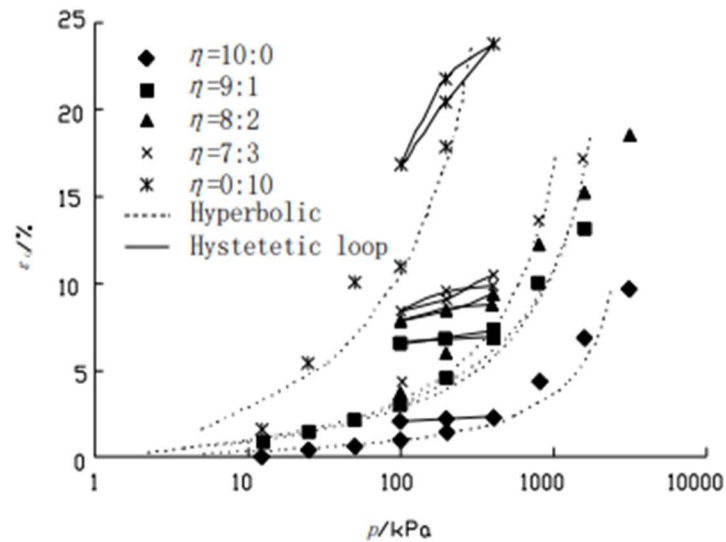


Fig. 2.2: p ε c - curves (η is proportion). (After Bai et al. 2020)

Incorporating rubber particles into clayey soils increased shear strength and reduced compressibility, mitigating expansiveness. Similar effects were observed in loess, expansive soils, and fly ash, improving dynamic characteristics and shear strength. The study highlights the potential of scrap tyre rubber for sustainable soil enhancement. This review emphasized its importance for environmental sustainability and soil mechanics.

Wangmo et al. (2020) addressed the environmental challenges of discarded tyres, proposing the use of waste tyre crumbs (2%-8% by volume) as subgrade soil stabilizers. The study collected tyre crumbs, ranging from fibrous filaments to fine powder, from Jaigaon, Bhutan, and mixed them with soil samples for analysis. Key tests, including CBR and Modified Proctor Tests, revealed a notable increase in strength with tyre additions, peaking at a 6% tyre mixture, achieving a maximum CBR of 9.48%. Beyond this point, CBR values declined. The study also examined road design parameters for Primary National Highway (Asian Highway No. 48), estimating 3.2 million standard axles (msa) over a 15-year design life, with a traffic volume of 200 Commercial Vehicles Per Day (CVPD), a 7.5% annual growth rate, a Vehicle Damage Factor (VDF) of 1.5, and a Design Factor (DF) of 0.75. Pavement thickness for unreinforced soil was calculated at 496 mm, while tyre-reinforced soil required only 404 mm, marking a 54.65% strength improvement. Cost analysis showed an 8.39% savings, with tyre-

reinforced soil costing Nu.11,969,183.93 per km, compared to Nu.13,065,922.8 for natural soil. The study demonstrated both environmental and economic benefits of tyre crumb stabilization in infrastructure development.

Yang et al. (2020) addressed the global issue of waste tyre accumulation and its environmental impacts. Traditional disposal methods like landfilling and incineration release toxic chemicals, posing ecological risks. However, research has shown that waste tyres can be repurposed in geotechnical engineering, offering a sustainable recycling solution. Experimental studies, including triaxial, CBR, UCS, direct shear, and consolidation tests, revealed that adding 20% rubber particles to expansive soil improved its strength and stability. A 30% rubber-sand mix has been used as an isolation layer for buildings. Despite these positive results, the long-term sustainability and chemical effects of tyre rubber in soil remain uncertain, warranting further research. The review highlighted practical applications of rubber-reinforced soils in retaining walls, road fillings, and shock absorption, noting improvements in shear strength, bearing capacity, and soil deformation. Overall, the study emphasized the potential of rubber reinforcement in sustainable waste tyre management and geotechnical engineering.

Dhorajiya et al. (2019) carried out a study using old rubber tyres as reinforcement in soft cohesive soil subgrades. CBR tests were conducted in both field and lab settings, comparing reinforced and unreinforced soil. Field tests involved soil fills in pits reinforced with tyre geogrids at depths of 8 cm, 5 cm, and 2 cm. Results showed significant improvements in CBR values, with a 208% increase in laboratory tests and a 225% increase in field tests for reinforced soils. These findings suggest a potential reduction in pavement thickness following IRC guidelines.



Fig. 2.3: Field CBR setup (After Dhorajiya et al 2019)

The research explored the influence of rubber tyre placement at various depths within the subgrade layer on the soil's engineering properties. The findings indicated a substantial enhancement in soak CBR values, particularly with a 208% increase at a depth of 2 cm in laboratory conditions, and a corresponding 225% increase in field tests at the same depth. This elevation in CBR values corresponded to the potential reduction in overall pavement thickness.

Jastrzębska (2019) explored how the shear strength of red clay was affected by the addition of tyre rubber waste, utilizing unconsolidated, undrained triaxial tests for the investigation. Rubber waste added in mass proportions of 5%, 10%, and 25%, in the forms of powder and granulate, resulted in a remarkable decrease in cohesiveness and a variable impact on the angle of internal friction. Specifically, the addition of granulate markedly enhanced the angle of friction more than powder did, with increments of up to 31% for granulate at 25% by mass as shown in Fig. 2.4.

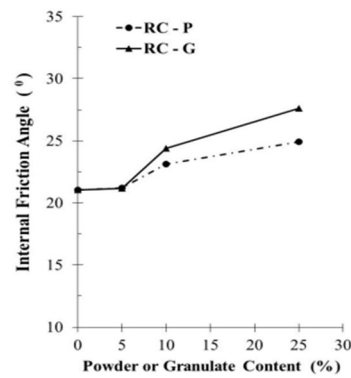


Fig. 2.4: Angle of internal friction with the rubber waste content

Conversely, cohesion significantly reduced with increasing rubber content and grain size, exhibiting reductions of up to 87% for granulate at 25% by mass as shown in Fig. 2.5.

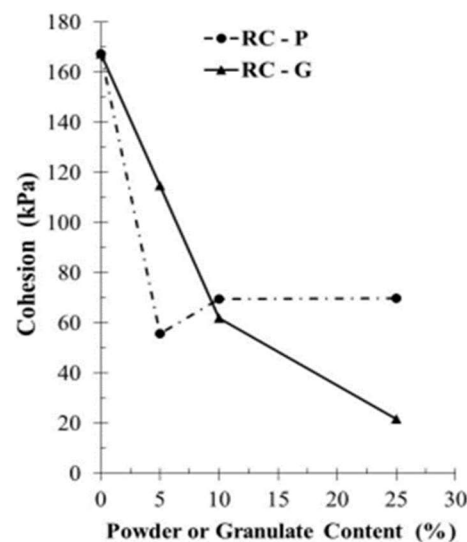


Fig. 2.5: Cohesion with the rubber waste content

These findings underscored the dual effects of rubber waste incorporation: reduced cohesion and enhanced friction angle, highlighting the potential for improving soil mixtures' strength and stability by optimizing rubber waste content and grain size.

Akshatha et al. (2018) studied the environmental concern of solid waste management, with a focus on the accumulation and recycling of waste tyres. The study investigated the use of scrap tyre rubber as an additive material for rural road building, especially when coupled with lateritic soil, which was common in coastal India. The purpose of the research was to find out how this combination affected the density, shear characteristics, and CBR of the soil. The

experimental program utilized two sizes of waste tyre rubber (WTR) materials: granulated rubber of sizes 2.36-4.75 mm and <2.36 mm. The impact of adding different proportions of WTR (5%, 10%, 15%, and 20%) to lateritic soil was examined, and the effects of rubber size were also considered.

Key findings include:

1. Incorporating WTR to lateritic soil reduced both its Liquid Limit (LL) and Plasticity Index (PI). For example, 5% WTR (2.36-4.75 mm) lowered the OMC from 20% to 18.90%, increasing the ODD from 1.73 to 1.80 g/cc.
2. WTR improved shear strength. With 15% WTR (<2.36 mm), the internal friction angle increased from 10° to 24°, and cohesiveness from 26 to 39 kN/m², as illustrated in Fig 2.6.

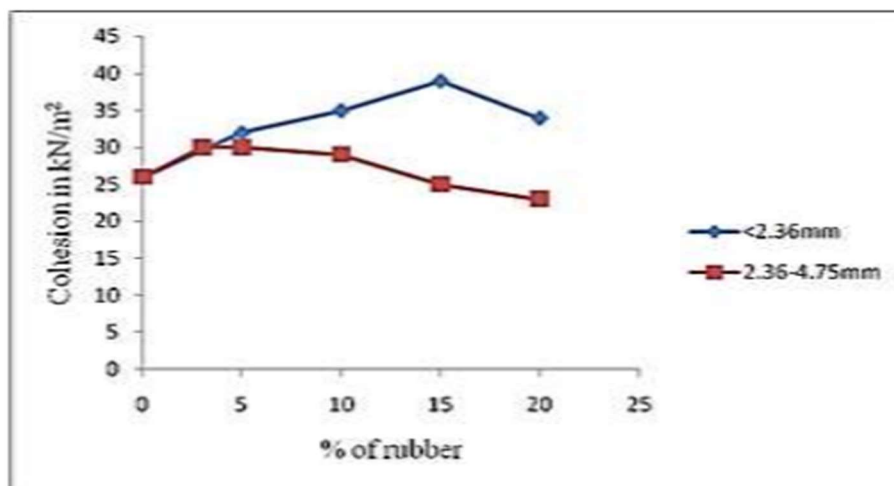


Fig. 2.6: Cohesion with waste tyre rubber. (After Akshatha et al 2018)

3. Incorporating WTR to lateritic soil improved CBR values. With 15% WTR (<2.36 mm), soaked CBR increased from 4.80% to 7.10% and unsoaked CBR from 7.40% to 11.47%. For 5% WTR (2.36-4.75 mm), soaked CBR rose to 9.44% and unsoaked CBR to 14.28%, as depicted in Figure 2.7.

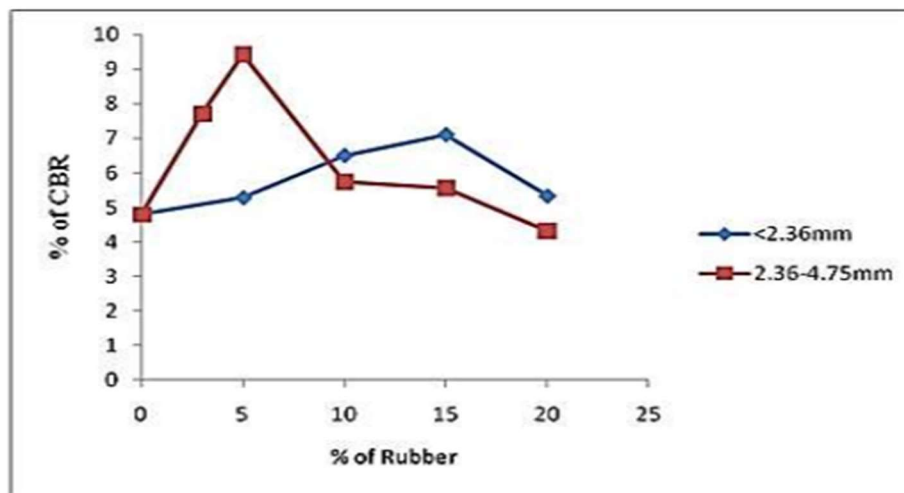


Fig. 2.7: Soaked CBR with different-sized tyre rubber. (After Akshatha et al 2018)

These findings indicated that integrating waste tyre rubber into lateritic soil could significantly enhance its mechanical qualities, making it a viable material for rural road building while also contributing to sustainable waste management methods.

Li and Li (2018) investigated the mechanical characteristics of scrap tyre crumbs mixed with clayey soil. This research was significant for its potential applications in civil engineering, particularly in ground improvement and landfill barrier materials. The research examined the effects of varying contents of scrap tyre crumbs (CSTC). The key findings of the research were-

1. With an increase in CSTC, a notable decline in both MDD and OMC was observed, making the mixture more appropriate for use as a lightweight fill material.
2. The mixture's shear strength observed an approximate increase of 20% when the CSTC reached up to 30%, although there was a decline in residual strength.
3. Compressive strength and consolidation settlement of the mixtures decreased as CSTC increased.

These findings indicated that scrap tyre crumbs could enhance the mechanical characteristics of clayey soil, making it appropriate for a variety of geotechnical applications. They also provided useful insights into the possibilities of employing scrap tyre crumbs to enhance the

mechanical characteristics of clayey soil. The study found that such mixes could be useful in civil engineering field, offering increased shear strength while reducing density and settlement. This research contributed to sustainable engineering practices by proposing an effective use of scrap tyre materials.

Al-Neami (2018) studied to enhance sandy soil properties using an innovative approach: waste tyre chips. This alternative aimed to replace conventional soil stabilization additives. Varying weight percentages (2%, 4%, 6%, and 8%) of tyre chips were manually mixed with sand in a predetermined ratio to create sand-tyre chip samples. To assess the geotechnical characteristics, examinations were conducted for compaction, specific gravity, CBR and direct shear. Results demonstrated waste tyre chips effectively improve sandy soil. Mixing in tyre chips led to an increase in shear strength, attributed to improved cohesion and friction angle. The specific gravity and MDD went to a significant decrease, whereas the OMC experienced a minor reduction of about 10%. These changes suggest that using tyre chips as fill material may lower the lateral earth pressure exerted on retaining walls. Shear strength improvement due to scrap tyre chip integration was evident. Reinforced physical bonds among soil particles led to heightened friction angle and cohesion. Soaked CBR values notably increased, up to 1.6 times that of unstabilized sand, particularly at 8% tyre chip content, as depicted in Fig. 2.8. This was attributed to elevated confining pressure and load-bearing capacity.

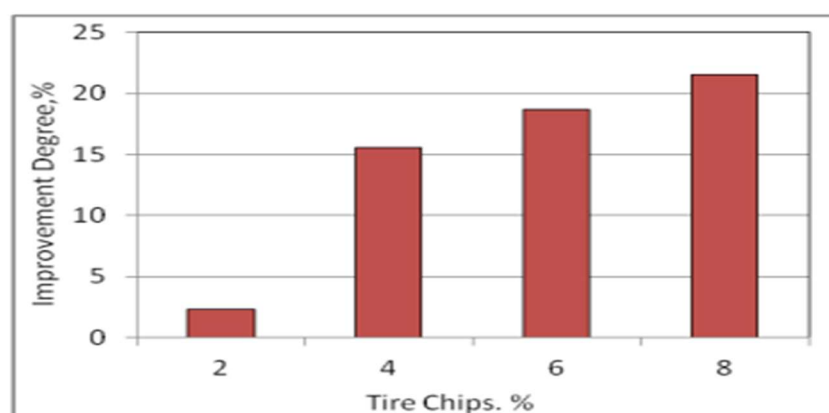


Fig. 2.8: Effect of tyre chips on CBR improvement of sand mixtures (After Al-Nemi 2018)

Incorporating waste tyre chips in construction not only enhanced soil properties but also offered economic benefits. It reduced costs and addresses disposal challenges. Embracing such eco-friendly practices contributed to sustainable development by curbing waste's environmental impact.

Peddaiah and Suresh (2017) conducted research on the enhancement of strength properties in expansive soils through the incorporation of lime and tyre chips. Targeting soils characterized by high compressibility, the investigation utilized Standard Proctor Tests and CBR tests on soil samples, both untreated and treated with varying amounts of tyre chips (4%, 8%, 12%, and 16%) alongside a fixed quantity of lime (10%). The findings revealed that the combination of tyre chips and lime markedly increased the MDD and CBR values, signifying a substantial enhancement in the strength. Specifically, the ideal combination of 12% tyre chips and 10% lime produced the highest MDD of 1.54 g/cc and CBR value of 10.3%, representing a 14.9% and 186.1% improvement over untreated soil, respectively. This study underscored the efficacy of using tyre chips and lime as cost-effective and environmentally sustainable stabilizers for enhancing the engineering characteristics of expansive soils, thereby offering a viable solution for enhancing soil stability and reducing construction costs for civil engineering applications.

Pradeep et al. (2016) investigated enhancing soil strength by partially replacing it with scrap tyre rubber and waste paper sludge ash (WPSA). WPSA, a byproduct of paper sludge combustion, and scrap tyre rubber, known for civil engineering applications, aimed to synergistically improve soil strength. The study pursued several objectives. It examined how increasing WPSA and scrap tyre rubber replacements influenced OMC and MDD. Additionally, it sought to identify optimal concentrations through UCS and CBR ratio tests. Replacing soil with varying WPSA (3%, 6%, 9%, and 12%) and scrap rubber (4%, 8%, 12%, and 16%) percentages revealed that an 8% scrap tyre rubber and 6% WPSA combination yielded the greatest boost in UCS and CBR ratio. With curing time, UCS values shifted. A 6%

WPSA replacement increased from 67.457kPa to 97.007kPa after 7 days, and an 8% scrap tyre rubber replacement increased from 67.457kPa to 80.33kPa over the same period. The peak UCS value, 106.302kPa, emerged at the optimal mix of 8% scrap tyre rubber and 6% WPSA after 7 days. In terms of CBR ratio, 6% WPSA replacement achieved 26.9%, and 8% scrap tyre rubber replacement reached 9.09kPa. In contrast, raw soil had a 7.27kPa CBR ratio. Impressively, combining 6% WPSA and 8% scrap tyre rubber yielded a 27.99% CBR ratio. Ultimately, the study underscored the potential of WPSA and scrap tyre rubber as effective stabilizers, significantly enhancing soil properties like UCS and CBR ratio. This research offered valuable insights into sustainable engineering practices through the utilization of industrial waste and recycled materials. With increases of about 27% in CBR ratio and 74.03% in UCS, the findings supported the conclusion that WPSA and scrap tyre rubber could effectively improve soil strength properties.

Apriyono et al. (2016) focused on the use of woven scrap tyres as reinforcement for soft clay subgrades in order to reduce construction costs, avoid structural collapse of highways, and minimize environmental risks resulting from Indonesia's increasing waste tyre buildup. The study used experimental studies with different woven tyre stripe distances: 2, 2.5, 3, 3.5, and 4 cm soft clay samples were created, each reinforced with one of the tyre configurations. Every sample was subjected to CBR tests, which measured CBR values at 0.20 and 0.10 inches of displacement. The study established a correlation between stripe distances and CBR values, facilitating the identification of the optimal woven tyre stripe distance yielding the highest CBR value. Results indicated that a 3 cm stripe distance was optimal, resulting in a CBR value of approximately 20%. This marked a 115% increase compared to unreinforced soft clay. The study concluded that strengthening soil with woven scrap tyres significantly improves soil carrying capacity. The optimal spacing between stripes was determined to be 3.5 cm, which produced an impressive 115.29% increase in CBR in comparison to unreinforced soil. This

utilization of waste tyres for soil reinforcement offered dual benefits: enhancing road structure stability while addressing environmental pollution concerns.

Singh and Sonthwal (2016) employed soil stabilization methods to enhance soil properties, utilizing shredded rubber tyres. Various sizes of shredded rubber tyres (10mm, 20mm, 30mm in width and 20mm, 40mm, and 60mm in length) were employed for investigation purposes, with proportions of 5%, 10%, and 15% in the investigation mixtures. The use of shredded rubber tyres for soil improvement had gained significant attention in recent times. This study investigated the impact on pavement subgrade behaviour through the improvement of subgrade soil with shredded tyres. The research revealed that the optimal proportion for shredded rubber tyres is 5%, with a size of 10mm \times 20mm. This proportion led to a 28.66% improvement in the CBR compared to the unmodified soil as shown in Fig. 2.9.

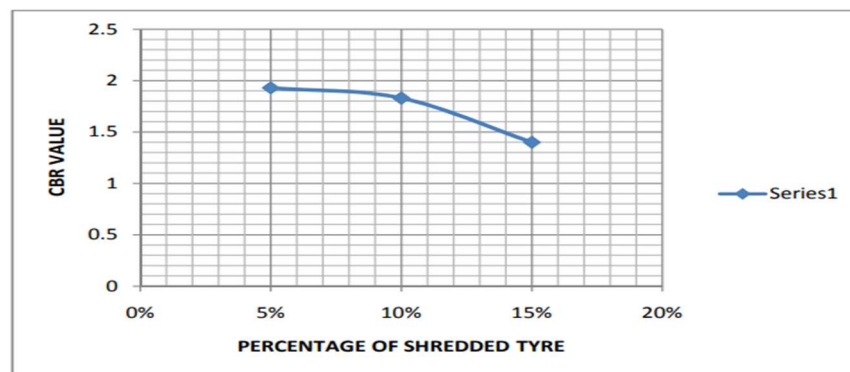


Fig. 2.9: CBR Value of Soil-Tyre Mixture (10mm \times 20mm) (After Singh and Sonthwal 2016)

Based on the research conducted, the following observations were drawn:

1. Increasing shredded tyre content raised OMC and lowered MDD due to tyre waste tyre lightweight and absorption properties.
2. Adding 5% shredded tyres (10mm \times 20mm) boosted CBR by 28.66%.
3. The 28.66% CBR increase in soaked conditions can reduce pavement thickness and costs.

Ravichandran et al. (2016) Examined the enhancement of weak soil stabilization by incorporating waste tyre crumb rubber (CR). Using different percentages of crumb rubber

(5%, 10%, 15%, and 20%), two types of problematic clay soils were stabilized. Two varieties of clay soils were stabilized by incorporating varying amounts of crumb rubber, including 5%, 10%, 15%, and 20%. The impacts on drainage properties and CBR values were then investigated. Subsequently, the effects on drainage characteristics and CBR values were explored. The incorporation of crumb rubber resulted in significant improvements in permeability and strength properties. Following the addition of 10% CR, as illustrated in Figure 2.10, there was a significant rise in CBR values, with an increase of 161% for soil type A1 and 130% for soil type A2, respectively.

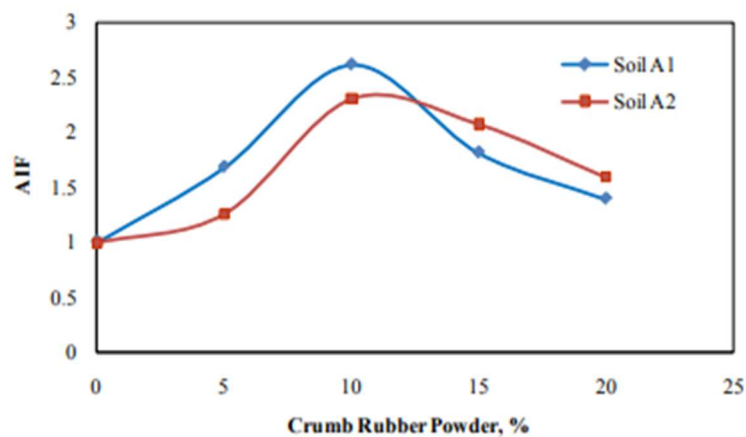


Fig. 2.10: Alteration in the effect of admixture influence factor (AIF) on CBR values due to the inclusion of Crumb Rubber Powder (CRP).

This enhancement suggested that crumb rubber could be a viable material for soil stabilization, offering environmental benefits by repurposing waste tyres while improving soil properties for construction purposes, particularly in road construction where increased CBR values could lead to reduced pavement thickness and associated costs.

Teja and Siddhartha (2015) explored the utilization of waste tyres for subgrade stabilization, which represented a safe disposal method. The incorporation of waste tyres into road construction had facilitated the efficient management of used tyre waste, mitigating disposal challenges. The soil examined in this study was obtained from near Tangutur, Ongole, along NH5, Prakasam District, Andhra Pradesh, India. The soil samples were meticulously prepared,

incorporating waste tyre fragments in various proportions, ranging from 0% to 10%, featuring tyre dimensions that fluctuate, with diameters spanning 15 to 20 mm and lengths from 20 to 25 mm. The findings revealed an enhancement in CBR value by up to 5% with the incorporation of waste tyres, as depicted in Figure 2.11. This enhancement of 1.63% in the CBR value could significantly reduce pavement thickness and, consequently, the overall project cost.

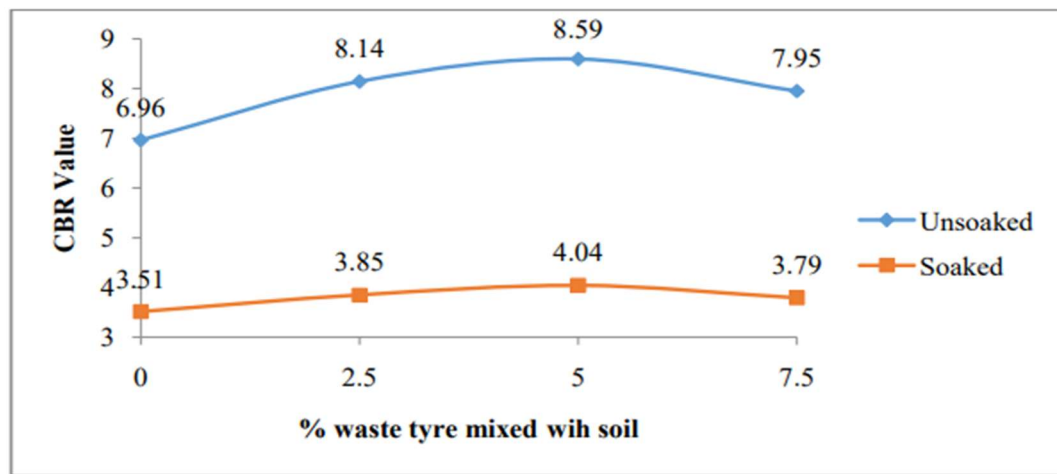


Fig. 2.11: Comparative analysis of CBR values (After Teja and Siddhartha 2015)

The present investigation examined the effects of partially replacing subbase layer aggregates with waste tyre pieces. The results indicated a significant rise in CBR value up to a 5% increase in tyre content, after which it dropped with subsequent increases in tyre content. Within the subbase layer of the pavement structure, aggregates that were partially replaced with discarded tyre pieces showed a significant reduction in their abrasion, crushing, and impact values, indicating that they were superior composite materials.

Munnoli et al. (2014) focused on addressing the growing issue of scrap tyre management. The researchers explored the application of crumb rubber (CR) derived from discarded tyres to strengthen subgrade soil, which was a significant environmental concern. They found that incorporating CR into the soil could effectively increase its strength, making it a viable solution for both waste management and construction purposes. They collected scrap tyres

from the surrounding area, which were then shredded to 4.75mm or less using a buffing machine at Karnataka Tyres, Dharwad. Meanwhile, BC soil was sourced from Krishi Nagar, Dharwad, Karnataka, and stored at the Soil Mechanics Laboratory of SDM College and Technology. The moisture content and dry density of the BC soil were found to be 18% and 2.43, respectively. As shown in Table 2.6, a CBR test with varying percentages of crumb rubber mixed into the soil revealed an increase in soil strength up to a 10% CR addition, beyond which the strength diminished, achieving a maximum CBR value of 1.54 at 10% CR content, nearly matching the control CBR value of 1.63 without CR.

Table 2.6: Outcomes from the conducted soaked CBR test. (Munnoli et al.2014)

	Pilot Reading	1 st trail	2 nd Trail	3 rd Trail	4 th Trail	5 th Trail
CR	-	6%	8%	10%	12%	14%
Result	1.63	1.16	1.37	1.54	1.03	0.91

The study concluded that adding crumb rubber to the soil not only enhanced its strength but also offered a partial solution to the disposal problem of waste rubber tyres. This research presented an innovative approach to recycling and waste management, particularly in the context of civil engineering and environmental sustainability.

Promptthangkoon and Karnchanachetanee (2013) investigated the use of recycled tyre chips as a geomaterial for building roads and embankments, mixed with low-strength soil and stabilized with cement. This innovative approach aimed at addressing the environmental problem posed by discarded tyres while also offering an eco-friendly approach to the construction industry. The findings showed that the strength and longevity of the built roads could be greatly increased by using a mixture stabilized by cement and up to 15% recycled tyre chips. Incorporating cement led to a notable rise in CBR values, which indicated improved shear strength and penetration resistance. Specifically, for mixtures with 15% cement content, the CBR values in soaked conditions ranged from 570% for 2% tyre

chips to 42% for 25% tyre chips, and UCS values increased from 1213 kPa with 2% tyre chips to 287 kPa with 25% tyre chips, demonstrating the potential of this geomaterial to reduce construction costs and mitigate environmental impacts effectively.

Marefat and Jigheh (2011) explored the innovative utilization of tyre chips mixed with clay to enhance soil stabilization, focusing on laboratory evaluations of the mechanical behaviour of these mixtures. Integrating environmental sustainability with engineering, this research addressed the pressing issue of tyre waste by repurposing it for ground improvement. Preliminary results indicated a notable improvement in the strength and compressibility of clay when mixed with tyre chips, suggesting potential for practical applications in geotechnical engineering. The findings underscored the viability of clay-tyre mixtures for landfill liners and covers, embankments, and backfill material, offering a dual benefit of waste reduction and soil stabilization. This pioneering work paved the way for further exploration into eco-friendly materials for construction and civil engineering projects.

Walubita et al. (2011) delved into the comprehensive collection and analysis of materials and pavement performance data across various highway test sections in Texas. This ambitious five-year project aimed to gather data from at least 100 test sections to refine mechanistic-empirical (M-E) design models for flexible pavements and overlays, significantly impacting future roadway investments. The report meticulously outlined data analysis plans encompassing laboratory tests on asphalt binders, Hot-Mix Asphalt (HMA) compositions, and materials for base and subgrade soil, field tests assessing cracking, rutting, and other performance indicators, alongside traffic, environmental, and climatic data analyses. Key findings from initial analyses underscored the possibility of enhancing crumb rubber soil stabilization, with an emphasis on enhancing the CBR values by 161% and 130% for specific soil types, thereby suggesting cost-effective solutions for road construction while addressing waste tyre disposal issues. Additionally, the study explored the incorporation of new materials

like tyre shreds into construction materials, showcasing their utility in reducing compressibility and enhancing shear strength, aligning with sustainable development goals.

Zornberg et al. (2004) investigated the mechanical properties of mixtures of tyre shred and sand, concentrating on the ideal content of tyre shred and aspect ratio for increased shear strength in geotechnical applications. Through large-scale triaxial testing, the research identified a tyre shred content of approximately 35% as optimal for maximizing shear strength, with a notable impact of the aspect ratio of tyre shreds on strength outcomes. The study emphasized the material's dilatant behaviour and a distinctly identified peak shear strength, apart from specimens that showed contractive behaviour and less apparent peak strength and had a significant percentage of tyre shreds. By suggesting a sustainable way to utilize tyre shreds in construction materials, this research provided a substantial addition to the area of geotechnical engineering by validating tyre shred-sand mixes as a workable solution for low soil shear strength difficulties.

Garga and O'Shaughnessy (2000) investigated the innovative application of scrap tyres in building retaining walls and earth fills, addressing the environmental problem of tyre disposal. Approximately 10,000 complete and sidewall-removed tyres were used in the building of a test fill measuring 57m by 17m that integrated reinforced slope sections and retaining walls. With the use of a thorough testing regimen that encompassed plate loading tests, field pull-out experiments, evaluation of water quality, and additional laboratory examinations, the study highlighted the viability of employing scrap tyres for earth reinforcement. The results provided design guidelines for tyre-reinforced structures by highlighting the significance of the role of negative wall friction in amplifying active thrust as the wall became more compressible compared to the backfill. This method not only presented an eco-friendly answer to scrap tyres but also approached a cost-effective alternative in geotechnical engineering practices.

2.2.2 Pavement Design and Traffic Studies

Pandey et al. (2022) carried out an extensive investigation aimed at optimizing the design of flexible pavement using various methodologies. The core objectives of their investigation were to design a flexible pavement in accordance with the IRC 37-2018 standards, assess depths through IITPAVE software, analyse strains at critical points using the same software, and ultimately achieve an optimal pavement design. Additionally, Soil tests gave a CBR value of 5.3%, while traffic estimated at 4.3 MSA. The researchers followed the depth selection procedure outlined in IRC 37-2012. They calculated the Maximum Allowable Strain for Rutting ($\epsilon_v \text{ max} = 809.25 \times 10^{-6}$) and Fatigue ($\epsilon_t \text{ max} = 536 \times 10^{-6}$). Employing the IITPAVE software, they determined strains at specific depths and radial distances: $\epsilon_t @ 95\text{mm} = 410.05 \times 10^{-6} < \epsilon_t \text{ max}$, and $\epsilon_v @ 495\text{mm} = 157.77 \times 10^{-6} < \epsilon_v \text{ max}$, by comparing the tensile and compressive strains acquired from the manual method based on IRC 37-2018 with those obtained by inputting layer thickness values into the software, the researchers identified significant disparities. As a result, they decided to decrease the thickness of every pavement layer by a certain extent to minimize the divergence in strain values between the two methods. The following strain values were obtained:

1. $\epsilon_t \text{ max} = 536 \times 10^{-6}$
2. $\epsilon_v \text{ max} = 809.25 \times 10^{-6}$
3. $\epsilon_t @ 95\text{mm} = 410.05 \times 10^{-6} < \epsilon_t \text{ max}$.
4. $\epsilon_v @ 495\text{mm} = 157.77 \times 10^{-6} < \epsilon_v \text{ max}$.

Their analysis concluded that a further reduction in layer thickness was feasible without exceeding safe strain limits.

Mehta et al. (2021) aimed to devise a flexible pavement design utilizing guidelines of IRC:37-2018 and the IIT-PAVE software. Their approach involved evaluating stress and strain at a pivotal location across distinct pavement layers. The design hinged on sub-grade soil strength and traffic load. The process encompassed gathering data on traffic levels and sub-grade soil

CBR values. Traffic was assessed through Equivalent Standard Axle Load (ESAL) considering an 80 KN load on a solitary axle with dual wheels. Layer combinations were explored while maintaining a consistent top bituminous concrete surface across trials. Compositions for base and sub-base layers, as suggested by IRC:37-2018, underwent modifications. Adjustments included variations such as Granular Base, Granular Sub-base, cement-based Sub-base, and layers treated with bitumen emulsion Reclaimed Asphalt Pavement (RAP), each defined by design thickness and resilient modulus.

The pavement's resistance to rutting and fatigue life was evaluated using IIT-PAVE. Certain trials considered perpetual pavement designs. Results indicated that the common choice was Trial 1, involving bituminous concrete, Granular base, and sub-base layers for the design of the highway. In case of an unavailable granular sub-base, Cement Treated Sub Base (CTSB) could replace it. The use of the RAP layer was less common in India due to disposal practices. Perpetual pavements were ideal for vital roads but required substantial initial investment, limiting widespread adoption. Overall, the study recommended the Trial 1 combination for its practicality and performance.

Hussainbhi et al. (2021) employed IIT PAVE software and IRC: 37-2018 guidelines to design safe flexible pavements for a 200 km road in Andhra Pradesh, India. They analysed both flexible and rigid pavements, considering subgrade CBR values from 5% to 15% and an initial traffic load of 150 MSA. For flexible pavements, they followed IRC: 37-2012 and 2018, focusing on fatigue and rutting failure criteria. Rigid pavements were designed per IRC: 58-2015, with slab thicknesses of 330mm, 320mm, and 320mm for 5%, 8%, and 15% CBR subgrades, respectively.

Their findings indicated that flexible pavement designs, using bituminous layers with granular bases like Wet Mix Macadam (WMM) and foam bitumen stabilized RAP, were safe for high traffic conditions. Rigid pavements also met safety criteria for various CBR values. However, flexible pavement Case-1 was about twice as expensive as Case-2 for CBR values between

5% and 10%, and 1.5 times higher for CBR values from 12% to 15%. At high traffic levels of 6000 CVPD, rigid pavement costs were 1.28 to 1.39 times higher than flexible pavement Case-2. The study highlighted the effectiveness of using IIT PAVE software and IRC guidelines for cost-effective and reliable road infrastructure development.

Kumar and Kumar (2020) conducted a field investigation to assess traffic patterns and subgrade soil CBR values, following IRC: 37-2012 guidelines for flexible pavement design. They used IITPAVE Software to ensure compliance with specifications, focusing on durability and deformation resistance. Additionally, they employed HDM-4, a World Bank tool, to evaluate the economic and engineering aspects of the project using Economic Net Present Value (ENPV) and Economic Internal Rate of Return (EIRR).

Data collection included axle load studies, traffic volume counts, and geotechnical analyses. Manual vehicle surveys and portable weighing pads tracked axle weights over a day, while soil investigations involved Field Dry Density, Grain Size Analysis, Modified Proctor, and Soaked CBR tests conducted over four days. Traffic volume and axle figures were calculated, and the pavement design was evaluated using IITPAVE, confirming safety as per IRC: 37-2012 standards, as detailed in Tables 2.7 and 2.8.

Table 2.7: Horizontal tensile strains (After Kumar and Kumar 2020)

Section	Allowable Strains from IRC:37- 2012	Actual Strains from IIT PAVE	Remark
Madhugiri - Gauribidanur	298.00×10^{-6} strains	266.40×10^{-6} strains	Safe
Gauribidanur - Chikkaballapur	425.60×10^{-6} strains	351.40×10^{-6} strains	Safe

Table 2.8: Vertical compressive strains (After Kumar and Kumar 2020)

Section	Allowable Strains from IRC:37- 2012	Actual Strains from IIT PAVE	Remark
Madhugiri - Gauribidanur	577.73×10^{-6} strains	345.50×10^{-6} strains	Safe
Gauribidanur - Chikkaballapur	784.40×10^{-6} strains	500.20×10^{-6} strains	Safe

Economic evaluation utilizing HDM-4 yielded economic indicators like ENPV and EIRR. For alternative 1, ENPV was Rs 1615.94 million with EIRR of 27.40% while alternative 2

had ENPV of Rs 1286.80 million and EIRR of 24.80% at a 12% discount rate. Given higher ENPV and EIRR, alternative 1 was chosen for the project.

Murana et al. (2019) assessed the detrimental impact of overloaded trucks along the Jebba-Mokwa-Bokani route in Niger State, Nigeria, with a focus on understanding axle load distribution and failure patterns. Their study aimed to address the deteriorating state of the highway due to excessive loading and propose effective solutions. The primary goal of their research was to evaluate distribution of axle loads and patterns of failure on the road between Jebba, Mokwa, and Bokani in Niger State, Nigeria, with a specific emphasis on the negative effects of overloaded trucks. To achieve this, they conducted a meticulous seven-day survey to classify traffic and measure axle loads. This survey allowed them to determine the Average Daily Traffic (ADT) and the proportion of large vehicles. The results highlighted a concerning reality: the examined highway experienced an alarming eightfold increase beyond Nigeria's standard axle load limit of 80 kN. This extensive overloading had placed significant stress on the road, leading to rapid pavement deterioration. To counter this urgent crisis, the researchers strongly recommended swift implementation of robust axle load control systems to safeguard the road's integrity. Key insights from the data analysis included:

- i. About 40% of trucks on the highway are categorized as heavy vehicles.
- ii. A significant 58% of overloaded trucks belong to the 4-axle category.
- iii. The highway operates at an average equivalent standard of 8.0, highlighting the severity of overloading.

Furthermore, a notable traffic pattern emerged, with the majority of truck traffic flowing from South to North. This resulted in a higher load concentration on the North-bound carriageway, exacerbating the situation. The comprehensive traffic analysis clearly underscored the substantial impact on road deterioration. Urgent actions were essential for regulatory authorities to enforce stringent control mechanisms, effectively curbing excessive axle loads.

Goutami et al. (2017) investigated life cycle costs of different pavement compositions on Solapur to Sangareddy stretch of NH-9. They acquired data on traffic, axle loads, and subgrade CBR values. Employing IRC: 37-2012 guidelines, they devised a flexible pavement. Relative to alternate materials in IRC: 37-2012 and leveraging IIT PAVE software, they found thinner alternatives effective for similar traffic loads, except Cement-treated Base (CTB) and Granular Sub Base (GSB) pavements. Traffic analysis of the Solapur to Sangareddy section revealed significant directional disparities, with traffic measuring 106 MSA in one direction and 83 MSA in the other. Subgrade soil analysis identified between Ch. 423.750Km and Ch. 493.000Km as appropriate for the construction of subgrades, boasting CBR values of 5% and 10% respectively. Under IRC 37:2012 guidelines, conventional pavement mandated 725 mm and 735 mm thicknesses for Subgrade CBR of 5%, accommodating traffic of 83 MSA and 106 MSA correspondingly. The same requirements were 600 mm and 610 mm for Subgrade CBR of 10%. Employing IIT Pave software along with IRC 37:2012 for the development of alternate pavement options demonstrated comparable traffic handling capabilities with decreased overall thickness, barring CTB and GSB pavements. Notably, the lower CBR (5%) subgrade yielded a higher reduction in pavement thickness than the higher CBR (10%) subgrade. Furthermore, the reduction in pavement thickness was more pronounced for pavements designed for lower traffic (80 MSA) compared to higher traffic (102 MSA). Lower CBR (5%) subgrade and higher traffic direction led to increased total pavement thickness. In cases of CBR 10% and 106 MSA traffic, treated RAP pavement demanded lesser quantities compared to other alternatives.

Harish (2017) studied to address the evolving traffic patterns and increased use of heavier vehicles, which had outpaced the design standards for pavements, leading to early deterioration. The study pivoted from the application of traditional methods towards the use of local, recycled, and engineered marginal aggregates for construction purposes due to environmental and legal constraints. The primary cause of asphalt pavement failure was

identified as fatigue cracking and rutting, resulting from excessive strain on pavements. The research focused on alternative pavement materials such as cement-based products and reclaimed asphalt, examined through the use of IITPAVE software. A specific road stretch around Bangalore was selected, where the engineering characteristics of the subgrade soil were analysed. The study compared different pavement compositions, including bases and sub-bases made of cement-like materials with aggregate interlayers for crack relief, and foamed bitumen or bitumen emulsion-treated materials. The key finding was those alternative compositions, particularly the cemented base and sub-base featuring a Stress Absorbing Membrane Interface (SAMI), significantly enhance pavement serviceability. This combination effectively reduced strains, thickness, and cost. The presence of SAMI acted as a stress-relieving layer, dissipating energy and reducing tensile stress in the bituminous layer, which delayed crack propagation and reduced maintenance costs. Overall, the study recommended these alternative materials for their improved serviceability and cost-effectiveness in pavement construction.

2.2.3 Falling Weight Deflectometer (FWD) Test

Flores et al. (2023) investigated FWD testing to assess the structural properties of concrete slabs, with a focus on their asymmetric response. This study presents an innovative method by using multi-directional Falling Weight Deflectometer (FWD) testing, moving away from traditional unidirectional tests. FWD tests were conducted on two rectangular concrete slabs, measuring vertical deflections in eight directions using geophones. Notable asymmetries were found in a 22-year-old slab marked for replacement, while the new slab exhibited nearly symmetrical behavior. The researchers employed Kirchhoff–Love plate theory with unconstrained boundary conditions and modelled the support using a Winkler foundation. To replicate the observed deflections, they optimized the subgrade reaction modulus, but initial results were inconclusive. To improve accuracy, an auxiliary surface load was introduced as a second optimization variable, along with the Winkler foundation pressure. This improved the

model's ability to simulate subgrade pressure distribution. Calculating this pressure enabled the determination of the effective subgrade reaction modulus distribution. The study also considered inertia forces, enhancing the effective subgrade moduli by up to 3.5%, improving understanding of the structural responses under different loads. Multi-directional FWD testing offered deeper insights into the slab's non-uniform subgrade degradation under prolonged asymmetric loading. An index was also developed to measure structural asymmetry, aiding in decision-making for slab repair. Statistical hypothesis testing validated this index, establishing thresholds for symmetric and asymmetric behavior in FWD test results. This research advances pavement engineering by introducing a novel method to assess the structural integrity and asymmetry of concrete slabs.

Alam et al. (2020) conducted a study to develop an intelligent pavement performance model aimed at optimizing the maintenance and repair of highway networks, a significant part of state budgets. Their research highlighted the importance of such models for prioritizing pavement maintenance and rehabilitation. These models helped predict the remaining service life of pavements and identify their rehabilitation needs, enabling better planning of maintenance activities. This approach was intended to minimize costs for road agencies and users alike. The study primarily focused on flexible pavement performance or deterioration models, accounting for factors like vehicle interactions, environmental influences, pavement structure, and surface conditions.

Alam et al. particularly examined pavement distresses such as cracking, ravelling, potholes, and roughness, crucial for understanding pavement degradation patterns. This knowledge enabled informed decisions on pavement strengthening measures. The study highlighted that traffic volume, environmental conditions, and climate all impact the pavement's remaining lifespan. To estimate the remaining lifespan, the study employed Falling Weight Deflectometer (FWD) tests at regular intervals.

The research was conducted on a section of State Highway (SH)-12A (S-2) in Punjab, covering 79.000Km to 108.800Km. Deflection data collected from this area was aggregated into seven sections for detailed analysis as outlined in Table 2.9. The findings revealed a decline in pavement modulus value over time, signalling deterioration in the flexible pavement.

Table 2.9: Summary of Average Deflection (After Alam 2020)

Chainage (Km)		Distance from Load Centre (mm)						
		0	200	500	900	1400	1900	2400
From	To	D1	D2	D3	D4	D5	D6	D7
79.2	80	1.33	0.89	0.47	0.22	0.12	0.08	0.07
80	85	1.12	0.75	0.41	0.18	0.09	0.06	0.06
85	90	0.98	0.63	0.32	0.15	0.07	0.05	0.05
90	95	1.13	0.75	0.36	0.16	0.08	0.06	0.05
95	100	1.07	0.66	0.32	0.15	0.08	0.06	0.05
100	105	0.98	0.58	0.28	0.13	0.07	0.05	0.04
105	108.8	0.96	0.55	0.26	0.13	0.07	0.06	0.05

Following the criteria outlined by IRC 37, the pavement was engineered to accommodate a specific number of standard axles. As the number of standard axles passing over the pavement increased, its life decreased. Therefore, regular deflection tests were essential to assess the pavement's ability to handle traffic loads and to determine when an overlay should be applied for strengthening.

Rabbi and Mishra (2019) presented an innovative approach to pavement rehabilitation decision-making at Boise State University. Pavement assessment techniques have depended on both functional and structural information, such as evaluations of visible damage and the use of FWD testing. However, these often hinged on accurately determining pavement layer thicknesses, a resource-intensive process not always feasible within operational constraints. The study proposed using Deflection Basin Parameters (DBPs), derived from FWD data, are presented as a more effective option for evaluating the structural state of pavements. This approach circumvented the requirement for precise measurements of layer thickness. The research involved a detailed finite-element modelling to validate the use of DBPs. They tested

typical modulus values across various pavement layers, finding that DBP values generally aligned with established ranges for different layer conditions. This confirmation led to field analyses of four selected pavement sections in Idaho, comparing the DBP-based method with traditional visual distress assessments. Results indicated that DBPs, particularly those not requiring surface layer data (like the Surface Curvature Index), could reliably indicate the state of pavement layers beneath the surface. This method's advantage was its independence from layer thickness data, making it more adaptable to operational limitations. The study's application in Idaho demonstrated that combining DBPs with functional condition data provides a comprehensive view of pavement conditions, aiding in identifying problematic layers and facilitating more informed rehabilitation decisions. The team of researchers effectively proposed methods of rehabilitation to the Idaho Transportation Department based on this integrated approach, indicating the potential for broader application in network-level pavement maintenance programs. However, they emphasize the crucial role of accurate FWD data collection, as errors in this process could lead to incorrect assessments of pavement conditions. Continued research and application of this method could lead to more effective and economical pavement preservation practices.

Singh et al. (2019) directed their efforts toward devising efficient strategies for pavement maintenance and management along a segment of the National Highway (NH) located in Haryana, India. Their primary goal was to assess the pavement material characteristics and structural strength. Using Falling Weight Deflectometer (FWD) and KGPBACK software, dynamic loads were applied to the pavement, and the resulting deflections were analyzed to determine the elastic moduli of the layers. The pavement, a 7-meter-wide two-lane flexible structure, included a 200mm bituminous layer, a 325mm base/sub-base, and a subgrade. Test pits were dug to measure pavement thickness, and historical data on rehabilitation and traffic were gathered. The study identified various pavement distresses due to design flaws, material issues, and construction errors, dividing the pavement into segments as per IRC 115 (2014)

standards. IITPAVE software was used to design overlays based on the elastic moduli, while HDM-4 predicted pavement degradation over time. The HDM-4 model showed that bituminous overlays reduced distresses like cracking, rutting, and roughness. FWD deflection measurements were crucial in determining the recommended overlay thickness, validated by HDM-4 results. This study provided guidelines for estimating funds for highway maintenance, stressing the need for consistent monitoring.

Lee et al. (2019) introduced an innovative approach for assessing subgrade strength employing a Dynamic Cone Penetrometer (DCP) equipped with a load cell and an accelerometer at the tip of the cone. This development addressed the limitations of traditional Dynamic Cone Penetration Test (DCPT), such as the influence of conveyed energy and the uprightness of the penetrometer, by providing a more accurate measure of subgrade strength. Laboratory tests conducted on weathered soil compacted at different dry unit weights demonstrated that the dynamic cone resistance, a novel index of strength proposed in this study, increased with soil depth and compactness. The capability of the instrumented DCP to directly record dynamic reactions at the cone tip offered a significant advantage over standard DCP tests, making it less susceptible to errors associated with energy transfer and penetrometer tilting. This study presented a strong case regarding the instrumented DCP as an encouraging on-site testing approach for dependable characterization of subgrade strength, suggesting that it could enhance pavement design and structural analysis by providing a more sensitive measure of stiff soil's variance in strength compared to traditional methods.

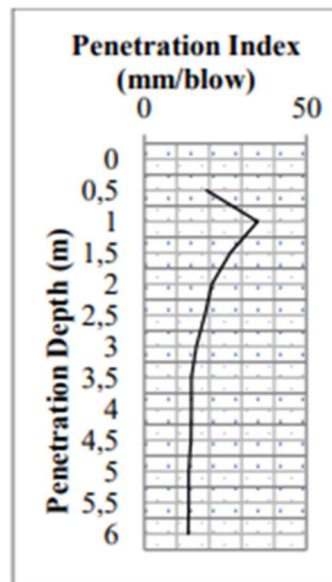
Razali et al. (2018) explored the application of the FWD in evaluating the bond condition of subgrades within flexible pavements, especially under tropical soil environments. This research was essential for understanding how subgrade deflection impacts the debonding of flexible pavements, which was a significant concern in Malaysia. The study employed FWD, a non-destructive testing method, to measure pavement vertical displacements. This approach was crucial for monitoring the state of adhesion between the pavement and the subgrade. The

research was conducted in Sungai Dua, Pulau Pinang, Malaysia, focusing on the deflection of pavement to understand the subgrade conditions. The research emphasized the significance of deflection as a key indicator of subgrade condition, with variations noted across different road segments. Understanding the bonding state between pavement and subgrade was vital for maintaining pavement integrity and preventing premature failures. Early detection of subgrade issues through FWD could reduce maintenance costs significantly. Razali et al. offered valuable insights into flexible pavement maintenance, particularly in tropical environments. The study emphasized the importance of FWD testing in the early detection of potential issues, thereby enabling cost-effective maintenance strategies and ensuring pavement longevity. This approach was particularly relevant for areas with challenging soil conditions, like Malaysia, where subgrade integrity is a critical factor in pavement performance.

Nwanya and Okeke (2018) demonstrated that the DCPT method was utilized to evaluate the CBR and bearing pressures of the subsurface soils in areas of Owerri, Southeastern Nigeria. Six (6) DCPTs were measured to a depth of 6 m. Through field measurements to a depth of 6 meters, three distinct soil layers were identified, spanning from loose to medium and dense conditions with penetration resistances varying from 11.4 to 55.5 mm/blow. The study demonstrated a correlation between soil depth and strength, with CBR values increasing from 5% at 1 meter depth to 16% at depths of 5 and 6 meters. Similarly, bearing pressures showed a significant increase from 104.8 KN/m² to 301.1 KN/m² over the same depth range. A sample DCP reading and soil profile for sample 1 were shown in Table 2.10 and Fig.2.12, indicating the varied soil layers and their corresponding penetration index values, which were crucial for understanding the geotechnical properties and designing foundations in the region.

Table 2.10: DCP measurement for sample 1 within the research zone

Penetration Records (in mm/blow)			CBR		Bearing Pressure	Description
S/no	# Blows	Depth	DPI	(%)	(KN/M2)	
0	0	0	0	0	0	0
1	15	0.5	33.3	6	122	medium soil
2	13	1	38.5	5	104.9	medium soil
3	11	1.5	45.5	4	90.3	medium soil
4	13	2	38.5	5	104.9	medium soil
5	22	2.5	22.7	9	180.5	medium soil
6	25	3	20.8	10	196.2	medium soil
7	24	3.5	15.6	14	265.4	medium soil
8	32	4	16.1	13	250.7	dense soil
9	31	4.5	15.6	14	265.4	dense soil
10	32	5	16.7	12	250.7	dense soil
11	30	5.5	17.2	12	237.5	dense soil
12	29	6	17.2	12	237.5	dense soil

**Fig. 2.12:** Soil Profile for Sample 1

This investigation not only highlighted the variability of subsurface soil characteristics but also underscored the importance of such assessments in civil and geotechnical engineering projects for ensuring structural stability and safety.

Skels et al. (2017) explored the reinforcement of non-bound layers in road structures using RAP, employing both laboratory and field assessments. The focus was on the design criteria and examination methods for stabilized Recycled Asphalt Pavement in road base layers. Four sections of the State Main Road A7 were examined. The location and design of the analyzed road sections are shown in Fig. 2.13.

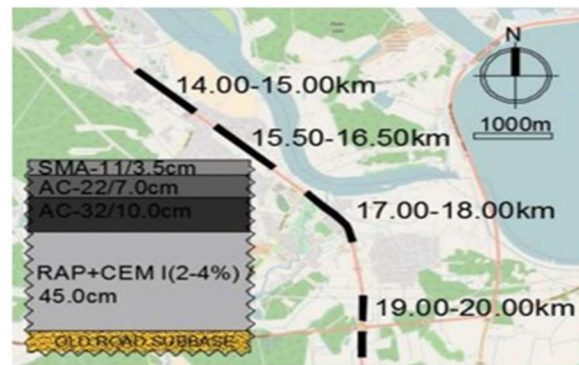


Fig. 2.13: Location of research sections along the road A7 Riga—Bauska—Lithuanian border and designed pavement structure. (After Skels et al.2017)

The equivalent modulus of elasticity (E_{eq}) was retroactively determined through analysis of data from the FWD, supplemented by laboratory tests. The study revealed E_{eq} values of 370 MPa at the surface, 170 MPa at a 30 cm depth, and 100 MPa at a 60 cm depth. A total of 67 FWD measurements from 1.0 km sections demonstrated the viability of using cement-stabilized RAP over traditional materials like dolomite or granite. The distribution of FWD deflection values is depicted in Fig. 2.14.

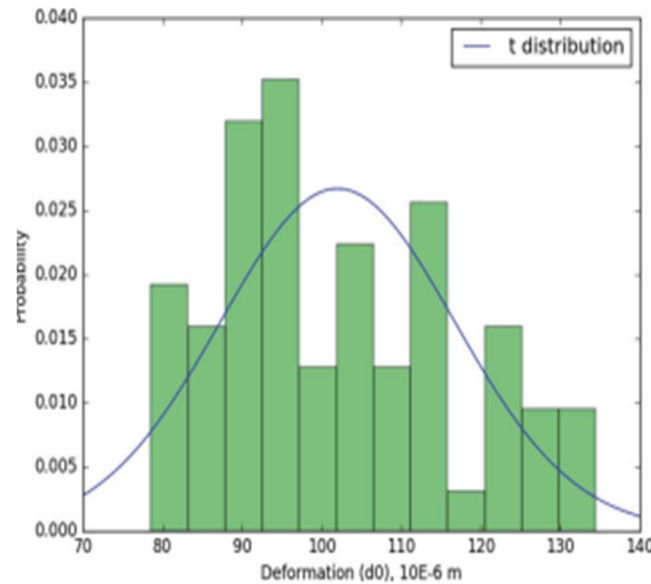


Fig.2.14: FWD measurement and t distribution for the studied four road A7 sections (After Skels et al.2017)

The elasticity modulus for cement-reinforced RAP showed high variability, with values up to 4000 MPa, indicating significant anisotropy. The modulus of elasticity results from laboratory tests on stabilized RAP samples were described in Table 2.11.

Table 2.11: Cement (2–4% CEM I) stabilized RAP testing results (After Skels et al.2017)

Sample ID No.	Sample height/diameter, mm	Max. compressive strength, MPa	E-modulus, MPa
1	196/150	3.34	1574
2	196/150	2.83	1446
3	195/150	3.89	2155
4	158/150	<u>1.48</u>	703
5	168/150	2.40	1057
6	221/150	3.13	<u>4390</u>
7	231/150	2.02	979
8	190/150	2.08	<u>557</u>
9	167/150	4.99	3883
10	141/150	<u>6.23</u>	3784
11	157/150	2.02	758
Median		2.83	1446

The study confirmed the technical, economic, and environmental feasibility of using cement-stabilized RAP in road construction. However, the variability in results necessitated improved design and construction specifications for stabilized RAP. Additionally, the study identified key parameters for pavement structures, emphasizing the need for more detailed investigations into pavement structures with stabilized road bases.

Solanki et al. (2016) conducted an extensive study along the Barnala-Mansa State Highway in Punjab, covering a 20 km stretch. Their investigation employed the Falling Weight Deflectometer (FWD) to assess pavement conditions both before and after overlay. Deflection data was collected at intervals of 0, 300, 600, 900, 1200, 1500, and 1800 millimeters from the load cell. This data was used to calculate the Surface Curvature Index (SCI), Middle Layer Index (MLI), and Lower Layer Index (LLI), which assessed the structural integrity of the pavement layers.

The SCI, representing the condition of the bituminous layer, indicated that values over 240 microns signified poor conditions, while values below 100 microns reflected good conditions. Before the overlay, most SCI values exceeded 240 microns, showing significant deterioration. The MLI, which reflects the base and sub-base layers, showed similar values (140 and 100)

for old and new layers, indicating good structural condition. The LLI, corresponding to the subgrade, reported values of 15 for the old pavement and 10 for the new, suggesting uniform subgrade conditions. Modulus values for the upper bituminous layer ranged from 600 to 2000 MPa, while the middle and lower layers had ranges of 100-450 MPa and 80-300 MPa, respectively, confirming the overall good structural integrity of the pavement.

Nega et al. (2016) concentrated on employing FWD testing for assessing the structural condition of pavements and projecting layer moduli via a back-calculation method. The research recognized that, despite its efficacy, FWD assessments can sometimes lead to inaccuracies in the estimated moduli of pavement layers, despite the calculated and observed deflection basins being within acceptable ranges, as shown in Figure 2.15.

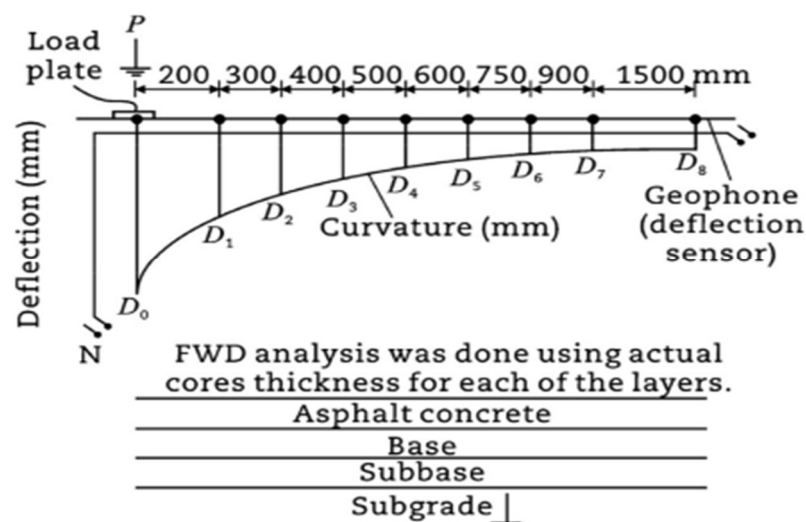


Fig. 2.15: Configuration design of a standard FWD, placement of the loading plate, geophones, and the recorded deflection basin. (After Nega et al. 2016)

Such variances may be ascribed to a range of elements, including the properties of the pavement framework, like layer depth and temperature shifts, affecting the structural capability of the pavement and the retroactively calculated layer modulus.

The primary goal of the study was to examine FWD testing results on flexible pavement in Western Australia to predict the structural capacity of the pavement. The research involved

collecting FWD data, and core information, and carrying out assessments on pavement deterioration. Key findings of the study were:

1. The study successfully applied dynamic analysis and enhanced algorithms to predict the flexible pavement layer moduli.
2. The investigation showed that moduli values across most sections were consistently and accurately predicted, with some discrepancies in certain areas.
3. The research utilized the BISDEF program for back-calculating layer moduli across seven sites, covering a 7 km stretch with 105 points in total. The research suggested using multilayer computer programs like BISAR and WESLEA to improve the precision of layer moduli predictions.
4. Figure 2.16 presented the dynamic deflection basin for a sample project, revealing the complexities of analysing FWD deflection data.
5. The study highlighted difficulties in gathering a single set of moduli representative of field conditions, particularly when using back-calculation methods like BISDEF.
6. The study emphasized the need to account for air or surface pavement temperatures during FWD testing, as temperature fluctuations can impact asphalt concrete thickness and layer modulus.

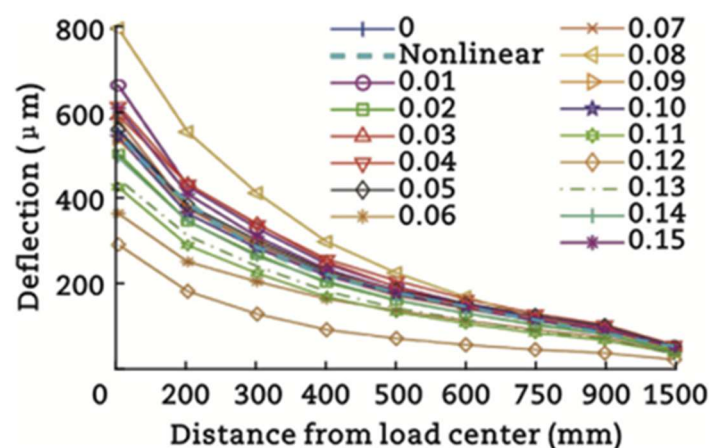


Fig. 2.16: The nonlinear analysis identified dynamic deflection basins at various locations for Project 5 (After Nega et al. 2016)

Chai et al. (2013) explored the CBR of subgrades for thin bituminous pavements using FWD data, highlighting the inadequacies of existing models which overestimated subgrade CBR by relying on deflections recorded at 900 mm from the load centre (D900). Their research, conducted across eleven pavement sites in Brisbane, Australia, demonstrated that these models failed to account for the small deflections and the inherent non-linearity of thin pavement structures. By developing a new model that utilized deflections at 450 mm from the load centre (D450), the study provided a more accurate estimation of the in-situ subgrade CBR, particularly for pavements with asphalt layers less than 50 mm. This new model, verified against DCP data, showed improved correlation and reduced prediction error, suggesting a significant advancement in the methodology for evaluating subgrade strength in thin bituminous pavements.

Talvik and Aavik (2009) Performed an investigation into the correlation between FWD deflection basin parameters, including SCI, Base Damage Index (BDI), and Base Curvature Index (BCI) and the condition of road pavements in Estonia. Utilizing data from the Estonian Road Databank, the research aimed to establish threshold values for these deflection basin parameters to effectively evaluate pavement structural conditions. Analysis revealed strong correlations between indicators of the upper layers, denoted by SCI and BDI, which were examined alongside the pavement's equivalent modulus (E_{eq}), revealing correlation coefficients (R^2) spanning from 0.5 to 0.9. However, the relationship between the subgrade indicator (BCI) and E_{eq} was weaker, indicating that weak subbases and subgrades compromised the structural capacity of Estonian roads. The research methodology involved normalizing FWD-measured deflections to a standard load and temperature to facilitate comparison across various pavement conditions. Despite efforts, no definitive correlation was established between deflection basin parameters and surface defects or rut depths in the pavement, likely due to the discrepancy between the localized nature of FWD measurements

and the continuous assessment of pavement defects. The study concluded with the creation of formulas for computing the maximum allowable values of SCI, BDI, and BCI for different pavement types, based on the minimum required equivalent modulus. These findings represented a significant advancement in utilizing FWD data for pavement condition assessment, providing a practical approach to identifying road network sections with inadequate structural capacity.

Sahoo and Reddy (2009) studied the correlation between DCP and CBR values in fine-grained soils through lab and field tests, revealing a notable relationship between the two, providing a reliable method for estimating subgrade strength—an essential parameter in highway pavement design. Specifically, the research established logarithmic models correlating lab DCP values with lab CBR values and field DCP values with field CBR values. The derived relationships, represented as $\log_{10} \text{LAB CBR} = 2.758 - 1.274 \log_{10} \text{LAB DCP}$ and $\ln \text{CBR} = 67.898 - 17.483 \ln(\text{FIELD DCP})$, suggested a consistent and accurate approach for in-situ subgrade evaluation. Fig. 6, depicting the field DCP-field CBR relationship for combined data, illustrated the robustness of their derived correlation across diverse soil samples, reinforcing the utility of DCP as a cost-effective tool for pavement layer assessment and design optimization. Fig 2.17 represents DCP-field CBR relationship.

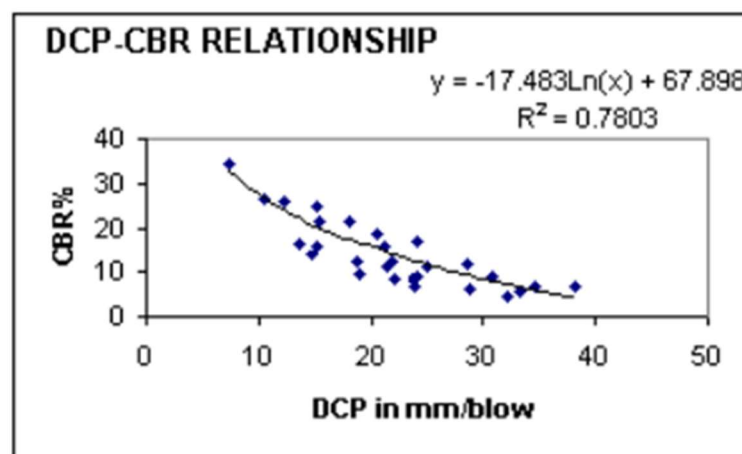


Fig. 2.17: Field DCP-CBR relationship (merged data) (After Sahoo and Reddy,2009)

This finding underscored the utility of DCP as an efficient, cost-effective tool for pavement layer and subgrade assessment, enhancing the process of pavement evaluation and design.

Horak (2008) explored the use of FWD for non-destructive testing of pavement structures. FWD data, combined with an analysis that blends semi-mechanistic and semi-empirical approaches, originating from South Africa, allowed for the benchmarking of pavements' structural conditions without detailed as-built data. This methodology utilized deflection bowl parameters to evaluate individual layer strengths and identify rehabilitation needs. Horak introduced an additional correlation investigation connecting calculated surface moduli with deflection bowl parameters for granular base pavements, improving the benchmarking technique. The study suggested that maximum deflection values, radius of curvature, and other deflection bowl parameters could effectively gauge pavement integrity, offering a practical tool for Pavement Management Systems (PMS) and project-level design investigations. Horak's method divided the deflection bowl into three zones, correlating each with specific pavement layers. This zoning facilitated the understanding of pavement response to loading and aided in pinpointing structural weaknesses. The paper also discussed the correlation between parameters of deflection bowls and surface moduli derived from calculations, offering a refined approach to pavement benchmarking.

2.2.4 Simulation of FWD Test by Finite Element Method (FEM)

Momin and Hamim (2022) presented a detailed analysis of the creation of a system for managing pavements in Bangladesh, focusing on a deflection prediction model for flexible pavements. Utilizing data from 252.6 km of road, including both national and regional highways, the research applied multiple linear regression analysis to establish a model correlating pavement deflection with International Roughness Index (IRI), the Annual Average Daily Traffic (AADT), width of the road, and duration since the last overlay. Significant findings included deflection values ranging from 0.5 to 2.0 mm, with most between 0.5 and 1.25 mm, and IRI measurements ranging between 2 and 12, mostly between

2 and 6. The correlation analysis revealed IRI as the strongest predictor of pavement deflection ($r = 0.775$, $p < 0.001$), with a model accuracy of 61.8% variance explanation ($R^2 = 0.618$). The research concluded the insignificance of pavement width and AADT in deflection prediction, highlighting IRI and pavement age as key factors. This model provided a foundation for decision-makers to select appropriate rehabilitation or maintenance strategies, demonstrating a method to enhance pavement longevity and serviceability with an emphasis on non-destructive testing approaches.

Adigopula (2022) presented a novel approach for predicting the modulus values of pavement layers based on data obtained from Light Weight Deflectometer (LWD). This research was pivotal for thin asphalt pavement analysis, particularly in determining the layer moduli through empirical equations. The study utilized LWD data, integrated with the FEM analyses, to predict the moduli of various pavement layers. Fig. 2.18 demonstrated the Dynatest 3031 testing with different drop weights.

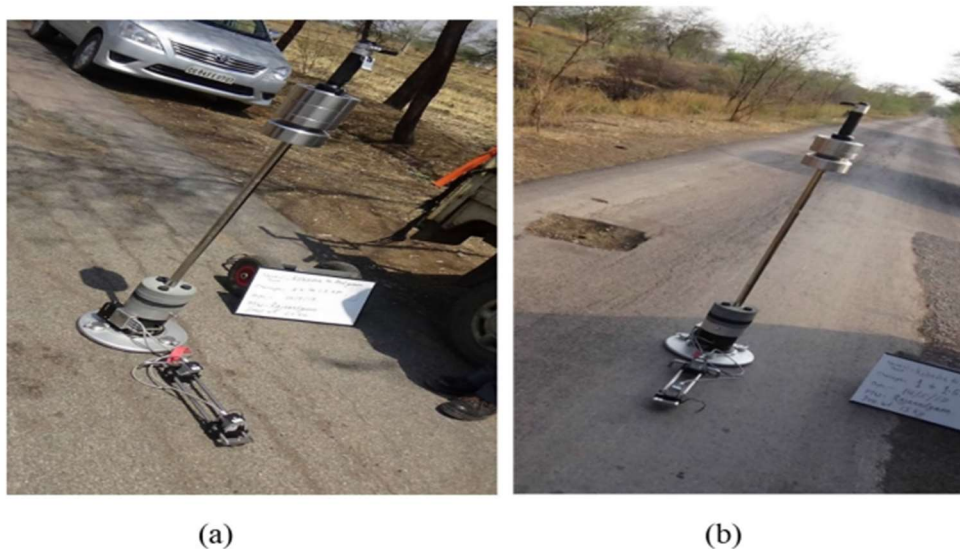


Fig. 2.18: Dynatest 3031 assessment involving (a) a 20 kg drop weight and (b) a 15 kg drop weight. (After Adigopula 2021)

A significant contribution was the formulation of an empirical expression for in-situ layer moduli estimation, eliminating the need for complex back calculation processes. Fig. 2.19 Outlined the methodology for developing empirical equations.

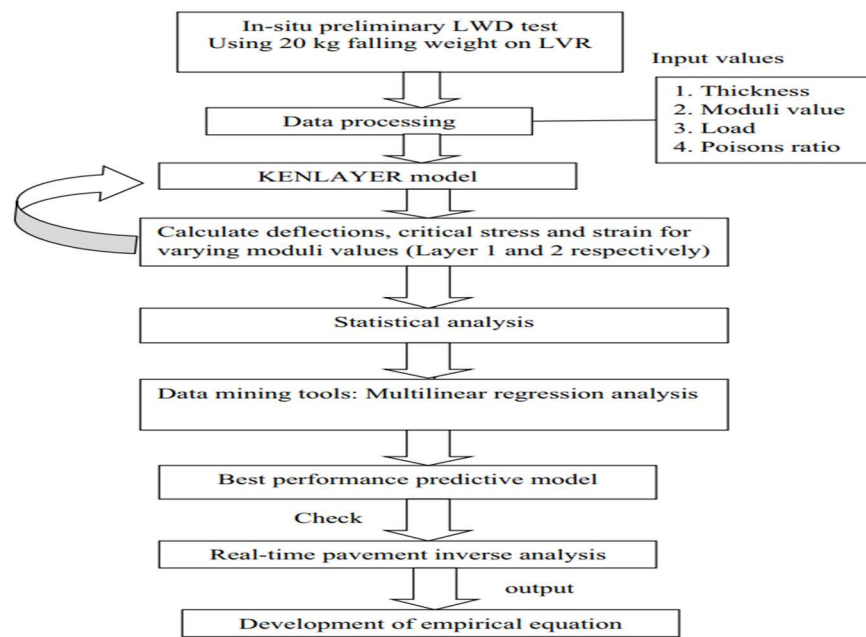


Fig.2.19: Approach employed in formulating empirical equations. (After Adigopula 2021)

The research focused on thin asphalt pavements, highlighting the efficacy of LWD in analyzing such structures. Adigopula's study successfully demonstrated a simplified method for estimating pavement layer moduli, offering a practical tool for pavement evaluation and design. Table 2.12. Described the description of the input values utilized in generating the dataset for modelling the pavement system.

Table 2.12: Assumed input values for generating the dataset in the pavement system model using KENLAYER. (After Adigopula 2021)

Data set	Asphalt layer 1 thickness, H1 (mm)	Base layer 2 thick- ness, H2 (mm)	Geophones offset (mm)	LWD falling weight (kg)	Layers	Poisons ratio	Modulus, M_R (MPa)
1	50	350–475	0, 300 and 600	20	Asphalt	0.35	500–700
					Base	0.40	280–480
					Subgrade	0.45	20–100

This empirical approach, validated through FEM and laboratory results, signified a step forward in pavement engineering, especially for low-volume roads and thin asphalt pavements.

Pai et al. (2020) investigated the feasibility of integrating slag-lime-treated indigenous soil as a subbase material in flexible pavement applications, aiming to reduce natural aggregate use and overall construction costs. Utilizing Ground Granulated Blast Furnace Slag (GGBS) and lime, the research treated expansive soil, known for its problematic construction and maintenance characteristics because of inadequate strength and pronounced swelling-shrinkage. The optimized mixtures, based on CBR and UCS tests, included soil with 12% GGBS, 6% GGBS + 3% lime, and 8% GGBS + 4% lime. Finite element analysis using PLAXIS 3D indicated a pavement service life increase of up to 65% with the treated soil subbase, leading to a 15.5% cost reduction. The findings suggested that slag-lime-treated native soil could serve as an economical and environmentally friendly alternative to conventional GSB materials in road construction.

Loizos and Scarpas (2013) explored the validation of FWD back analysis outcomes through Dynamic Finite Element (FE) modelling. The FWD was extensively used for non-destructive testing of pavements, primarily to estimate pavement material properties. This research examined the appropriateness of employing static versus dynamic models in the back analysis of FWD data, specifically focusing on estimating the elastic modulus of pavement materials. Dynamic FE simulations, both 2D and 3D, were used to verify the results of FWD back analysis procedures. Field data collected from both new and pre-existing asphalt pavements, utilizing various types of FWD were utilized, along with laboratory-tested core data for preliminary validation. Comparative analyses using Dynamic FE simulations and various back analysis methods, including MODCOMP, MODULUS, and ELMOD, were conducted. The investigation demonstrated the effectiveness of Dynamic FE modelling for validating the elastic modulus obtained through back analysis, offering a more accurate depiction of pavement response under dynamic conditions. Dynamic FE models were found to be valuable for validating and optimizing quasi-static back analysis methods, leading to more reliable pavement design and maintenance estimations. The study highlighted that while static models

are widely used due to their simplicity, dynamic models offer enhanced accuracy, especially under certain conditions. The utilization of Dynamic FE analysis for FWD back analysis verification was a promising approach in pavement engineering. It not only validated the back analysed data but also assisted in optimizing the pavement material properties used in construction and rehabilitation. This methodology offered a practical tool for engineers to validate and refine pavement designs and maintenance strategies.

Howard and Warren (2009) explored the effects of variability on the evaluation of thin flexible pavement performance through finite element analysis. The investigation focused on a pavement structure that included a slender asphalt surface, granular base, geosynthetics, and a fine-grained subgrade were considered. Employing PLAXIS software, the investigation integrated stationary transient loading and stress-dependent material models to replicate actual conditions. The findings highlighted the significant impact of variability on pavement behaviour, even within standards deemed acceptable for construction. Specifically, asphalt strain variations ranged from 8% to 141% due to variability, with vertical sensor positioning affecting strain readings by $\pm 31\%$. This level of variability questioned the reliability of using asphalt strain gauges in thin pavements due to potential measurement errors. Additionally, subgrade stress experienced changes from 17% to 45% because of variability, underscoring the complexity of accurately assessing pavement performance. The research underscored the necessity of accounting for variability in pavement design and analysis to avoid misleading interpretations of instrumented measurements.

2.3 SUMMARY

The previous section has presented a comprehensive review of the available literature about soil property improvement by tyre scrap, pavement design and traffic studies, FWD test and simulation of FWD test in Finite Element method. These investigations have encompassed experimental studies as well as numerical and analytical approaches. Numerous studies have

investigated the effects of different-sized tyre scraps on various soil types, focusing on their impact on properties such as shear strength, bearing capacity, and CBR values. Key findings from literature include optimal tyre content levels for enhancing soil mechanics and the environmental benefits of using recycled materials. Additionally, the chapter highlighted the effectiveness of tyre-reinforced soils in geotechnical applications like subgrades for flexible pavements. The chapter has been concluded by emphasizing the potential for sustainable engineering practices using scrap tyres.

2.4 MOTIVATION

In regard to the literature review previously mentioned, it is observed that there have several advantages of using scrap tyres as a reinforcing agent in civil engineering field. The special qualities of the raw materials utilized in the manufacture of tyres include strength, flexibility, resilience, and high frictional resistance. The special qualities of scrap tyres may be put to good use when they are recycled as an alternative building material rather than being burned. Generally, waste or scrap tyres are used mainly in granulated or shredded format and exhibit interesting physical, mechanical and dynamic properties. There have been various effects of reusing waste tyres in geotechnical-related issues, such as-

1. Improving Road Infrastructure: The potential of waste tyres to enhance the mechanical properties of subgrade soil can lead to more durable, cost-effective, and resilient road infrastructures, especially in regions with challenging soil conditions. From many research works it has become a fact that scrap tyres may improve effectively the performance of embankments and backfills by reducing deflections, (Ibrahim et al. (2022), Akshatha et al. (2018), Apriyono et al. (2016), Johns et al. (2022)).

2. Innovative Engineering Solutions: Exploring the use of waste tyre materials in geotechnical applications opens avenues for innovative engineering solutions, contributing to the advancement of the field. Recently, rubbers have been used as lightweight construction

material. (Tabasum et al. (2023), Mangi and Sarki (2021), Bai et al. (2020), Yang et al. (2020), Li and Li (2018), Peddaiah and Suresh (2017), Zornberg et al. (2004)).

3. Addressing Traffic Load Challenges: As traffic loads and vehicle sizes increase, there is a growing need for more robust and adaptable road infrastructures. Utilizing waste tyres in pavement subgrade can offer enhanced performance under these changing conditions. When embankment fill was constructed using cohesive soil and tyre shreds, heavy truck traffic and settlements demonstrated satisfactory long-term performances under traffic exposure. (Wangmo et al. (2020), Dhorajiya et al. (2019), Teja and Siddhartha (2015), Ravichandran et al. (2016))

4. Waste Management and Economic Benefits: Repurposing waste tyres in construction not only addresses waste management issues but also offers economic benefits by reducing the need for traditional, often more expensive, materials.

In view of the above context for the research, by highlighting the significant potential of utilizing tyre scraps in practical applications to create a healthier environment for humanity. It underscores that, based on existing literature, scrap tyres can enhance soil properties and strength, which is a crucial consideration for geotechnical engineering. The current study is thus conducted with the aim of evaluating the performance of clayey subgrade mixed with scrap tyre material. (Amin et al.2023, Juliana et al. 2020, Munnoli et al. 2014, Promputthangkoon and Karnchanachetanee 2013).

CHAPTER 3

OBJECTIVE AND SCOPE

3.1 OVERVIEW

This chapter outlines the principal objective and scope of work of the present investigation.

3.2 OBJECTIVE

The objective is to evaluate the performance of soft cohesive subgrade in flexible pavement by incorporating tyre scrap, with comparison to the performance of the same without any modification.

3.3 SCOPE OF WORK

The primary goal is to assess the effectiveness of using tyre scrap as an admixture for improving subgrade layers in flexible pavements. The study compares the performance of this material, with existing original soil subgrade.

The performance of two different subgrade types is specifically compared in this study:

- i. Subgrade consisting solely of cohesive soil, and
- ii. Subgrade that combines cohesive soil with tyre scraps.

With the integration of waste tyre materials into the subgrade layer, the comparison aims to evaluate improvements in the strength, durability, and overall performance of the pavement structure. The evaluation of subgrade properties in a flexible pavement system is crucial for ensuring its ability to support traffic loads and maintain long-term performance and integrity.

The key parameters for structural evaluation of the pavement subgrade include deflection, CBR, and Elastic Modulus (E_s). CBR test is used for evaluating the load-bearing capacity of subgrade soil. It quantifies the relative strength of the subgrade material by measuring its resistance to penetration under a standardized load, compared to that of crushed stone material.

The Elastic modulus (E_s) of a soil is a parameter that is commonly used in the estimation of settlement for pavement design and evaluation. It indicates how well the subgrade can distribute loads and reduce deformation. The focus of this study is to assess the effectiveness of incorporating scrap tyres into the pavement subgrade. The research site chosen for this investigation is the Jibantala-Taldi Road, which spans 12.45 Km in length and 5.5 m in width, located near Canning in the South 24 Parganas District of West Bengal, India. A sample stretch of the road section has been shown in Fig. 3.1. This road is under the jurisdiction of the Public Works Department (PWD), Government of West Bengal. Permission was obtained from the Department to conduct the necessary study on the road. The permission letter is included in ANNEXURE I. Original soil samples from the road site have been collected to determine essential soil parameters. while scrap tyres were obtained from a local car garage in Jadavpur, Kolkata, West Bengal, India.



Fig. 3.1: Sample stretch of Jibantala-Taldi Road

The study has been done with a three-dimensional analysis, which includes:

- i. Laboratory tests,
- ii. Field tests, and
- iii. Numerical work.

All these tests and associated studies are outlined below:

3.3.1 Laboratory Tests

This phase involves several tests to understand the properties of the original soil and the modified soil (with tyre scrap). These tests include:

- i. Soil Characterization: Laboratory tests such as Grain size analysis, Atterberg Limits, moisture content and specific gravity tests have been used to determine the basic properties of soils.
- ii. Shear strength: Unconsolidated Undrained test (UU) has been done to obtain shear strength parameters, specifically cohesion (C) and the angle of internal friction (ϕ).
- iii. Compaction Characteristics: OMC and MDD have been determined by the Modified Proctor Test, which are crucial for understanding the soil compaction behaviour.
- iv. Bearing capacity of subgrade: Both unsoaked and soaked CBR tests have been conducted to understand the strength and stability of the soil under various conditions.

The study includes various tests to observe changes in soil strength after mixing different sizes of scrap tyres (ranging from 10mmX10mm to 30mmX30mm) with soil at varying percentages (from 5% to 30%) to determine the maximum achievable improvement. Soil-tyre mixtures have been prepared by combining road subgrade soil with shredded tyre scrap based on dry weight proportions, exploring ratios of 100:0, 95:5, 90:10, 85:15, 80:20, 75:25, and 70:30. To fulfil the purpose of the study, two standardised methods for testing have been undertaken for soil-tyre mixtures:

- a) Modified Proctor test
- b) CBR test

The innovative aspect of this study has been done by experiments with various sizes of scrap tyre pieces, mixed in various ratios with the soil as described.

3.3.2 Field Study

Based on these laboratory findings, a 30m long and 5.5m wide flexible pavement section has been constructed by following the design methodology of IRC 37:2018. This construction has been situated at 20.0 m away from 7.0Km Ch. of the existing pavement and utilized the optimally determined tyre scrap mix combined with the original soil collected from selected areas near the existing road. The purpose of this construction is to replicate the laboratory-obtained proctor and CBR values of the tyre mix soil under field conditions. A comprehensive traffic study, including an axle load test, has been carried out on the existing road to collect necessary data. This part of the study involves the collection of necessary field data, which is then combined with laboratory findings to complete the study. It includes-

- i. Traffic study: To understand the volume and type of traffic and the effect of various axle loads on the pavement surfaces under consideration.
- ii. Dynamic Cone Penetrometer Test (DCPT): The field CBR or in-situ CBR value has been estimated using this test.
- iii. Falling Weight Deflectometer (FWD): To measure the deflection and Elastic Modulus (E_s) of the subgrade, which is an indicator of its ability to support loads.

3.3.3 Numerical Work

The study involves significant numerical work, including:

- i. Pavement Design: IIT PAVE software, a tool for designing pavements based on various parameters, has been utilized to complete the design.
- ii. Finite Element Modelling: The PLAXIS 3D software has been utilized to simulate the model for the present study. Then FWD test results, obtained from the analysis have been analysed to understand how the subgrade behaves under load in a more detailed and comprehensive manner.

3.3.4 Regression Analysis

An attempt has been made to obtain modified CBR with respect of normal CBR, tyre size and proportions as input variables using MINITAB, a statistical software.

By combining laboratory tests, field data, and numerical modelling, the study aims to provide a thorough evaluation of tyre scrap as a material for subgrade improvement. This can lead to more sustainable methods for building and maintaining roads, especially in areas with challenging soil conditions.

CHAPTER 4

METHODOLOGY

4.1 OVERVIEW

The study investigates the use of scrap tyres in pavement subgrades using a comprehensive methodology. The main methods and procedures encompass material collection for the study, laboratory testing, field studies, and numerical work.

4.2 LABORATORY TESTING AND MECHANISM

In the present work, the following tests have been performed-(i) Grain size distribution (ii) Atterberg Limits (iii) Water Content (iii) Specific Gravity (iv) Unconsolidated Undrained (UU) test (v) Modified Proctor compaction test and (vi) CBR test.

Tests are conducted to evaluate the impact of integrating tyre scrap of varying sizes (10mm X 10mm to 30mm X 30mm) and proportions (5% to 30%) into the soil. The goal is to identify the optimal tyre scrap inclusion for enhancing soil properties. For these mixtures, Modified Proctor and CBR tests are performed. It is worth mentioning that the road under study (Jibantala-Taldi) is classified as a major district road by the PWD. As stipulated in clause 6.1 of IRC:37-2018, the Modified Proctor Compaction test has been used to evaluate the value of Optimum moisture content (OMC) and Maximum Dry Density (MDD). The tests described above for soil and soil tyre scrap mix have been carried out using the IS Code techniques outlined in Table 4.1.

Table 4.1: Test programme for soil and soil tyre scrap mix

Sl. No.	Tests	Relevant IS Code
1	Grain Size Distribution	IS:2720(PART-IV):1985
2	Atterberg Limits Liquid Limit Plastic Limit	IS:2720(PART-V):1985
3	Water Content	IS:2720(PART-II):1973
4	Specific Gravity	IS:2720(PART-III/Section1):1980
5	Unconsolidated Undrained (UU) Test	IS:2720(PART-XI):1993
6	Modified Proctor Compaction Test (OMC, MDD)	IS:2720 (PART-VIII): 1983
7	CBR Test	IS:2720 (PART-XVI): 1987

4.2.1 Grain Size Analysis

The soil grain sizes have been determined using IS:2720(PART-IV): 1985 at several points along the road. The results are visually represented using grain size distribution curves, which displayed cumulative particle percentages on a logarithmic scale.

4.2.2 Atterberg Limits

4.2.2.1 Liquid Limit

It is defined as the water content at which soil flows cohesively along a groove in a standardized cup under 25 impacts in Casagrande's apparatus, employing a 200g air-dried soil sample combined with water to determine soil consistency. This method is crucial for assessing the Liquid Limit of soil samples collected at Km intervals along roads.

4.2.2.2 Plastic Limit

The Plastic Limit, which is determined by the water content at which soil stops forming threads of 3 mm diameter without fragmentation, involves combining approximately 50 g of

oven-dried soil with water to assess its plasticity. This test, conducted according to IS 2720 (part V), is crucial for evaluating soil samples collected at intervals along the road.

4.2.3 Water Content

The percentage that represents the water to solid weight ratio in soil determines the moisture content, which is important for the study. Soil samples from specific road chainages have been analysed using the oven drying technique outlined in IS:2720(PART-II):1973.

4.2.4 Specific Gravity

Specific gravity, defined as the weight ratio of soil solids to distilled water at the same volume and temperature, is critical for understanding unit weight. The original soil sample has been tested for specific gravity in accordance with IS 2720 (Part III/Section 1).

4.2.5 Unconsolidated Undrained (UU) test

UU triaxial compression test, per IS 2720 (Part-XI):1993, assesses soil shear strength without directly measuring pore water pressure. Conducted on unconsolidated soil samples from various pavement subgrade chainages, it determines shear strength parameters. Samples are prepared to match field conditions by adjusting density and moisture content, eliminating structure and anisotropy through remoulding and compaction. This ensures homogeneity and meets the requirements for the UU triaxial test.

4.2.6 Modified Proctor Compaction Test

A 2.5 kg air-dried soil sample, sieved to pass through a 4.75 mm sieve, is blended with water incrementally from 5% to 20%. Compacted in Proctor moulds in five layers with 25 blows each, the modified Proctor test determines OMC and MDD following IS:2720 (PART-VIII): 1983 guidelines.

4.2.7 California Bearing Ratio (CBR)

The CBR test involves penetrating a soil sample with a 5 cm diameter plunger at a constant rate into a mould containing soil compacted in three layers using a 2.6 kg hammer. CBR

values, determined at penetrations of 2.5 mm and 5.0 mm, are computed following IS:2720 (PART-XVI): 1987 guidelines, conducted on various soil and soil-tyre mixtures at OMC.

4.3 FIELD STUDIES

In this present study, a series of field tests have been done methodically, covering numerous aspects of traffic and pavement analysis. These tests consist of Traffic Study, DCPT and FWD test.

4.3.1 Traffic Study

The traffic study aims to comprehensively assess traffic volume and diversity using advanced census methodologies, systematically counting and categorizing vehicles to analyze traffic patterns. It is structured into Traffic Census and Axle Load Survey segments to understand vehicular flow, types, and weight distribution per axle, providing insights into traffic density and its impact on road infrastructure.

4.3.1.1 Traffic Census

In designing pavement thickness, a crucial step involves conducting an exhaustive traffic study to ensure accommodating anticipated volumes and environmental factors, considering material attributes, traffic load frequency, magnitudes, and environmental conditions for longevity estimation of flexible pavements within 15 to 20 years.

Commercial Vehicles Per Day (CVPD), Passenger Car Unit (PCU), and Average Daily Traffic (ADT) are essential traffic engineering concepts vital for traffic flow management, roadway design, and transportation infrastructure decision-making, detailed further below.

i. Commercial Vehicles Per Day (CVPD)

CVPD, representing the count of passenger vehicles passing a point on a roadway within a day, is a fundamental unit in traffic engineering, crucial for traffic planning, road design, capacity analysis, and traffic forecasting, aiding in assessing vehicle traffic volume for transportation authorities and engineers.

ii. Passenger Car Unit (PCU)

PCU standardizes the impact of different vehicle types on traffic flow by assigning values to account for their varying effects on congestion, aiding in the analysis of roadway capacity, congestion, and service levels through the conversion of vehicle counts into Traffic Volume.

iii. Average Daily Traffic (ADT)

ADT, the average daily traffic count of vehicles passing a specific roadway point over a year, aids in traffic management and infrastructure planning, informing decisions about maintenance, expansion, signal timing, and traffic control devices by offering insights into overall traffic load. By collecting and analyzing data related to CVPD, PCU, and ADT, transportation professionals can make evidence-based decisions to improve road networks, and enhance traffic flow, and safety through a comprehensive traffic census spanning a continuous 7-day period.

A 7(seven) day traffic survey is carried out to find out the (CVPD) for a specific location, following these steps:

A. Define Study Objectives: Clearly define the objectives of the survey. In this case, the objective is to determine the CVPD for the location over a 7-day period.

B. Select Survey Location: Choose the location or specific road segment where to measure CVPD.

C. Equipment and Personnel: Procure the essential equipment and personnel for the survey, including automatic traffic counters (ATC) or manual traffic counters, and when necessary, data collection personnel.

D. Data Collection Plan: Develop a data collection plan that includes the following:

a) Data Collection Period: Plan to collect data for 7 consecutive days to obtain a comprehensive view of traffic patterns.

b) Data Collection Times: Determine the specific times of day when data will be collected.

This could include multiple time blocks during the day.

c) **Data Collection Locations:** Identify the specific locations within the study area where data will be collected, and ensure these locations are representative of the entire area.

d) **Data Collection Method:** Specify the collection method whether it will be using automated counters or manual methods to collect data.

E. Data Collection: Execute the data collection plan, ensuring consistent and accurate data collection as per the specified schedule and locations. Ensure that data is recorded separately for each day

F. Data Analysis: After the 7-day data collection period, analyse the collected data to determine the CVPD. Calculate the combined volume of passenger vehicles (cars) and delivery vehicles (trucks, vans) for each day and calculate the daily average.

G. Report and Documentation: Compile the results of the analysis into a comprehensive report. This report should include:

- a) Daily and average CVPD values for each day of the survey.
- b) Any variations or trends observed over the 7-day period.
- c) A description of the study methodology, including data collection equipment and procedures.
- d) Any limitations or challenges encountered during the survey.

H. Recommendations and Interpretation: Provide recommendations or interpretations based on the CVPD data. This might include suggestions for road improvements, traffic management measures, or insights into the use of the surveyed area.

I. Follow-Up and Ongoing Monitoring: Consider whether ongoing monitoring is necessary to track changes in CVPD over time or assess the effectiveness of any recommended measures. Remember to follow any local regulations, standards, or guidelines for traffic surveys, and ensure the accuracy and reliability of your data collection methods to obtain meaningful results.

CVPD provides daily vehicle counts, which can be averaged over a year to calculate ADT, considering daily and seasonal variations. PCU standardizes the impact of different vehicle types on traffic flow, aiding in capacity analysis, traffic management, and road design by converting vehicle counts into PCU values to assess combined effects on road capacity and congestion, thus facilitating understanding and analysis of traffic patterns and road performance.

4.3.1.2 Axle Load Survey

An axle load test assesses road pavements and bridges' structural integrity and load-carrying capacity, aiding in maintenance decisions by applying controlled loads and measuring deflections and strains. A systematic survey determines the Vehicle Damage Factor (VDF) crucial in road design, ensuring both ease and safety in conducting representative samplings. The primary objective of this survey is to ascertain the Vehicle Damage Factor (VDF) by following IRC 37:2018. The Vehicle Damage Factor (VDF) is a critical coefficient in road design, estimating the damage diverse vehicles may inflict on pavements, and guiding the creation of durable surfaces capable of withstanding anticipated traffic loads.

The VDF plays a crucial role in converting data on commercial vehicles' axle configurations and loads into standard axle load repetitions, with surveys conducted meticulously over 24 hours. Special attention is given to vehicles over 3 tons, recognizing their inherent stress on road surfaces, essential to assess how vehicle loads may impact pavement wear or damage in order to plan maintenance and construction. To calculate the VDF in an axle load survey, these steps need to be followed-

i. Gather Data: Collect data on actual axle loadings of vehicles. This data is usually obtained through field surveys to measure and record the weights of various types of vehicles using weigh-in-motion (WIM) systems, portable scales, or other data collection methods.

ii. Determine Vehicle Classifications: Categorize the vehicles into appropriate classes based on their characteristics, such as the number of axles and axle spacings. Common vehicle classes may include passenger cars, single-unit trucks, and multi-unit trucks.

iii. Calculate Equivalent Single-Axle Loads (ESALs):

For each vehicle class, calculate the Equivalent Single-Axle Load (ESAL) using the formula:

$$\text{ESAL} = (\text{Load on Axle}) * (\text{VDF for the Vehicle Class})$$

The load on the axle is typically measured in kilonewtons (kN) or pounds-force (lbf).

iv. Calculate VDF:

Calculate the VDF for each vehicle class by dividing the ESAL by the actual load on the axle:

$$\text{VDF} = \text{ESAL} / (\text{Load on Axle})$$

v. Aggregate VDF Values:

In case of multiple vehicle classes, to aggregate the VDF values to calculate an overall VDF for the entire survey. This is done by taking a weighted average of the VDF values for each vehicle class, with the weights based on the proportion of each class in the total traffic.

vi. Quality Control:

Ensure the accuracy of your data and calculations. Check for any outliers or errors in the data and address them to ensure the reliability of your VDF estimates.

vii. Documentation:

Document the methodology and assumptions used in calculations, including the source of the data, the formulas, and any specific criteria for classifying vehicles. This material is crucial for transparency and future reference. It is noteworthy that the VDF values are subject to variation based on the specific road type, survey site, and vehicle characteristics in the area. Therefore, it is essential to tailor calculations to the specific conditions and requirements of the study. Additionally, consulting relevant transportation engineering standards and guidelines can provide further guidance on calculating VDF in axle load surveys for pavement analysis and design.

4.3.2 Dynamic Cone Penetration Test (DCPT)

The Dynamic Cone Penetrometer (DCP) facilitates rapid in-situ assessment of subgrade strength crucial for evaluating its capacity to support pavement loads in road construction.

The central thrust of this investigation encompasses two primary objectives:

- i. Thoroughly scrutinizing the engineering attributes of the subgrade soil through the utilization of the DCPT methodology.
- ii. Conducting a comparative analysis between the results obtained from the DCPT and the laboratory-calculated CBR values.

The current study utilizes DCPT to assess subgrade strength, measuring in-situ CBR by applying a standard weight to drive a cone into the ground, presenting dynamic cone resistance, a strength index derived from the instrumented DCP, and comparing it with laboratory testing for both types of pavements. Scala developed the Scala Penetrometer in Australia in 1956, which prompted the development of the Dynamic Cone Penetrometer (DCP) for subgrade soil testing. This device, similar to the current DCP, featured a 9 kg hammer dropping from 510 mm to apply force onto a cone. Later, van Vuuren (1969) developed a comparable tool with a 10 kg hammer dropping from 460 mm, establishing a correlation between DCP results and CBR values. Using a DCP with an 8 kg hammer and a 574 mm drop height, the Transvaal Roads Department in South Africa compared cones with apex angles of 30° and 60° in 1973 (Kleyn 1975). Further studies by Kleyn and Savage (1982) involved similar configurations for subgrade testing. The methodology and data analysis for DCPT may be divided into four parts and are described below-

4.3.2.1 Setup of Dynamic Cone Penetrometer (DCP)

The DCP is an instrument specifically engineered for the swift, in-situ assessment of subgrade properties. Fig.4.1 illustrates the standard configuration of the DCP. Upper and lower shafts make up the DCP in this arrangement. The lower shaft is attached to the upper shaft by an anvil, which holds an 8 kilogram drop hammer with a 575 mm drop height. The lower shaft

has a cone with a 60-degree angle and an anvil fastened at the end of it. An additional rod, marked in millimetres, is attached to the lower shaft to serve as a measurement device. Two people are usually needed to run the DCPT. While one operator takes measurements, the other releases the hammer. The cone tip is first placed on the test surface to start the test. While the reading rod remains stationary on the test surface the entire time, the lower shaft with the cone moves on its own. Since the ground surface is loose and disturbed, and because the testing equipment weighs a lot, the initial reading is usually not zero. The value of this initial reading is regarded as the initial penetration, which corresponds to below zero.

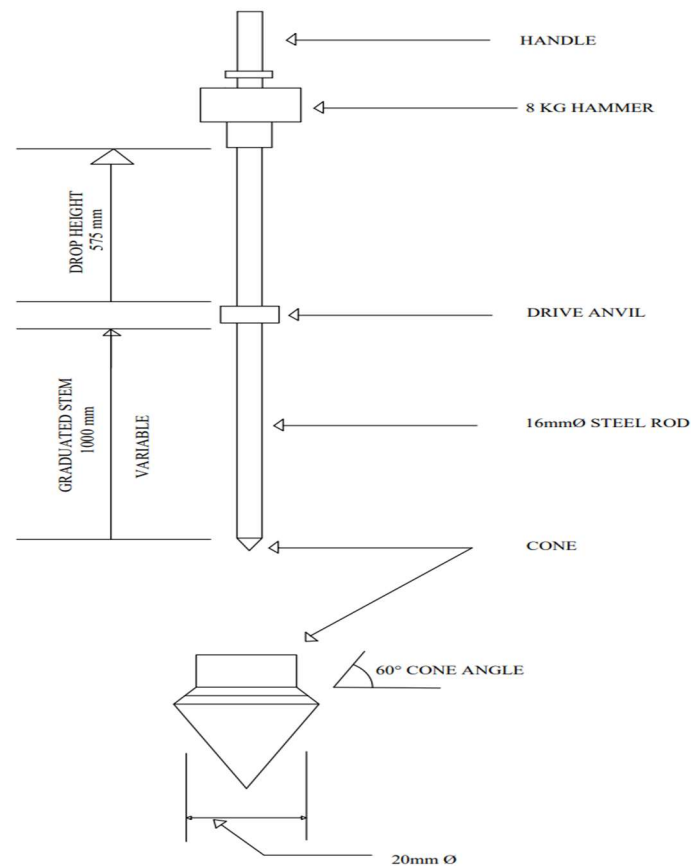


Fig. 4.1: Schematic diagram of the DCPT instrument

4.3.2.2 DCPT mechanism

For the operation of the DCPT, two people are usually necessary. While the other takes measurements, one operator lets go of the hammer. The cone tip is first placed on the test surface to start the test. While the reading rod remains stationary on the test surface the entire

time, the lower shaft with the cone moves on its own. Due to the weight of the testing apparatus and the loose, disturbed nature of the ground surface, the initial reading is usually not zero. As it corresponds to below zero, the value of this initial reading is regarded as the initial penetration. The penetration result after the initial hammer drop is shown in Fig. 4.2. Hammer blows are applied repeatedly, and following each blow, the penetration depth is measured. Until the desired penetration depth has been achieved, this process is repeated.

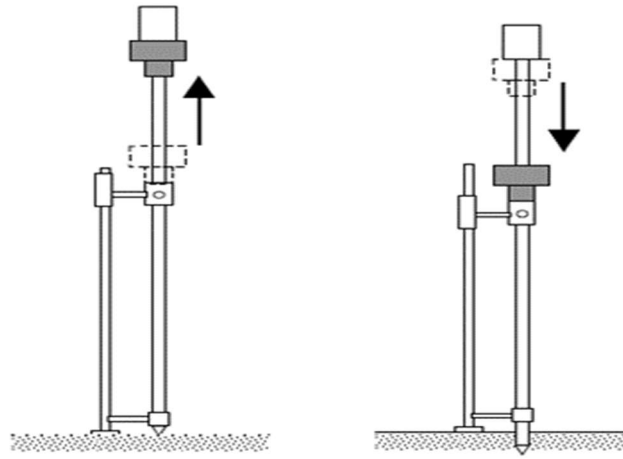


Fig. 4.2: DCP test before and after hammer drooping effect

4.3.2.3 Preparation of DCPT outcome data

The depth of penetration is measured after each impact, expressed as millimeters per blow (mm/blow). The DCPT offers rapid subgrade strength evaluation and generates significant data in a short time; however, it may not provide laboratory-soaked CBR values, as it correlates penetration depth to blow counts. Since the recorded blow counts are cumulative values, outcomes of DCPT are reported as incremental values defined as:

$$PI = \frac{\Delta D_p}{\Delta BC} \dots \dots \dots (4.1)$$

Where, **PI** = DCP penetration index in units of length divided by blow count;

ΔD_p = penetration depth;

BC = blow counts corresponding to penetration depth ΔD_p .

As a result, values of the penetration index (PI) represent DCPT characteristics at certain depths. Fig. 4.3 shows a typical DCPT results.

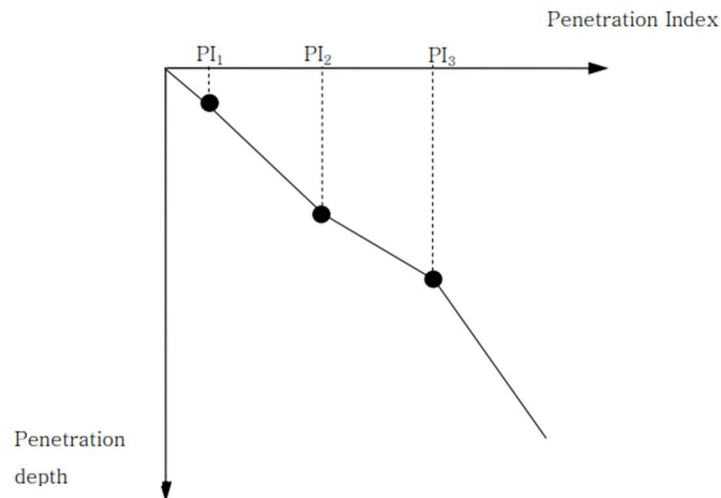


Fig. 4.3: Typical DCP test result

4.3.2.4 Relationship between Penetration Index (PI) and CBR Values

Several authors have delved into the relationships between CBR and the DCP penetration index PI. CBR values are frequently applied to pavement and road design. For the PI and CBR correlation, two different kinds of equations have been taken into consideration. Those are the inverse and log-log equations. The following general forms can be used to represent the log-log and inverse equations for the relationship:

log-log equation: $\log CBR = A - B(\log(PI))^C$ (4.2)

inverse equation: $CBR = D(PI)^E + F(2.3)$ (4.3)

where CBR = California Bearing Ratio; PI = penetration index obtained from DCPT in units of mm/blow or in/blow; A, B, C, D, E, and F = regression constants for the relationships.

According to Harison's (1987) statistical research, the inverse equation was shown to be inadequate and error-prone, while the log-log equation is more reliable for correlating DCP Penetration Index (PI) with CBR. Several coefficients (A, B, and C) for the log-log equation were provided by later researchers, notably Livneh in 1987 and 1989. These proposals were

based on their findings from the laboratory and field, and they further refine the equation for use in pavement assessment and design.

$$\log CBR = 20.2 - 71.0 \log(PI) \dots \dots \dots (4.4)$$

$$\log CBR = 14.2 - 69.0 \log(PI) \dots \dots \dots (4.5)$$

where CBR = California Bearing Ratio; PI = DCP Penetration Index. Although eqn. (4.4) was suggested based on eqn. (4.3), differences in results from eqn. (4.3) and eqn. (4.4) are small.

Following a further examination of data by various writers, Livneh et al. (1994) suggested the following equation as the optimal correlation:

$$\log CBR = 46.2 - 12.1 \log(PI) \dots \dots \dots (4.6)$$

Typical log-log equations for the CBR-PI correlation proposed by various authors are summarized in Table 4.2. The penetration for each blow has been noted down in the field data sheet and after that, the field CBR from the DCPT test has been calculated using the correlation between CBR and PI (Penetration Index), the correlation has been given in Table 4.2.

Table 4.2: Correlations between CBR and PI (After Harison 1987 and Gabr et al. 2000)

Author	Correlation	Field or Laboratory Based Study	Material Tested
Kleyn (1975)	$\log CBR = 2.62 - 1.27 \log(PI)$	Laboratory	Unknown
Harison (1987)	$\log CBR = 2.56 - 1.16 \log(PI)$	Laboratory	Cohesive
Harison (1987)	$\log CBR = 3.03 - 1.54 \log(PI)$	Laboratory	Granular
Livneh et. al. (1994)	$\log CBR = 2.46 - 1.12 \log(PI)$	Field and Laboratory	Granular and Cohesive
Ese et. al. (1994)	$\log CBR = 2.44 - 1.07 \log(PI)$	Field and Laboratory	Aggregate base course (ABC)
NCDOT (1998)	$\log CBR = 2.60 - 1.07 \log(PI)$	Field and Laboratory	ABC and Cohesive
Coonse (1999)	$\log CBR = 2.53 - 1.14 \log(PI)$	Laboratory	Piedmont residual soil
Gabr (2000)	$\log CBR = 1.40 - 0.55 \log(PI)$	Field and Laboratory	Aggregate base course (ABC)

The correlation for cohesive soil has been used to convert the DCPT into CBR. For the existing subgrade soil is appraised as cohesive soil by visual means, the correlation by Harrison formula has been used for the present purpose. Though, CBR has been calculated by formulas given by Klern (1975) and Livneh et al (1994) also to compare the CBR values which have been obtained by Harrison's (1987) formula. The summarized co-relation table has been illustrated in Table 4.3.

Table 4.3: Correlations between CBR and PI

Author	Correlation	Field or Laboratory Based Study	Material Tested
Kleyn (1975)	$\log CBR = 2.62 - 1.27 \log(PI)$	Laboratory	Unknown
Harison (1987)	$\log CBR = 2.56 - 1.16 \log(PI)$	Laboratory	Cohesive
Livneh et. al. (1994)	$\log CBR = 2.46 - 1.12 \log(PI)$	Field and Laboratory	Granular and Cohesive

4.3.3 Falling Weight Deflectometer (FWD) Test

Assessing flexible pavement performance involves subjecting them to traffic-like loads, measuring elastic deflection, and conducting data analysis considering factors like subgrade strength, layer thickness, and drainage conditions.

The Falling Weight Deflectometer (FWD) closely replicates real-world loading conditions, generating load pulses as a moving wheel load traverses the pavement. Utilizing the energy potential of a raised weight, the FWD applies load pulses to the pavement surface, simulating vehicle wheel loads, with data collected from sensors for post-test analysis of pavement properties.

According to Walubita et al. and Solanki et al., The FWD is a key Non-Destructive Testing (NDT) equipment for evaluating pavement strength, capable of calculating the elastic modulus of individual layers. In the current study, the primary objective is to conduct a comparative analysis between the subgrade deflection and elastic modulus of existing pavement and

modified pavement. For conducting the FWD survey, a loading force within the range of 0-100 kN is utilized. This range allows the FWD to effectively simulate various types of vehicles loads on the pavement surface. In FWD study, the setup includes deflection sensors or geophones which are strategically placed at specific distances from the center of the loading plate. According to IRC 115:2014, the distances are - 0 mm (D0), 300 mm (D1), 600 mm (D2), 900 mm (D3), 1200 mm (D4), 1500 mm (D5), and 1800 mm (D6). These sensors have been used to measure the surface deflection resulting from dropped weights such as 40kN (0.56 MPa contact stress) over a contact area of diameter 300 mm. The loading time of the FWD typically ranges between 25 to 30 milliseconds. A typical FWD Schematic representation has been illustrated in Fig.4.4.

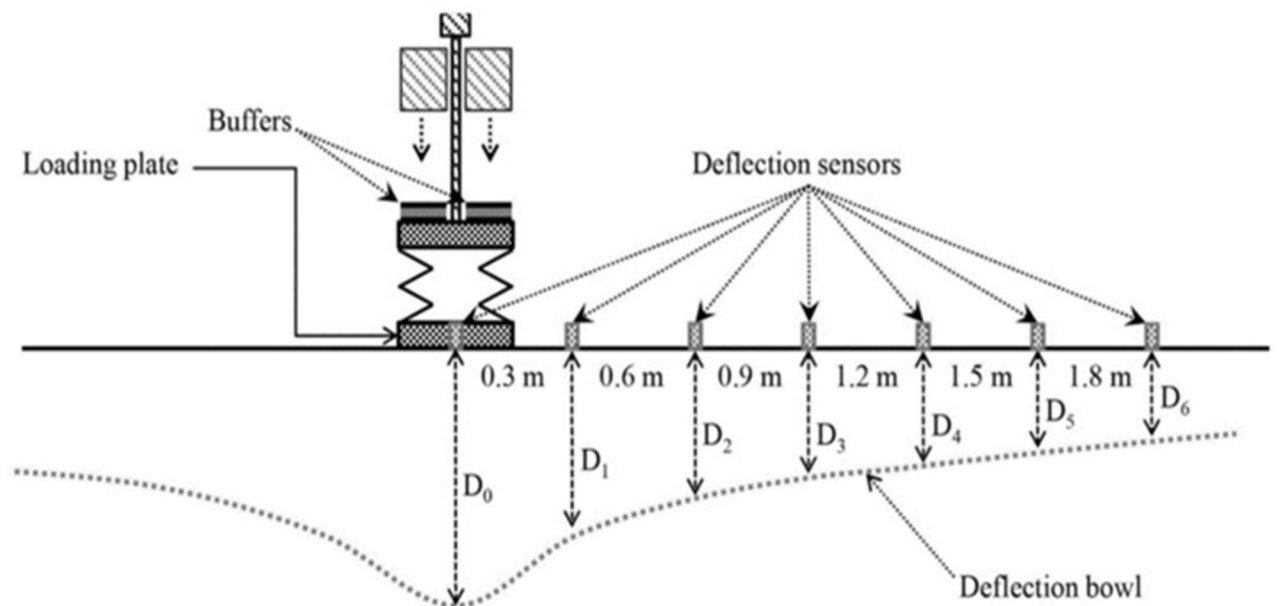


Fig. 4.4: Typical representation of FWD operation.

The FWD is used to impart a dynamic load to the existing pavement, and the response is recorded. The acquired deflection values are then used in the KGPBACK program to calculate the elastic moduli of the modelled pavement layers, in accordance with IRC: 115-2014. Figure 4.5 illustrates that the deflection bowl observed beneath a loaded wheel can be technically divided into three distinct regions.

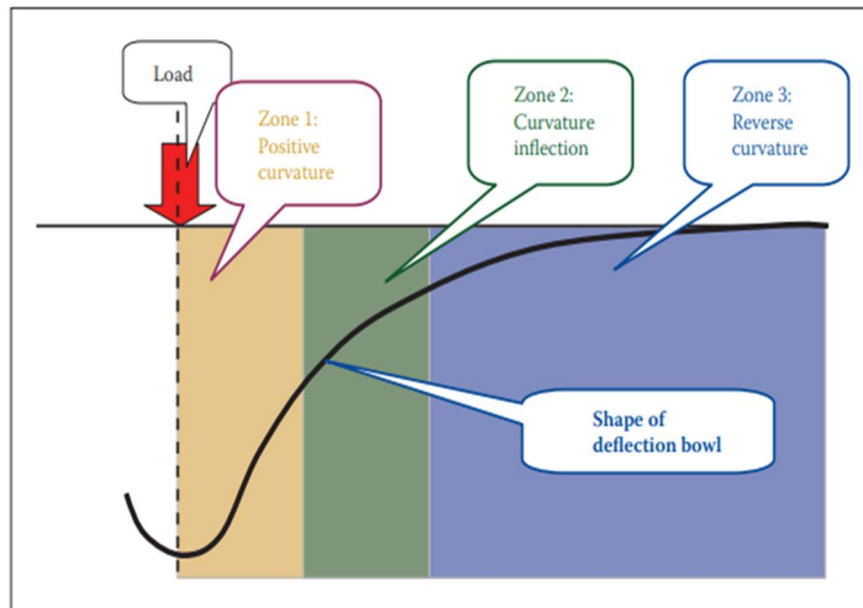


Fig. 4.5: Curvature zones of a deflection bowl (After Horak,2008)

Zone 1, the deflection bowl that is nearest to the loading point, has a positive curvature with a radius of around 300 mm. Zone 2, or the transitional area, extends between 300 and 600 mm from the loading point and indicates the change from positive to reverse curvature. The location of the inflection point depends on the composition of the pavement layer. Zone 3, which is the furthest away from the loading area and reaches the road surface, has a reverse curvature. spanning approximately 600 mm to 18000 mm, with dimensions influenced by pavement depth and subgrade response. The performance mechanism for FWD is described below-

4.3.3.1 FWD deflection testing points & measurement:

At each measurement point, four drops have been executed: the first is the 'seating drop,' while the remaining three record deflections. The bituminous layer's pavement temperature has been also logged following IRC: 115-2014, Section 5.4.7. The steps for measuring deflections at a test point are as follows:

- i. Mark the test point on the pavement.

- ii. Center the load plate over it.
- iii. With adequate contact and no surface water, lower the loading plate onto the pavement.
There can be no more than a 10% slope.
- iv. Lower the geophone frame to touch the pavement surface.
- v. Raise the mass to reach a 40 kN target load (+10%).
- vi. Execute one seating load drop without recording data.
- vii. Using the data collecting system, raise and lower the mass while recording load and deflection data. At different radial points, note the peak load and deflections. For accuracy, make sure there are at least two drops in each spot.
- viii. If deflections vary or deflection/load pulses are improper in the previous steps, repeat the drop.
- ix. Proceed to the next test site after raising the load plate and geophone frame.
- x. When the pavement temperature exceeds 45°C, no deflection measurements should be taken.

4.3.3.2 Analysis of data

The FWD applies a dynamic load to the pavement, and its response is measured, with deflection values used in KGPBACK software to calculate elastic moduli of modelled pavement layers as per IRC: 115-2014. The KGPBACK program, a version of BACKGA, is utilized for back-analysis, relying on FWD deflection measurements to assess in-service pavement structural condition by determining in situ elastic moduli. Here is a technical modification and brief explanation of how KGPBACK works:

i. Objective: KGPBACK is designed to determine the in situ elastic moduli of individual pavement layers by iteratively adjusting the assumed moduli values until the calculated deflection values closely match the observed deflections.

ii. Input Data:

- **Measured Surface Deflections:** Data obtained from FWD testing.

- **Tyre Contact Pressure:** The pressure applied by the FWD's tyres on the pavement.
- **Geophone Positions:** Locations of the geophones used to measure deflections.
- **Poisson's Ratio:** A material property related to the pavement's deformation behaviour.
- **Range of Moduli for Each Layer:** Assumed elastic moduli values for each pavement layer.

iii. Process:

- Start with an initial set of assumed elastic moduli values for each layer.
- Calculate deflection values based on these assumed moduli values.
- Compare and analyse the computed and observed deflection values.
- For the subsequent iteration, adjust the estimated elastic moduli values.
- Until the calculated and observed deflection values converge to a smaller difference, continue through this iterative process.

iv. Iteration: The software iterates through these processes until the discrepancy between the calculated and observed deflection values becomes much lower, suggesting that the assumed moduli values have been improved to closely reflect the real pavement attributes.

v. Output: The results of the analysis are the in situ elastic moduli values for each pavement layer, which represent the actual properties of the layers, as closely as possible, based on the observed deflections and input parameters.

The iterative back-calculation process depicted in Figure 4.6 refines the initial assumptions to provide a more accurate representation of the elastic properties of pavement. This is a crucial tool in pavement engineering for assessing the structural integrity of roads and making informed decisions regarding maintenance and rehabilitation.

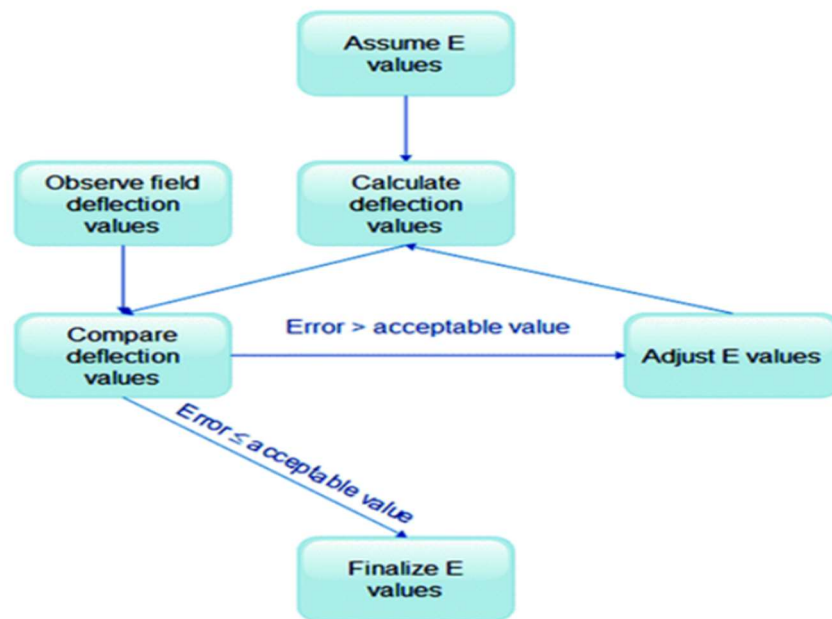


Fig. 4.6: Back calculation process (After Singh et al.,2019)

Temperature and seasonal corrections are necessary after KGPBACK calculation to account for the variations in pavement material properties caused by temperature changes and seasonal effects. These corrections are important for the following reasons:

- i. **Temperature-Related Changes:** Pavement materials, including asphalt and subgrade soils, exhibit different mechanical properties at varying temperatures. As temperature fluctuates, the stiffness and modulus of the materials change. This means that the back-calculated pavement layer moduli obtained using KGP methods may not accurately reflect the actual material properties if temperature effects are not considered.
- ii. **Seasonal Effects:** Seasonal changes can lead to variations in environmental conditions, such as moisture content and frost susceptibility of the subgrade. These fluctuations can affect the structural behaviour of the pavement. To obtain a more accurate representation of the pavement's structural condition, it is essential to account for seasonal variations.
- iii. **Accurate Performance Prediction:** Correcting for temperature and seasonal effects ensures that the back-calculated pavement layer properties align with the conditions

the pavement experiences throughout the year. This accuracy is crucial for making informed decisions regarding maintenance, rehabilitation, or design modifications to enhance pavement performance.

- iv. Long-Term Structural Integrity: Neglecting temperature and seasonal corrections can lead to incorrect assessments of pavement structural integrity. This, in turn, can result in suboptimal maintenance strategies and may reduce the overall service life of the pavement.

In summary, temperature and seasonal corrections are required after KGPBACK calculation to improve the accuracy of pavement layer moduli and to account for real-world variations in temperature and seasonal conditions, which can significantly impact pavement performance and longevity.

i. Correction for Temperature

The temperature of the pavement affects the back-calculated moduli values of the bituminous layers assessed by the FWD survey. The standard pavement temperature for India is recommended as 35°C, so the back-calculated moduli obtained at temperatures other than the identified standard temperature will have to be corrected using a suitable correction factor using equations 4 and 5 of IRC:115-2014, and the same is extracted below for easy reference.

$$E_{T1} = \lambda E_{T2} \dots\dots\dots (4.7)$$

Where, λ , temperature correction factor, is given as

$$\lambda = (1 - 0.238 \ln T_1) / (1 - 0.238 \ln T_2) \dots\dots\dots (4.8)$$

Where, E_{T1} = Back-calculated modulus (MPa) at temperature T_1 (°C) E_{T2} = Back-calculated modulus (MPa) at temperature T_2 (°C)

ii. Correction for Seasonal Variation

The strength of the subgrade and granular subbase/base layers is dependent on the moisture content. The type of subgrade soil, the gradation and makeup of the fines in the granular layers, and other factors will determine how much the strength is impacted. The pavement layer

moduli values are supposed to correspond to the time when the subgrade is at its weakest when following these criteria. This time frame falls within India's monsoon recession. Therefore, it is preferable to monitor deflections during this time. If doing the same is not practical, a correctional process ought to be used. Equations 6 and 7 of IRC:115-2014 can be used to estimate the modulus value of a subgrade layer based on modulus values back-calculated from deflections measured in the winter and summer, respectively. In a similar manner, the modulus value of the granular layer can be estimated using Equations 8 and 9 of IRC:115-2014, which derive the modulus value from deflections measured in the winter and summer, respectively.

$$E_{sub_mon} = 3.351 * (E_{sub_win})^{0.7688} - 28.9 \dots\dots\dots (4.9)$$

$$E_{sub_mon} = 0.8554 * (E_{sub_sum}) - 8.461 \dots\dots\dots (4.10)$$

Where, E_{sub_mon} = Subgrade modulus in monsoon (MPa)

E_{sub_win} = Subgrade modulus in winter (MPa)

E_{sub_sum} = Subgrade modulus in summer (MPa)

$$E_{gran_mon} = -0.0003 * (E_{gran_sum})^2 + 0.9584 * (E_{gran_sum}) - 32.989 \dots\dots\dots (4.11)$$

$$E_{gran_mon} = 10.5523 * (E_{gran_win})^{0.624} - 113.857 \dots\dots\dots (4.12)$$

Where, E_{gran_mon} = Granular layer modulus in monsoon (MPa)

E_{gran_win} = Granular layer modulus in winter (MPa)

E_{gran_sum} = Granular layer modulus in summer (MPa)

4.4 NUMERICAL WORK

In the current research, two distinct numerical components were developed. The first part involves pavement design utilizing IITPAVE, a software specifically tailored for pavement design based on Indian conditions. This approach focuses on creating a structural design for pavements, considering factors such as traffic load, material properties, and environmental conditions.

The second numerical component is centred around pavement deflection analysis using PLAXIS 3D. This segment of the study leverages the capabilities of PLAXIS 3D for finite element analysis, providing insights into how pavements respond to loads typically measured by a FWD. This analysis helps in understanding the deformation and stress distribution within the pavement structure under various loading conditions, which is crucial for assessing pavement durability and service life. Together, these two parts offer a comprehensive approach to pavement analysis, combining structural design with detailed deflection and stress analysis.

4.4.1 Pavement Design and Analysis by IIT PAVE Software

In the present study, the pavement thickness for both suggested subgrades—original soil and soil mixed with tyre scraps has been calculated sequentially using the IIT PAVE software. MoRTH Research Scheme R-56 "Analytical design of Flexible Pavement" funded the development of the Indian Institute of Technology Kharagpur's IIT PAVE program, which is an improved version of FPAVE. It is utilized in pavement research, particularly in the analysis of flexible pavements. This program is essential for planning and researching flexible pavements in the field of transportation engineering. The FEM is used by the IIT PAVE project to evaluate how flexible pavements react to different loads. The program provides a thorough examination of pavement behavior, taking into account variables including traffic volumes, meteorological conditions, and material quality. By simulating different loading scenarios, the software may provide stress and strain data at crucial places in the pavement structure, allowing for an examination of the pavement's performance over time. The IITPAVE program's intuitive interface makes data entry, structural adjustments, and outcome visualization easier. By providing a more accurate and timely method for pavement design and analysis, IITPAVE software has played a major role in the field of pavement engineering. IITPAVE, a multi-layer analysis program, is used to analyze flexible pavement and locate critical pavement locations where stresses and strains are present. To design a flexible

pavement, the thickness of each layer needs to be determined based on the strength characteristics of the pavement materials. This can be done by using the CBR value as well as traffic data, and by using IITPAVE software which computes the actual value of strains coming on the pavement due to wheel load. This software requires the input of pavement layer thickness, applied loads on the pavement surface, tyre pressure, wheel spacing, and Poisson's ratio. Upon running the software, it generates output data, specifically the actual horizontal tensile strain and vertical compressive strains at critical pavement locations. The software computes many functional parameters, including stresses, strains, and deflections, assuming that the pavement is a linear elastic layered system. The software can be used to calculate the strains and stress parameters required to check for sub-grade rutting and fatigue cracking of bituminous layers. These strains are vertical compressive strain and horizontal tensile strain. Overall, the design process involves using the IITPAVE software to determine the thickness of component layers. The procedure is based on the strength characteristics of the pavement materials, as specified by IRC 37 :2018.

4.4.2 Finite Element Analysis by PLAXIS 3D

In the current study, FE analysis using PLAXIS 3D (Version 20) is employed to establish a correlation between FWD deflections and PLAXIS-derived deflections. Technical brief on the methodology is illustrated below-

4.4.2.1 Model Setup in PLAXIS 3D:

The steps for model set up are as follows:

- i. Geometry Creation: The first step involves creating a three-dimensional model of the pavement structure, including layers representing the subgrade, base, and surface layers.
- ii. Material Properties: Assign appropriate material properties (like elasticity, Poisson's ratio, and density) to each layer based on laboratory tests or standard values.

- iii. Boundary Conditions: Set boundary conditions to replicate the actual field conditions.

This often includes specifying the base and lateral boundaries to simulate the infinite extent of the ground.

4.4.2.2 Loading Conditions:

Steps for loading condition include:

- i. FWD Simulation: Implement a loading mechanism in PLAXIS 3D to mimic the FWD test. This involves applying a transient dynamic load. Magnitude and duration is similar to that of the FWD.
- ii. Mesh Refinement Around Load: Ensure the mesh is sufficiently refined around the load application area to capture detailed responses.

4.4.2.3 Analysis and Calculation:

Steps are as follows:

- i. Conduct a FE analysis to calculate the deflection of each pavement layer under the simulated FWD load.
- ii. The analysis should capture the vertical displacement of the Pavement's surface, which corresponds to the deflection measured by FWD in the field.

4.4.2.4 Correlation with FWD Data:

- i. Compare the PLAXIS 3D model's deflection results with actual FWD deflection data collected from the field.
- ii. Use statistical or analytical methods to establish a correlation between the two sets of data. This may involve regression analysis or other statistical tools to understand the relationship and validate the model.

4.4.2.5 Interpretation and Validation:

- i. Interpret the results to understand the pavement behaviour under load.
- ii. Validate the PLAXIS model by ensuring the correlation with FWD data is within acceptable limits of accuracy.

4.4.2.6 Adjustments and Iterations:

i. If necessary, adjust the model parameters based on the correlation results and rerun the analysis for improved accuracy.

This approach provides a detailed understanding of the pavement's structural behaviour and aids in validating finite element models using real-world data, thus enhancing the reliability of pavement design and analysis.

4.5 FLOWCHART OF THE STEPS:

Figure 4.7 depicts the successive stages taken in the investigation in a flowchart manner. Each node in the flowchart likely symbolizes a unique activity or decision point, visually illustrating the procedure used throughout the research study. The flowchart aids in understanding the methodology and sequence of the analysis's procedures.

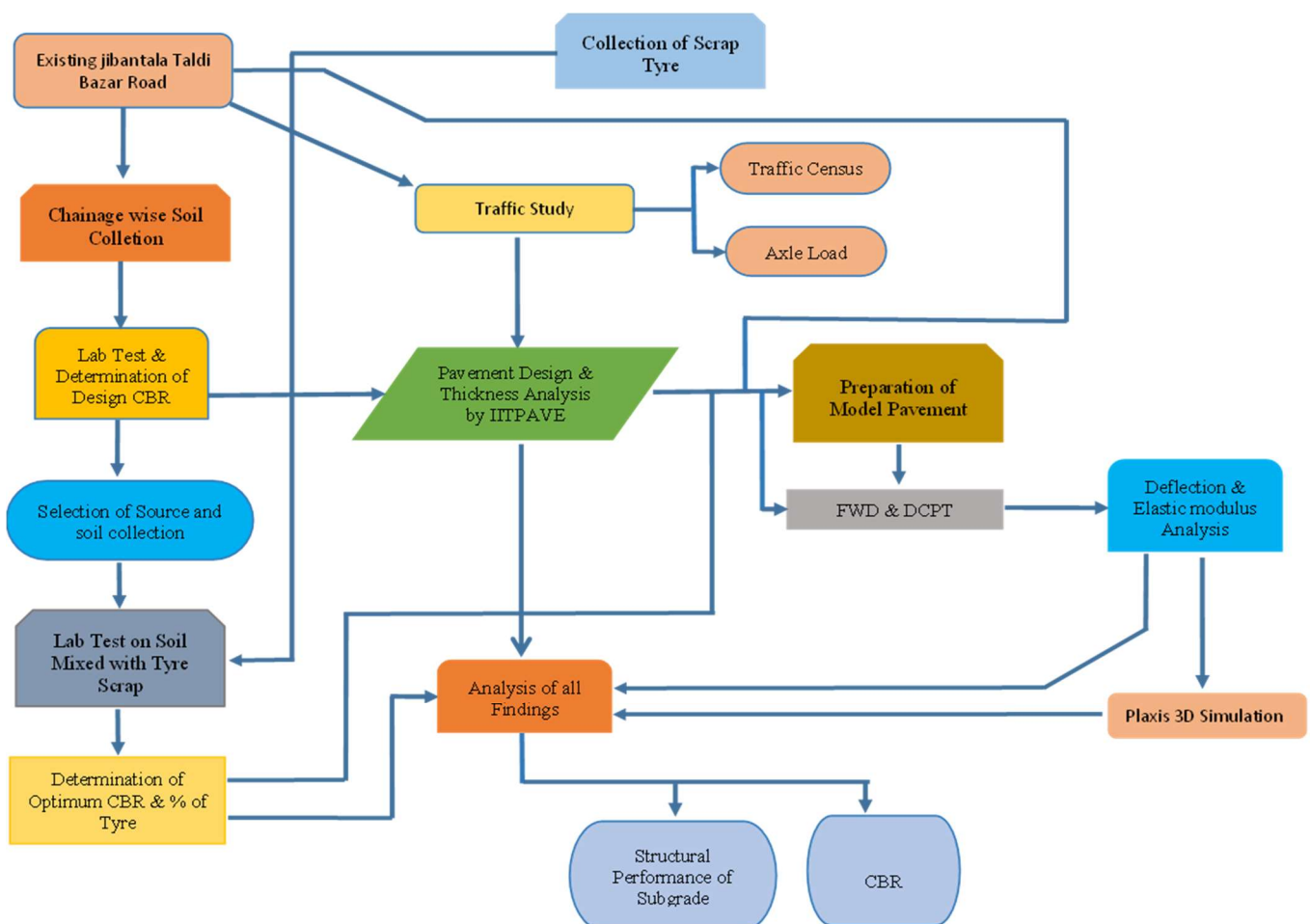


Fig. 4.7 : Flowchart of steps

4.6 SUMMARY:

This chapter has presented the methodology employed in the investigation, encompassing both laboratory and field studies. An overview of the tests conducted on the existing subgrade soil and tyre scrap materials, including grain size analysis, Atterberg limits, and California Bearing Ratio (CBR) testing has been outlined. Furthermore, the preparation of soil-tyre mixtures and the procedures for dynamic cone penetration and falling weight deflectometer tests has been described. Finally, numerical modelling using IIT PAVE and PLAXIS 3D is also outlined, providing a comprehensive framework for analyzing pavement performance. The methodologies are systematically presented to ensure the reproducibility and reliability of the research findings.

CHAPTER 5 LABORATORY TESTS

5.1 OVERVIEW

The laboratory tests for the current investigation have been performed in two stages. The original soil has been tested in the first phase, followed by soil mixed with shredded tyre scrap in the second. To examine the original soil, samples have been collected at every Km chainage along the Jibantala-Taldi Road, which has a length of 12.45 Km as shown in Fig.5.1

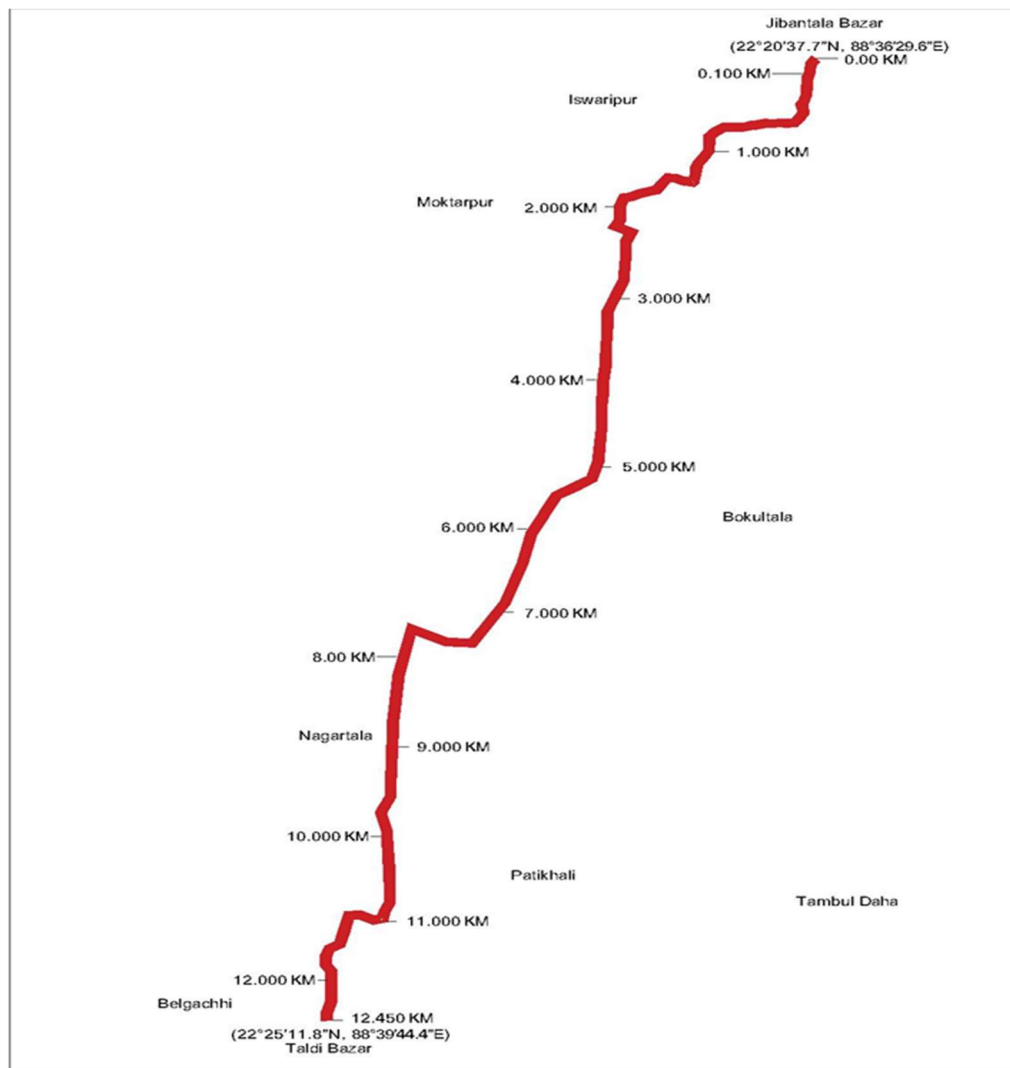


Fig. 5.1: Sample collection chainages on the road

The samples have been collected from locations adjacent to the road, at a depth of 1.0 m below the Existing Ground Level (EGL). Soil samples have been collected from 1.0 m below the existing ground level (EGL) for California Bearing Ratio (CBR) and other relevant tests, as

the existing road subgrade is located at this depth. According to IRC 37:2018, the subgrade bottom must maintain a minimum clearance of 1.0 m (or 0.6 m for roads with no history of overtopping) from the water table or high flood level. In this case, the water table is approximately 2.0 m below the existing road level. Hence, the subgrade depth of the existing road also complies with IRC specifications. Soil sample collection has been illustrated through Fig. 5.2.



Fig. 5.2: Soil sample collection from Jibantala-Taldi Road

5.2 TEST PROGRAM FOR SOIL

The laboratory tests for the current investigation have been performed in two stages. The original soil has been tested in the first phase, followed by soil mixed with shredded tyre scrap in the second. To examine the original soil, samples have been collected at every Km along the Jibantala-Taldi Road, which has a length of 12.45 Km. The samples have been collected from locations adjacent to the road, at 1.0 m below the EGL. The test program for soil sample has been outlined in Table 5.1.

Table 5.1: Test program for soil

Sl. No.	Tests	Number of tests
1	Grain Size Distribution	14
2	Atterberg Limits	Liquid Limit
		Plastic Limit
3	Water Content	03
4	Unconsolidated Undrained (UU) Test	03
5	Specific Gravity	14
6	Modified Proctor Compaction Test (OMC, MDD)	14
7	CBR Test	14

5.3 TEST PROGRAMME FOR SCRAP TYRE MIX SOIL

Table 5.2, shows the details of test program for soil mixed with shredded tyre scrap. For the present study, various sizes of scrap tyres (10mm x 10mm, 15mm x 15mm, 20mm x 20mm, 25mm x 25mm and 30mm x 30mm) have been utilized. One of the sample tyre scraps of size 15mm X 15mm is depicted in Fig. 5.3.

Table 5.2: Test program for tyre scrap mix soil

Sl.No.	Tests	Number of tests
1	Modified proctor compaction test (OMC, MDD)	30
2	CBR at OMC (Unsoaked and soaked)	30

**Fig. 5.3:** Sample tyre scrap of size 15mm X 15mm

5.4 LABORATORY TEST RESULTS

In order to fulfill the objectives of the study, all the tests listed in Table 5.1 have been conducted, and the outcomes obtained are displayed individually for both the original soil and the soil mixed with tyre scrap.

5.4.1 Test Results for Original Soil

The original soil samples are collected from the Jibantala-Taldi Road surroundings and brought to the Soil Mechanics Laboratory of Jadavpur University, Kolkata, West Bengal, India, for further analysis. The samples have been subjected to an initial process of oven drying and sieving using a 2.36 mm IS sieve. Following this, the soil specimens have undergone a drying process in an oven set at 105°C for 24 hours to ensure thorough desiccation. Sample photographs of Laboratory tests have been depicted in Fig. 5.4.



(A)



(B)

Fig. 5.4(A) and (B): Laboratory sample preparation and data collection.

Grain Size Analysis has been conducted to ascertain the particle size distribution within the soil samples. Additionally, Liquid Limit (LL) and Plastic Limit (PL) tests have been carried out to evaluate the plasticity characteristics. Shear strength properties of the soil have been determined through Unconsolidated Undrained (UU) tests. The compaction characteristics of the soil have been reassessed using the Modified Proctor Test, which involved compacting the

soil at various moisture contents to determine the MDD. Furthermore, CBR tests have been conducted on the collected samples to measure the load-bearing capacity and mechanical strength of the road subgrade. The results of these laboratory tests for the normal soil at the specified road chainage has been illustrated in Table 5.3. Particle size distribution curves of the original soil has been shown in Fig. 5.5.

Table 5.3: Laboratory test results on road soil with respect to chainage

Chainage (in Km)	Description of soil	Modified proctor		Atterberg Limits			Grain size analysis (%)			Laboratory CBR value (%)	
		MDD (g/cc)	OMC (%)	LL (%)	PL (%)	PI (%)	Sand	Silt	Clay	Soaked	Unsoaked
0.100	Grey clayey silt	1.760	15.18	45.70	21.80	23.90	12	61	27	3.80	5.27
1.000	Grey silty clay/clayey silt	1.751	15.25	46.80	21.30	25.50	10	60	30	3.75	4.98
2.000	Brownish grey silty clay	1.741	16.80	48.50	21.28	27.22	7	60	33	3.62	4.96
3.000	Grey silty clay	1.724	17.06	50.20	21.20	29.00	4	62	34	3.39	4.60
4.000	Grey silty clay	1.720	17.42	51.20	20.26	30.94	4	61	35	3.15	4.15
5.000	Grey silty clay	1.710	18.14	53.90	20.10	33.80	2	62	36	3.05	4.01
6.000	Brownish grey silty clay	1.730	16.50	48.60	21.30	27.30	6	61	33	3.30	4.45
7.000	Grey silty clay/clayey silt	1.728	17.12	46.70	21.90	24.80	7	62	31	3.45	4.65
8.000	Brownish grey clayey silt	1.750	15.60	45.60	21.20	24.40	10	64	26	3.75	5.09
9.000	Grey silty clay	1.740	15.86	47.20	22.60	24.60	6	67	27	3.57	4.90
10.000	Brownish grey silty clay	1.740	16.20	47.50	21.30	26.20	5	69	26	3.55	4.89
11.000	Grey silty clay	1.730	17.16	48.70	22.40	26.30	5	64	31	3.41	4.47
12.000	Grey silty clay	1.730	16.90	50.20	22.00	28.20	6	61	33	3.28	4.55
12.450	Greyish brown silty clay	1.730	17.05	47.70	22.40	25.30	8	62	30	3.40	4.59

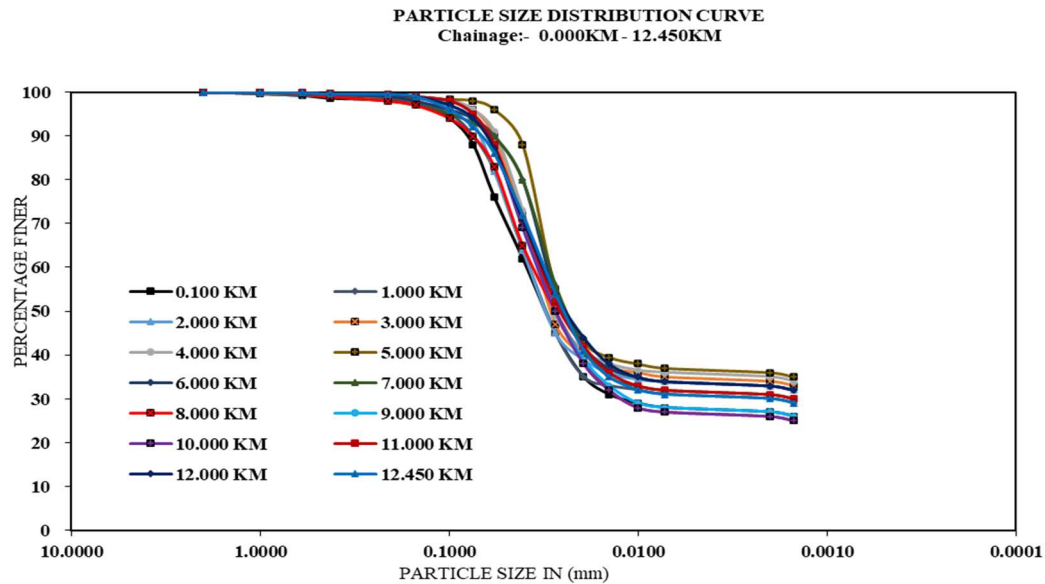


Fig. 5.5: Particle size distribution curve

The compaction curves for the road subgrade soil are depicted in Fig. 5.6, while Fig. 5.7 to 5.10 illustrate the CBR curves.

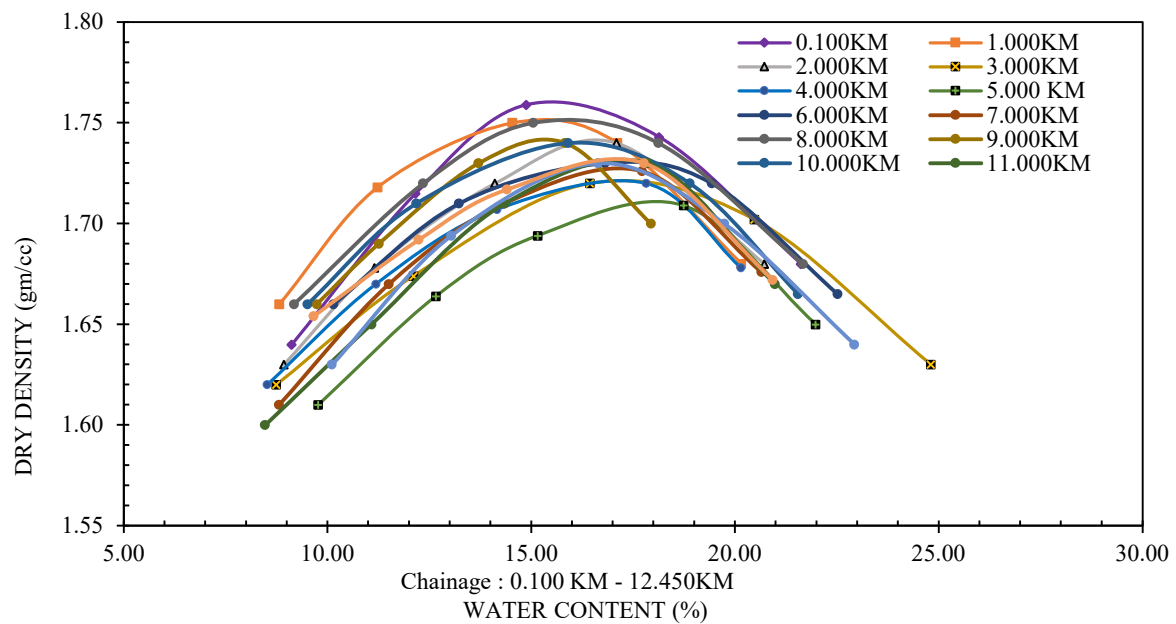


Fig. 5.6: Modified Proctor Compaction Curve for existing road subgrade between chainages 0.100 Km and 12.450 Km

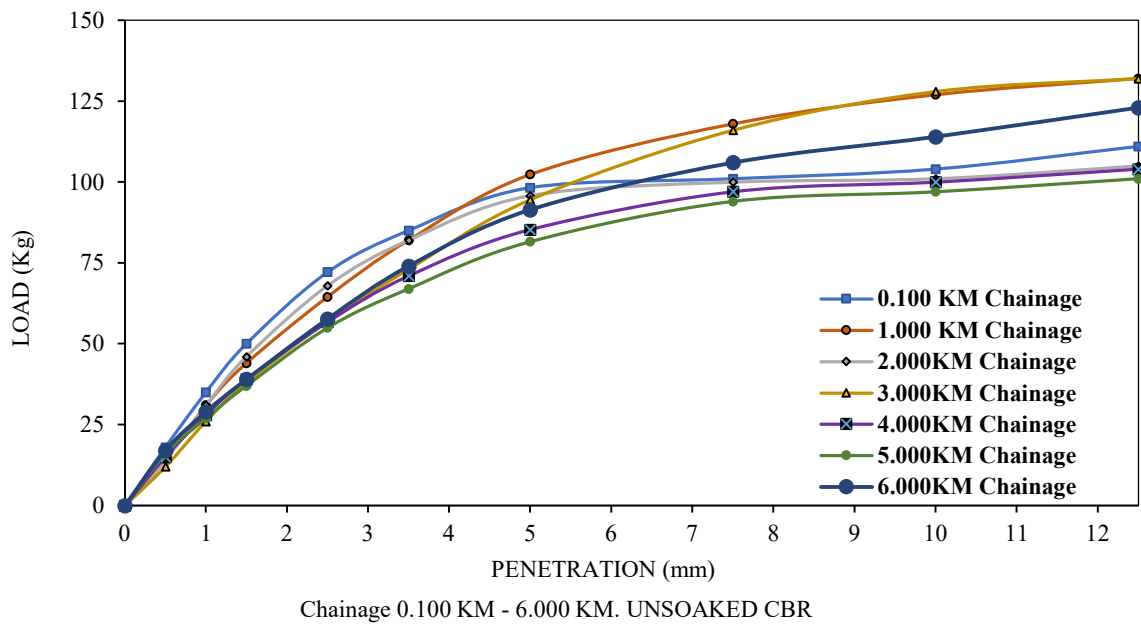


Fig. 5.7: Load vs. Penetration curve for existing road subgrade between 0.100 km and 6.000 km in unsoaked condition

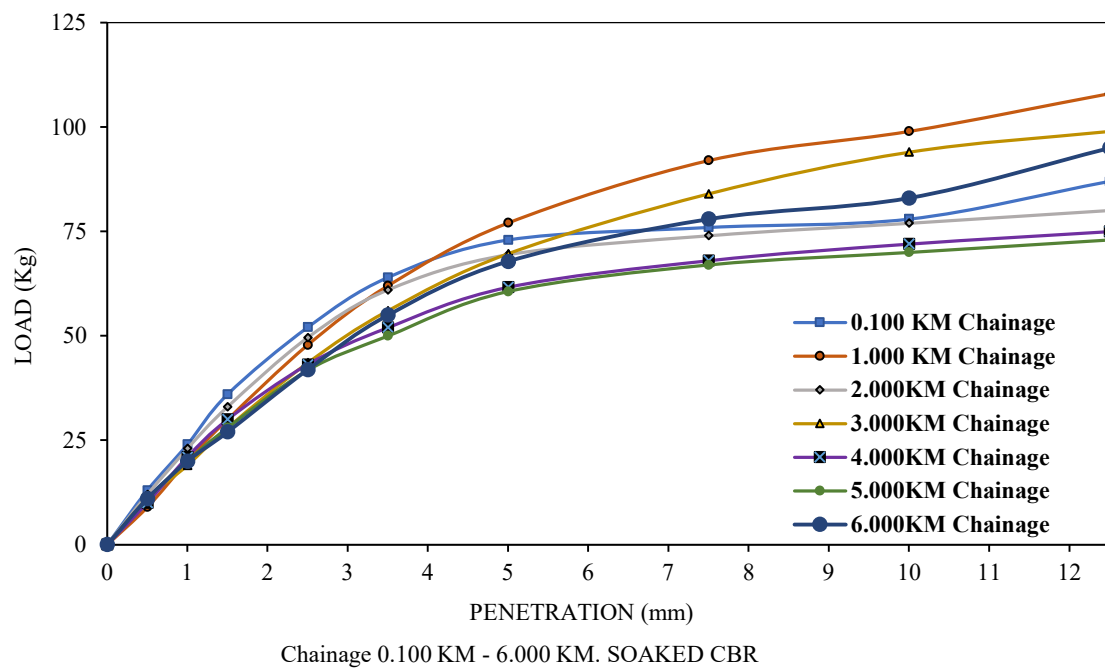
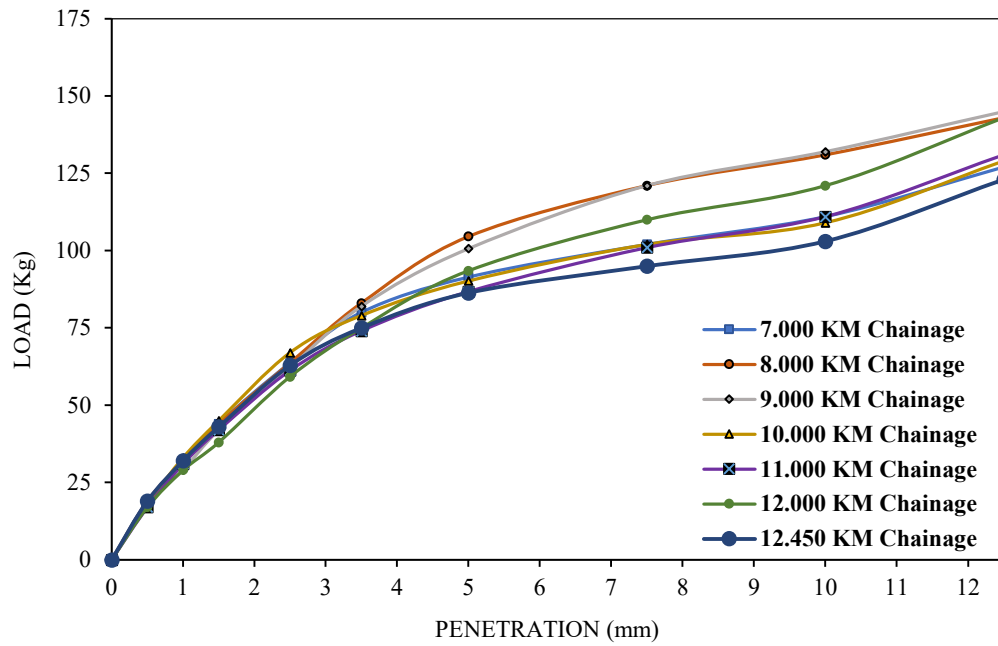
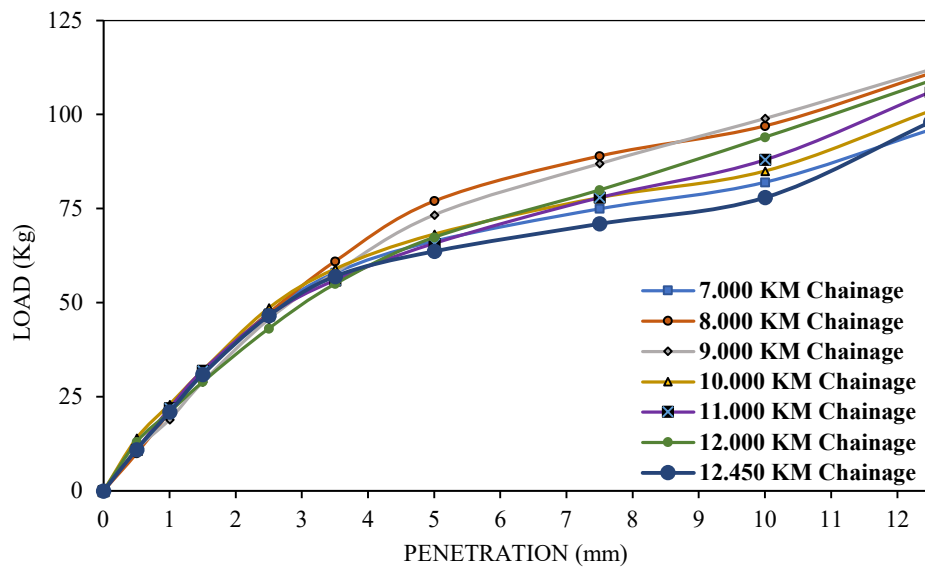


Fig. 5.8: Load vs. Penetration curve for existing road subgrade between 0.100 km and 6.000 km in soaked condition



Chainage 7.000 KM.- 12.450 KM UNSOAKED CBR

Fig. 5.9: Load vs. Penetration curve for existing road subgrade between 7.000 km and 12.450 km in unsoaked condition



Chainage 7.000 KM.- 12.450 KM SOAKED CBR

Fig. 5.10: Load vs. Penetration curve for existing road subgrade between 7.000 km and 12.450 km in soaked condition

5.4.2 Evaluation of Design CBR And Soil Sample Collection for Tests on Soil Tyre Mix

The 80th percentile CBR value, as specified in Clause 6.2.2 of IRC:37-2018, can be used to calculate the design CBR of a road if the design traffic volume is below 20 msa during the pavement design. Therefore, for further analysis, it is advisable to ascertain the CBR value of

the soil by averaging at least three specimens prepared using the specific soil. In accordance with this clause, Fig.5.11 presents an 80th percentile CBR graph, illustrating a value of 3.36 for the 80th percentile CBR. This value can be effectively utilized for subsequent design processes.

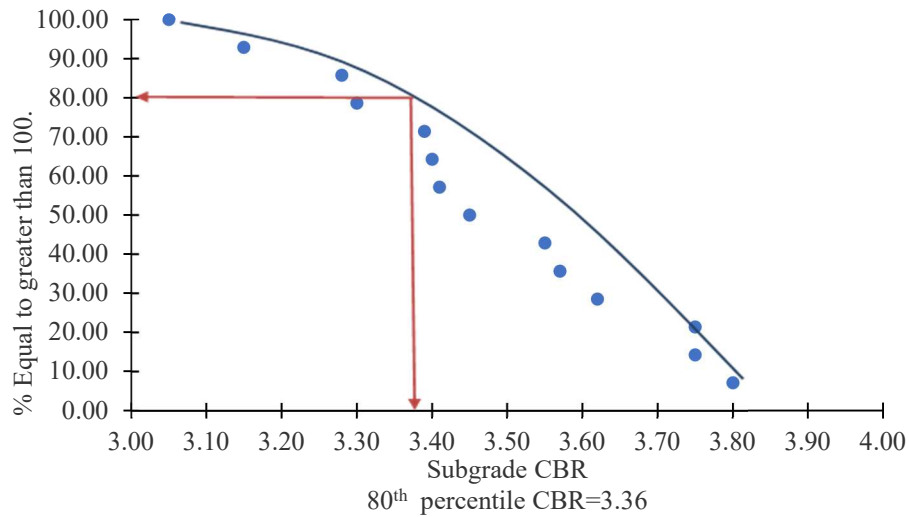


Fig. 5.11: Design CBR curve

5.4.3 Property Of Scrap Tyre Material Used in This Study

The waste tyre material, in the form of shredded tyres used in this investigation, has been purchased from a local car garage in the Jadavpur area of Kolkata. The outer circle steel reinforcement around the tyre has been removed using a hexablade. The remaining of the tyre has been sliced into fragments ranging from 10 to 25 mm in length and width, and 2 to 3 mm in thickness, considering an aspect ratio ($AR = \text{Length of shred}/\text{Width}$) of 1. Table 5.4 displays some properties of the scrap tyre material that was tested at a NABL Lab in Kolkata.

Table 5.4: Properties of scrap tyre

Sl No	Property	Sample 1	Sample 2
1	Density	1.11 gm/cm ³	1.13 gm/cm ³
2	Melting Point	232°C	236 °C
3	Specific Gravity	1.13	1.15
4	Water Absorption Capacity	NIL	NIL
5	Elastic Modulus	1.01Mpa	1.03Mpa

****NABL Lab report has been attached in Annexure II**

5.4.4 Test Results for Shredded Tyre Scrap Mixed Soil

5.4.4.1 Collection and preparation of soil samples for tyre scrap mixing

The design CBR value of 3.36, as shown in Fig.5.11, is based on the 80th percentile CBR graph. The next phase aims to match this CBR value with soil that will be considered for mixing with shredded tyre scrap. For these purposes, Soil samples have been collected from various points (chainages) along the existing road at 3.00Km, 6.00Km, 7.00Km, 11.00Km, 12.00Km, and 12.45Km. The CBR values of these locations are 3.39, 3.30, 3.45, 3.41, 3.28, and 3.40, which are closely aligned with the target design CBR value of 3.36. Manual mixing has been conducted to achieve a homogeneous mixture of soil and scrap tyre. In the laboratory, the soil sample was combined with various sizes of scrap tyre, ensuring a uniform blend while taking appropriate precautions throughout the process. After mixing these soils, three samples have been collected from the mixture and tested as remoulded samples. The test results have been presented in Table 5.5.

Table 5.5: Property of mixed soil formed by collecting soil from different chainages of 3.00Km, 6.00Km, 7.00Km, 11.00Km, 12.00Km, and 12.45Km. (Atterberg Limits, Bulk Density, Moisture Content and Grain Size Analysis)

Sl. No	Sample No.	Description of soil	Atterberg Limits			Bulk Density (Y _b) (gm/cc)	Moisture Content (%)	Grain Size Analysis (%)		
			LL (%)	PL (%)	PI (%)			Sand	Silt	Clay
1	SAMPLE 1	Grey silty clay	48.68	21.93	27.01	2.11	19.23	7	62	31
2	SAMPLE 2	Grey silty clay	48.88	21.91	26.96	2.02	20.02	6	62	32
3	SAMPLE 3	Grey silty clay	48.73	21.87	26.82	2.13	19.77	6	64	30
	Suggested values		48.68	21.87	26.82	2.02	19.23	6	62	32

Figure 5.12 represents particle size distribution of mix soil

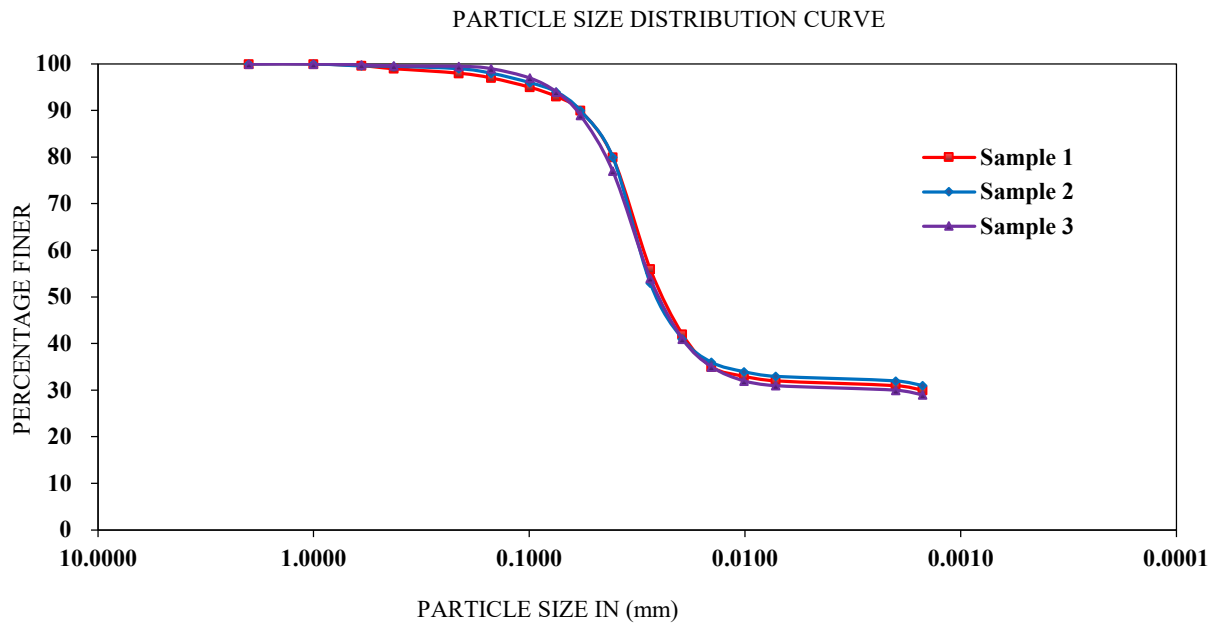


Fig. 5.12: Particle size distribution curve for mix soil

Table 5.6, showing an average CBR value of 3.37, which is mostly equal to the design value of 3.36.

Table 5.6: Property of mixed soil formed by collecting soil from different chainages of 3.00Km, 6.00Km, 7.00Km, 11.00Km, 12.00Km, and 12.45Km. (Modified Proctor, Unconsolidated Undrained (UU) and Laboratory CBR (%))

Sl. No	Sample No.	Description of soil	Modified Proctor		Unconsolidated Undrained (UU)		Laboratory CBR (%)	
			MDD (gm/cc)	OMC (%)	Cohesion(C) (t/m ²)	Angle of internal Friction(ϕ)	Soaked	Unsoaked
1	SAMPLE 1	Grey silty clay	1.729	16.99	2.52	2.2	3.37	4.55
2	SAMPLE 2	Grey silty clay	1.730	16.97	2.50	2.0	3.39	4.58
3	SAMPLE 3	Grey silty clay	1.730	16.98	2.51	2.3	3.39	4.56
Suggested values			1.729	16.97	2.50	2.0	3.37	4.55

The corresponding compaction and CBR curve for mix soil are displayed in Fig.5.13 and 5.14 respectively.

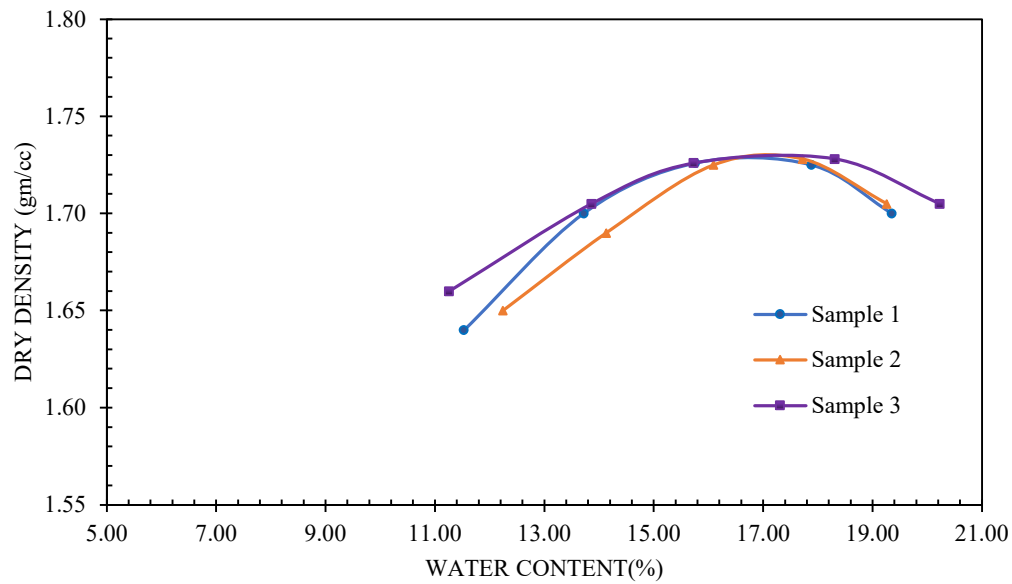


Fig. 5.13: Modified Proctor Compaction Curve for mix soil

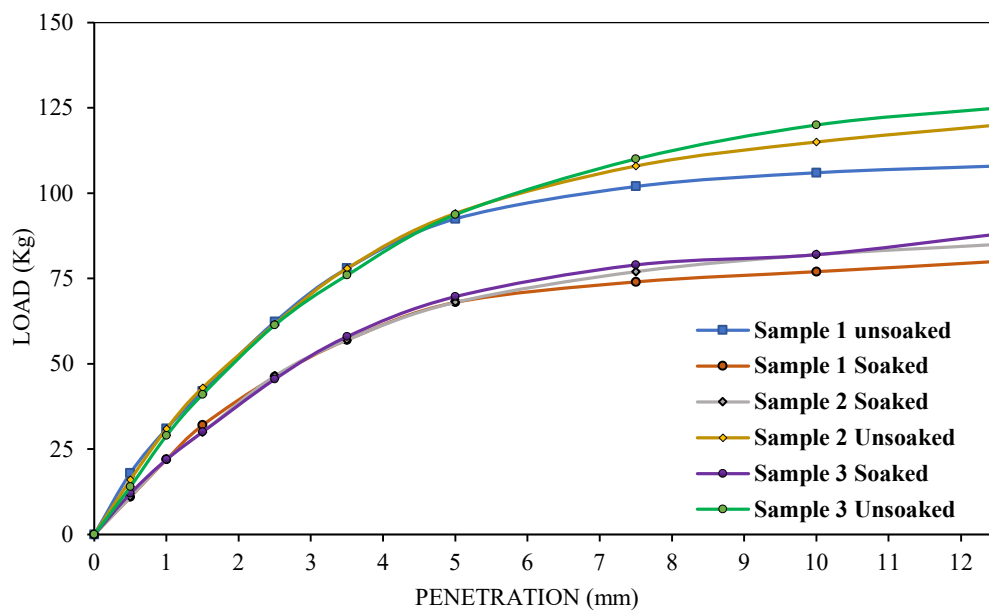


Fig. 5.14: Load vs. Penetration Curve for mix soil

UU curves for mix soil samples have been presented in ANNEXURE -III

This mix soil mass is then further processed with different sizes and proportions of tyre scrap as stated earlier. The test results for the soil-shredded tyre scrap mix are presented in Table 5.7.

Table 5.7: Laboratory test results for soil- shredded tyre scrap mix.

Tyre Size (in mm)	Percentage (%) of Soil	Percentage (%) of Tyre	Modified Proctor		Laboratory CBR value (%)	
			OMC (%)	MDD (gr/cc)	Soaked	Unsoaked
10 X 10	95	5	16.70	1.74	7.60	8.40
	90	10	16.45	1.70	7.90	9.30
	85	15	17.40	1.68	7.00	8.70
	80	20	18.24	1.63	6.04	7.90
	75	25	20.30	1.58	5.10	6.50
	70	30	20.88	1.55	4.67	6.35
15 X 15	95	5	17.10	1.70	7.80	9.10
	90	10	17.10	1.68	8.90	10.25
	85	15	18.10	1.64	7.30	8.60
	80	20	18.56	1.60	6.10	7.80
	75	25	20.65	1.53	5.80	7.00
	70	30	21.24	1.51	4.56	6.50
20 X 20	95	5	17.55	1.67	7.67	8.34
	90	10	18.24	1.65	8.45	9.13
	85	15	18.93	1.62	7.13	8.10
	80	20	18.98	1.58	6.08	7.57
	75	25	21.22	1.50	5.53	6.66
	70	30	21.56	1.50	4.52	6.12
25 X 25	95	5	18.45	1.65	6.45	8.13
	90	10	18.95	1.63	6.56	8.96
	85	15	19.01	1.60	5.34	7.78
	80	20	19.68	1.56	5.43	7.12
	75	25	21.68	1.49	4.53	6.23
	70	30	21.98	1.49	4.25	6.03
30 X 30	95	5	19.36	1.65	6.22	8.00
	90	10	19.55	1.61	6.31	8.46
	85	15	19.14	1.55	5.49	7.53
	80	20	20.44	1.53	4.88	6.58
	75	25	22.05	1.49	4.33	6.02
	70	30	22.12	1.48	4.01	5.89

The corresponding compaction curves for road subgrade soil are displayed in Fig.5.15 to Fig.5.19 and the CBR curves are plotted in Fig.5.20 to 5.29 respectively. Modified Proctor Compaction curves for soil scrap tyre mixture on the basis of Table 5.7, are illustrated below:

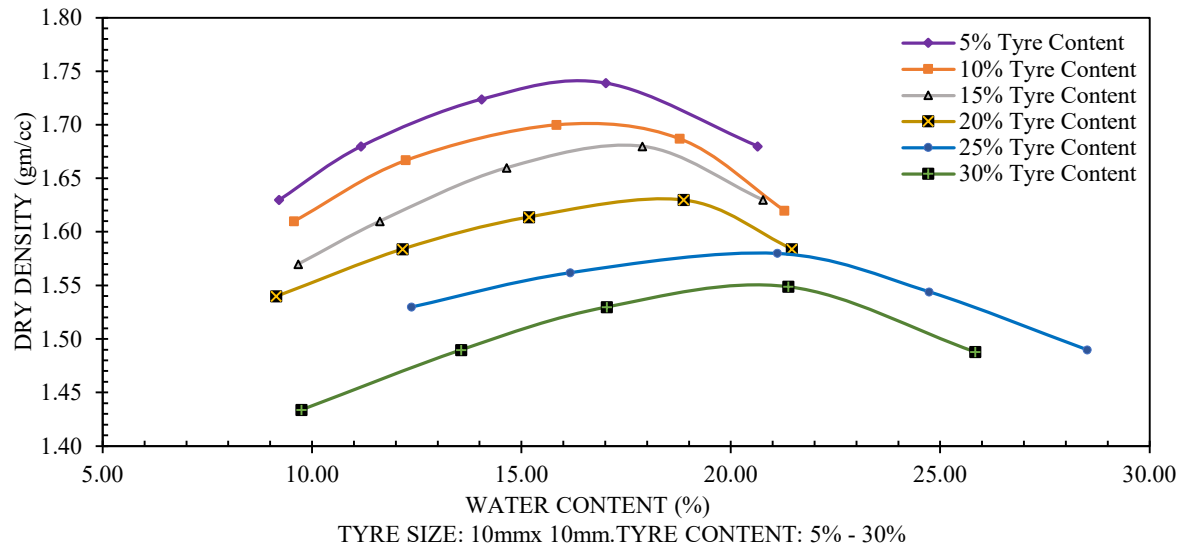


Fig. 5.15: Modified Proctor Compaction Curve for Original Soil mixed with Various Percentages of 10 mm x 10 mm tyre Scrap

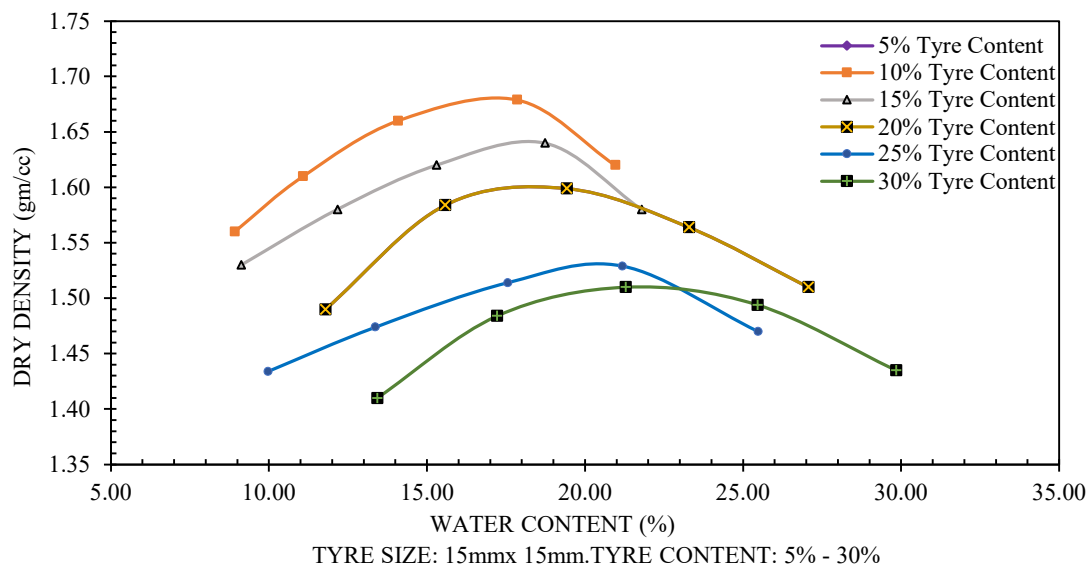


Fig. 5.16: Modified Proctor Compaction Curve for original soil mixed with Various Percentages of 15 mm x 15 mm tyre Scrap

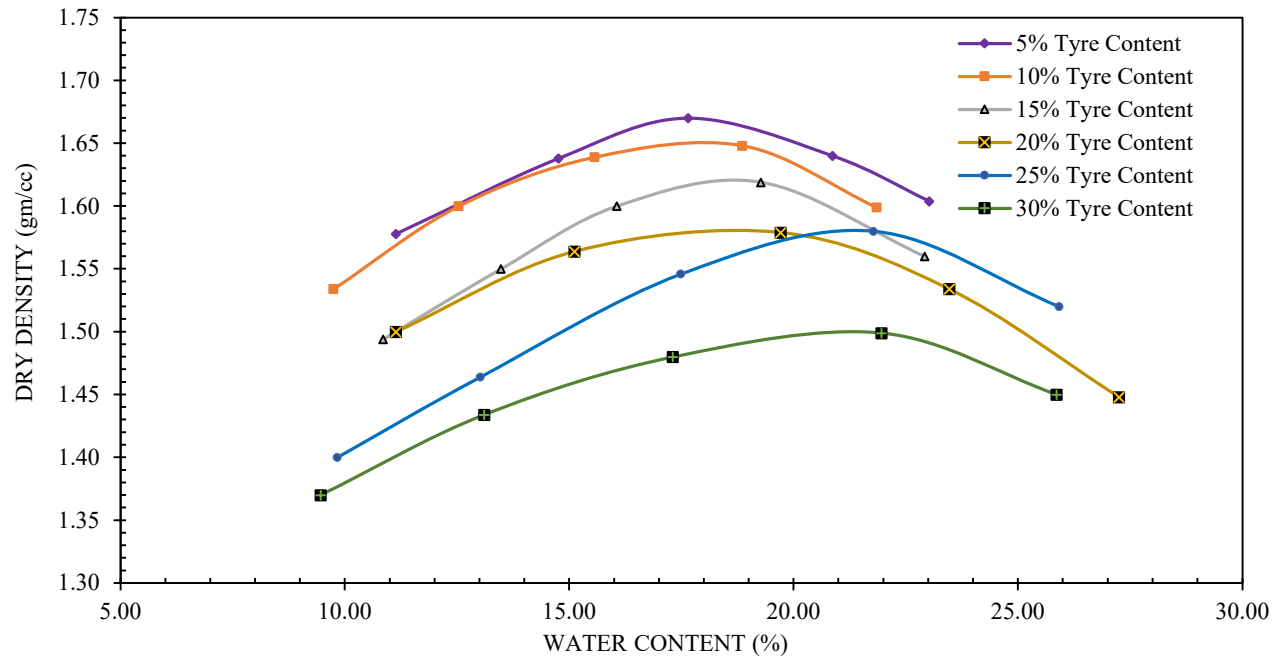


Fig. 5.17: Modified Proctor Compaction curve for original soil mixed with various Percentages of 20 mm x 20 mm tyre Scrap

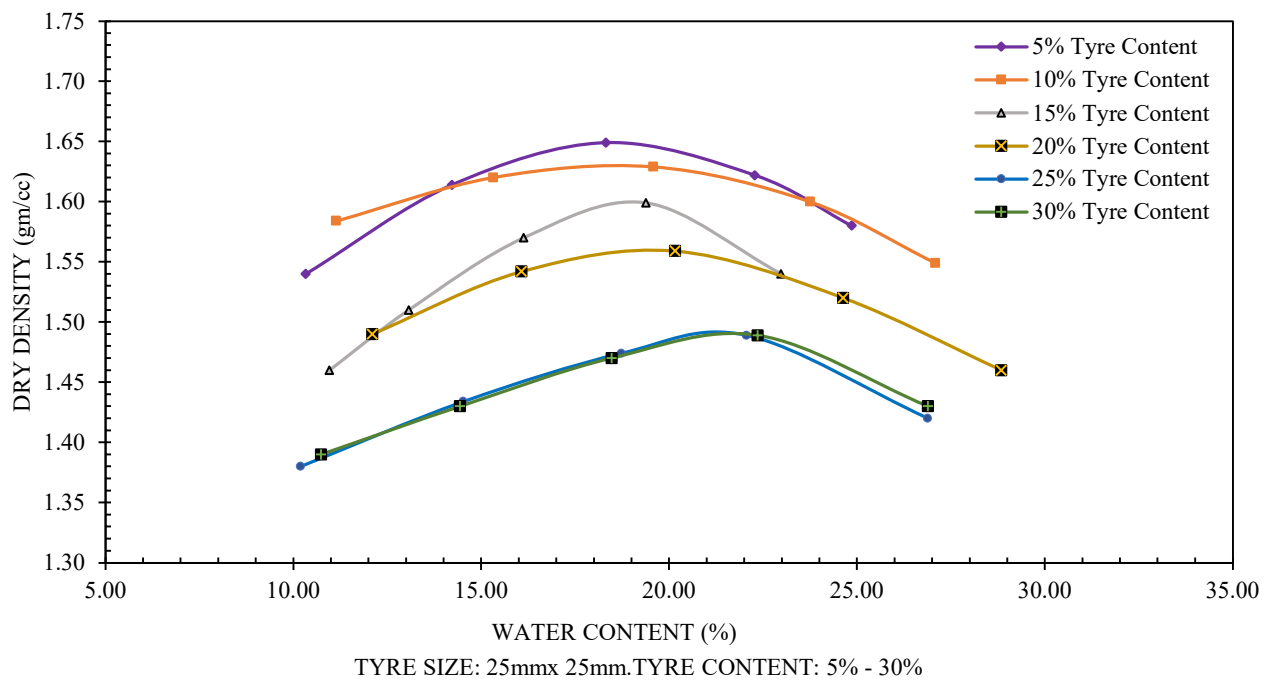


Fig. 5.18: Modified Proctor Compaction curve for original Soil mixed with various Percentages of 25 mm x 25 mm tyre Scrap

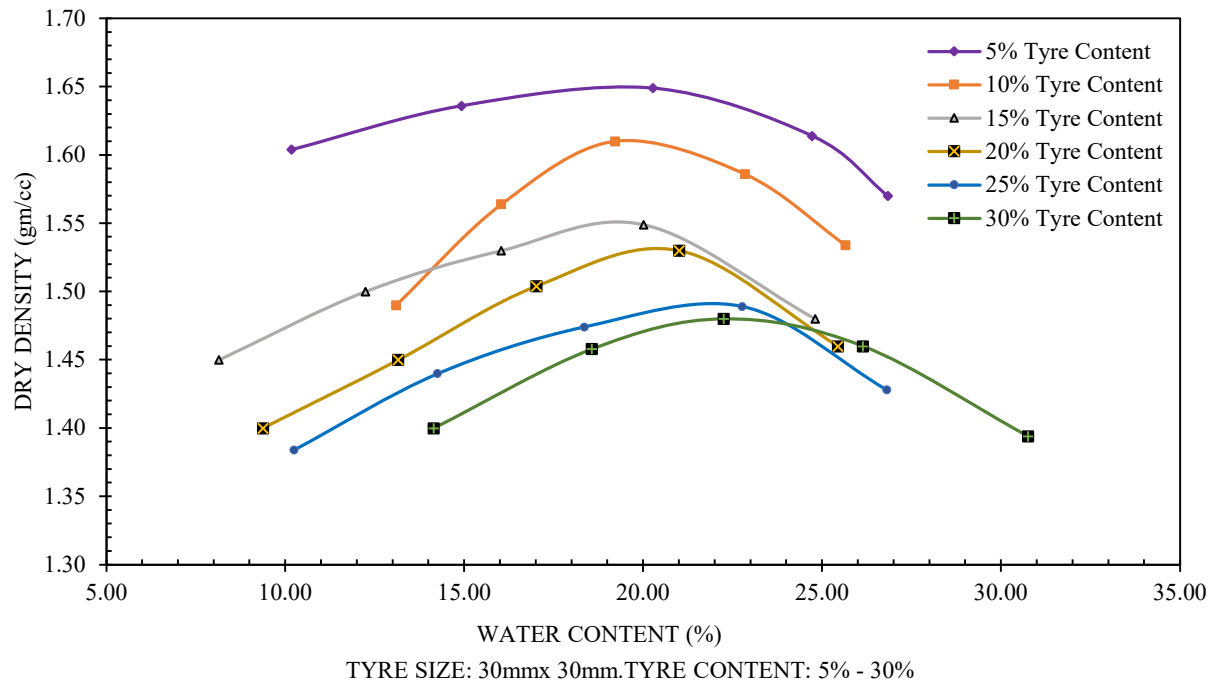


Fig. 5.19: Modified Proctor Compaction curve for original Soil mixed with various Percentages of 30 mm x 30 mm tyre Scrap

CBR curves for soil scrap tyre mixture on the basis of Table 5.7 are illustrated below-

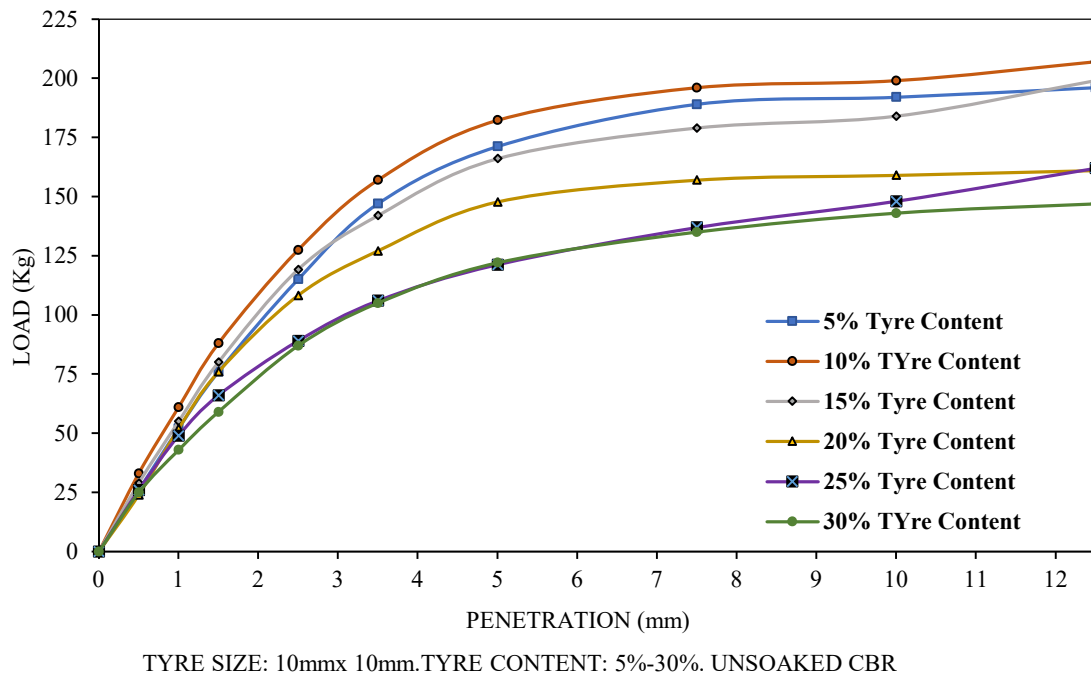
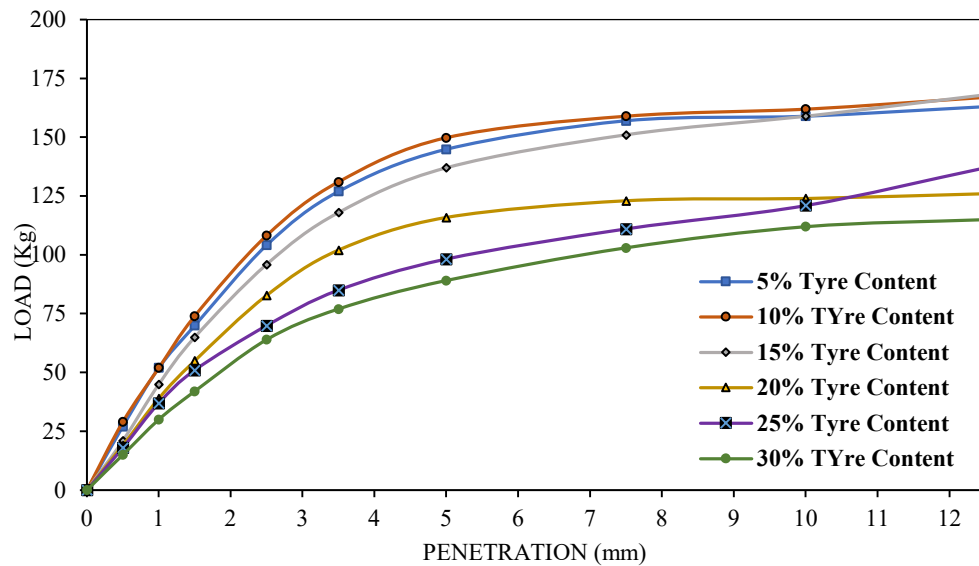
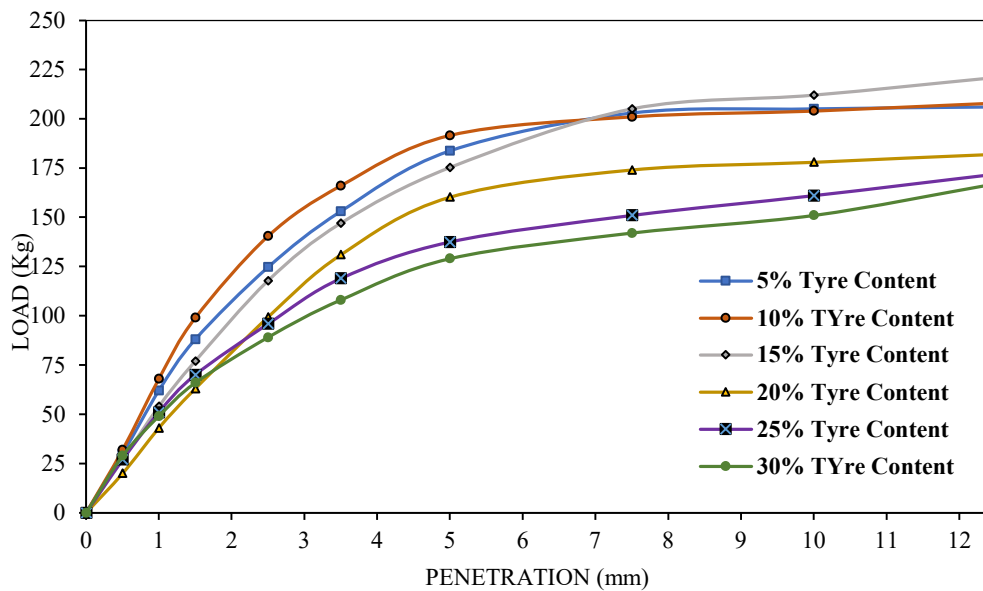


Fig. 5.20: Load vs. Penetration Curve for Original Soil Mixed with Different Percentages of 10 mm x 10 mm tyre scrap, in unsoaked condition



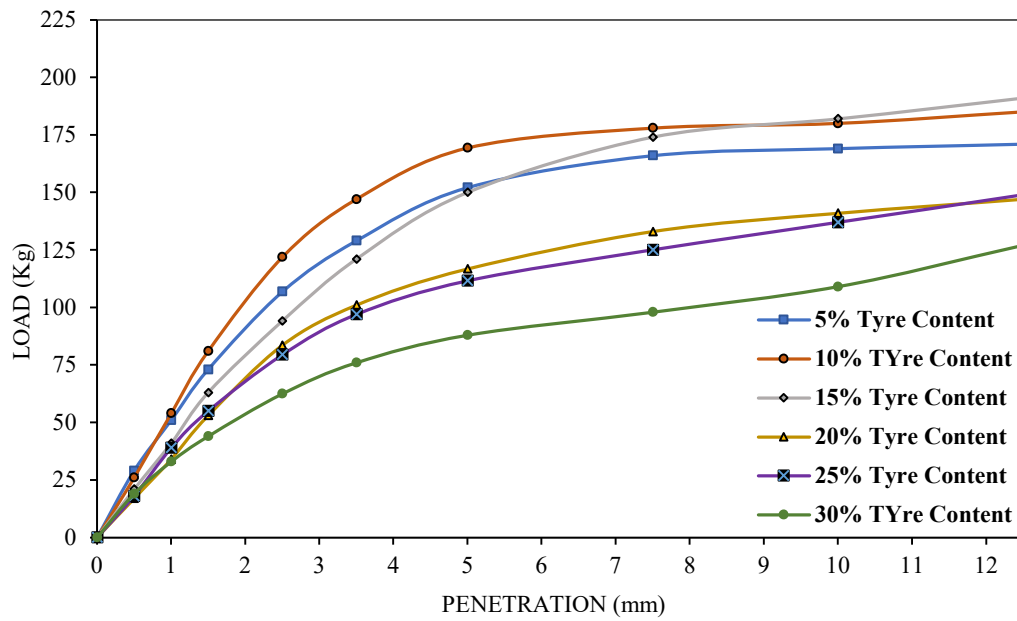
TYRE SIZE: 10mmx 10mm.TYRE CONTENT: 5%-30%. SOAKED

Fig. 5.21: Load vs. Penetration Curve for Original Soil Mixed with Different Percentages of 10 mm x 10 mm tyre scrap, in soaked condition



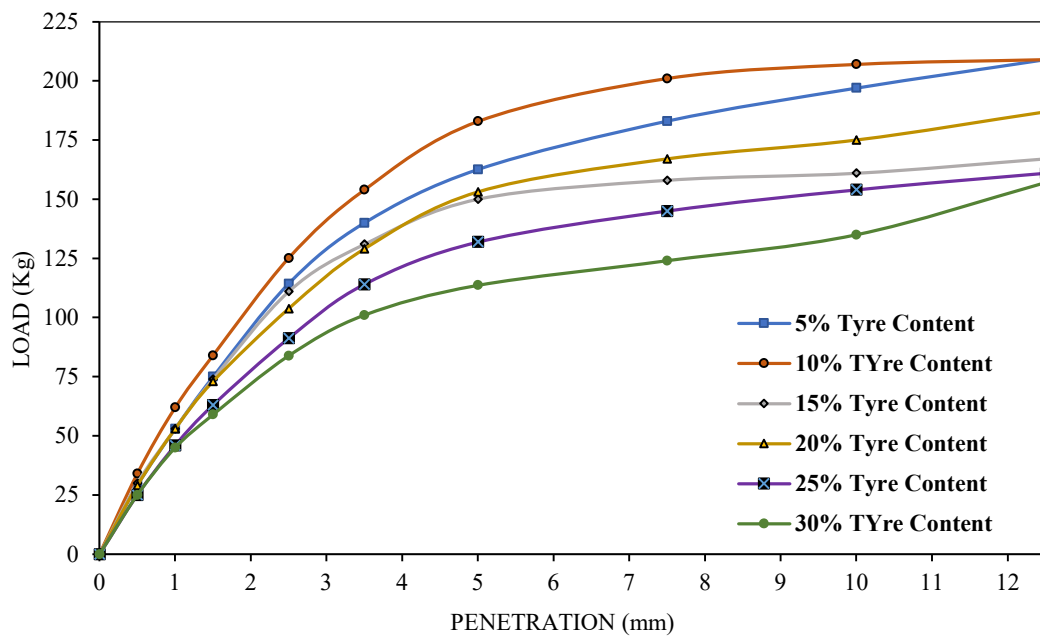
TYRE SIZE: 15mmx 15mm.TYRE CONTENT: 5%-30%. UNSOAKED

Fig. 5.22: Load vs. Penetration Curve for Original Soil Mixed with Different Percentages of 15 mm x 15mm tyre scrap, in unsoaked condition



TYRE SIZE: 15mmx 15mm.TYRE CONTENT: 5%-30%. SOAKED CBR

Fig. 5.23: Load vs. Penetration Curve for Original Soil Mixed with Different Percentages of 15 mm x 15mm tyre scrap, in soaked condition.



TYRE SIZE: 20mmx 20mm.TYRE CONTENT: 5%-30%. UNSOAKED

Fig. 5.24: Load vs. Penetration Curve for Original Soil Mixed with Different Percentages of 20 mm x 20mm tyre scrap, in unsoaked condition

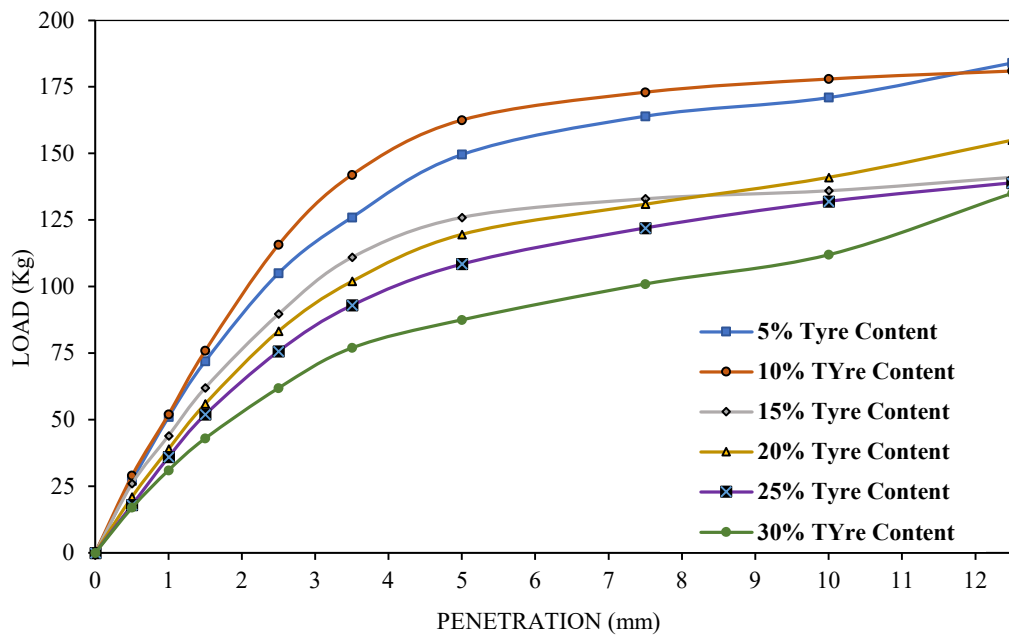


Fig. 5.25: Load vs. Penetration Curve for Original Soil Mixed with Different Percentages of 20 mm x 20mm tyre scrap, in soaked condition

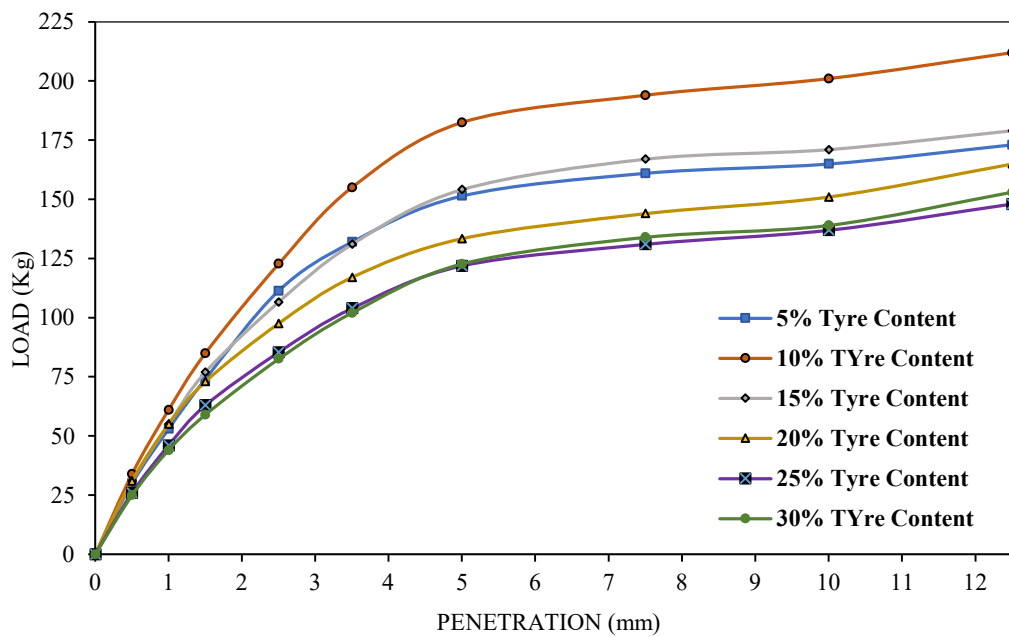


Fig. 5.26: Load vs. Penetration Curve for Original Soil Mixed with Different Percentages of 25 mm x 25mm tyre scrap, in unsoaked condition

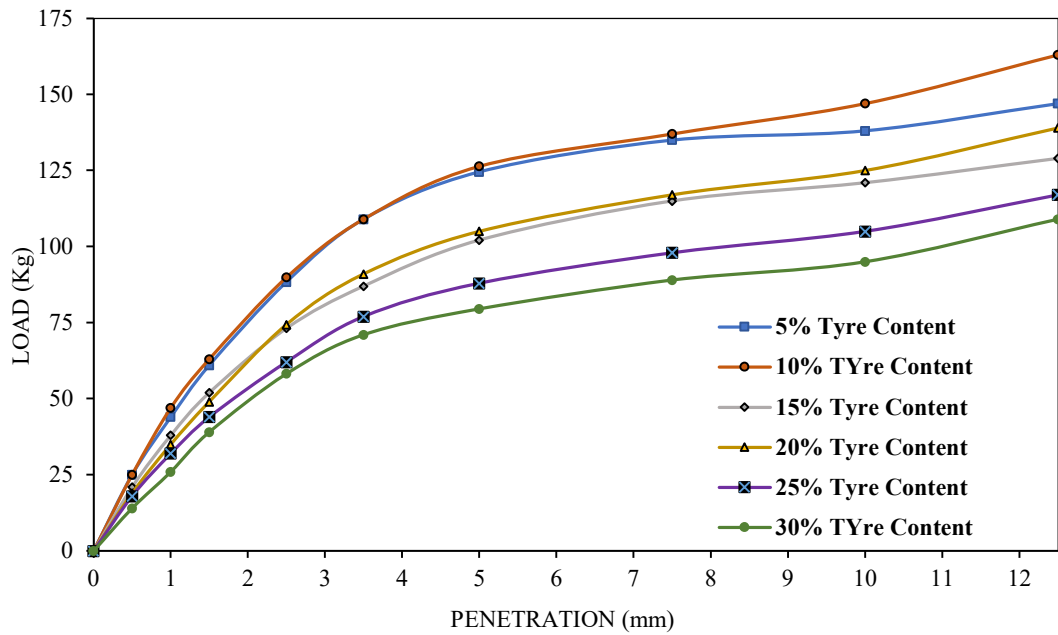


Fig. 5.27: Load vs. Penetration Curve for Original Soil Mixed with Different Percentages of 25 mm x 25mm tyre scrap, in soaked condition

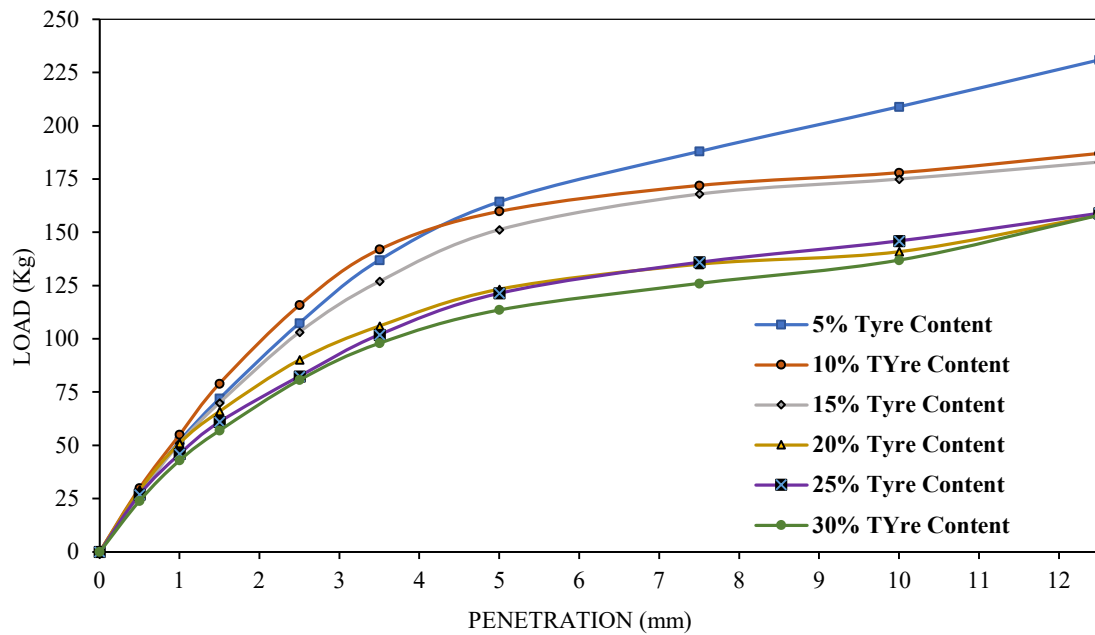


Fig. 5.28: Load vs. Penetration Curve for Original Soil Mixed with Different Percentages of 30 mm x 30mm tyre scrap, in unsoaked condition

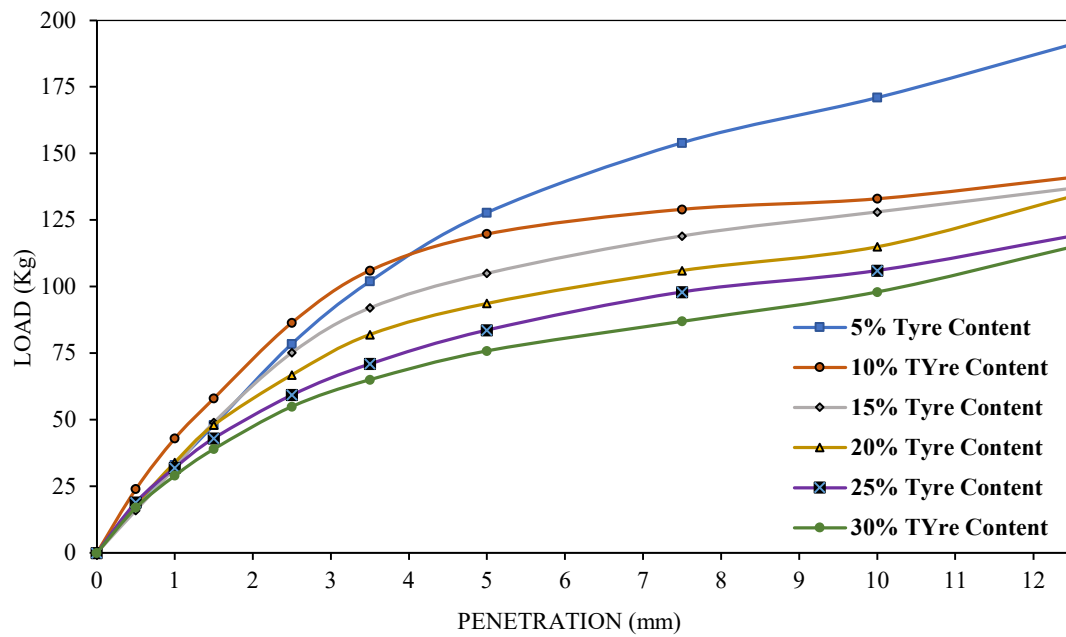


Fig. 5.29: Load vs. Penetration Curve for Original Soil Mixed with Different Percentages of 30 mm x 30mm tyre scrap, in soaked condition

Based on Table 5.7, it is evident that the optimum CBR of 8.90 (Soaked) has been found at a tyre scrap size of 15mm x 15mm with a tyre percentage of 10%. This scrap tyre-mixed soil has been then further tested for bulk density (γ_b) and UU tests for future study. Mix soil sample have been collected from the respective chainage points as stated in Section 5.4.4.1 and have been prepared for UU test. The test results are presented in Table 5.8.

Table 5.8: UU and Bulk Density of soil mixed with tyre scrap of size 15mm x 15mm at a percentage of 10%

Sl. No	Sample No.	Unconsolidated Undrained (UU)		Bulk Density (γ_b) (t/m^3)
		Cohesion(C) (t/m^2)	Angle of internal Friction(ϕ)	
1	SAMPLE 1	4.62	8°	1.99
2	SAMPLE 2	4.50	8°	1.97
3	SAMPLE 3	4.58	8°	2.03
Suggested values		4.50	8°	1.97

UU curves for mix soil samples have been illustrated in Annexure III

5.5 SUMMARY

This chapter has presented the results of various laboratory tests conducted to evaluate the properties of both original subgrade soil and soil mixed with shredded tyre scrap. Detail analyses of grain size distribution, Atterberg limits, compaction characteristics, and California Bearing Ratio (CBR) values have been included. The findings have been revealed significant improvements in the strength and compaction properties of the subgrade when mixed with specific proportions and sizes of tyre scrap. Additionally, the chapter has highlighted the optimal mix ratios that enhance subgrade performance, providing a solid foundation for the subsequent field studies and numerical analyses.

CHAPTER 6

FIELD TESTS AND ASSOCATED STUDY

6.1 OVERVIEW

This research work encompasses various field studies aimed to evaluate different aspects of pavement design. The principal objective of this study is to assess and compare the structural performance of two distinct pavement subgrade: one is existing road subgrade and another is subgrade modified with scrap tyres. To assess this performance by the study, the following field tests are considered: Traffic Survey along with Pavement Design and structural performance assessment of the subgrade using FWD and other allied works.

6.2 TRAFFIC STUDY AND PAVEMENT DESIGN

This study includes the collection of essential data about axle loads and traffic volume, which are crucial for pavement design. It comprises the following key components:

- i. Traffic Census.
- ii. Axle Load Survey.
- iii. Pavement Design.

Along the project route, a number of traffic data have been collected, such as axle load surveys and traffic volume counts. To obtain the basic traffic study parameters for this work, traffic analysis and axle load survey have been conducted to initiate the pavement design.

6.2.1 Traffic Census

In this present investigation, a traffic analysis has been performed by using an Auto Traffic Counter and Classifier (ATCC) with model KVC01 Hardware + Software made by Kotai, India. This involves employing automated devices to gather data regarding vehicular traffic patterns and volume on a specific section of the Jibantala-Taldi Road. These traffic counters have been strategically placed to provide valuable insights for transportation planning, road design, and traffic management. To collect data, a video camera has been

utilized to record various information such as vehicle counts, vehicle types (e.g., cars, trucks), speed, and vehicle classifications (e.g., passenger cars, buses, motorcycles). The video camera has been installed at chainage 11.50 Km to capture vehicle-related information. Data collection has taken place continuously over a period of seven (7) days. Following data collection, the ATCC has been employed to conduct traffic analysis, resulting in a classified traffic count presented in the form of a traffic census. This census aims to determine the annual variation of traffic over consecutive seven days along the Jibantala-Taldi Road section. The primary objective is to calculate the total average CVPD to assess traffic flow rates. A seven-day traffic study is conducted and is summarized in Table 6.1. This data is analyzed to inform the design of pavements in accordance with Clause 4.1.2 of IRC 37:2018. Detailed vehicle information Supported by daily traffic data have been provided in Annexure-IV. Graphical representations of ADT and PCU have been shown in Fig. 6.1 and Fig 6.2.

Table 6.1: Summary of Traffic census

Road: Jibantala bazar to Taldi bazar. Chainage:11.50 Km. Location: Taldi
 Direction of traffic: Up- From Jibantala to Taldi, Down- From Taldi to Jibantala
 Assumed year of traffic opening:2021

TRAFFIC DATA ANALYSIS																				
(Summary Sheet)																				
Road :	Jibantala Bazar to Taldi bazar Road																			
Chainage:	11+50 km							Location : Taldi												
Direction of Traffic :	Up	From: Jibantala							To: Taldi	Down	From: Taldi							To: Jibantala		
Time Period	Motorised Vehicle												Non-motorised Vehicles							
	Fast Passenger					Fast Goods					Slow Goods		Total Motorised Vehicles	Animal / Hand Drawn	Cycle	Cycle Rickshaw	Others	Total Non-motorised Vehicles		
	Two Wheeler	Auto Rickshaw	Car / Jeep / Van	Motorized Van	Bus		Truck			Agriculture Tractor	Agriculture Tractor with Trailer									
					Mini / RTVs	Standard	LCV	2-Axle	3-Axle			MAV								
09.06.2019	992	44	511	26	0	0	90	184	64	13	75	223	2162	0	290	48	0	338		
10.06.2019	955	61	573	24	0	0	100	206	46	7	94	202	2271	0	334	47	0	381		
11.06.2019	945	92	612	35	0	0	85	205	66	6	77	165	2288	0	308	45	0	353		
12.06.2019	997	64	594	32	0	0	94	208	43	9	81	163	2276	0	323	49	0	372		
13.06.2019	874	46	483	45	0	0	80	198	65	8	64	190	2053	0	346	52	0	398		
14.06.2019	922	59	498	47	0	0	96	176	53	9	50	162	2072	0	338	49	0	387		
15.06.2019	870	50	498	47	0	0	106	191	60	11	63	180	2076	0	322	53	0	375		
Average	936	59	538	37	0	0	93	195	57	9	72	184	2171	0	323	49	0	372		
Equivalency Factor	0.5	1.0	1.0	1.0	1.5	3.0	1.5	3.0	3.0	4.5	1.5	4.5		6.0	0.5	2.0	4.5			
Daily PCU	468	59	538	37	0	0	140	586	170	41	108	826	2973	0	162	98	0	260		
Total average Comercial Vehicle per day (CVPD)						445	(195+57+9+184)													
Total Passenger Car Unit (PCU)=						3233	(2973+260)													

GRAPHICAL PRESENTATION OF PCU (PASSENGER CAR UNIT) AND ADT (ANNUAL DAILY TRAFFIC)

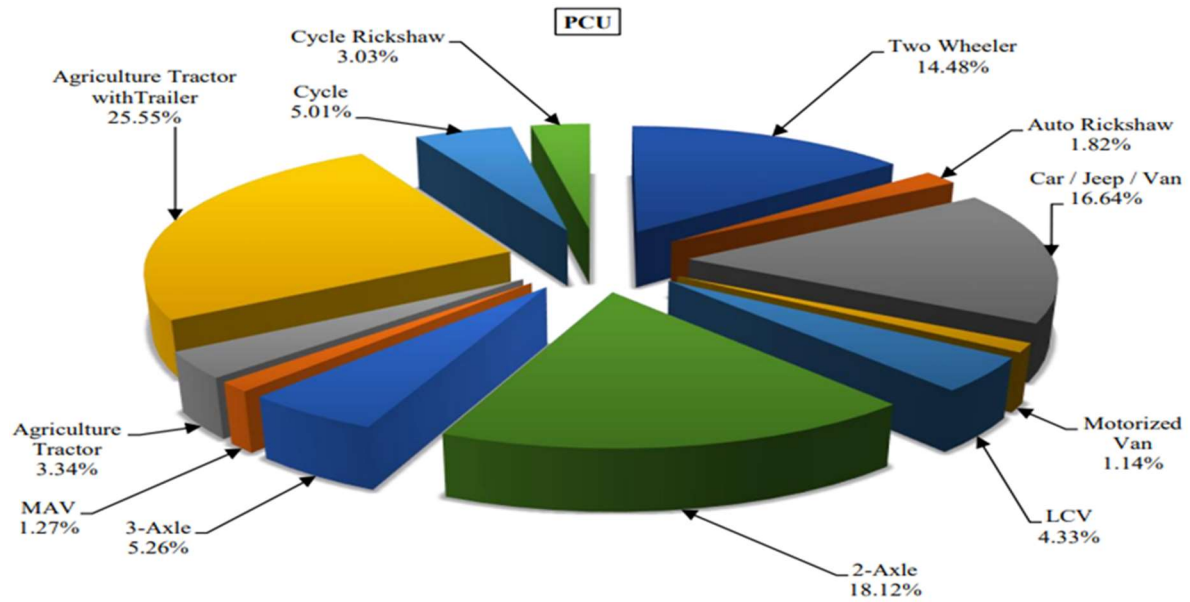


Fig. 6.1: Vehicle distribution chart as per PCU

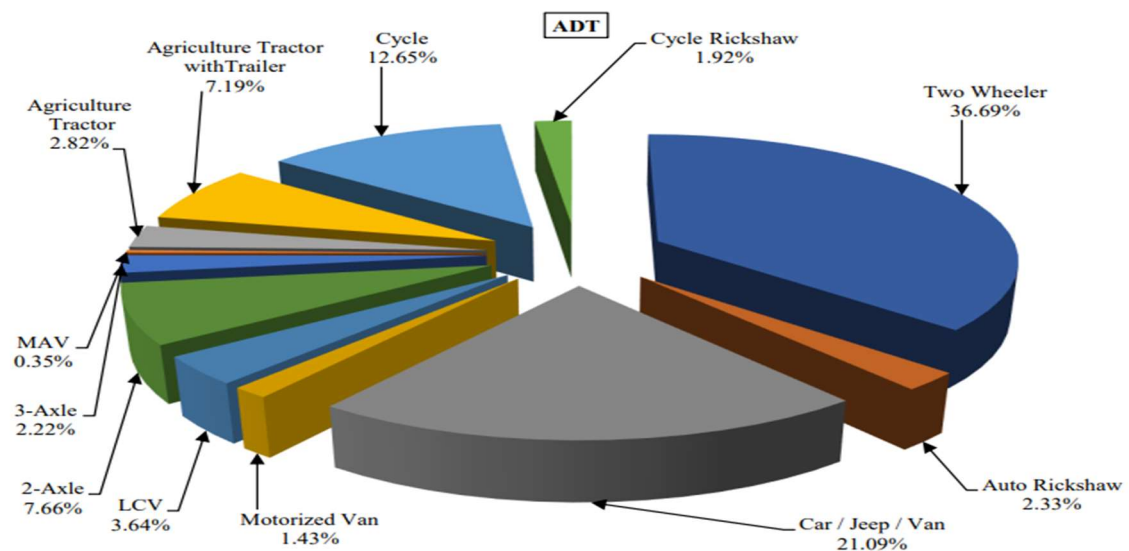


Fig. 6.2: Vehicle distribution chart as per ADT

6.2.2 Axle Load Survey

On regular working days, a continuous 24-hour axle load survey has been carried out at chainage 11.50 km on the project route. For this study, a portable axle weigh pad model no. SEPT-912 made by S.P Engineering & Technology, India, has been utilized to measure the load, as illustrated in Fig.6.3 and Fig. 6.4.



Fig. 6.3: Axle load test



Fig. 6.4: Axle load test data collection

Vehicles have been randomly stopped and their loads on each axle were measured to obtain the loading pattern, and data are continuously monitored and recorded to find out the VDF. Detail VDF analysis for different types of vehicles along with summary of Axle Load Test

results are depicted in Table 6.2, and the supporting vehicular load information to find out VDF are presented in Annexure-V. Finally, the VDF is computed in compliance with IRC 37:2018 clause 4.4 and is provided in Table 6.2.

Table 6.2: Summary of Axle load test results

Name of the Road: Jibantala Taladi Road, Location: Taladi
 Direction- Up: From Jibantala to Taladi, down: From Taladi to Jibantala
 Date :09-06-2019 to 10-06-2019
 Chainage-11.500 Km

Road: JIBANTALA TALDI ROAD									
Location: TALDI									
Up: From JIBANTALA to TALDI									
Down: From TALDI to JIBANTALA									
Date: 09-06-2019 to 10-06-2019									
Sl. No.	Type of Vehicle	No. of Samples	UP			No. of Samples	Down		
			VDF	ADT	Total Damaging Effect		VDF	ADT	Total Damaging Effect
1	LCV	10	2.51	47	117.97	15	2.418	46	111.24
2	TRAILER	20	2.514	92	231.29	20	1.52	92	139.84
3	2 - Axle Truck	20	6.7	98	656.6	20	5.125	97	497.13
4	3 - Axle Truck	8	7.95	29	230.55	7	7.582	28	212.3
5	MAV	3	9.65	5	48.25	3	8.562	4	34.25
Total		61	29.324	271	1284.66	65	25.208	267	994.77
Combined VDF			4.74			3.73			
Adopted VDF			4.74						

All of the needed traffic data has been collected from Jibantala-Taladi Road, and the pavement is designed for a 15-year term utilizing IRC 37:2018, using these data along with effective CBR. Same traffic data has been considered to design pavement of tyre scrap mix modified subgrade.

6.2.3 Pavement Design

To accomplish the primary objective of the research IIT PAVE software has been used to determine the pavement thickness for both of proposed subgrade consisting of original soil and tyre scrap mixed soil sequentially. The multi-layer analysis program, IIT PAVE software

is utilized to analyse flexible pavement, aiming to ascertain stresses and strains at critical pavement points (Harish, 2017). The strength properties of the pavement materials need to be taken into consideration when designing a flexible pavement to determine the thickness of each layer. This can be done by using the CBR value as well as traffic data, and by using IIT PAVE software which computes the actual value of strains coming on the pavement due to wheel load. The software calculates various functional parameters, such as stresses, strains, and deflections, under the assumption that the pavement behaves as a linear elastic layered system. The software may be used to calculate the strains and stress parameters for both vertical compressive strain and horizontal tensile strain, which are crucial mechanistic aspects to check for sub-grade rutting and bottom-up cracking of bituminous layers. In general, the design procedure involves using the IIT-PAVE program to ascertain the component layer thicknesses, derived from the strength characteristics of the pavement materials, in accordance with IRC 37:2018.

6.2.3.1 Determination of pavement thickness by IITPAVE using original soil as subgrade

The following steps have been utilized to ascertain the thickness of flexible pavement: -

i. Calculation of Design Traffic

The traffic design has been calculated using equation 4.5 from IRC 37:2018. This equation estimates the traffic design by considering the projected number of standard axles that the pavement will encounter over its design life period. The equation is as follows:

$$N_{des} = \frac{365[(1+r)^n - 1] \times A \times D \times F}{r} \dots\dots\dots (6.1)$$

Where, N_{des} = Cumulative number of standard axles to be carried during the design period of 'n' years,

A = Initial traffic (CPVD) in the year of completion of construction.

D = Lane distribution factor.

F = Vehicle damage factor (VDF),

n = Design period (years).

r = Annual inflation rate of commercial vehicles in decimal.

The expected traffic in the completion year of a construction project can be calculated using the equation referenced in Equation 4.6 of IRC37:2018.

$$A = P(1 + r)^x \dots\dots\dots (6.2)$$

Where, P = Count of commercial vehicles per day as per the previous record,

x = difference in the number of years between the last record and the year of termination of construction,

The input parameters for determining the design traffic of Jibantala-Taldi Road in the present study have been provided in Table 6.3.

Table 6.3: Input Parameters for design traffic calculation of Jibantala-Taldi Road

Sl. No.	Description of input parameters	Particulars	Reference
1	CVPD During Census (P)	445	Table 6.1
2	Year of Traffic Census	2019	Table 6.1
3	Assume the Year of Opening Traffic	2021	Table 6.1
4	Difference in the number of years (x)	2	2021-2019
5	Considered Rate of Increment (r)	5%	Clause 4.2.2 of IRC37:2018
6	CVPD at Opening year of Traffic	490.61	From eqn. 6.2
7	Lane Distribution Factor (D)	0.75	Clause 4.5.1.2 of IRC37:2018
8	VDF	4.74	Table 6.2
9	Design Life	15 Yrs.	Clause 4.3.2 of IRC37:2018
10	Type of pavement considered	Flexible	According to the project

From equation 6.2,

$$A = 445(1 + 0.05)^2 = 490.61 \text{ CVPD.}$$

The design traffic has now been calculated by putting these numbers into equation 6.1 and taking into account the increasing number of standard axles that will be accommodated over a 15-year design period-

$$N_{\text{des}} = \frac{365[(1 + 0.05)^{15} - 1] \times 490.61 \times 0.75 \times 4.74}{0.05} = 13.74 \text{ MSA}$$

ii. Analysis based on performance criteria of pavement

The following performance criteria for flexible pavement design are suggested by IRC: 37-2018 recommendations:

A. Subgrade Rutting Performance Criteria

When a mean rut depth of 20 mm or greater is recorded over the wheel tracks, critical rutting conditions are considered. Clause 3.6.1 of IRC 37:2018 discusses and provides empirical equations to calculate the sub-grade rutting life. The guidelines outlined in clause 3.7 of IRC 37:2018 recommend using the performance equation for subgrade rutting (equation 6.3) with 80% reliability, particularly when designing for traffic volumes less than 20 MSA.

$$N_R = 4.1656 \times 10^{-08} \left[\frac{1}{\epsilon_v} \right]^{4.5337} \text{ (for 80 \% reliability) } \dots\dots\dots (6.3)$$

where, N_R = subgrade rutting life. ϵ_v = Maximum vertical compressive strain at the top of the sub grade.

B. Fatigue Cracking Criteria for Bituminous layer

A section of pavement is deemed to be in a critical or failure condition if fatigue cracking has developed and affects 20% or more of the paved surface area. The fatigue life of the bituminous layer can be determined by using clause 3.6.2 of IRC 37:2018. The guidelines outlined in clause 3.7 of IRC 37:2018 recommend using the performance equation for fatigue (equation 6.4) with 80% reliability, especially when designing for traffic volumes less than 20 msa.

$$N_f = 1.6064 \times C \times 10^{-04} \left[\frac{1}{\epsilon_t} \right]^{3.89} \times \left[\frac{1}{M_{Rm}} \right] \text{ (for 80 \% reliability) } \dots\dots\dots (6.4)$$

Where, C = adjustment Factor = 10^M and $M = 4.84((V_{be}/V_a + V_{be}) - 0.69)$,

V_a = per cent volume of air void in the mix used in the bottom bituminous layer,

V_{be} = per cent volume of effective bitumen in the mix used in the bottom bituminous layer,

N_f = fatigue life of bituminous layer,

ϵ_t = max horizontal tensile strain at the bottom of the bituminous layer,

M_{Rm} = resilient modulus (MPa) of the bituminous mix used in the bottom Bituminous layer,

The input parameters necessary for analysing the performance criteria of bituminous pavement are outlined in Table 6.4.

Table 6.4: Input parameters for the analysis of pavement performance criteria for normal soil and scrap tyre modified soil

Sl. No.	Description of input parameters	Particulars	Reference
1	Air voids (V_a)	3.50%	Clause 12.3 of IRC37:2018
2	Binder content (V_{be})	11.50%	Clause 12.3 of IRC37:2018
3	Resilient Modulus of Bitumen (M_r)	3000 mpa	Table 9.2 of IRC37:2018
4	CBR of material under Subgrade	3.36%	Clause 12.3 of IRC37:2018
5	Sub Base - 1 (Separation layer)	GSB - Gr. - V	Clause 7.2.1 of IRC37:2018
6	Sub Base - 2 (Drainage layer)	GSB - Gr. -III	Clause 7.2.1 of IRC37:2018
7	Base – 1	WMM	Clause 7.2.1 of IRC37:2018
8	Binder Course	DBM	Clause 7.2.1 of IRC37:2018
9	Wearing Course	BC	Clause 7.2.1 of IRC37:2018
10	Ambient Temperature	35° C	Pavement Temperature
11	Design Traffic (Rutting life for granular layer)	13.74 MSA	Equation 6.1
12	Design Traffic (Fatigue life for bituminous layer)	13.74 MSA	Equation 6.1

By using the values from Table 6.4 the following strain values can be determined for both normal and tyre modified soil subgrade-

a) Maximum vertical compressive strain at the top of the sub grade (ϵ_v) = 0.0006276 (from equation 6.3).

b) Maximum horizontal tensile strain at the bottom of the bituminous layer (ϵ_t) = 0.0003325 (from equation 6.4).

iii. Subgrade CBR value

The soaked CBR for normal soil subgrade of Jibantala-Taldi Road is 3.36, while the scrap tyre mixed soil yields a CBR value of 8.90. It is worth noting that incorporating 15mm×15mm tyre scraps with a thickness of 2mm to 3mm into the original soil at 10% of its dry weight produces a modified CBR value of 8.90.

iv. Pavement thickness analysis trial by using IIT PAVE software

Numerous functional characteristics, including stresses, strains, and deflections, are calculated assuming the pavement to be a linear elastic layered structure. The IIT-PAVE software is useful for planning and analysing flexible pavements and can be used to analyse linear elastic layered systems. The vertical compressive strain and horizontal tensile strain are critical mechanistic factors to assess subgrade rutting and bottom-up cracking of bituminous layers, and to evaluate the satisfactory performance of flexible pavements, this method is employed. Pavements can be designed utilizing any combination of inputs through this approach. The program is used to calculate these stresses and strains parameters. The initial parameters needed for pavement design have been established in the context of this work. The selection of a suitable pavement thickness is of utmost importance, and it can be achieved as per the IRC guidelines. Figure 12.1 of IRC 37:2018 provides a range of trial pavement thicknesses for 5% CBR. In the present study, Fig. 6.5 represents the trial pavement thickness chart for 5% CBR, following IRC 37:2018. This chart can serve as a reference for categorizing the thickness components of bituminous and granular layers obtained from IITPAVE analysis.

Using IIT PAVE software, trial pavement thickness research has been conducted to assess the rutting strain within the subgrade and the tensile strain at the interface between the bituminous and granular layers with an 80 percent reliability. The outcomes of the analysis are shown in Table 6.5. Figures 6.6 and 6.7, respectively, illustrate a standard input and output interface of an IITPAVE study for a typical soil subgrade. All of the previously listed parameters in Table 6.4 are inputs for the software

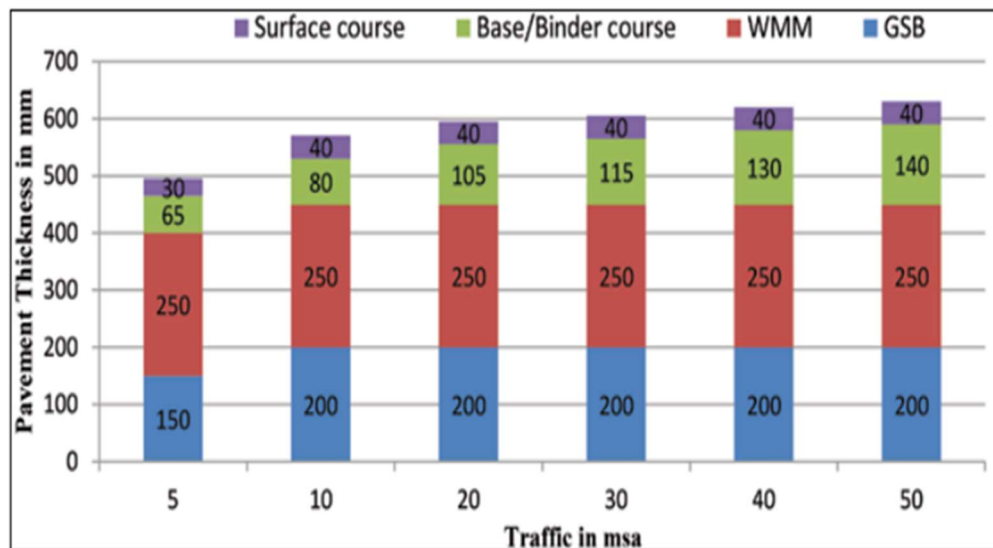


Fig. 6.5: Trial pavement thickness for 5% CBR. (After IRC 37:2018)

No of Layers: HOME

Layer: 1 Elastic Modulus(MPa) Poisson's Ratio Thickness(mm)

Layer: 2 Elastic Modulus(MPa) Poisson's Ratio Thickness(mm)

Layer: 3 Elastic Modulus(MPa) Poisson's Ratio

Wheel Load(Newton) Tyre Pressure(MPa)

Analysis Points

Point:1 Depth(mm): Radial Distance(mm):

Point:2 Depth(mm): Radial Distance(mm):

Point:3 Depth(mm): Radial Distance(mm):

Point:4 Depth(mm): Radial Distance(mm):

Wheel Set (1- Single wheel
2- Dual wheel)

Submit Reset

Fig. 6.6: Typical input window of IITPAVE analysis for normal soil subgrade

Table 6.5: Trial pavement thickness analysis for normal soil subgrade by IITPAVE

Trial No.	Thickness of bituminous layer(mm)	Thickness of granular layer(mm)	CBR Value	Resilient modulus (Subgrade)	Resilient modulus (Granular)	Resilient modulus (Bituminous)	Calculated horizontal tensile strain & vertical strain		Calculated maximum allowable horizontal tensile strain & vertical strain		Remarks
							Calculated tensile strain at bottom of bituminous layer	Calculated vertical strain on subgrade	Maximum tensile strain at the bottom of bituminous layer	Maximum vertical strain on subgrade	
1	105	440	3.36%	33.60	103.97	3000	0.3476×10^{-3}	0.7007×10^{-3}	0.3325×10^{-3}	0.6276×10^{-3}	Design unsafe
2	110	450	3.36%	33.60	105.03	3000	0.3310×10^{-3}	0.6599×10^{-3}	0.3325×10^{-3}	0.6276×10^{-3}	Design unsafe
3	120	450	3.36%	33.60	105.03	3000	0.3048×10^{-3}	0.6168×10^{-3}	0.3325×10^{-3}	0.6276×10^{-3}	Design safe

After several trial runs, the safe thickness has been obtained from Table 6.5. Specifically, in trial 3, the bituminous layer has a thickness of 120mm, while the granular layer has a thickness of 450mm.

<input type="checkbox"/> OPEN FILE IN EDITOR <input checked="" type="checkbox"/> VIEW HERE <input type="button" value="BACK TO EDIT"/> <input type="button" value="HOME"/>										
No. of layers	3									
E values (MPa)	3000.00 105.03 33.60									
Mu values	0.350.350.35									
thicknesses (mm)	120.00 450.00									
single wheel load (N)	20000.00									
tyre pressure (MPa)	0.56									
Dual Wheel										
Z	R	SigmaZ	SigmaT	SigmaR	TaoRZ	DispZ	epZ	epT	epR	
120.00	0.00-0.9990E-01	0.1229E+01	0.9984E+00-0.1368E-01	0.7804E+00-0.2931E-03	0.3048E-03	0.2011E-03				
120.00L	0.00-0.9990E-01-0.8891E-02-0.1695E-01-0.1368E-01	0.7804E+00-0.8650E-03	0.3048E-03	0.2011E-03						
120.00	155.00-0.9139E-01	0.1080E+01	0.5582E+00-0.3994E-01	0.8028E+00-0.2216E-03	0.3055E-03	0.7073E-04				
120.00L	155.00-0.9139E-01-0.9676E-02-0.2794E-01-0.3994E-01	0.8028E+00-0.7448E-03	0.3055E-03	0.7073E-04						
570.00	0.00-0.1864E-01	0.2631E-01	0.2328E-01-0.2854E-02	0.5661E+00-0.3427E-03	0.2350E-03	0.1961E-03				
570.00L	0.00-0.1863E-01	0.1602E-02	0.6488E-03-0.2852E-02	0.5661E+00-0.5779E-03	0.2350E-03	0.1967E-03				
570.00	155.00-0.1978E-01	0.2785E-01	0.2589E-01-0.3623E-02	0.5792E+00-0.3674E-03	0.2448E-03	0.2196E-03				
570.00L	155.00-0.1978E-01	0.1671E-02	0.1041E-02-0.3638E-02	0.5792E+00-0.6168E-03	0.2449E-03	0.2196E-03				

Fig. 6.7: Typical output window of IITPAVE analysis for normal soil subgrade

Using the aforementioned data, a standard pavement cross-section is provided in Figure 6.8.

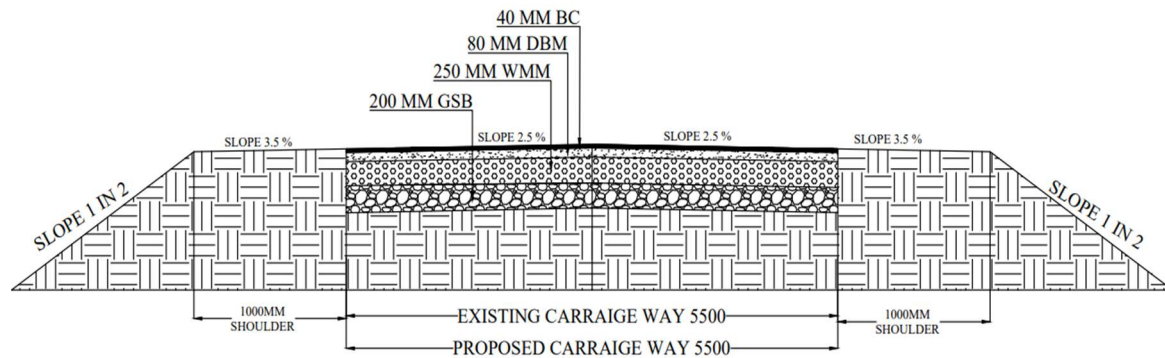


Fig. 6.8: Typical Cross Section of pavement for original Soil Subgrade of CBR 3.36

6.2.3.2 Determination of pavement thickness by IITPAVE using shredded tyre scrap mixed soil as subgrade

To determine the safe thickness for shredded tyre scrap mixed soil as subgrade, the peak CBR value has been considered within the investigation. The CBR value obtained is 8.90 for a mixture containing 10% tyre scrap with a size of 15mm X 15mm. The same equations and methods described earlier (section 6.2.3.1) have been utilized to determine the thickness using IIT PAVE trial method. All parameters, including traffic data, design traffic, and performance criteria, have remained unchanged. For the IIT PAVE design, multiple trial runs have conducted to achieve a pavement design that is both safe and cost-effective. In this case, three (3) test iterations have been conducted, and the findings are delineated in Table 6.6. Figure 12.5 of IRC 37:2018 provides a range of trial pavement thicknesses for 9% CBR. In the present study, Fig. 6.9 represents the trial pavement thickness chart for 9% CBR, following IRC 37:2018. This chart can serve as a reference for categorizing the thickness components of bituminous and granular layer properties derived from IITPAVE analysis.

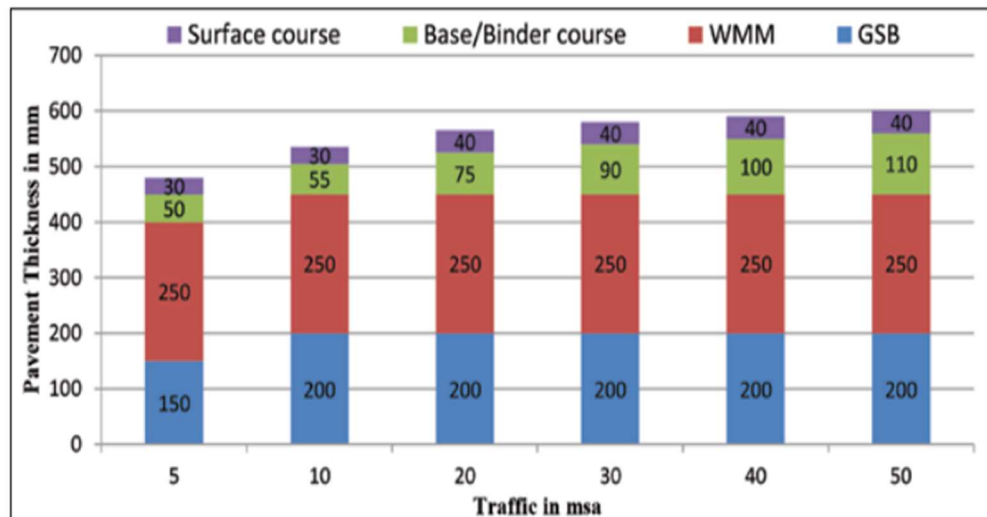


Fig. 6.9: Trial pavement thickness for 9% CBR. (After IRC 37:2018)

Using IIT PAVE software, trial pavement thickness research has been conducted to assess the rutting strain in the subgrade and the tensile strain at the interface between the bituminous and granular layers with an 80 percent reliability. The findings of the analysis are depicted in Table 6.6. Figure 6.10 and Figure 6.11, respectively, depict the standard soil subgrade input and output windows for an IITPAVE study. The input for the software includes all of the parameters described earlier.

The screenshot shows the IITPAVE analysis input window with the following parameters:

- No of Layers:** 3
- Layer 1:** Elastic Modulus(MPa) 3000, Poisson's Ratio 0.35, Thickness(mm) 80
- Layer 2:** Elastic Modulus(MPa) 211.39, Poisson's Ratio 0.35, Thickness(mm) 400
- Layer 3:** Elastic Modulus(MPa) 71.31, Poisson's Ratio 0.35
- Wheel Load(Newton):** 20000
- Tyre Pressure(MPa):** 0.56
- Analysis Points:** 4
- Point:1:** Depth(mm): 80, Radial Distance(mm): 0
- Point:2:** Depth(mm): 80, Radial Distance(mm): 155
- Point:3:** Depth(mm): 480, Radial Distance(mm): 0
- Point:4:** Depth(mm): 480, Radial Distance(mm): 155
- Wheel Set:** 2 (1- Single wheel, 2- Dual wheel)
- Buttons:** Submit, Reset

Fig. 6.10: Typical input window of IITPAVE analysis for tyre scrap modified soil subgrade.

Table 6.6: Trial pavement thickness analysis for tyre scrap modified soil subgrade by IITPAVE

Trial no.	Thickness of bituminous layer	Thickness of granular layer	CBR Value	Resilient Modulus (Subgrade)	Resilient Modulus (Granular)	Resilient Modulus (Bituminous)	Calculated horizontal tensile strain & vertical strain from IITPAVE software		Calculated maximum allowable horizontal tensile strain & vertical strain		Remarks
							Calculated tensile strain at bottom of bituminous	Calculated Vertical Strain at Subgrade	Maximum tensile strain at the bottom of the bituminous layer	Maximum vertical strain on subgrade	
1	75	340	8.90%	71.31	196.48	3000	0.3235×10^{-3}	0.6194×10^{-3}	0.3325×10^{-3}	0.6276×10^{-3}	Design unsafe
2	80	340	8.90%	71.31	196.48	3000	0.3128×10^{-3}	0.5992×10^{-3}	0.3325×10^{-3}	0.6276×10^{-3}	Design unsafe
3	80	400	8.90%	71.31	211.39	3000	0.2963×10^{-3}	0.4915×10^{-3}	0.3325×10^{-3}	0.6276×10^{-3}	Design safe

After several trial runs, the safe thickness has been obtained from Table 6.6. Specifically, in trial 3, the bituminous layer has a thickness of 80mm, while the granular layer is 400 mm thick.

<input type="checkbox"/> OPEN FILE IN EDITOR <input checked="" type="checkbox"/> VIEW HERE										
BACK TO EDIT HOME										
No. of layers 3 E values (MPa) 3000.00 211.39 71.31 Mu values 0.350.350.35 thicknesses (mm) 80.00 400.00 single wheel load (N) 20000.00 tyre pressure (MPa) 0.56 Dual Wheel										
Z	R	SigmaZ	SigmaT	SigmaR	TaoRZ	DispZ	epZ	epT	epR	
80.00	0.00	-0.2206E+00	0.1136E+01	0.9250E+00	-0.1937E-01	0.5189E+00	-0.3139E-03	0.2963E-03	0.2016E-03	
80.00L	0.00	-0.2206E+00	-0.3042E-01	-0.4525E-01	-0.1937E-01	0.5189E+00	-0.9185E-03	0.2963E-03	0.2016E-03	
80.00	155.00	-0.1555E+00	0.7459E+00	-0.4571E-01	-0.9628E-01	0.5223E+00	-0.1335E-03	0.2721E-03	-0.8411E-04	
80.00L	155.00	-0.1555E+00	-0.2528E-01	-0.8106E-01	-0.9628E-01	0.5223E+00	-0.5596E-03	0.2721E-03	-0.8411E-04	
480.00	0.00	-0.3067E-01	0.4161E-01	0.3404E-01	-0.5654E-02	0.3417E+00	-0.2704E-03	0.1913E-03	0.1429E-03	
480.00L	0.00	-0.3062E-01	0.3116E-02	0.5569E-03	-0.5652E-02	0.3417E+00	-0.4475E-03	0.1913E-03	0.1428E-03	
480.00	155.00	-0.3339E-01	0.4521E-01	0.3946E-01	-0.8515E-02	0.3542E+00	-0.2982E-03	0.2038E-03	0.1671E-03	
480.00L	155.00	-0.3339E-01	0.3339E-02	0.1393E-02	-0.8468E-02	0.3542E+00	-0.4915E-03	0.2039E-03	0.1670E-03	

Fig. 6.11: Typical output window of IITPAVE analysis for tyre scrap modified soil subgrade

Using the aforementioned data, a standard pavement cross-section is provided in Fig.6.12

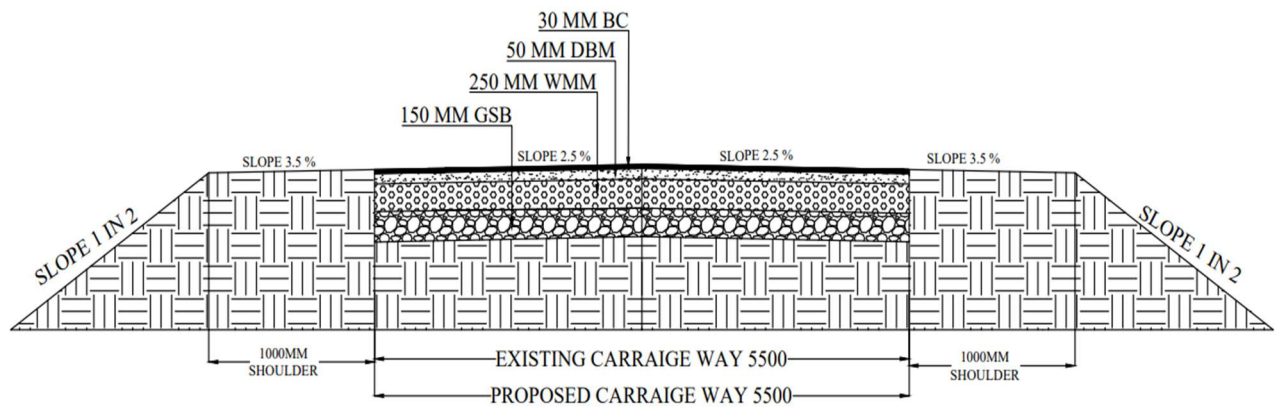


Fig. 6.12: Typical Cross Section of pavement for scrap tyre modified subgrade of CBR 8.90

6.3 STRUCTURAL PERFORMANCE ASSESSMENT STUDY OF SUBGRADE

This step involves the execution of FWD tests and DCPT on both pavement types to evaluate their structural performance. This phase involves preparation of a new Pavement with scrap tyre-modified Subgrade.

By conducting these field studies and assessments, the study aims to offer valuable insights into the performance along with feasibility of utilizing scrap tyre-modified subgrades in pavement construction. In the current study, a FWD has been utilized to evaluate pavement performance. The FWD investigation initially encompasses the full 12.45 km length of an existing road. This comprehensive FWD analysis aims to understand the deflection patterns of the subgrade. Subsequently, a focused study is conducted on a specific 30m segment of the road, between 3.00 km and 3.03 km along the Jibantala-Taldi Road. This section has been selected because it uniquely conformed to the designed pavement cross-section and smooth surface which has a thickness of 570 mm as outlined in Section 6.2.31 of the thesis report. And also, this segment having CBR value at 3.00 km, which was 3.39 as per laboratory tests.

This value is remarkably similar to the intended design value of 3.36, ensuring that the segment is representative for subgrade strength of the entire road. To enhance the study, an additional pavement section, identical in length (30m) and width (5.5m), has been constructed at a distance of 20m from 7.0km chainage point of the existing road. Both the pavement sections have a subgrade depth of 500mm. This new section features a subgrade modified with tyre scrap. Comparative analyses have been performed on both the existing and the newly constructed pavements to evaluate their performances. A detailed methodology for constructing the new pavement is presented below.

6.3.1 Pavement Preparation for Scrap Tyre-Modified Subgrade

To fulfil the main goal of the study, a new pavement of length 30m and width 5.5m has been constructed near the Jibantala-Taldi Road, located within a 20m distance from the existing road. The pavement design calculations (Table-6.6) have computed a safe thickness of 480mm for a modified CBR of 8.90. According to Table-5.7, it has been found that incorporating 10% scrap tyre material, with a size of 15mm x 15mm, mixed with 90% original soil having an approximate CBR of 3.36, results in a combined CBR of 8.90. The following procedures have been established to develop the pavement. Fig. 6.13 represents the site for pavement preparation.



Fig. 6.13: Site before model pavement preparation

6.3.1.1 Preparation of subgrade

To maintain uniformity in the CBR, which is targeted at 3.36, soil samples have been collected from various segments of the Jibantala-Taldi Road where the CBR values approximated 3.36. The subgrade preparation with tyre scrap mixed soil has been executed following the steps described below:

i. Calculation of required soil and tyre scrap in subgrade: To construct the new pavement, the specifications for the subgrade dimensions have been specified as 500mm in depth, 5.5m in width, and 30m in length. Thus, the calculated volume of the Subgrade (V) is $(0.500 \times 5.5 \times 30.0) = 82.5 \text{ m}^3$.

According to Table 5.7 of Chapter 5, the optimum CBR of 8.90 for scrap tyre-modified soil in soaked conditions is observed with an OMC of 17.10% and a MDD of 1.68 g/cc.

Hence, the total dry weight of soil and tyre, required to make the subgrade = $(1.68 \times 82.5) \text{ Ton} = 138.6 \text{ Ton}$

Given that the scrap tyre content constitutes 10% of the dry weight of the soil, the calculation follows as:

Dry weight of soil + 10% of dry weight of soil (Scrap tyre) = 138.6 tons.

Hence, the total dry weight of soil (W_s) is $(138.6/1.1) = 126 \text{ tons}$, and the total weight of scrap tyre is $= 138.6 - 126 = 12.6 \text{ tons}$.

ii. Calculation for bulk volume of soil used in subgrade: Soil samples are collected from specified chainages as detailed in Section 8.3, mixed, and then dumped at the site for subgrade preparation. The required scrap tyre has been also dumped at the site. The moisture content (w) of the blended soil is found to be 19.23% (according to Table 5.5 of Section 5.4.4.1), and the Bulk Density (γ_b) is 2.02 gm/cc. To calculate the amount of bulk soil needed to achieve the required dry soil weight, the following calculation is made,

Here, $w = W_w / W_s = 0.192$, (Where W_w = Weight of water and W_s = Weight of solid = 126 Ton)

Or, $1 + W_w / W_s = 1 + 0.192$

$$\text{Or, } W_w + W_s / W_s = 1.192$$

Hence, $W / W_s = 1.192$ (where $W = W_w + W_s$ = Bulk Weight of mixed soil at Moisture Content(w) of 19.23%)

$$W / 126 = 1.192$$

$$\text{Hence, } W = 150.23 \text{ Ton}$$

$$\text{Total Bulk Volume} = 150.23 / 2.02 = 74.37 \text{ m}^3$$

Therefore, a total bulk volume of 74.37 m^3 of soil, can produce 126 tons of dry soil.

iii. Mixing of soil and scrap tyre for subgrade construction: This 74.37 m^3 of soil, mixed uniformly with 12.6 tons of scrap tyre, to construct pavement of 500mm deep subgrade, 30m length and 5.5m of width. Bulk soil samples have been collected from various points (chainages) along the existing road at 3.00 km, 6.00 km, 7.00 km, 11.00 km, 12.00 km, and 12.45 km, and have been transported to the site using small vehicles. Fig 6.14 shows scrap tyre mixing with subgrade soil.



Fig. 6.14: Scrap tyre mixing with subgrade soil

iv. Subgrade Preparation Process: The subgrade has been compacted manually by ramming and mechanically by using a roller, dividing the total 500mm thickness into three

parts (150mm + 150mm + 200mm). Table 6.7 outlines the soil and scrap tyre requirements for each layer.

Table 6.7: Soil and scrap tyre requirements for each layer

Depth of Sub Grade	Requirement of soil	Requirement of Scrap tyre
150mm	22.31m ³	3.78 T
150mm	22.31m ³	3.78 T
200mm	29.75m ³	5.04 T

By keeping the same soil parameters and calculation guidelines for a pavement with a length of 1 km, width of 5.5 m, and a subgrade depth of 500 mm, the calculated volume of the Subgrade (V) is $(0.500 \times 5.5 \times 1000) = 2750 \text{ m}^3$.

The required amount of bulk soil for the modified pavement will be 2478 m³ and the scrap tyre amount will be 420 tons to achieve the same condition of obtaining a modified CBR of 8.90 from a normal soil CBR of 3.36. Fig. 6.15 shows the subgrade preparation at site.



Fig. 6.15: Preparation of subgrade

6.3.1.2 Preparation of Base and Subbase

i. Granular Sub-Base (GSB) of thickness 150mm: -

The sub-base materials consist of natural sand, moorum, gravel, laterite, kankar, brick metal, crushed slag, crushed stone, reclaimed crushed concrete/reclaimed asphalt pavement, riverbed material, or combinations thereof, tailored to meet grading and physical standards. Granular sub-base (GSB) must adhere to the MORTH Road and Bridge Specifications. The composition of a GSB layer for 1 m³ is as follows:

- 0.2560 m³ of 37.50mm stone chips.
- 0.2560 m³ of 22.40mm stone chips.
- 0.1920 m³ of 11.20mm stone chips.
- 0.3200 m³ of 5.60mm stone chips.
- 0.2560 m³ of Sand.

GSB volume needed for 30m of road, width 5.5m and GSB thickness 0.150m = $(30 \times 5.50 \times 0.15) = 24.75 \text{ m}^3$

Based on this volume, the required materials have been collected to prepare the GSB.

ii. Wet Mix Macadam (WMM) of thickness 250mm: -

This procedure entails supplying, distributing, compacting, and laying graded stone aggregate in accordance with WMM specifications. It also includes screening granular and aggregate materials, pre-mixing them at Optimum Moisture Content (OMC) in the wet mix plant, transporting the blended material to the site, and spreading it in consistent layers. According to Clause 406 of the Specifications for Road & Bridge Works of the Ministry of Road Transport & Highways (5th Revision), the composition of a GSB layer for 1 m³ is as follows:

- 0.3960 m³ of 26.50mm stone chips.
- 0.2640 m³ of 13.20mm stone chips.
- 0.3564 m³ of 5.60mm stone chips.
- 0.3036 m³ of stone dust

WMM volume needed for 30m of road, width 5.5m and WMM thickness 0.150m= (30 x 5.50 x 0.25) = 41.25 m³

Based on this volume, the required materials have been collected to prepare the WMM. Fig. 6.16 shows the subbase preparation at site.



Fig. 6.16: Preparation of subbase layer

ii. Dense Bituminous Macadam (DBM) of thickness 50mm: -

The preparation of DBM entails supplying and deploying dense bituminous macadam through a Hot Mix Plant capable of manufacturing an average of 75 tonnes of material per hour. The plant uses coarse, fine, and filler aggregates as well as bituminous binder in accordance with the design Job Mix Formula that complies with the Marshall Method specifications. Additionally, chip cleaning and screening are done, and the plant creates a uniform and high-quality mix that ensures all of the mineral aggregate particles are coated evenly. The heated mixture is subsequently conveyed to the construction site, where the blended materials are placed at the specified temperature. In accordance with Clause 505 of the Specifications for Road & Bridge Works of the Ministry of Road Transport & Highways (5th Revision), composition of DBM layer for 1 m³ as follows-

- 0.2197 m³ of 26.50mm stonechips.
- 0.2197 m³ of 22.40mm stonechips
- 0.3662 m³ of 11.20mm stonechips
- 0.2197 m³ of 5.60mm stonechips
- 0.4394 m³ of stone dust and grit.
- 44kg of lime stone dust.
- 111kg of Bitumen 30grade

DBM volume needed for 30m of road, width 5.5m and DBM thickness 0.05m= (30 x 5.50 x 0.05) = 8.25 m³.

Based on this volume, the required materials have been collected to prepare the DBM. Fig. 6.17 shows the surface layer preparation at site.



Fig. 6.17: Preparation of surface layer

iii. Bituminous Concrete (BC) of thickness 30mm: -

In this process, bituminous concrete is provided and laid using a Hot Mix Plant incorporating coarse aggregates, fine aggregates, filler materials, and bituminous binder that meets the necessary specifications. Additionally, chips are screened, cleaned, and a uniform and high-quality mix is prepared in the Hot Mix Plant, guaranteeing that all of the mineral aggregate

particles are coated evenly. The heated mixture is then conveyed to the construction site, where the blended materials are laid at a pre-determined temperature. In accordance with Clause 507 of the Specifications for Road & Bridge Works of the Ministry of Road Transport & Highways (5th Revision), composition of BC layer for 1 m³ as follows-

- 0.2959 m³ of 13.20mm stonechips.
- 0.2959 m³ of 11.20mm stonechips.
- 0.2959 m³ of 5.60mm stonechips.
- 0.5919 m³ of stone dust and grit.
- 45kg of lime stone dust.
- 137kg of Bitumen 30grade.

BC volume needed for 30m of road, width 5.5m and DBM thickness 0.03m= (30 x 5.50 x 0.03) = 4.95 m³.

Based on this volume, the required materials have been collected to prepare the BC. Fig. 6.18 shows the finished pavement at site.



Fig. 6.18: Finished pavement under FWD study

6.3.2 FWD Study on Pavement

The FWD is a key NDT equipment for evaluating pavement strength, capable of calculating the elastic modulus of individual layers (Walubita et al. 2011 and Solanki et al. 2014). In the current study, the primary objective is to conduct a comparative analysis between the subgrade deflection and elastic modulus of existing pavement and pavement modified with scrap tyre materials. Transportation engineers typically employ FWD measurements for overlay design purposes. In order to conduct the FWD survey on the project road, GEOTRAN FWD, which is a Fully-Automatic Trailer-mounted system was employed as shown in Fig. 6.19. This specialized FWD system has the capability to apply a loading force within the range of 0-100 kN, allowing it to effectively simulate various types of vehicles loads on the pavement surface.



Fig. 6.19: GEOTRAN FWD operation under process

6.3.2.1 Locations of FWD Test

The focus is on the 3.00 km to 3.03 km stretch of Jibantala-Taldi Road, chosen for its smooth surface and uniform cross-section, which is ideal for FWD tests. Both the modified and

existing pavements, each 30.00m in length, have been divided into four equal segments of 10.0m for testing, allowing for direct performance comparison. This methodological approach has ensured a precise evaluation of the impact of tyre scrap on pavement quality. Table 6.8 shows the different chainage points under study.

Table 6.8: Test points and Chainages

Sl. No	Pavement type	Selected Chainage (m) for FWD test	FWD test points			
			1st point	2nd point	3rd point	4th point
1	Existing pavement	3.00×10 ³ m to 3.03×10 ³ m	At 3.00×10 ³ m	At 3.01×10 ³ m	At 3.02×10 ³ m	At 3.03×10 ³ m
2	Modified pavement	0.00 m to 30.00m	At 0.00m	At 10.00m	At 20.00m	At 30.00m

6.3.2.2 Details of FWD equipment

The equipment is equipped with a backup battery and is conveniently trailer-mounted, complete with all necessary accessories for pavement evaluation. The following describes the primary parts of the GEOTRAN FWD system.:

- i. The Vehicle: To accommodate the whole FWD system, including the hydraulic and electrical connections, the car has undergone unique modifications. These adjustments are made to make room for necessities like working people, electronic circuits, and personal computers. To extract electricity from the car's engine for the purpose of charging the batteries, an alternator is integrated. The computer and electronic circuitry are powered by a sine wave inverter. A 550 mm diameter hole is created in the floor of the vehicle to facilitate the passage of the loading plate and falling mass during the FWD testing process. To warn other drivers during testing, especially at night, the vehicle also has flashing lights installed.
- ii. Supporting Frame: A sturdy rectangular frame is constructed and firmly attached to the floor of the vehicle to protect the FWD system from harsh weather conditions.

iii. Mass and Rubber Pad Arrangement: The FWD system includes a two-stage cylinder, with its base secured to the upper horizontal element of the supporting frame. The cylinder's bottom flange is where the loading plate assembly is attached. To measure load impact, a load sensor with a capacity of 100 kN, known as the Strain Impact Sensor, is positioned on the loading plate assembly. This assembly comprises a 300 mm diameter bottom plate with a rubber sole affixed to its underside to ensure the even distribution of the load during testing.

iv. Loading Plate Assembly: A universal joint is installed at the base of the top plate of the assembly to provide flexibility and ensure uniform placement on the pavement. To house the central geophone, a casing is constructed.

v. Geophone Arrangement: To gauge the deflections of the pavement surface, seven geophones are situated within a geophone frame at radial intervals of 0, 300, 600, 900, 1200, 1500, and 1800 from the center of the loading plate. The loading plate assembly contains the first geophone. The hydraulic system moves the geophone frame vertically and straightens and folds it. Moreover, this instrument mostly exceeds or matches all the criteria given in the IRC: 115- 2014.

6.3.2.3 Testing procedure & frequency

The detailed test methodology and the procedure have been described in IRC: 115-2014 “Guidelines for Structural Evaluation and Strengthening of Flexible Road Pavements Using Falling Weight Deflectometer (FWD) Technique”. However, as per the requirement, the sampling procedure has been customized in this project. In adherence to the same, structural evaluation of the existing ‘pavement and subgrade system’ by measuring its response in terms of deflection has been carried out using FWD for the project roads in the month of January 2022 (16/01/2022 to 17/01/2022). In the present work, FWD is applied to measure subgrade deflection of the pavements, in line with the procedures outlined in Section 3 of IRC 115: 2014. This analysis involves testing at various locations as described in Table 6.8. For both pavements the intermediate distance for testing is 10.0m, for the newly constructed modified

pavement, the entire length of 30.0m is partitioned into four (4) segments, each measuring 10.0m in length. Using a load of 40 kN or a contact pressure of 565.9 kPa, Maree and Bellekens (1991) and Maree and Jooste (1999) analysed deflection bowls obtained during FWD testing. They concentrated on a range of common pavement structures seen in South Africa, such as bituminous, cemented base pavements, and granular pavements. High-density (FWD) surveys covering the outside and inside wheel tracks of the slow, fast, and shoulder lanes on various roadways have been conducted at intervals of 5.0m to 10.0m. After that, elastic moduli have been ascertained using back-analysis techniques that considered the known layer thicknesses.

6.3.2.4 Testing Equipment:

The equipment used for the testing is-

- i. The GEOTRAN FWD Trailer Mounted FWD is equipped with one loading plate and seven geophones positioned at intervals of 0, 300, 600, 900, 1200, 1500, and 1800 mm from the centre of the loading plate.
- ii. Towing Vehicle.
- iii. GPS, Air Temperature and Pavement Surface Temperature sensors as part of the FWD instrument.
- iv. Red flags and red cones and flashing lamps for traffic arrangement.

6.3.2.5 Pavement composition details:

The existing details of the pavement crust have been furnished and the pit results have been presented in Table 6.9 for both types of pavements. Further analysis of the FWD data has been conducted based on these pit results.

Table 6.9: Crust thickness for both the pavements

Category	Layers	Pavement thickness of existing road Subgrade	Pavement thickness for scrap tyre modified subgrade
Bituminous Layer	BC	40mm	30mm
	DBM	80mm	50mm
Granular layer	WMM	250mm	250mm
	GSB	200mm	150mm
Total thickness		570mm	480mm

6.3.2.6 CBR determination for FWD

This study has been divided into field and laboratory components to examine and compare the performance between the existing and modified pavements. In the current study, a specific 30.0 m stretch of the Jibantala-Taldi Road, precisely between the 3.00 km to 3.03 km chainage has been selected. This segment has been selected due to its CBR value at 3.00 km, which was 3.39 as per laboratory tests. This value is remarkably similar to the intended design value of 3.36, ensuring that the segment is representative for subgrade strength of the entire road. The modified model pavement length is 30.0m, hence for further study, 30m length has been considered for the old pavement also. This methodological approach ensures a precise evaluation of the impact of tyre scrap on pavement quality. Table 6.10 shows the different chainage points under study.

Table 6.10: CBR Test points and chainage

Sl. No	Pavement type	Selected Chainage (m) for/Lab test and DCPT test	Test points			
			1 st point	2 nd point	3 rd point	4 th point
1	Existing pavement	3.00×10 ³ m to 3.03×10 ³ m	At 3.00×10 ³ m	At 3.01×10 ³ m	At 3.02×10 ³ m	At 3.03×10 ³ m
2	Modified pavement	0.00 m to 30.00m	At 0.00m	At 10.00m	At 20.00m	At 30.00m

Hence, the determination of the CBR value, used for the FWD test according to IRC: 115-2014, has been divided into two parts: one is the in-situ or field CBR determination by DCPT, and the other is CBR determination by laboratory tests. The aspects of both tests are discussed below-

i. In-situ CBR determination by Dynamic Cone Penetration Test (DCPT)

In accordance with clause 5.5.4 of IRC: 115-2014, CBR values have been obtained through the DCPT within the designated pavement section provide the foundation for determining the elastic modulus of that specific segment. In several studies, DCPT has been performed to determine the in-situ CBR or field CBR of the soil. Nwanya and Okeke (2018), used the DCPT in Owerri, southeastern Nigeria, to assess subsurface soils up to 6 meters deep, determining CBR and bearing pressure. The study identified three (3) soil layers with varying densities and resistances. The penetration resistance ranged from 11.4 to 55.5 mm/blow, revealing layers of loose, medium, and dense soils. CBR values increased from 5% to 16% with depth, while average bearing pressures rose significantly from 104.8 to 301.1 KN/m², indicating increasing soil strength with depth. Sahoo and Reddy (2018), studied, using DCPT to estimate soil strength, specifically targeting the relationship between DCPT and CBR values in fine-grained soils. They conducted laboratory experiments to explore the correlation between CBR values and DCP penetration depth across different fine-grained soil types. Their results indicated a strong correlation between CBR and DCP values for each soil type and across the combined data set. To encapsulate this relationship, they formulated logarithmic equations: $\text{Log}_{10} \text{LAB CBR} = 2.758 - 1.274 \text{Log}_{10} \text{LAB DCP}$ and $\text{Ln CBR} = 67.898 - 17.483 \text{Ln (FIELD DCP)}$, further confirming the strong link between CBR and DCPT values. These studies collectively contribute to a deeper understanding of pavement engineering, offering innovative methodologies for assessing, designing, and maintaining pavement performance.

Lee et al. (2019), evaluated subgrade strength using DCP. It highlights the limitations of standard DCPs and introduces an advanced version with a load cell and accelerometer integrated at the cone tip. This instrumented DCP records dynamic responses and computes the dynamic cone resistance, serving as a novel strength index. Tests on weathered soils indicate this method offers a more reliable subgrade strength profile, with the potential for improved pavement design and construction quality assurance. Within this current research study, the scope of DCPT testing encompasses the section from the 3.0 km chainage point to the 3.03 km chainage point. The project area is characterized by a consistent soil profile primarily comprised of Grey/Brownish Silty Clay. To facilitate a comprehensive assessment of subgrade characteristics, 1m x 1m test pits were excavated at 30.0m intervals, organized in a staggered pattern. This procedure was replicated for the newly constructed scrap tyre modified subgrade, with DCPT measurements conducted at Four (4) distinct locations, spaced at 10m intervals, as specified in Table 6.10. Within each of these test pits, the DCPT method was utilized to determine the in-situ CBR of the subgrade. In the present study, DCP was made by EIE Instruments Pvt. Ltd. India. Notably, the subgrade maintains a consistent thickness of 500mm. Vakili et al. (2021), demonstrated that adding lime to marl soil improved its mechanical properties, including UCS and CBR, validating the effectiveness of DCPT in soil behaviour analysis. In the present work, the comprehensive summary of the test results is presented in Table 6.11. The DCPT-oriented in-situ CBR test results have been obtained by using 3 different methods as described in Table 4.3 of Chapter 4. DCPT operation on the existing subgrade has been shown in Fig. 6.20.



Fig. 6.20: DCPT operation on subgrade

To determine the worst-case scenario, the minimum CBR value among the three has been considered for further study.

Table 6.11: Summary of DCPT test results

Sl. No	Chainage (in m)	Side	Visual classification of soil	Average CBR by Harrison	Average CBR by Kleyn	Average CBR by Livneh	DCPT inferred CBR
For existing pavement							
1	3.00×10^3 m	L/S	Grey silty clay	4.99	3.82	4.6	3.82
2	3.01×10^3 m	R/S	Grey silty clay	5.01	3.83	4.62	3.83
3	3.02×10^3 m	L/S	Grey silty clay	5.1	3.91	4.69	3.91
4	3.03×10^3 m	R/S	Grey silty clay	5.8	4.5	5.32	4.5
For Scrap tyre modified pavement							
5	0.00m	L/S	Grey silty clay	11.16	9.21	10	9.21
6	10.00m	R/S	Grey silty clay	10.26	9.3	10.09	9.3
7	20.00m	L/S	Grey silty clay	11.27	9.33	10.1	9.33
8	30.00m	R/S	Grey silty clay	11.37	9.4	10.18	9.4

Fig.6.21 and Fig.6.22 show the sample DCPT curves for existing subgrade and modified subgrade.

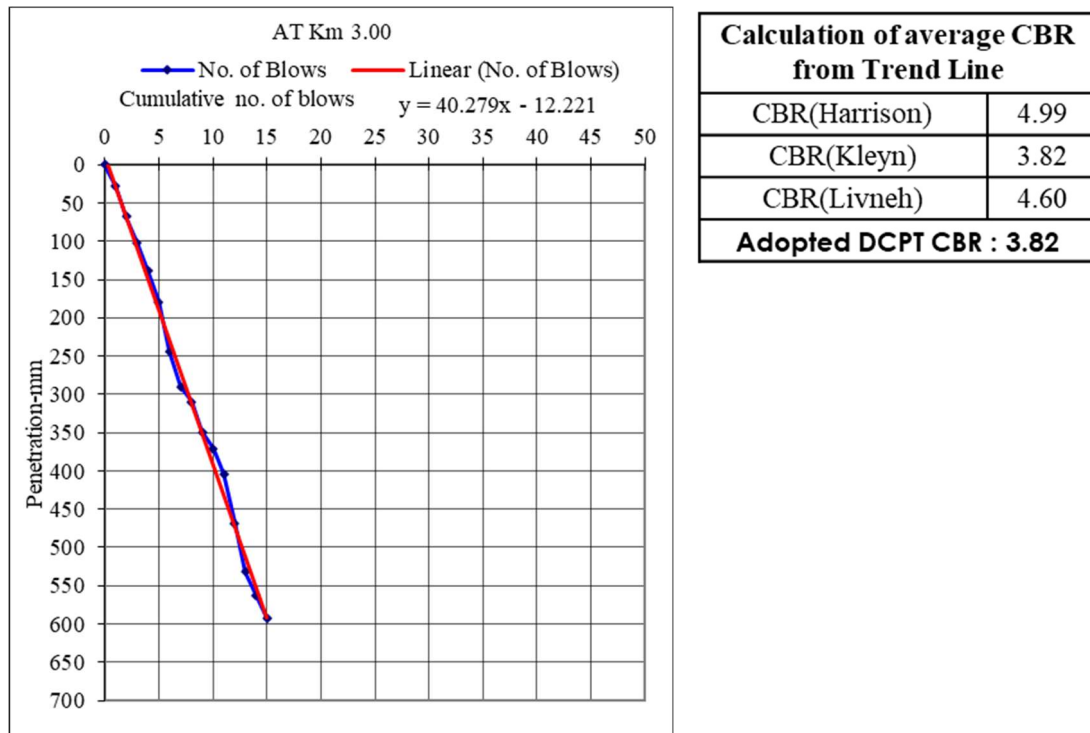


Fig. 6.21: DCPT Test Result Graph for existing subgrade at Chainage 3.0×10^3 m

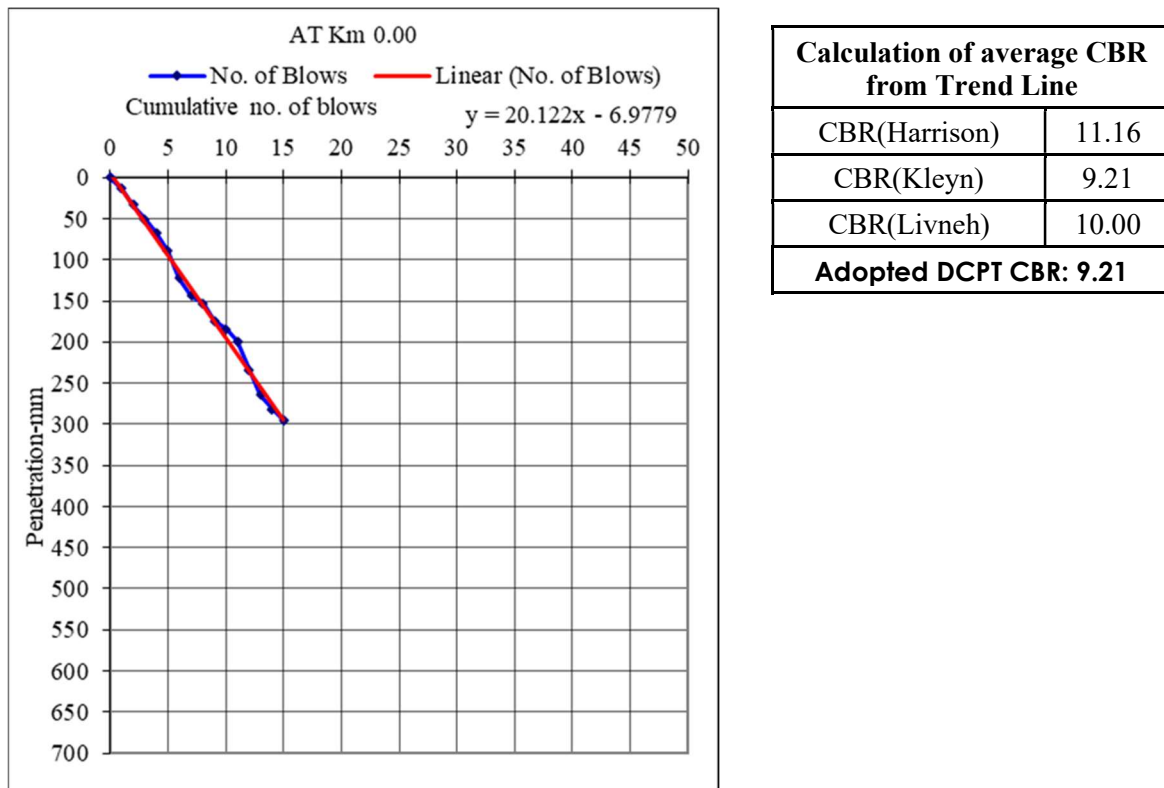


Fig. 6.22: DCPT Test Result Graph for modified subgrade at Chainage 0.00m.

ii. CBR determination by Laboratory testing

Modified proctor and CBR tests have performed on the collected samples from the existing road subgrade and modified subgrade. The test values along with locations are have been illustrated in Table 6.12.

Table 6.12: Modified Proctor and CBR test results for existing and modified subgrade soil

Sl. No	Chainage (in Km)	Side	Visual classification of soil	OMC (%)	MDD Density(gm/cc)	Lab CBR %(Soaked)
1	3.00×10 ³ m	L/S	Grey silty clay	17.11	1.714	3.40
2	3.01×10 ³ m	R/S	Grey silty clay	17.09	1.719	3.43
3	3.02×10 ³ m	L/S	Grey silty clay	17.09	1.720	3.37
4	3.03×10 ³ m	R/S	Grey silty clay	17.06	1.720	3.39
5	0.00m	L/S	Grey silty clay	16.59	1.629	8.79
6	10.00m	R/S	Grey silty clay	16.61	1.628	8.84
7	20.00m	L/S	Grey silty clay	16.59	1.631	8.83
8	30.00m	R/S	Grey silty clay	16.62	1.631	8.80

Fig.6.23 and Fig. 6.24 show the modified proctor and CBR curve for both the pavements

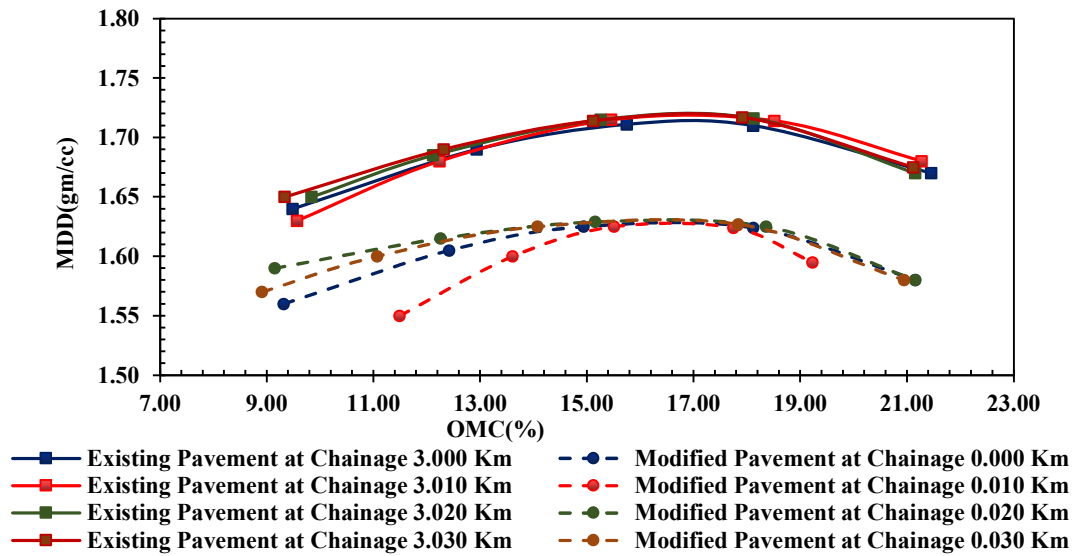


Fig. 6.23: Variation in modified proctor for different pavements

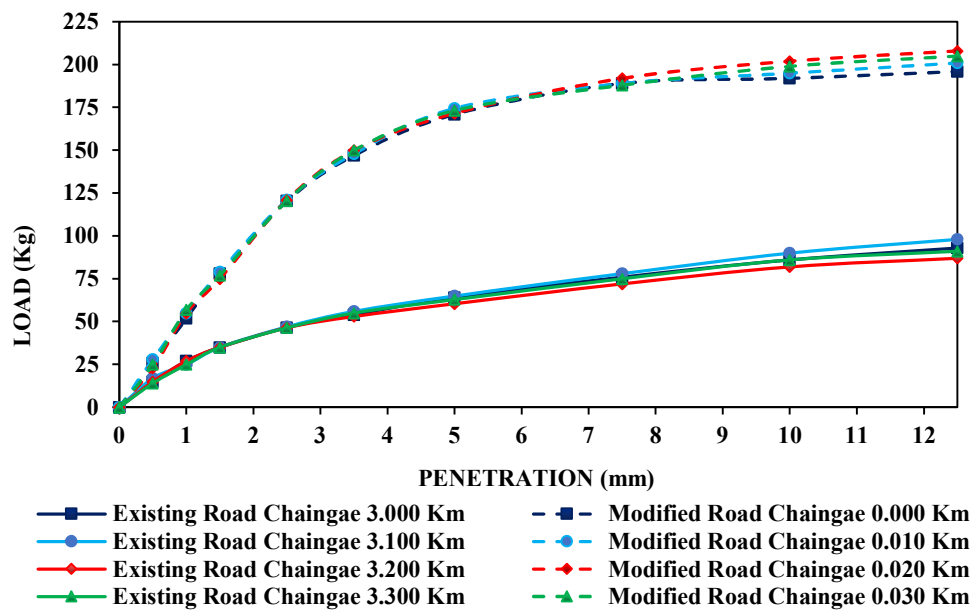


Fig. 6.24: Variation in CBR for different pavements

iii. DCPT test results analysis for FWD test

DCPT penetration resistance values have been obtained at various test locations along the road stretch. These values have been used to calculate the field CBR using relevant correlations.

To determine the laboratory CBR, soil samples have been collected from the chainage points specified in Table 6.10. The calculated field CBR values are then compared with the laboratory CBR values, which are given in Table: 6.13.

Table 6.13: Comparison table between field and laboratory CBR

Sl. No.	Chainage (in m)	Lab CBR % (Soaked)	DCPT inferred CBR
CBR Values for existing subgrade			
1	3.00×10 ³	3.40	3.82
2	3.01×10 ³	3.43	3.83
3	3.02×10 ³	3.37	3.91
4	3.03×10 ³	3.39	4.50
CBR Values for modified subgrade			
5	0.00	8.79	9.21
6	10.00	8.84	9.30
7	20.00	8.83	9.33
8	30.00	8.80	9.40

From the above table, it is evident that based on the DCP tests conducted along the road stretch from Jibantala Bazar to Taldi Bazar, field CBR values have been calculated and compared with the corresponding laboratory CBR values. This analysis reveals a valuable insight into the load-bearing capacity of the subgrade soil. For the existing pavement, laboratory CBR values range from 3.39 to 3.43, while for the tyre scrap modified subgrade pavement, they range from 8.79 to 8.84. In contrast, the DCPT values range from 3.82 to 4.50 for the existing pavement and 9.21 to 9.40 for the subgrade-modified pavement. To ensure a conservative analysis for further processing in FWD and to account for the worst-case scenario, the minimum CBR values obtained from laboratory tests have been considered for further analysis. These values are 3.39 and 8.79 for the existing subgrade and scrap tyre-modified subgrade, respectively. It is worth noting that Solanki et al. (2016) employed laboratory CBR

values in their FWD analysis for the Barnala - Mansa Section of SH13, which spans a length of 20 km in the district of Barnala, Punjab, India.

6.3.2.7 FWD test on existing pavement and tyre scrap modified pavement

i. Identification of test points

A) Chainage wise test points for both the pavements

The test point locations are pre-determined, and points are calculated for each section of the project. These sections are then subdivided based on the data from the visual pavement condition survey and test pit information. To account for various factors and establish comparability between the two pavements, both roads are partitioned into four equal parts for conducting the FWD test. All the FWD test points with chainage are outlined in Table 6.14

Table 6.14: FWD test points and chainage

Sl. No	Pavement type	Selected Chainage (m) for FWD test	FWD test points			
			1st point	2nd point	3rd point	4th point
1	Existing pavement	$3.00 \times 10^3 \text{m}$ to $3.03 \times 10^3 \text{m}$	At $3.00 \times 10^3 \text{m}$	At $3.01 \times 10^3 \text{m}$	At $3.02 \times 10^3 \text{m}$	At $3.03 \times 10^3 \text{m}$
2	Modified pavement	0.00 m to 30.00m	At 0.00m	At 10.00m	At 20.00m	At 30.00m

B) Standardized Representation of test points

The study compares two pavements by dividing each into four equal segments by establishing specific Reference Chainage (RC) points for further analysis. Both pavements are 30.0m long but with different chainages. To simplify deflection data representation, the chainages are categorized as RC1 (0.00m for modified and $3 \times 10^3 \text{m}$ for existing pavement), RC 2 (10.0m for modified and $3.01 \times 10^3 \text{m}$ Km for existing pavement), RC 3 (20.0m for modified and $3.02 \text{Km} \times 10^3 \text{m}$ for existing pavement), and RC 4 (30.0m for modified and $3.03 \times 10^3 \text{m}$ for existing pavement).

ii. Collection of deflection data from FWD

To satisfy the criteria of the present study, FWD tests were conducted between 3.0 km and 3.03 km chainage points on the existing pavement. Fig. 6.25 depicts the FWD test and deflection recording on the Jibantala-Taldi Road to obtain deflection data for individual geophones.



Fig. 6.25: FWD deflection recording on Jibantala -Taldi Road

For the existing subgrade deflection data from four points as specified in Table 6.14 are gathered specifically for structural performance analysis of subgrade, and these data points are presented in Table 6.15.

Table 6.15: Summary of average deflection (For Existing pavement)

Chainage (m)	Distance from Load Centre(mm)						
	0	300	600	900	1200	1500	1800
	Deflection(mm)						
	D0	D1	D2	D3	D4	D5	D6
3.00×10³m	0.519	0.322	0.197	0.099	0.063	0.048	0.022
3.01×10³m	0.509	0.324	0.217	0.109	0.065	0.047	0.037
3.02×10³m	0.529	0.34	0.236	0.093	0.063	0.047	0.038
3.03×10³m	0.518	0.342	0.146	0.096	0.062	0.047	0.036
Average deflection	0.519	0.332	0.199	0.099	0.063	0.047	0.033

FWD test has been also conducted on the scrap tyre modified subgrade pavement at various specified intervals between 0.00Kmp to 0.030Kmp. The deflection data from four chainage points for the modified subgrade are specified in Table 6.16.

Table 6.16: Summary of average deflection (for modified subgrade)

Chainage (m)	Distance from Load Centre(mm)						
	0	300	600	900	1200	1500	1800
	Deflection(mm)						
	D0	D1	D2	D3	D4	D5	D6
0.00m	0.412	0.172	0.078	0.051	0.029	0.019	0.013
10.00m	0.422	0.165	0.08	0.049	0.027	0.021	0.018
20.00m	0.387	0.15	0.075	0.044	0.038	0.025	0.015
30.00m	0.393	0.158	0.074	0.051	0.025	0.022	0.012
Average deflection	0.404	0.161	0.077	0.049	0.03	0.022	0.015

Fig.6.26 represents deflection records of scrap tyre modified subgrade. The deflection data for both the subgrades have been gathered specifically for performance analysis of pavement subgrade. Fig. 6.27 illustrates the deflection data collected for the subgrades.



Fig. 6.26: FWD deflection recording on scrap tyre modified subgrade pavement

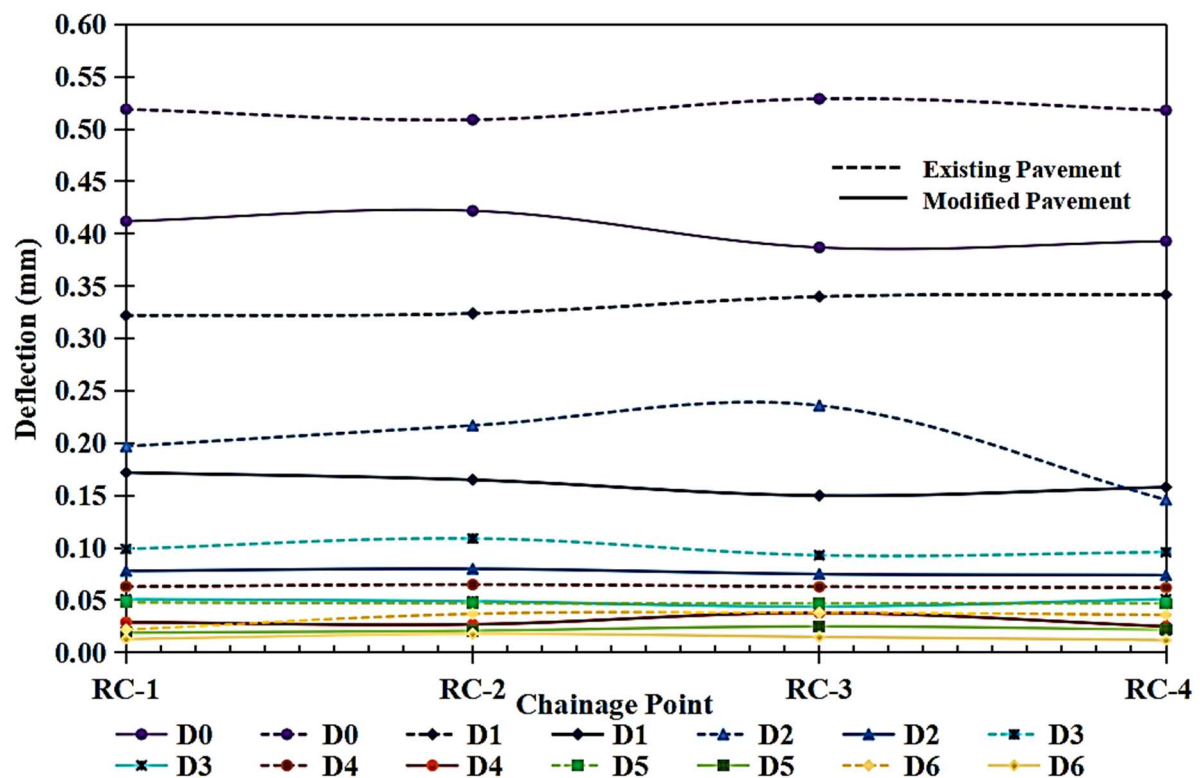


Fig. 6.27: Deflection data collected for the subgrades

6.3.2.8 Back Calculation of Layer Modulus (KGPBACK) for both type of pavement

The FWD is used to impart a dynamic load to the existing pavement, and the response is recorded. Using the deflection values that were acquired, the KGPBACK program is then used in accordance with IRC: 115-2014 recommendations to ascertain the elastic modulus of the pavement layers that were modelled. The KGPBACK software has been utilized for back calculating the layer modulus. The bituminous layer, granular layer, and subgrade make up the three layers of the pavement system that have been modelled. The transportation engineering department at IIT Kharagpur, India, created the KGPBACK software, a customized version of the BACKGA program, which is an essential tool for the back-analysis process that determines the elastic modulus of pavement surfaces. The deflection measurements used in this computation come from the FWD. By calculating the in situ elastic modulus of various pavement layers, this process aims to evaluate the structural health of in-

service pavements. The pavement layer modulus is obtained by using the KGPBACK software with normalized data and the extra input parameters specified in Table 6.17.

Table 6.17: Input parameters for KGPBACK software analysis

Sl.No	Parameters	Values			
		For existing pavement		For scrap tyre modified subgrade pavement	
1	Single Wheel Load (N)	40000		40000	
2	Contact Pressure (MPa)	0.56 (As per IRC: 115-2014)		0.56 (As per IRC: 115-2014)	
3	Number of deflections	7		7	
4	Radial distance between each geophone (mm)	0	300 600 900 1200 1500 1800	0	300 600 900 1200 1500 1800
5	Design CBR (%)	3.36		8.90	
6	Measured Deflections (mm)	As per Table 6.15		As per Table 6.16	
7	Pavement Layer Thickness(mm)	570		480	
8	Poisson's ratio values	0.5 ,0.4, 0.4 (bituminous layer, granular layers & subgrade as per IRC: 115-2014)		0.5 ,0.4, 0.4 (bituminous layer, granular layers & subgrade as per IRC: 115-2014)	
9	Moduli range (as per Clause III.8.4 of IRC:115 2014 guidelines) in MPa	BT Layer	750 to 3000	BT Layer	750 to 3000
		Granular	100 to 500	Granular	100 to 500
		Subgrade	16.8 to 67.2	Subgrade	44.5 to 178.0
		(5* CBR to 20*CBR)		(5* CBR to 20*CBR)	

The sample inputs and outputs of the KGPBACK are illustrated from Fig. 6.28 to Fig. 6.31

```

!!!!!!          PRINT INPUT DATA          !!!!!
!!!!!!    PL. SEE THE MANUAL SUPPLIED FOR HELP    !!!!!

TYPE PEAK FWD LOAD (N), CONTACT PRESSURE (MPa)
Standard Values are 40000 0.56
40000 .56

HOW MANY DEFLECTIONS WERE MEASURED (4 TO 10)?
7

PRINT RAD.DISTANCES (mm) WHERE DEFLECT. WERE MEASURED
eg: 0, 300, 600, 900, 1200, 1500 is a Typical
    Configuration for six Geophones

0 300 600 900 1200 1500 1800

PRINT MEASURED DEFLECTIONS IN mm.
.519 .322 .197 .099 .063 .048 .022
GIVE THE PAVEMENT RELATED INPUTS (3-LAYER SYSTEM)
TYPE EACH LAYER THICKNESS(mm). START FROM TOP
120 450

TYPE POISSON RATIO OF EACH LAYER. START FROM TOP
Suggested values are 0.5 0.4 0.4
.5 .4 .4

INPUT RANGE (lower and upper) FOR EACH LAYER MODULUS
Please note that Backcalculation Results will depend
on the selection of appropriate Ranges. The selection
of Ranges has to be made judiciously on the basis of
of the Pavement Condition

PRINT LOWER AND UPPER BOUND MODULI (MPa) LAYERS
Pl. See the Manual supplied for guidance

750 3000
100 500
16.8 67.2

```

Fig. 6.28: Sample Input window of KGPBACK for existing pavement

```

#####
#          !!! THANKS FOR USING KGPBACK !!!          #
#          THE RESULTS ARE GIVEN BELOW                #
#####

#####
# INPUT DATA #
#####
No. of Layers                = 3
FWD Load (N)                = 40000.00
Contact Pressure (MPa)      = .56
No. of Deflection points    = 7
Deflections measured using FWD (mm) = .51900 .32200 .19700 .09900 .06300 .04800 .02200
Radial distances from centre of load(mm) = .0 300.0 600.0 900.0 1200.0 1500.0 1800.0
Layer thickness (mm)        = 120.00 450.00
Poisson ratio values        = .50 .40 .40
Layer Modulus (MPa) Ranges Selected :-
(a) Bituminous Surfacing    = 750.0 3000.0
(b) Granular Base           = 100.0 500.0
(c) Subgrade                = 16.8 67.2

#####
# OUTPUT DATA #
#####

Backcalculated Layer Moduli are:
Surface (MPa) = 2296.2
Base (MPa)    = 102.3
Subgrade (MPa) = 67.2

```

Fig. 6.29: Sample output window of KGPBACK for existing pavement


```

TYPE PEAK FWD LOAD (N), CONTACT PRESSURE (MPa)
Standard Values are 40000 0.56
40000 .56

HOW MANY DEFLECTIONS WERE MEASURED (4 TO 10)?
7

PRINT RAD.DISTANCES (mm) WHERE DEFLECT. WERE MEASURED
eg: 0, 300, 600, 900, 1200, 1500 is a Typical
Configuration for six Geophones

0 300 600 900 1200 1500 1800

PRINT MEASURED DEFLECTIONS IN mm.
.412 .172 .078 .051 .029 .019 .013
GIVE THE PAVEMENT RELATED INPUTS (3-LAYER SYSTEM)
TYPE EACH LAYER THICKNESS(mm). START FROM TOP
80 400

TYPE POISSON RATIO OF EACH LAYER. START FROM TOP
Suggested values are 0.5 0.4 0.4
.5 .4 .4

INPUT RANGE (lower and upper) FOR EACH LAYER MODULUS
Please note that Backcalculation Results will depend
on the selection of appropriate Ranges. The selection
of Ranges has to be made judiciously on the basis of
of the Pavement Condition

PRINT LOWER AND UPPER BOUND MODULI (MPa) LAYERS
Pl. See the Manual supplied for guidance

750 3000
100 500
44.5 178

```

Fig. 6.30: Sample Input window of KGPBACK for modified pavement

```

#####
#      !!! THANKS FOR USING KGPBACK !!!      #
#      THE RESULTS ARE GIVEN BELOW           #
#####

#####
# INPUT DATA #
#####
No.of Layers                = 3
FWD Load (N)                = 40000.00
Contact Pressure (MPa)      = .56
No.of Deflection points     = 7
Deflections measured using FWD (mm) = .41200 .17200 .07800 .05100 .02900 .01900 .01300
Radial distances from centre of load(mm) = .0 300.0 600.0 900.0 1200.0 1500.0 1800.0
Layer thickness (mm)        = 80.00 400.00
Poisson ratio values        = .50 .40 .40
Layer Modulus (MPa) Ranges Selected :-
(a) Bituminous Surfacing    = 750.0 3000.0
(b) Granular Base           = 100.0 500.0
(c) Subgrade                = 44.5 178.0

#####
# OUTPUT DATA #
#####

Backcalculated Layer Moduli are:
Surface (MPa) = 2997.8
Base (MPa)    = 176.6
Subgrade (MPa) = 178.0

```

Fig. 6.31: Sample Output window of KGPBACK for modified pavement

The back-calculated modulus of each layer is computed and shown in Table 6.18 using the inputs listed in Table 6.17. Fig. 6.32 shows the back-calculated modulus chart for both the pavements.

Table 6.18: Back calculated moduli for pavement layers

Pavement type	Back calculated Moduli (MPa)			
	Chainage (m)	Bituminous	Granular	Subgrade
Existing pavement	3.00×10 ³ m	2296.20	102.30	67.20
	3.01×10 ³ m	2975.80	107.80	67.20
	3.02×10 ³ m	2300.60	111.30	67.20
	3.03×10 ³ m	2925.20	189.90	67.20
Modified pavement	0.00m	2997.80	176.60	178.00
	10.00m	2918.60	189.90	178.00
	20.00m	2958.20	232.20	178.00
	30.00m	2815.20	186.80	178.00

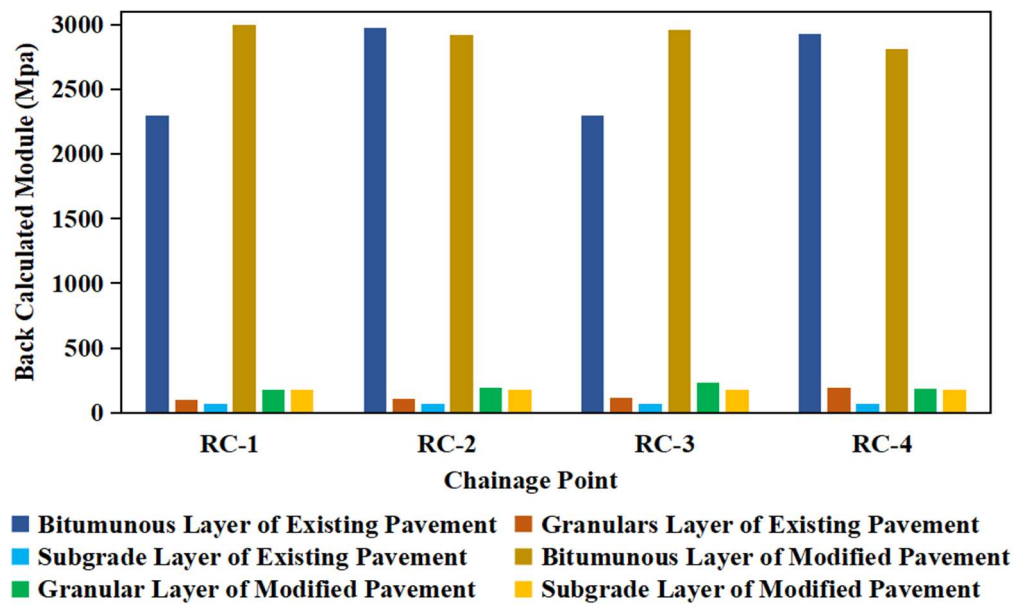


Fig. 6.32: Back calculated moduli chart for both the pavements

6.3.2.9 Determination of corrected back calculated moduli (MPa)

Back-calculated moduli of bituminous, granular, and subgrade layers obtained via software analysis have been modified using appropriate correction factors:

- i. A pavement temperature correction factor has been applied exclusively to the bituminous layer, following the guidelines outlined in clause 6.4.2 of IRC:115-2014. Table 6.19 illustrates the calculation of correction factors and the resulting corrected back-calculated moduli for the bituminous layer, specifically accounting for temperature variations.

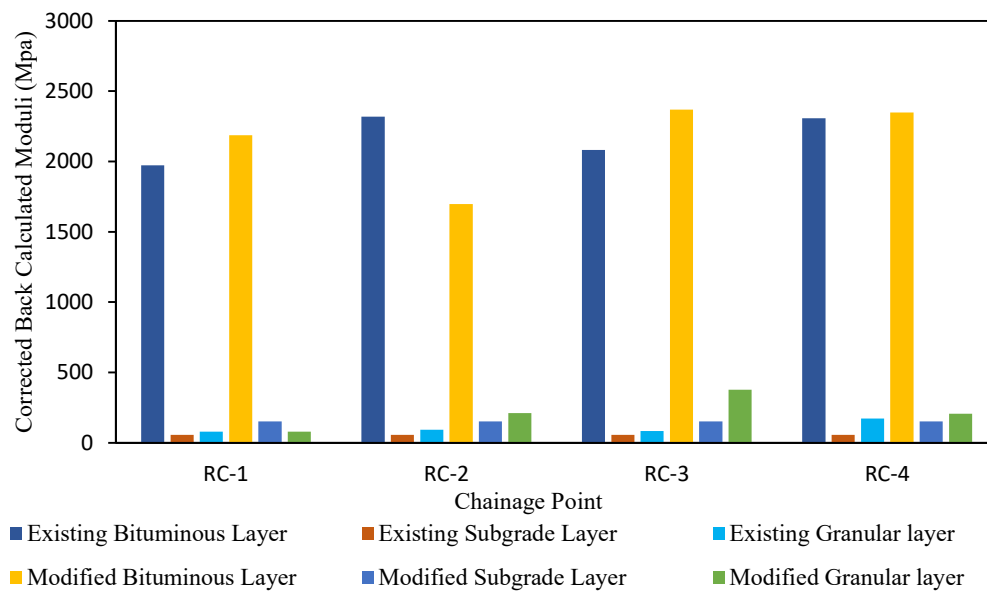
Table 6.19: Corrected Back Calculated moduli for bituminous layer of pavements

Pavement type	Chainage in Km	λ , temperature correction factor = $(1 - 0.238 \ln T1) / (1 - 0.238 \ln T2)$	Equation parameters		Back-Calculated moduli for bituminous layer (MPa)	Corrected Back-Calculated moduli for bituminous layer (MPa)
			T1 (In °C)	T2 (In °C) (Asphalt Temperature)		
Existing pavement	3.00×10 ³ m	0.8	35	29.7	2296.2	1836.96
	3.01×10 ³ m	0.78	35	29.2	2975.8	2321.12
	3.02×10 ³ m	0.78	35	29.3	2300.6	1794.47
	3.03×10 ³ m	0.79	35	29.5	2925.2	2310.91
Scrap tyre modified subgrade pavement	0.00m	0.78	35	29.1	2997.8	2338.28
	10.00m	0.79	35	29.5	2918.6	2305.69
	20.00m	0.79	35	29.4	2958.2	2336.98
	30.00m	0.79	35	29.6	2815.2	2224.01

- ii. Additionally, a correction for the seasonal variation factor has been implemented for the granular and subgrade layers, in accordance with clause 6.5.1 of IRC:115-2014. Table 6.20 illustrates the calculation of correction factors and the resulting corrected back-calculated modulus for the granular layer and subgrade layer, specifically accounting for seasonal variations. In this work, the winter season has been considered. Fig. 6.33 shows the corrected back-calculated modulus chart for both the pavements.

Table 6.20: Corrected Back Calculated moduli for granular ($E_{\text{gran_win}}$) and subgrade ($E_{\text{sub_win}}$) layers of pavement

Pavement type	Chainage in m	Back Calculated modulus of subgrade ($E_{\text{sub_win}}$ in MPa)	Back Calculated modulus of granular layer ($E_{\text{gran_win}}$ in MPa)	Corrected Back Calculated modulus for subgrade $E_{\text{sub_mon}}=3.351*(E_{\text{sub_win}})^{0.7688}-28.9(\text{MPa})$	Corrected Back Calculated modulus for granular layer $E_{\text{gran_mon}}=3.351*(E_{\text{gran_win}})^{0.624}-113.857(\text{MPa})$
Existing pavement	3.00×10^3 m	67.20	102.30	56.22	75.60
	3.01×10^3 m	67.20	107.80	56.22	81.89
	3.02×10^3 m	67.20	111.30	56.22	85.83
	3.03×10^3 m	67.20	189.90	56.22	164.85
	Average Back Calculated modulus			56.22	102.04
Modified pavement	0.00m	178	176.60	151.11	152.50
	10.00m	178	189.90	151.11	164.85
	20.00m	178	232.20	151.11	202.11
	30.00m	178	186.80	151.11	162.00
	Average Back Calculated modulus			151.11	170.36

**Fig. 6.33:** Corrected back calculated Moduli chart for both the pavements

The Tables (Table 6.18 to 6.20) above clearly illustrate that in the case of the scrap tyre-modified subgrade pavement, there has been an increase in the back-calculated moduli for each component of the pavement when compared to the existing pavement. These back-calculated moduli play a crucial role in analysing the in-service pavement and evaluating its structural condition as outlined in Clause 6.3.1 of IRC:115-2014.

6.3.2.10 Deflection and Elastic Modulus of Subgrade

In this study, the primary focus is dedicated to the analysis and comparison of subgrade deflection and elastic moduli for existing and modified pavement. To effectively characterize the subgrade condition and gauge its structural performance, deflections have been measured at two key distances: 1200 mm (referred to as D1200) and 1500 mm (referred to as D1500) from the centre of the load. The difference between these two deflections is referred to as the Lower Layer Index (LLI), which is a deflection bowl parameter derived from the results of deflection tests. LLI serves as a characterization of the subgrade condition and proves valuable in predicting performance and assessing the overall condition. The significance of these measurement points has been highlighted in prior studies conducted by Horak (2008), Talvik and Aavik (2009), as well as Solanki et al. (2019).

Table 6.21 provides a summary of the average deflection for D1200 and D1500 along with the LLI and average elastic moduli values for both types of pavements, offering insights into the subgrade's overall performance and condition.

Table 6.21: LLI for Subgrade Layer in both pavement types

Pavement type	Chainage (m)	Distance from Load Centre(mm)		Lower layer Index (LLI) in mm
		1200	1500	(D4-D5)
		Deflection(mm)		
		D4	D5	
Existing subgrade	3.00×10 ³ m	0.063	0.048	0.015
	3.01×10 ³ m	0.065	0.047	0.018
	3.02×10 ³ m	0.063	0.047	0.016
	3.03×10 ³ m	0.062	0.047	0.015
Average LLI for existing subgrade (LLI _{eps}) in mm				0.016
Scrap tyre modified subgrade pavement	0.00m	0.029	0.019	0.01
	10.00m	0.027	0.021	0.006
	20.00m	0.038	0.025	0.013
	30.00m	0.025	0.022	0.003
Average LLI for modified subgrade (LLI _{mps}) in mm				0.008

The average elastic modulus values for both pavements are shown in Table 6.22, as obtained from the data in Table 6.21.

Table 6.22: Average Elastic Moduli (E_s) for Subgrade Layer in both pavement types

Pavement type	Chainage (m)	Corrected Back Calculated modulus for subgrade (E_s) in Mpa
Existing subgrade	3.00×10 ³ m	56.22
	3.01×10 ³ m	56.22
	3.02×10 ³ m	56.22
	3.03×10 ³ m	56.22
Average E_{eps}		56.22
Scrap tyre modified subgrade pavement	0.00m	151.11
	10.00m	151.11
	20.00m	151.11
	30.00m	151.11
Average E_{mps}		151.11

6.4 SUMMARY

This chapter has presented the comprehensive field studies conducted to evaluate the performance of pavement subgrades modified with scrap tyres. A detailed traffic census and axle load survey have been conducted to gather essential data for pavement design. The chapter also discusses the structural performance assessment using Falling Weight Deflectometer (FWD) tests on both the existing and tyre-modified subgrades. The FWD tests have been indicated a significant increase in the stiffness and load-bearing capacity of the tyre-modified subgrade, demonstrating its effectiveness in improving pavement performance. These values of Elastic Modulus of subgrade have been used in numerical analysis. The analysis has been done by PLAXIS 3D to simulate FWD test. The numerical findings have corroborated the deflections acquired during FWD tests. The details of the analysis have been presented in the next chapter, Chapter 7.

CHAPTER 7

PLAXIS MODELLING

7.1 OVERVIEW

In this study, the main goal is to obtain a simplified numerical model and evaluate the results in FWD using experimental data. For the determination of the deflection bowl in the FWD test's 3D dynamic FE modelling, analytical data from the static back analysis has been used. It needs to be mentioned that the goal of this research is to create numerical models for determining deflection bowls for varying pavement thickness and soil subgrade parameters using the FWD peak falling load (40 kN). A comparison between measured deflection bowl, obtained from the in situ FWD test and the calculated deflection bowl from the FE simulation, may help to validate the back-analysed data. Another goal is to determine the deflection values of various layers of the pavement, as obtained during the FWD test.

A three-dimensional dynamic FE simulation of the test has been executed in this study to check and validate the results of the FWD back analysis technique using PLAXIS 3D.

In situ measurements from two types of soil subgrade pavement—one for existing soil condition and the other for modified soil subgrade condition, as well as the outcomes of their back analyses are utilized as input for the FE simulation.

7.2 PLAXIS 3D ANALYSIS ON MODEL PAVEMENT:

The load impact of the FWD test is simulated using PLAXIS 3D(V20) on the top surface of a 4-layered pavement, having a subgrade of 3.36% CBR and 8.90% CBR. To simulate a typical FWD load pulse, a dispersed load with a radius of 0.15 m is employed. To imitate a typical falling weight, a dispersed load with a radius of 0.15 m is employed. A dynamic surface load of 565 kPa has been applied on a circular contact surface with a 0.30 m diameter to instigate

the actual force because of a 40 kN single-axle wheel load. A typical FWD load pulse is exhibited assuming an impulse duration of 25ms (h et al. and Skels et al.2019). The current model works by utilising a transient load that is placed at a fixed spatial location, presumably to simulate traffic when the FWD load pulse occurs. Moreover, it is acknowledged that stationary pulses are not enough to provide a clear explanation of stress waves produced when a wheel leads forward and eventually exits the region of interest (Howard and Warren (2009), Skels et al. 2019; Loizos and Scarpas 2005). A typical FWD load pulse has been exhibited assuming an impulse duration of 25ms. Fig. 7.1 shows the FWD load pulse, and the chosen load configuration is appropriate for the scope of work.

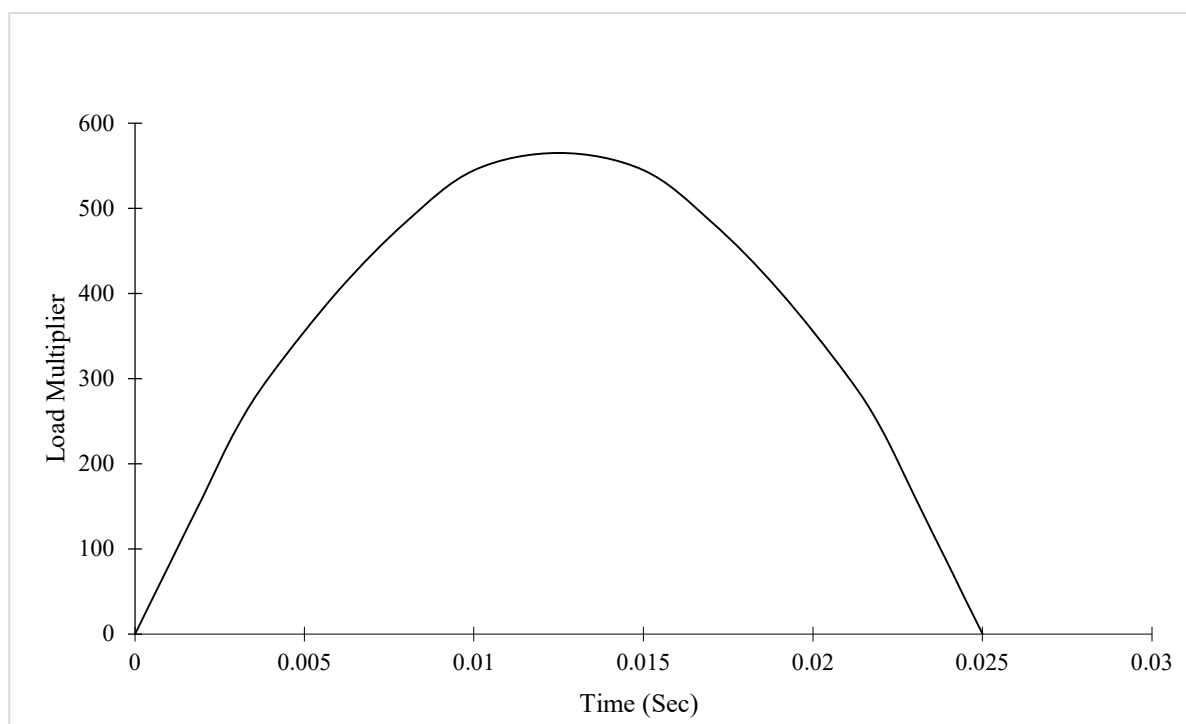


Fig. 7.1: The model of FWD test pulse load

The thickness of each layer of flexible pavement has been estimated for a traffic intensity of 13.74 MSA and subgrade CBR of 3.36% and 8.90%, respectively, using the templates, provided in IRC 37:2018.

When determining the limit pressure on the soil from different loads and types of impact, the Mohr–Coulomb criterion is frequently utilized in problem-solving techniques involving the

limiting equilibrium of the soil (Hambleton and Drescher, 2007, Korolev, 2014). It is frequently used to simulate soil deformation behaviour and shear strength. Laboratory data can be more easily correlated with numerical modelling when using the Mohr-Coulomb model since it is compatible with the results of triaxial and direct shear laboratory tests (Smith et al, 2013). The Mohr-Coulomb method has been utilized in PLAXIS 3D to represent the subgrade of soil. The layers which make up the pavement crust—BC, DBM, WMM and GSB—have been modelled using the linear elastic method (Pai et al, 2020). The linear elastic model for pavement crust is based on Burmister's elastic layered theory, which states that both horizontal tensile strain at the bottom of the asphalt layer and vertical compressive strain on top of the subgrade is limited (Huang, 2004). Fine meshing has been done to eliminate any calculation errors. Viscous boundary conditions have been used in the X-direction, Y-direction and as well as in the bottom of Z-direction of the model in the software to simulate the dynamic analysis. The top of the Z-direction remains free so that deflection can be obtained which is the actual case during in situ FWD testing. The typical pavement Finite Element model is displayed in Fig. 7.2.

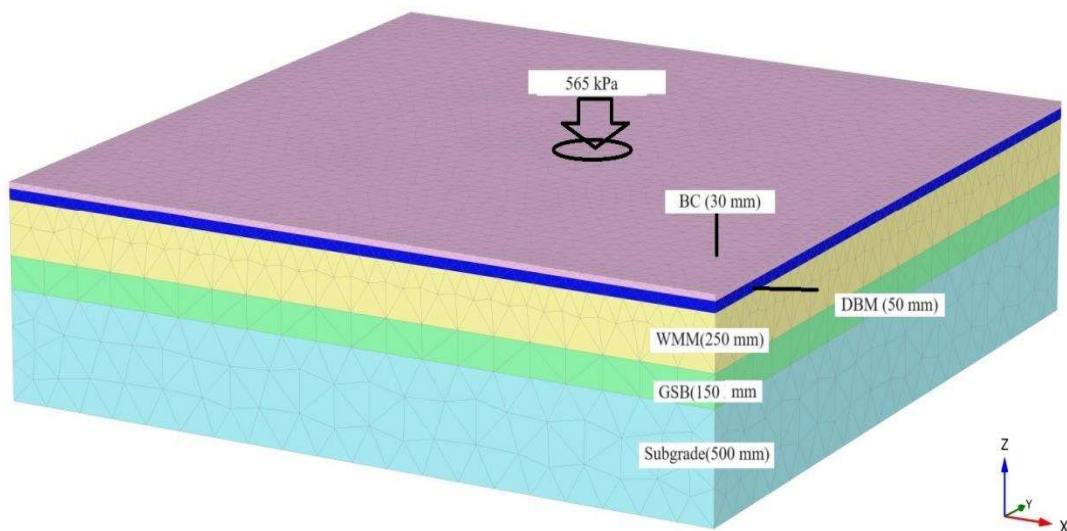


Fig. 7.2: FE model of flexible pavement with meshing

7.2.1 Input Parameters for PLAXIS Modelling

The material characteristics used for the numerical studies of the pavement reactions have been estimated using the findings from FWD tests. Back calculated modulus for different pavement layers from FWD test data has been used (Skels et al.). For soil subgrade, unit weight and shear parameters are obtained by testing the normal soil and scrap tyre-modified soil and used in this analysis.

Parameters adopted for FE analysis have been shown in Table 7.1 and Table 7.2.

Table 7.1: Parameters used for finite element analyses of normal soil subgrade pavement

Material	Model type	Unit weight (kN/m ³)	C (kN/m ²)	ϕ	E(MPa)	ν	Thickness(mm)
Subgrade	Mohr-Columb	20.20	25.00	2	56.22	0.40	500
GSB	Elastic	21.00	-	-	102.04	0.40	200
WMM	Elastic	22.30	-	-	102.04	0.40	250
DBM	Elastic	24.00	-	-	2065.87	0.50	80
BC	Elastic	25.00	-	-	2065.87	0.50	40

Table 7.2: Parameters used for finite element analyses of scrap tyre modified subgrade pavement

Material	Model type	Unit weight (kN/m ³)	C (kN/m ²)	ϕ	E(Mpa)	ν	Thickness(mm)
Subgrade	Mohr-Columb	19.70	45.00	8	151.10	0.40	500
GSB	Elastic	21.00	-	-	170.37	0.40	150
WMM	Elastic	22.30	-	-	170.37	0.40	250
DBM	Elastic	24.00	-	-	2301.24	0.50	50
BC	Elastic	25.00	-	-	2301.24	0.50	30

7.2.2 Output from PLAXIS 3D Analysis

Simulating FWD test in PLAXIS, vertical deflection for normal soil subgrade pavement and scrap tyre modified pavement have been obtained.

7.2.2.1 Vertical Deflections from PLAXIS:

Fig. 7.3 and Fig. 7.4 represent examples of vertical deflection of pavement surface and layered boundaries with time for normal soil (CBR=3.36%) and scrap tyre-modified soil (CBR=8.90%). A single response versus time curve was able to accurately depict the vertical deflection curve due to their geometry, and layer thicknesses. Vertical deflections obtained from PLAXIS 3D, at the top of BC at the centre of the loading are 0.593 mm and 0.451 mm respectively for two cases. These values are relatively closer to the values required from the FWD test. In both graphs, the coordinate (0,0,0) represents the centre of loading, at the top of BC. In Fig. 7.3, coordinates (0,0, -0.040), (0,0, -0.120), (0,0, -0.370) and (0,0, -0.570) represent top DBM, top of WMM, top of GSB and top of subgrade respectively for deflection calculation. Whereas the same layers are represented by coordinates (0,0, -0.030), (0,0, -0.080), (0,0, -0.033) and (0,0, -0.48) for modified pavement, as shown in Fig.7.4.

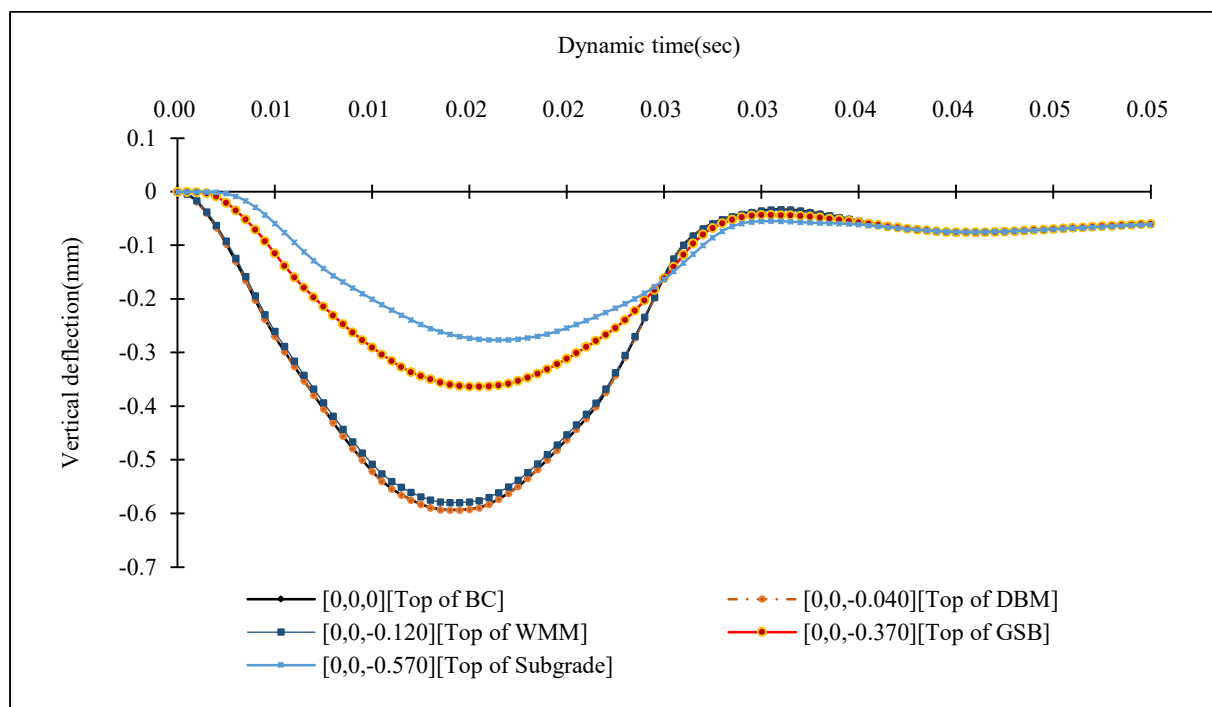


Fig. 7.3: Vertical deformation on the pavement surface and at layer boundaries as a function of dynamic time for normal soil

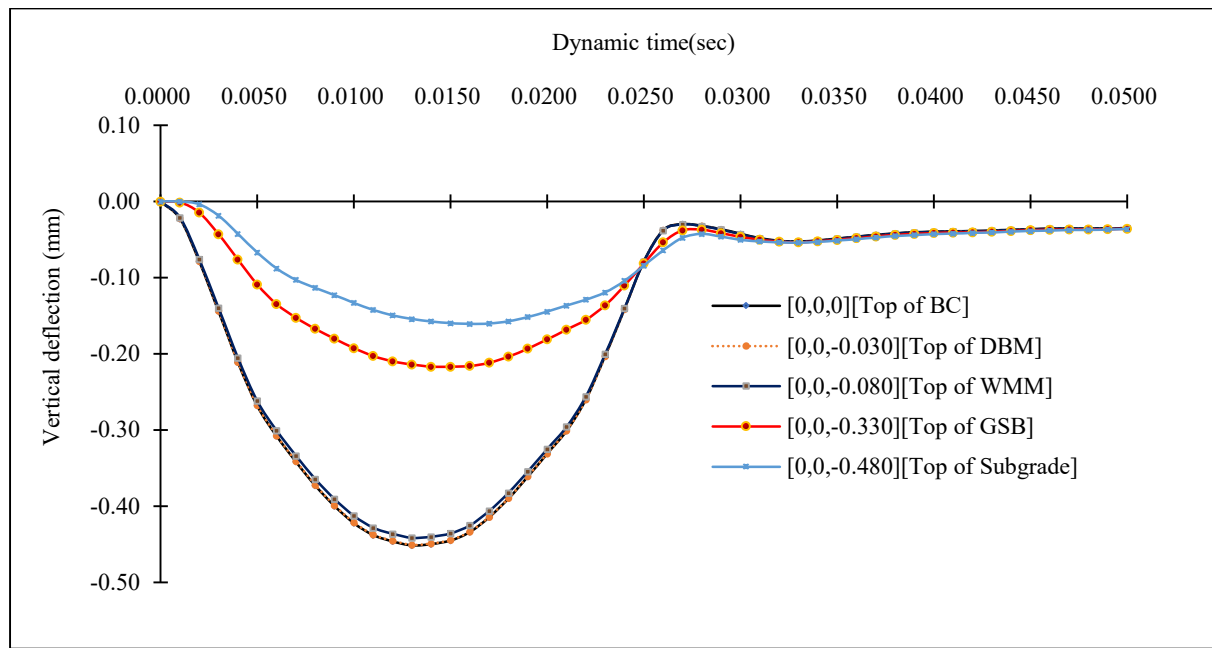


Fig. 7.4: Vertical deformation on the pavement surface and at layer boundaries as a function of dynamic time for scrap tyre modified soil

7.3 RESULTS OF FWD SIMULATION FROM PLAXIS ANALYSIS.

Simulating FWD test in PLAXIS 3D(V20) software, the vertical deflection curves over time for different radial distance from the centre of the loading are also obtained. Vertical deflection responses at different distances are obtained such a way that they are in accordance with the geophones installed during in situ FWD test. Data obtained from these responses are presented in Table 7.3

Table 7.3: vertical deflection data, obtained from FE analysis

Distance from Load centre(mm)	Deflection obtained from PLAXIS 3D for normal soil subgrade pavement(mm)	Deflection obtained from PLAXIS 3D for scrap tyre modified pavement(mm)
0	0.593	0.451
300	0.370	0.176
600	0.182	0.076
900	0.101	0.043
1200	0.063	0.03
1500	0.049	0.02
1800	0.034	0.013

The variation of deflection bowl can be shown in Fig. 7.5 for normal soil subgrade pavement and scrap tyre modified subgrade pavement, From the deflection bowl it can be said that for same load condition vertical deflection is less for modified soil.

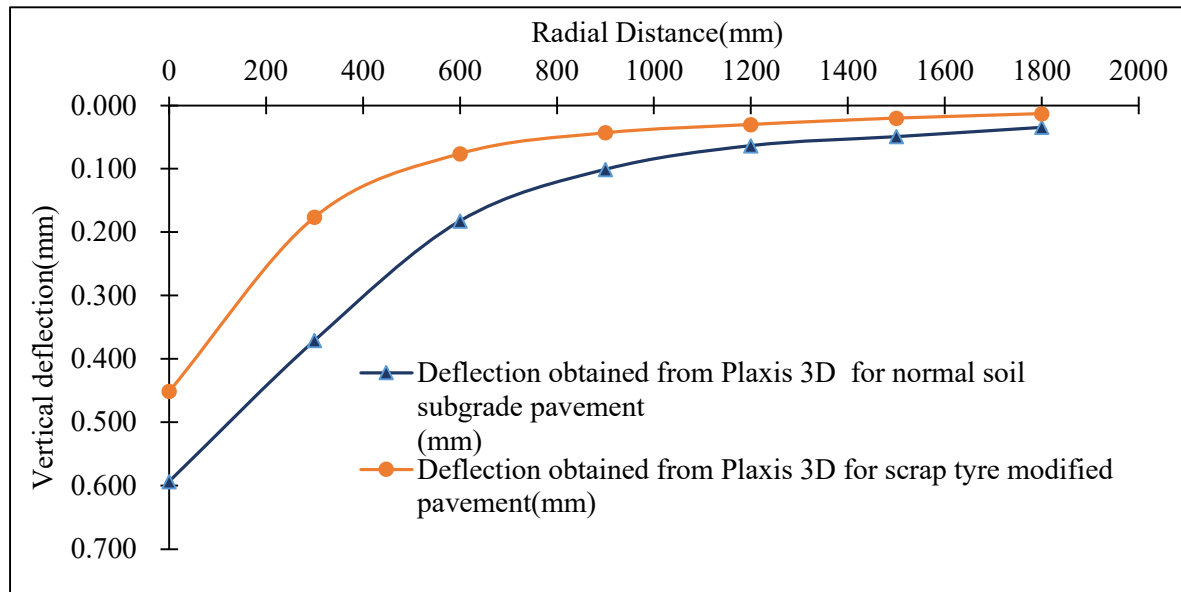


Fig. 7.5: Comparison of vertical deflection bowl for normal soil subgrade pavement and scrap tyre modified soil subgrade pavement

7.4 COMPARISON OF THE RESULTS OBTAINED FROM FWD TEST AND FWD SIMULATION IN PLAXIS 3D:

Deflection bowls obtained from FWD test and PLAXIS analysis, also have been compared.

The results indicate an alignment of the measured value and the FE analysis value. Obtained deflection values for two cases have been presented in Table 7.4 and Table 7.5.

Table 7.4: Vertical deflection data, obtained from FWD test and FE analysis for normal soil subgrade pavement

Radial distance(mm)	Deflection as per FWD test (mm)	Deflection obtained from PLAXIS 3D (mm)
0	0.519	0.593
300	0.332	0.371
600	0.199	0.182
900	0.099	0.101
1200	0.063	0.063
1500	0.047	0.049
1800	0.033	0.034

Table 7.5: Vertical deflection data, obtained from FWD test and FE analysis for tyre modified soil subgrade pavement

Radial distance(mm)	Deflection as per FWD test (mm)	Deflection obtained from PLAXIS 3D (mm)
0	0.404	0.451
300	0.161	0.176
600	0.077	0.076
900	0.049	0.043
1200	0.03	0.03
1500	0.022	0.02
1800	0.015	0.013

Comparison of surface deflection bowl for existing pavement and modified pavement has been shown in Fig. 7.6 and Fig.7.7.

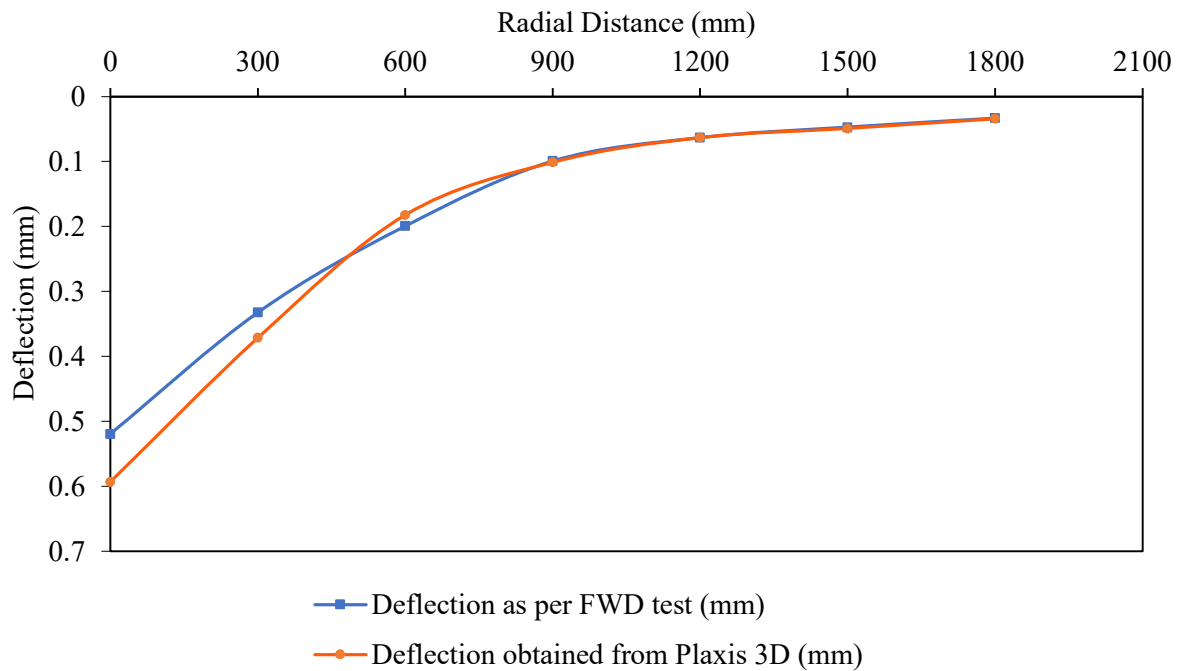


Fig. 7.6: Deflection bowl comparison, obtained from FWD test and FE analysis for existing pavement

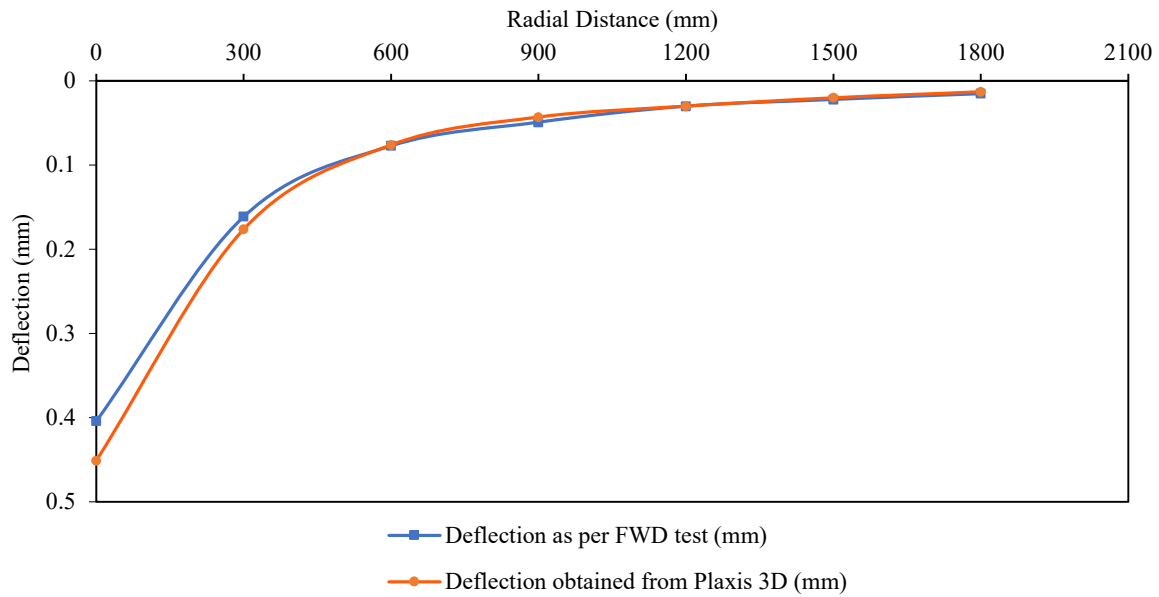


Fig. 7.7: Deflection bowl comparison, obtained from FWD test and FE analysis for modified pavement

7.5 SUMMARY

This chapter focuses on the use of PLAXIS 3D software to simulate the response of the pavement under load conditions. The chapter describes the setup of finite element models representing the pavement layers and subgrade, incorporating material properties derived from field tests. The simulations have been aimed to replicate the deflections observed in FWD tests. The results from PLAXIS modelling closely aligned with the empirical data, validating the use of scrap tyres in enhancing subgrade stiffness and providing a reliable method for predicting pavement performance.

CHAPTER 8

REGRESSION ANALYSIS

8.1 OVERVIEW

The aim of this analysis is to find out the correlation between modified soil CBR and parameters like normal soil CBR, scrap tyre size, and percentage of tyre scrap. This regression model will give an idea of how the input variable changes, so that it can predict the modified soil CBR for a variety of input parameters.

8.2 GENERAL:

Regression analysis is one of the statistical tools which can be used to examine the relationship that exists between a response, also known as a dependent variable, and sample measurements made on various factors, also known as independent variables or predictor variables.

To establish a relationship between multiple independent variables and only one dependent variable, generally multiple linear regression is used. It is used to predict the value of one dependent variable using known values for the independent variables. The weight of each predictor value indicates how much influence it has on the final prediction.

Equation 8.1 depicts the general form of the multiple linear regression model, while Equation 8.2 displays the fitted equation of the model.

$$Y = \beta_0 + \beta_1 X_1 + \beta_2 X_2 + \dots + \beta_k X_k + e \dots \dots \dots (8.1)$$

The fitted equation:

$$\hat{Y} = b_0 + b_1 x_1 + b_2 x_2 + \dots + b_k x_k \dots \dots \dots (8.2)$$

Where: Y = Dependent variable,

X_k = k^{th} independent variable,

β_k = Regression coefficient of k^{th} population,

e = residuals,

b_k = estimate of k^{th} population regression coefficient,

\hat{Y} = Response of the fitted model.

8.3 TERMINOLOGY USED:

During multiple regression analysis, different terminologies are used for describing the correlation between dependent variables and independent variables.

8.3.1 R^2 , Adjusted R^2 and Mean Squared Error (MSE), F Value and t-Value:

When determining the relationship between a set of explanatory variables and the dependent variable, R^2 is regarded as a fundamental and essential tool. R^2 is often used to demonstrate the variation of the dependent variable which can be predicted by the independent variables. R^2 typically estimates the linear regression's fit in an optimistic manner. As more effects are incorporated into the model, it always rises. This overestimation is attempted to be corrected for in adjusted R^2 . If a particular effect does not improve the model, adjusted R^2 may go down. Mean squared error is another term used in statistical analysis. MSE, is a statistical measure of model inaccuracy. The mean squared difference value is evaluated between observed and predicted value. MSE value is zero for a model which has no error. The value of it rises with increasing model inaccuracy. The degree to which a regression model accurately depicts the modelled data is shown by the regression sum of squares. If the data is not sufficiently fitted by the model, regression sum of square shows larger value. The variation of modelling errors is basically measured by the error sum of squares. In a regression analysis, it shows how the variation seen in the dependent variable cannot be explained by the model. Regression model explains the data better when the residual sum of squares has lower value; in contrast, when the residual sum of squares has higher value, the model performs less well.

A prediction model is considered dependable when value of R^2 is high and its MSE has lower value. The better the model matches the data, the greater the R^2 score.

In Analysis of Variance (ANOVA), the F value is utilized. Two mean squares are divided to compute it. This method calculates the ratio between explained variation to unexplained variance. The statistical significance of the test can be determined using t- value. The t-value, which is often referred to as the t-score, is the ratio of the variation between the two sample sets' means to the variance within each sample set. Higher t-score values indicate that the two sample sets differ significantly from one another. As the t-value decreases, the degree of similarity between the two sample sets rises.

8.4 REGRESSION MODEL:

A statistical model has been utilized to investigate potential correlations between the scrap tyres stabilized soil CBR(Soaked) and input variables, such as normal soil CBR(Soaked), scrap tyre size, and the percentage of scrap tyre.

The statistical program MINITAB is utilized to create the regression models for the data. The size of the scrap tyre, scrap tyre percentage in the soil and the normal soil CBR, have been employed as independent variables, and the scrap tyre modified soil CBR has been used as the dependent variable. Thirty samples have been subjected to a regression analysis correlating the soaked CBR value.

Best fit model has been used in MINITAB software to fit all the parameters for regression analysis. Table 8.1 represents regression model summary for prediction of stabilized soil CBR.

8.4.1 Results Obtained from Regression Model:

Table 8.1, Table 8.2 and Table 8.3 depict Regression model summary and different statistical parameters obtained from Regression analysis

Table 8.1: Regression model summary (Analysis of variance)

Model	Statistical Parameters			F-value
	Degree of freedom (df)	Sum of squares (ss)	Adjusted Mean squared (ms)	
Regression	3	43.238	14.4125	40.54
Error of Residual	26	9.244	0.3555	
Total	29	52.481		

Table 8.2: Regression model summary (Coefficients)

Model	Coefficients	Standard Error (SE)	t
Intercept	36	107	1.36
CBR _{unstabilized}	-7.8	31.9	-0.24
Size of scrap tyre(S)	-0.0724	0.0160	-4.54
Percentage of scrap tyre(P)	-0.1274	0.0129	-9.84

Table 8.3: Model summary

Number of variables	Variables	Regression sums of squares	Error sum of squares	Mean squared error (MSE)	R ²	Adjusted R ²
3	Normal soil CBR, Size of scrap tyre, Percentage of scrap tyre	43.238	9.244	0.596265	82.39 %	80.35 %

The equation obtained from the regression of the above model is presented in Equation 8.3

$$\text{CBR}_{\text{Stabilized}} = 36 - 7.8\text{CBR}_{\text{Unstabilized}} - 0.0724 S - 0.1274P \dots\dots\dots (8.3)$$

Where, S=Size of the scrap tyre (Length), P= Percentage of scrap tyre used (%).

This can be observed from the Fitted Value as well as Observation Order of the distribution presented in Figure 8.1, the residual values of the model are distributed uniformly and symmetrically around the neutral line.

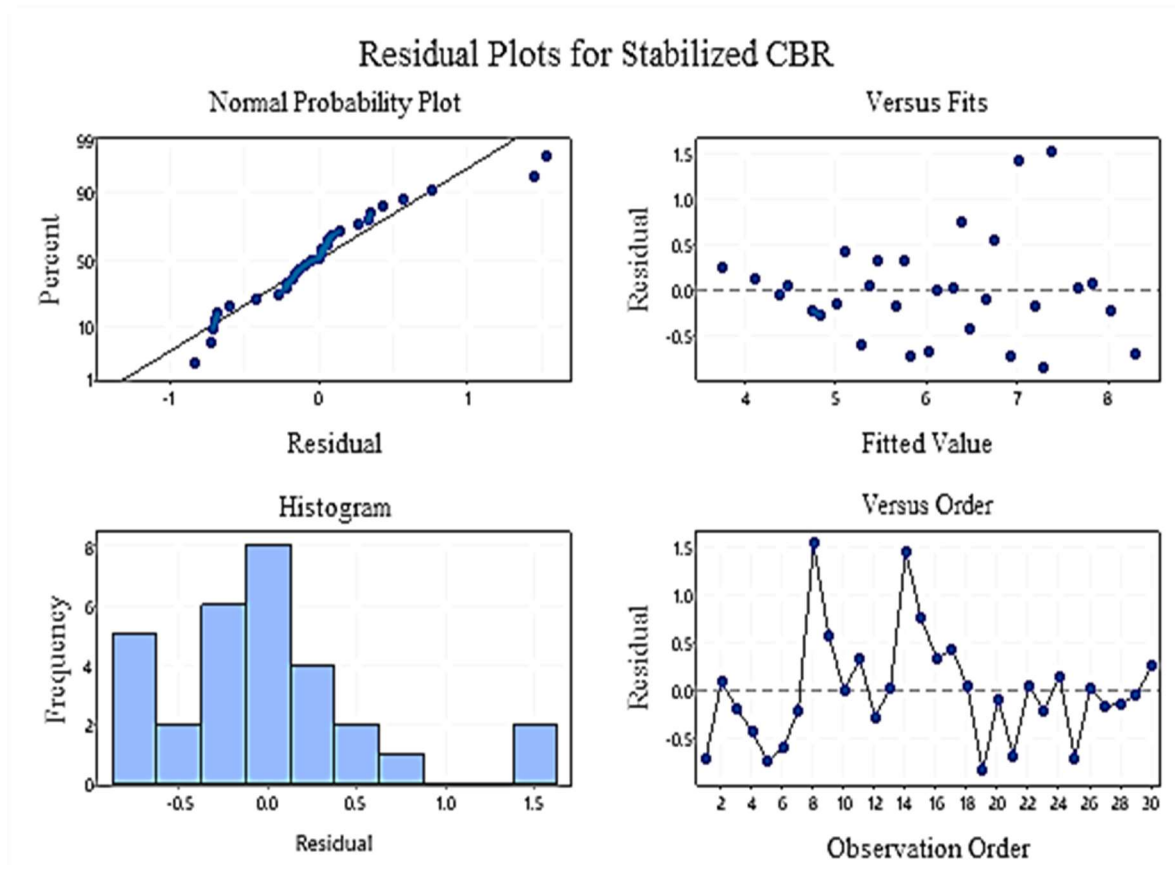


Fig. 8.1: Residual analysis of prediction of stabilized CBR

The extent to which a model captures the experimental data is determined by the model validation assessment. Predicted values have been determined using Equation 8.3, one of the best model equations, and subsequently compared against the total number of samples, to validate the model. As seen in Figure 8.2, experimental results are similarly plotted against the quantity of samples and compared. The experimental results are rather close to the expected values, as seen in Figure 8.2. a similar trend has been observed to that R^2 trend value from this figure.

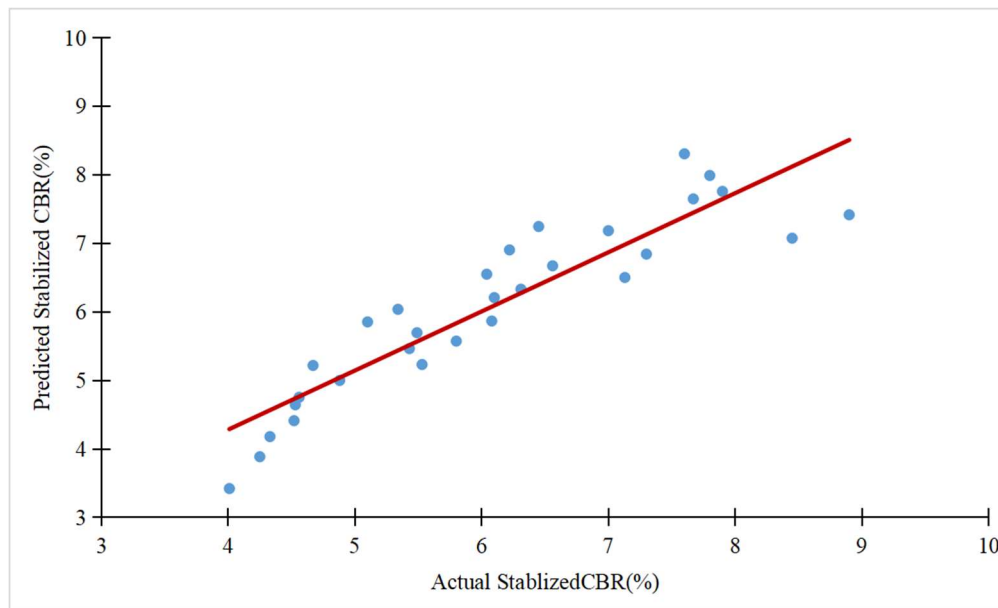


Fig. 8.2: Validation plot of stabilized CBR

Thirty (30) disturbed soil samples stabilized with five to thirty percent scrap tyres of varying sizes are subjected to regression analysis. The size of the scrap tyre, scrap tyre percentage, the normal soil CBR, and the thickness of the pavement are the independent variables, and the stabilized CBR is the dependent variable. The prediction models for the Soaked CBR of the soil transformed by scrap tyres appear to be reasonably accurate in predicting the corresponding real results. Significant correlations ($R^2 = 0.84$, adjusted $R^2 = 0.8163$) have been observed when these variables have been estimated using regression analysis. The model equation developed from this analysis produces a very good response prediction since the equation can be utilized to estimate soaking CBR. The test findings are consistent with the correlation equation established from regression analysis.

8.5 SUMMARY

This chapter has presented the results of the regression analysis conducted to establish relationships between various factors influencing the performance of the cohesive subgrade modified with tyre scrap. The chapter has provided a detailed explanation of the statistical models developed, including the choice of independent variables, the regression equations formulated, and the statistical significance of the results. The regression models demonstrated

good predictive capability, with high R-squared values indicating that the models effectively captured the variation in the data. Additionally, the chapter has been discussed the implications of these results in the context of subgrade design, offering insights into how tyre scrap modifications can be optimized for better pavement performance.

In summary, the chapter has been made a valuable contribution to the research by measuring the connections among tire scrap content, soil characteristics, and subgrade performance.

CHAPTER 9

DISCUSSION

9.1 OVERVIEW

Various observations from laboratory, field test and numerical analysis results have been obtained from the present work, which has been discussed in that section.

9.2 LABORATORY TEST RESULTS

One of the primary goals of the current study is to determine the CBR for both normal soil and soil modified with shredded tyre scraps. In order to do this, modified Proctor tests have been carried out on a variety of samples, resulting in a range of maximum dry density values, during both test phases that focused on compaction properties (i.e., OMC and MDD). Furthermore, CBR tests have been conducted on samples of both normal soils collected from existing road subgrade and soil mixed with shredded tyre material. These CBR tests are used to evaluate the mechanical strength of the road subgrade using a penetration test. The following observations have been derived from the laboratory tests conducted in both cases.

9.2.1 Modified Proctor and CBR Test Results

Figures 9.1, 9.2, and 9.3 show the changes in the Modified Proctor and CBR test results within the chainage range of 0.00 km to 12.45 km based on Table 5.3.

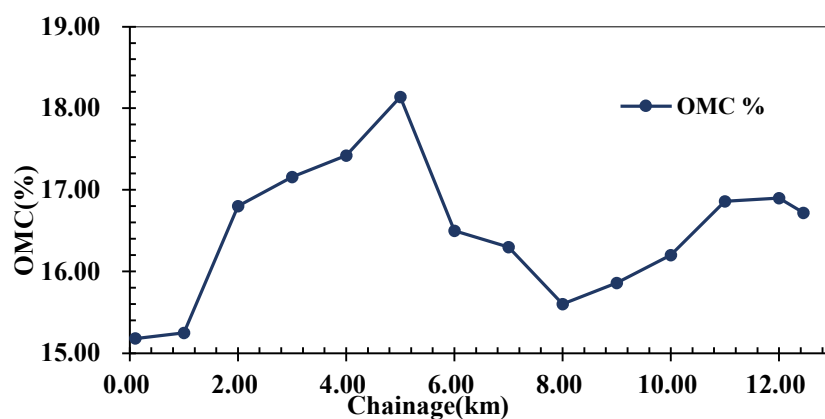


Fig. 9.1: Variations in Optimum moisture content (OMC) test results with respect to road chainage

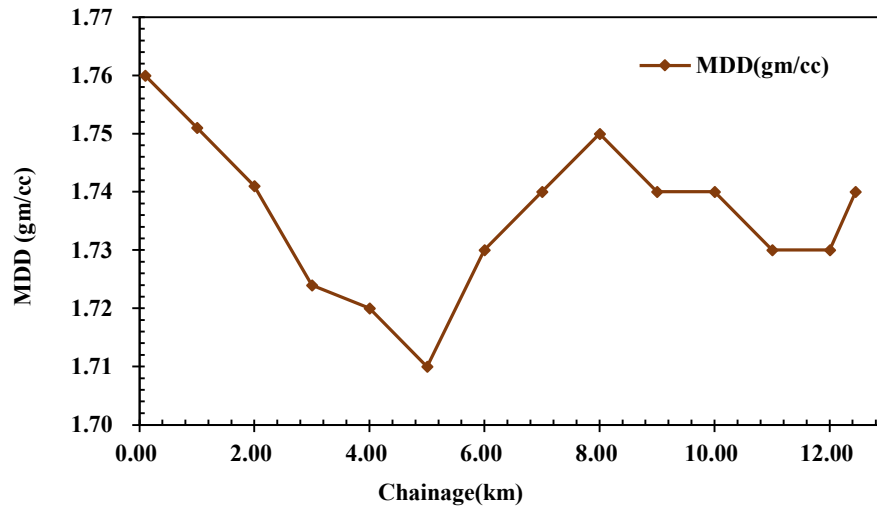


Fig. 9.2: Variations in Maximum dry density (MDD) test results, with respect to road chainage

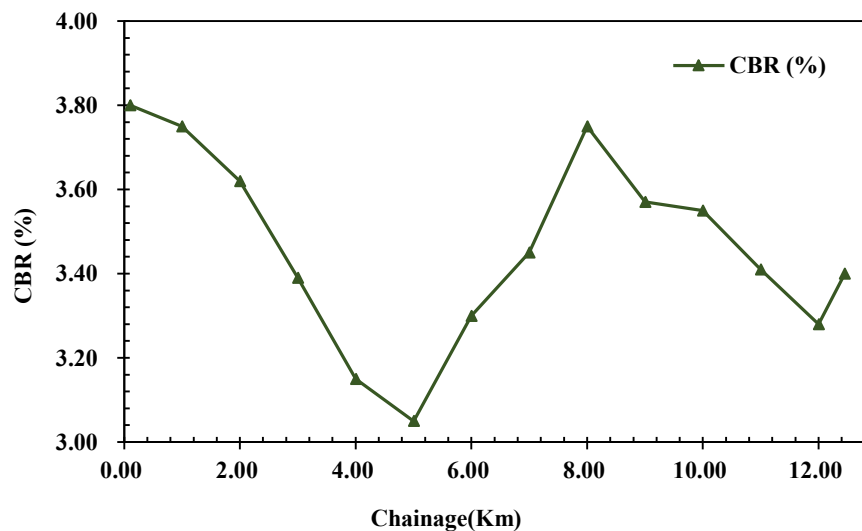


Fig. 9.3: Variations in CBR test results, with respect to existing road chainage

According to Table-5.3 and Figs.9.1,9.2 and 9.3, the test results show no significant variations across the chainage range. It can be assumed that the soil properties remain relatively consistent over the whole length of the road based on the soil description and other index properties. There are very slight variations in the subgrade soil's CBR value along the length of the pavement.

It has been observed from Table 5.7 that MDD of soil–shredded tyre scrap mixtures have reduced marginally. This reduction is attributed to the lower density of waste tyres compared

to clayey soil. Due to the high absorption capacity of waste tyre scrap mix soil, the OMC increases as the amount of tyre content increases (Md. Zain et al. 2022 and Akbarimehr et al. 2019). The variations in OMC, MDD, and CBR for soil mixed with varying sizes of shredded tyre scrap at different percentages are illustrated in Figures 9.4, 9.5, and 9.6.

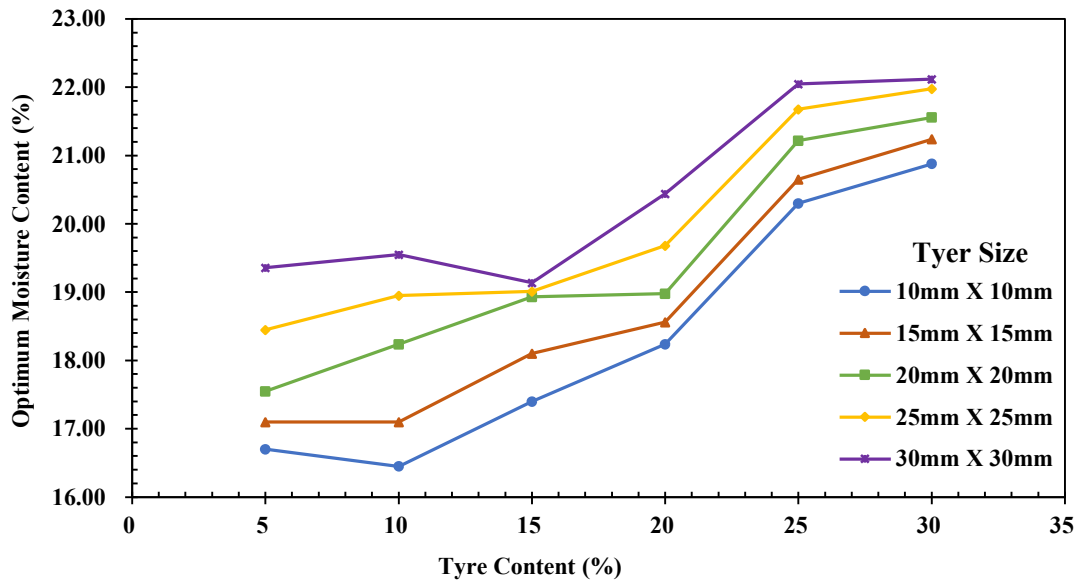


Fig. 9.4: Variation in Optimum moisture content (OMC) test results for soil mixed with different sizes of shredded tyre scrap of different percentages

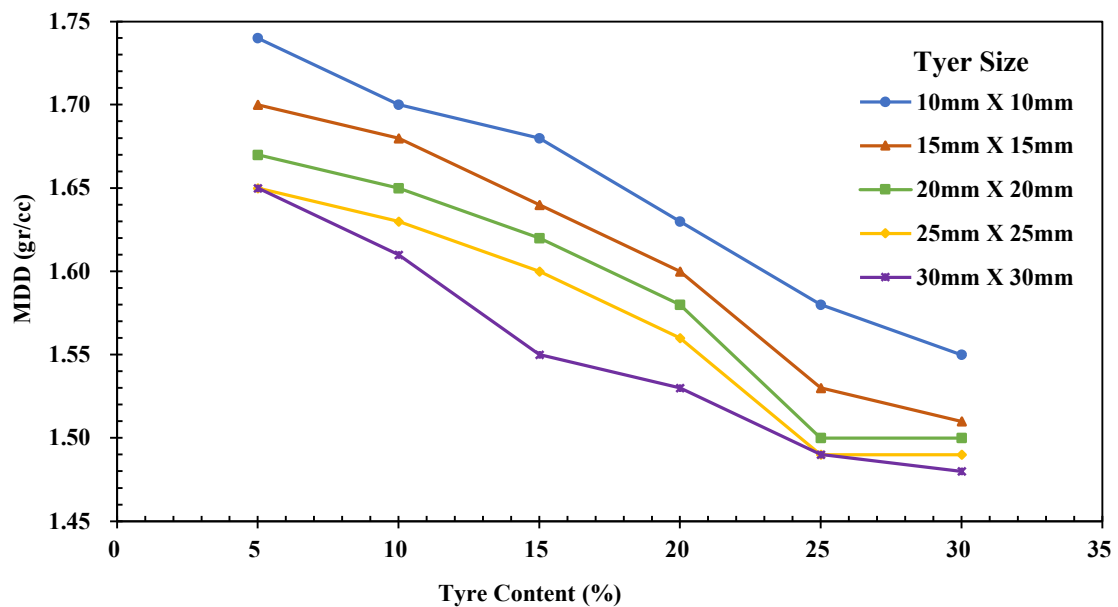


Fig. 9.5: Variation in Maximum dry density (MDD) test results for soil mixed with different sizes of shredded tyre scrap of different percentages

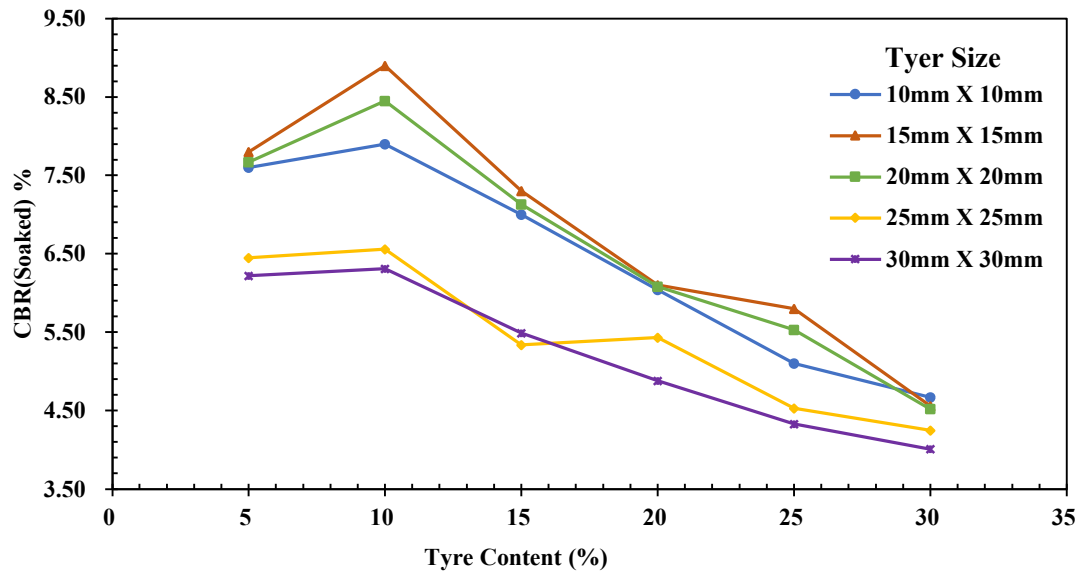


Fig. 9.6: Variation in soaked CBR test results for soil mixed with different sizes of shredded tyre scrap of different percentages

From the above depicted Figs.9.4, Fig.9.5, Fig.9.6 and Table 5.7, it is evident that the optimum value of soaked CBR obtained was 8.90 at 10% of tyre scrap for a size of (15mmX15mm). A significant improvement of about 164% or 2.64 times was observed compared to the soaked CBR value of 3.36 obtained for the normal soil.

The results show that adding the optimum 10% of scrap tyre material with dimensions of 15 mm × 15 mm significantly improves CBR. However, for all rubber size ranges, CBR gradually decreased beyond a certain proportion of tyre scrap. This may be attributed to the high elasticity of tyre scrap, which results in lower penetration resistance compared to soil.

9.3 FIELD TEST RESULTS

9.3.1 Traffic Study

- i. A 7-day traffic census was performed to determine CVPD, essential for estimating pavement thickness based on anticipated traffic volumes.

ii. In order to determine the VDF, which measures the effect of varying axle loads on the pavement and permits a design customized for different vehicle types, an axle load test has been conducted.

iii. Utilizing IIT PAVE software and following IRC 37: 2018 guidelines, the design process integrates CVPD and VDF to assess the pavement's ability to withstand expected traffic loads.

iv. The design was applied to two types of subgrades: normal soil and tyre mix soil, with the latter incorporating recycled tyre materials to enhance durability and sustainability.

v. The methodology included three trial runs for each subgrade type, focusing on analysing vertical strain at the top of the subgrade and tensile strain at the base of the bituminous layer, crucial for assessing the pavement's resistance to deformation and cracking.

vi. This comprehensive approach ensures the creation of a robust, durable pavement structure tailored to specific traffic demands and grounded in the latest research and standards.

9.3.2 Dynamic Cone Penetration Test (DCPT) Result

Based on Table 6.13, Fig.9.7 shows a comparison bar chart between in-situ CBR and Laboratory CBR.

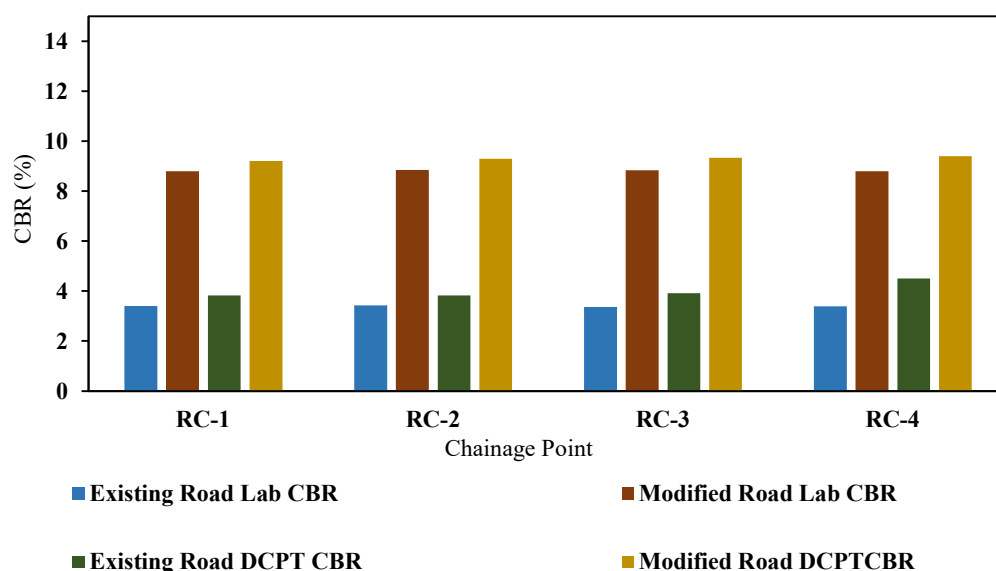


Fig. 9.7: Comparison bar chart between Laboratory CBR and In-situ CBR

It is evident from the data that there is no significant difference between the laboratory values and DCPT oriented in-situ CBR values for existing pavement. This may be due to the presence of nearby water bodies. In general, both laboratory and DCPT CBR values exhibit a consistent trend along the road stretch. In most instances, the DCPT CBR values slightly surpass the laboratory CBR values (Bandyopadhyay and Bhattacharjee, 2010). The original minimum in-situ CBR value mentioned is 3.82, which is the result of DCPT on the original soil without any modifications. After modifying the subgrade with scrap tyres, the minimum in-situ CBR value improved to 9.21. The improvement stated is about 141%, or 2.41 times the original CBR value, which suggests a significant increase in the strength and likely the load-bearing capacity of the modified subgrade pavement compared to the original soil condition.

9.3.3 FWD Oriented Result

9.3.3.1 Subgrade deflection

In this study LLI serves as a characterization of the subgrade condition and proves valuable in predicting performance and assessing overall condition, as indicated in studies by Horak (2008), Talvik and Aavik (2009), and Solanki et al. (2019). To calculate the LLI, the average deflection values of D1200 and D1500 for both types of pavements have been considered according to Table 6.21. The resulting LLI values are described below-

LLI for existing pavement subgrade = $LLI_{eps} = 0.016\text{mm}$

LLI for modified pavement subgrade = $LLI_{mps} = 0.008\text{mm}$

This means that the decrease of LLI for modified subgrade with respect to that of the existing subgrade becomes $[(0.016 - 0.008) \times 100 / 0.016] \% = 50 \%$.

Thus, the obtained data suggests that the improvement, in the form of decrease of LLI, is 50%.

Fig. 9.8 shows the variation of deflection for both pavements

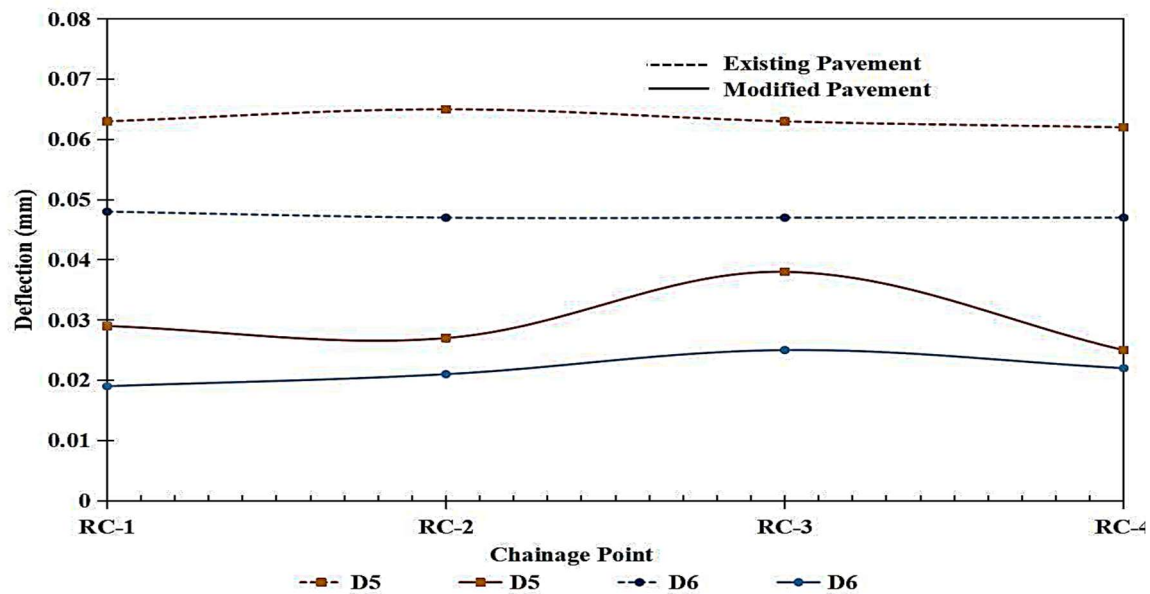


Fig. 9.8: Deflection variation in subgrade for both the pavements

LLI provides a quantitative measure of the subgrade's ability to distribute loads and effectively characterizes the stiffness and load-bearing capacity of the subgrade. The LLI values are indicative of the structural integrity of the subgrade (Horak,2008). This implies that the LLI is exceptionally capable of identifying possible structural issues in the subgrade. A lower LLI value suggests a stiffer subgrade that is better at distributing loads, thus implying a potentially longer lifespan and reduced maintenance needs for the pavement (Fuentes et al. 2022). Here, the LLI of the existing Pavement Subgrade indicates a relatively less stiff subgrade. This could translate to a higher likelihood of deformations under load, leading to potential issues like rutting or cracking in the overlying pavement layers. LLI of modified pavement subgrade suggests a considerable improvement in subgrade stiffness. This could be a result of modifications like the incorporation of materials (e.g., scrap tyres) that enhance the load-bearing capacity. A stiffer subgrade as indicated by this lower LLI value could lead to better load distribution, reduced strain on the pavement layers, and potentially a longer lifespan for the pavement.

9.3.4 Elastic Modulus (E_s) of Subgrade

Based on Table 6.18, Fig. 9.9 clearly illustrates that in the case of the scrap tyre-modified subgrade pavement. Comparing the modified pavement to the existing pavement, it has been observed that there has been an increase in the elastic modulus for subgrade.

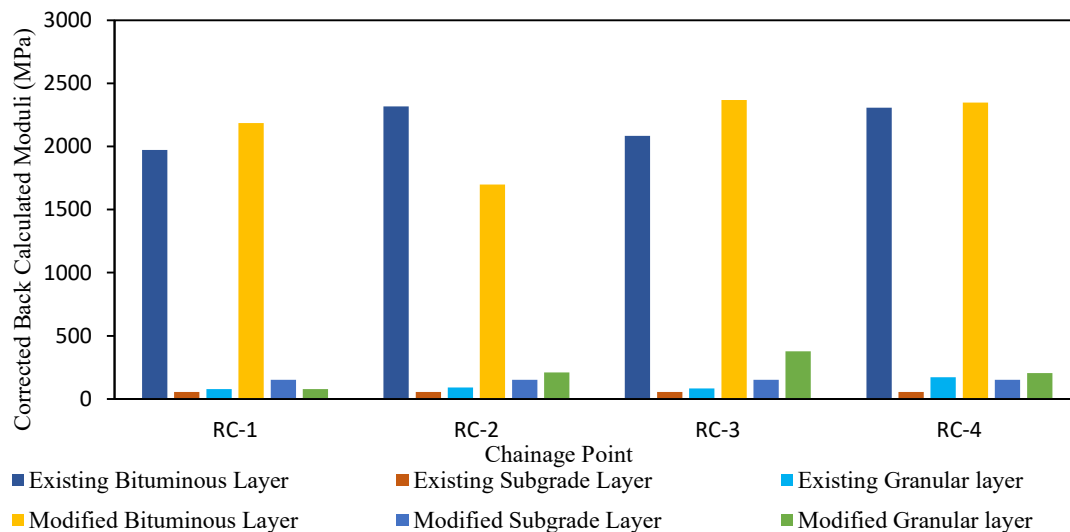


Fig. 9.9: Corrected back calculated Moduli chart for both the pavements

This study provides crucial insights into the comparative performance of existing pavement and scrap tyre modified subgrade pavement. Utilizing FWD for deflection measurements and the KGP-BACK software for back-calculating moduli values, the analysis aligns with the standards set forth in IRC:115-2014. For the existing pavement, the elastic modulus (E_{eps}) is measured at 56.22 MPa. This value falls within the typical range (20 to 100 MPa) for conventional pavement structures, indicating a standard level of stiffness. Such a modulus level suggests that the pavement is likely to perform adequately under normal traffic conditions (Solanki et al. 2016). However, this also implies potential limitations in its load-bearing capacity, possibly making it more susceptible to wear and degradation over time. In contrast, the modified pavement, characterized by an elastic modulus (E_{mps}) of 151.09 MPa, exhibits a markedly higher stiffness level of 2.68 times with respect to the existing pavement due to the integration of scrap tyre materials. This substantial increase in modulus points to an enhanced load-bearing capacity and overall structural integrity. Consequently, pavements

with such modifications are expected to offer improved durability, resist deformation more effectively, and potentially enjoy a longer service life (Talvik and Aavik 2009). The observation that the scrap tyre modified pavement has a much greater modulus than the existing pavement demonstrates the usefulness of using recycled materials to improve pavement performance.

9.4 NUMERICAL RESULTS

Deflection of different pavement layer with pulse duration for both existing and modified pavement has been illustrated in Fig. 9.10, based on Figs.7.3 and 7.4.

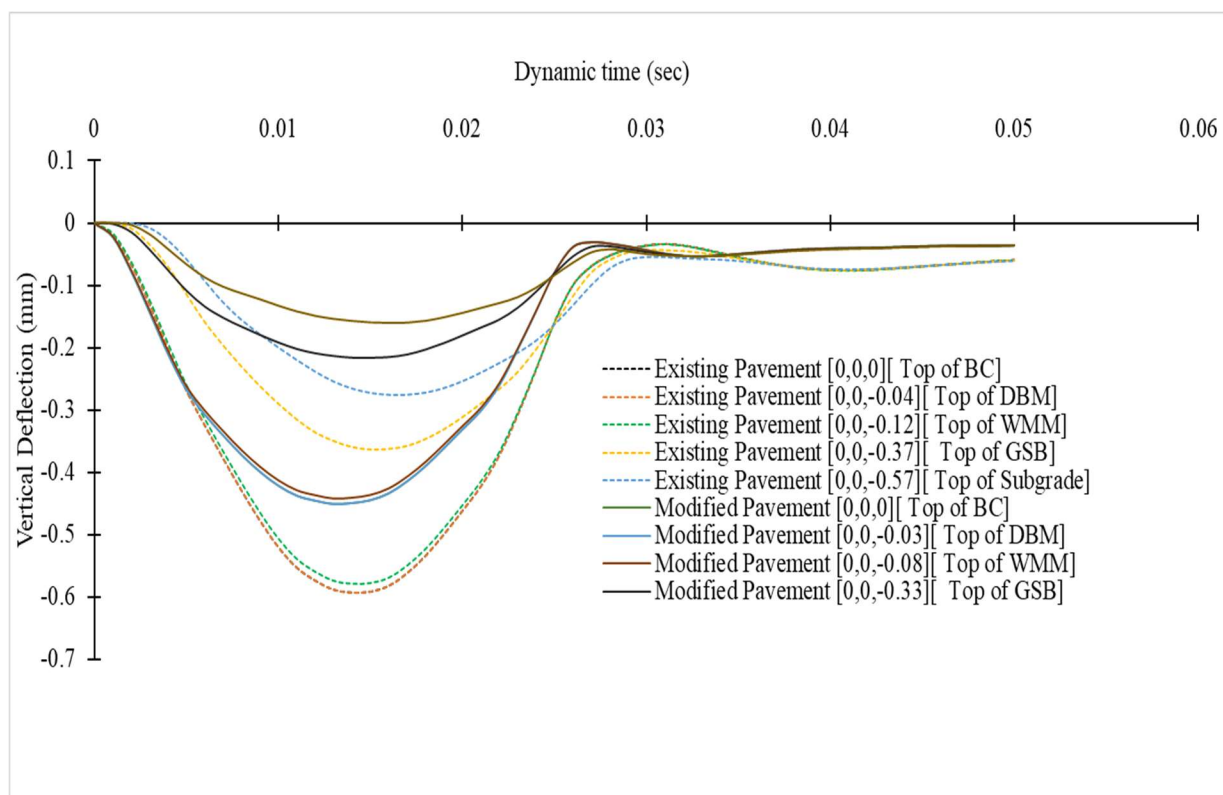


Fig. 9.10: Vertical deformation for both pavements as a function of dynamic time at the layer borders and on the pavement surface

It is evident from Fig. 9.10 that, vertical deflections of different boundary layers for modified pavement are less than that of existing pavement. It is due to the fact that resistance due to load of scrap tyre modified soil subgrade is higher than the existing soil, though the thickness of the pavement is less for modified soil subgrade pavement.

A comparison curve illustrating the surface deflection bowl for both existing and modified pavement is shown in Fig. 9.11, based on data from Table 7.3 and 7.4.

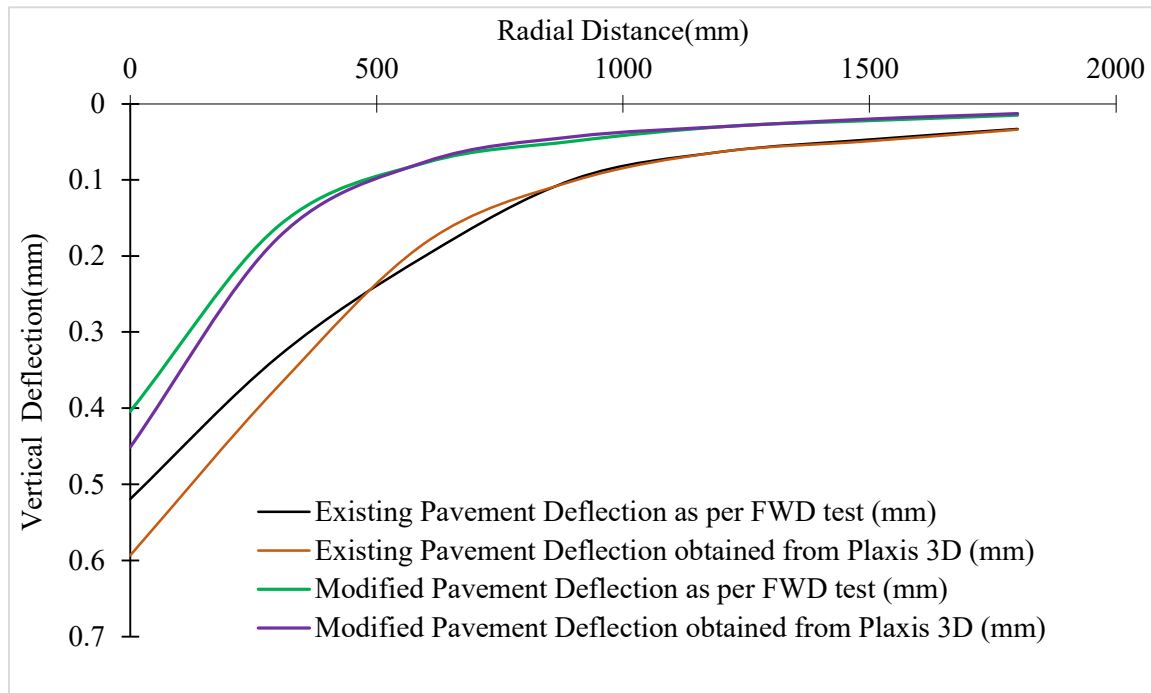


Fig. 9.11: Comparison of vertical deflection bowl for both the pavements

From Fig. 9.11, it is apparent that there is generally good agreement between the measured FWD test values and the PLAXIS 3D simulation results, with variations ranging from -8.54% to +14.26% for existing pavement and variations ranging from -13% to +12% for modified pavement. The discrepancies observed may be attributed to factors such as modelling assumptions, material properties, or boundary conditions. Further analysis and calibration may be needed to refine the numerical model for more accurate predictions.

Overall, the acceptance of dynamic FE analysis as a technique for FWD back analysis verification suggests that the procedure is quite promising. This result implies that this method might also be used to verify the material properties utilized in pavement construction. For instance, the dynamic FE analysis may be utilized to determine the expected deflection bowl.

9.5 EFFECT OF SCRAP TYRE ON SUBGRADE

9.5.1 Discussion on Impact of Thickness of Pavement

i. Based on the pavement thickness analysis presented in section 6.2.3.1, it is evident that the CBR value exerts a substantial impact on pavement design. Higher CBR values indicate stronger subgrade materials that can withstand heavier loads without excessive deformation. In such cases, thinner pavement layers may be required as the subgrade provides better support to the overlying pavement structure.

ii. For normal soil subgrade with a CBR of 3.36, the pavement thickness has been calculated as 570mm. By incorporating 10% shredded rubber tyres, the CBR value increased to 8.90, which allowed for a reduction in pavement thickness to 480mm. This modification resulted in a decrease of 90mm in pavement thickness, amounting to a significant reduction of 18.75%. This highlights the effectiveness of using a tyre-modified subgrade to reduce pavement thickness, as detailed in Table 9.1. The basic design analysis for pavement thickness has been discussed in section 6.2.3.

Table 9.1: Different layer pavement thickness for normal and tyre scrap mixed soil

Category	Layers	Pavement thickness of existing road Subgrade	Pavement thickness for scrap tyre modified subgrade
Bituminous Layer	BC	40mm	30mm
	DBM	80mm	50mm
Granular layer	WMM	250mm	250mm
	GSB	200mm	150mm
Total thickness		570mm	480mm
Difference in thickness		90mm	

9.5.2 Discussion on Impact of Subgrade Strain (ϵ_v)

The analysis and calculations derived from section 6.2.3, indicate important findings about the behaviour of pavement under stress and the impact of modifications on subgrade strain.

i. **Maximum Vertical Compressive Strain (ϵ_{mvc}) Analysis:** According to the analysis based on IRC 37:2018, for both kinds of pavements, the maximum vertical compressive strain at the

top of the subgrade is determined to be 0.6276×10^{-3} with a traffic load of 13.74 MSA. This value serves as a reference point for comparing the performance of existing and modified pavements.

ii. **Calculated Vertical Compressive Strain (ϵ_{cvc}) from Laboratory CBR:** After conducting IIT PAVE analysis using Laboratory CBR values for both pavement types, the ϵ_{cvc} for existing and modified pavements were found to be 0.6168×10^{-3} and 0.4915×10^{-3} respectively, according to Table 6.5 and Table 6.6. These values are crucial for evaluating the effectiveness of pavement modifications. Fig.9.12 shows the locations of critical strain in a pavement section.

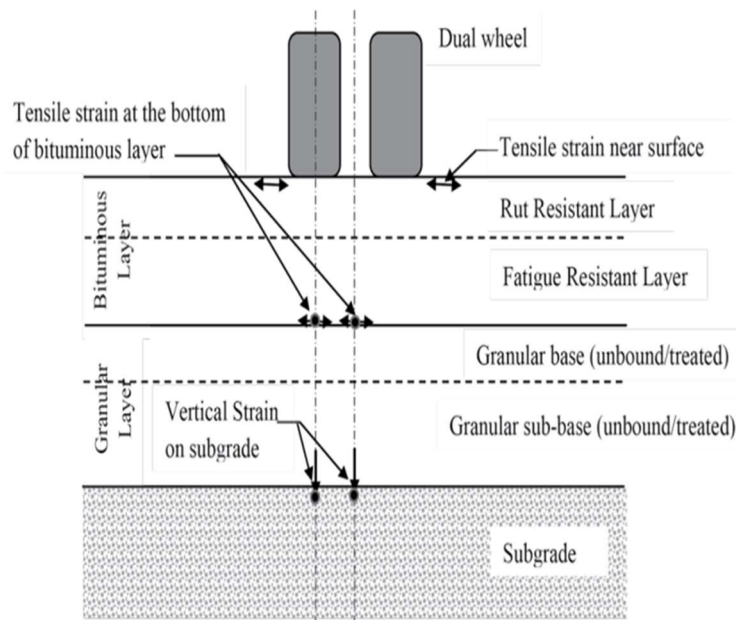


Fig. 9.12: Pavement Section Showing the Locations of Critical Strains. (IRC 37:2018)

iii. **Comparison of ϵ_{cvc} to ϵ_{mvc} :** The analysis reveals that for the normal subgrade, the ϵ_{cvc} is 1.72% less than the ϵ_{mvc} . In contrast, for the modified subgrade, ϵ_{cvc} is 21.68% less compared to ϵ_{mvc} . This significant reduction in strain for the modified pavement highlights the positive impact of the modifications on reducing subgrade stress. Fig. 9.13 illustrates the comparison chart between ϵ_{cvc} vs. ϵ_{mvc} .

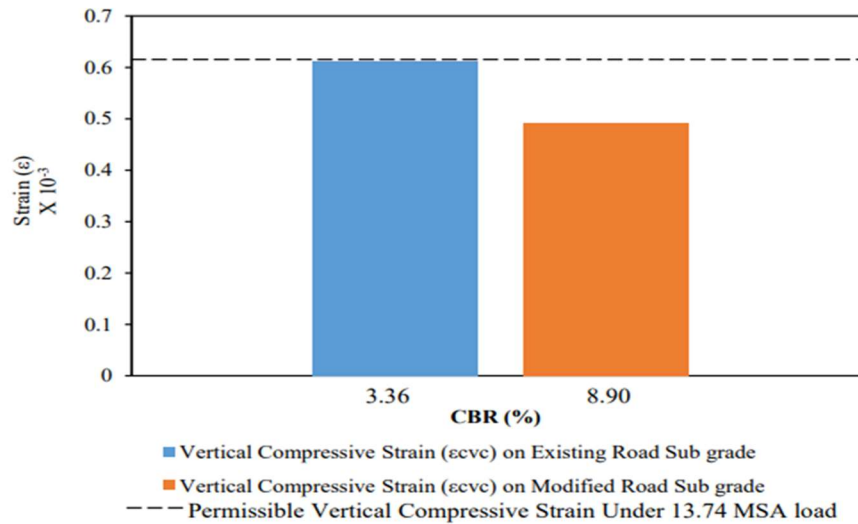


Fig. 9.13: Comparison chart between ϵ_{cvc} VS. ϵ_{mvc}

iv. **Impact of Modifications on Subgrade Strain:** The data indicates a substantial reduction in ϵ_{cvc} for the modified subgrade compared to the normal subgrade. Specifically, ϵ_{cvc} of the modified subgrade is 20.31% less than that of the normal subgrade. This reduction underscores the effectiveness of using scrap tyres in modifying the subgrade, which leads to a more stable and durable pavement by reducing the strain on subgrade soil.

The analysis showcases the advantages of pavement modifications, particularly the use of scrap tyres, in enhancing the stability and durability of the pavement by lowering the subgrade's vertical compressive strain significantly. This finding is instrumental for pavement engineering, offering a sustainable approach to improving pavement performance and longevity.

9.6 IMPACT OF COSTS ON MODIFIED PAVEMENT CONSTRUCTION

For a pavement of length 1 km, width of 5.5 m, and a subgrade depth of 500 mm, the calculated volume of the subgrade (V) is $(0.500 \times 5.5 \times 1000) = 2750 \text{ m}^3$. The required amount of soil for the modified pavement will be 2705 m^3 and the scrap tyre amount will be 420 ton to achieve the same condition of obtaining a modified CBR of 8.90 from a normal soil CBR of 3.36 and to achieve the subgrade volume of 2750 m^3 . Based on market prices, the costs for subgrade

soil and scrap tyres, including purchase, mobilization, and preparation, are detailed in Table-9.2.

Table 9.2: Quantity and cost analysis of flexible pavement for normal and tyre scrap modified subgrade

Material	Quantity required for per Km of existing pavement subgrade	Quantity required for per Km of modified pavement subgrade	Unit costs (INR) for material, mobilisation, and processing as per local market for pavement subgrade	Costs (INR) for material, mobilisation, and processing as per local market for existing pavement subgrade	Costs (INR) for material, mobilisation, and processing as per local market for modified pavement subgrade
Soil(m ³)	2750	2478	630	1732500.00	1561140.00
Tyre Scrap (Ton)	0	420	4600	0.00	1932000.00
Total costs				1732500.00	3493140.00

It has been observed from the thickness design that there had a thickness reduction in pavement of around 90mm. Due to this reduction a cost cut has been observed with respect to surface, base and subbase layer. According to the study scrap tyre material were mixed with subgrade soil. Hence for proper estimation, cost analysis for scrap tyre material has been made and presented on Table 9.3 by following WB Govt PWD, India, Roads Schedule of rates - 2018 with 10th Corrigendum. Detail cost estimate and rate analysis are attached in Annexure-VI.

Table 9.3: Thickness and costs analysis of flexible pavement for normal and tyre scrap modified subgrade

Pavement component	Layers	Thickness with untreated Soil Subgrade(mm)	Thickness with scrap tyre modified Soil Subgrade(mm)	Per Km costs (INR) for untreated pavement	Per Km costs (INR) for scrap tyre modified pavement
Bituminous Layer	BC	40	30	1888893.60	1416670.20
	DBM	80	50	3454066.36	2158791.23
Granular layer	WMM	250	250	3821620.00	3821620.00
	GSB	200	150	2914021.59	2185515.79
Subgrade		500	500	1732500	3493140
Total costs=				13811101.55	13075737.22
Hence cost difference=				735364.33	
Reduction in cost percentage with respect to existing pavement				5.30%	

India's 2021 Scrap Vehicle Policy, designed to replace old vehicles with new, environmentally friendly ones, has led to more vehicles and scrap tyres being scrapped. This has caused an increase in scrap tyre supply without a matching demand increase, typically leading to lower prices. With the policy continuing, the current 5.30% price reduction can be expected to grow. This trend aligns with economic principles and the expected ongoing impact of the policy on scrap tyre availability. This cost reduction will influence in case of pavement construction with very large length.

9.7 SUMMARY

The Chapter has presented the results from laboratory tests, field studies, and numerical simulations. The chapter highlights the improvements in subgrade performance due to the addition of scrap tyres, evidenced by increased CBR values and reduced deflections. The discussion also explores the implications of these findings for pavement design, emphasizing the potential for using tyre scrap as a sustainable material in road construction. Furthermore, cost analysis has been shown for untreated pavement and modified pavement with scrapped tyre.

CHAPTER 10

SUMMARY AND CONCLUSIONS

10.1 SUMMARY

To study the performance improvement of clayey subgrade with the addition of scrap tyre admixtures, soil samples were collected at each Km chainage along the Jibantala-Taldi Road, which spans 12.45 km in length and 5.5 m in width. Soil samples have been obtained from each chainage, and several tests have been carried out on them, such as the Modified Proctor Compaction test, CBR test, specific gravity, Atterberg Limits, and grain size distribution. The CBR values from 14 distinct chainage points have been taken into account in determining the design CBR value. Soil samples from chainages such as 3.00 km, 6.00 km, 7.00 km, 11.00 km, 12.00 km, and 12.45 km were collected based on the closest design CBR value, then mixed and retested mainly for UU, Modified Proctor, and CBR. The mixed soil was further combined with different sizes (10mm x 10mm, 15mm x 15mm, 20mm x 20mm, 25mm x 25mm, and 30mm x 30mm) and proportions (5%, 10%, 15%, 20%, 25%, and 30%) of tyre scrap to determine the optimum CBR value and the respective tyre size and proportion, which was found to be 15mm x 15mm and 10%. An axle load test and traffic census were conducted on the existing Jibantala-Taldi Road. Pavement design was carried out using IIT PAVE, considering the design CBR for the existing pavement to determine the actual pavement thickness of 570mm, and another design using the optimum CBR, keeping all conditions the same as the existing road, which resulted in a thickness of 480mm. A new or modified pavement stretch of 30m in length, 5.5m in width, and 480mm in thickness, with a tyre scrap-modified subgrade depth of 500mm, was constructed. DCPT on the modified subgrade and FWD on the pavement were performed to obtain field CBR, FWD-oriented deflection of subgrade in terms of LLI, and Elastic Modulus (Es). PLAXIS 3D Dynamic FE modelling of the FWD test was conducted to create an approximate simplified numerical model and use

experimental data to validate the findings. A regression method using MINITAB statistical software was employed to establish a relationship among modified CBR as the dependent variable and normal soil CBR, size of scrap tyre, percentage of scrap tyre, and pavement thickness as independent variables.

10.2 CONCLUSIONS

Based on the current investigation, the following conclusions can be made:

- a) The existing road subgrade soil properties indicate minimal variation in soil characteristics. Considering the different change values, the design CBR has been determined to be 3.36 from 14 different chainage CBR values.
- b) Soil from various chainages was collected based on the closest design CBR value, then mixed and retested for UU, Proctor and CBR. The CBR of the mixed soil was 3.37, after which it was mixed with tyre scrap for further testing.
- c) The addition of 10% shredded rubber tyre, sized 15mm \times 15mm, to normal mixed soil produces a modified CBR value of 8.90, which increases the soaked CBR value from 3.36 by 164%. However, further addition decreases it. Thus, 10% is the optimal amount for soaked conditions.
- d) An effort was made to determine the pavement design by considering both the existing pavement CBR and the optimum CBR. The design was made for both CBR values, based on the condition of the existing Jibantala-Taldi Road. To achieve this, a traffic census and axle load survey were conducted.
- e) The pavement thickness was determined using the IRC method through IIT PAVE software. Incorporating 10% shredded rubber tyre (15mm \times 15mm) reduced the pavement thickness by 18.75%, from 570mm to 480mm, which is a 90mm reduction compared to the normal soil subgrade.

f) A new pavement of stretch 30m, width 5.5m, thickness 480mm and tyre scrap modified subgrade depth 500mm was constructed to test DCPT on the modified subgrade and FWD on the pavement, to get field CBR and FWD oriented deflection in terms of LLI and Elastic Modulus (E_s).

g) The current study showed that incorporating 10% shredded rubber tyre, sized 15mm \times 15mm, into the subgrade soil significantly improved its CBR value for both laboratory and in-situ CBR values determined by DCPT. Specifically, for the modified pavement, the in-situ DCPT-measured CBR increased by 141%, compared to the existing pavement.

h) The modified subgrade with 50% lower LLI with respect to the existing subgrade, indicates enhanced stiffness and load-bearing capacity, likely due to scrap tyre material, leading to improved load distribution, less strain on layers, and extended pavement lifespan.

i) The scrap tyre-modified pavement's modulus is 2.68 times higher than the existing pavement, indicating that using recycled tyres improves pavement performance and offers a sustainable solution for more durable roads.

j) Overall acceptance of dynamic FE analysis suggests promising applications in pavement construction. Resistance due to load in modified soil subgrade results in lower vertical deflections.

k) Regression analysis on 30 soil samples stabilized with varying scrap tyre percentages and sizes. Strong correlations have been found ($R^2 = 0.84$, Adjusted $R^2 = 0.8163$) between modified soil CBR and input parameters. Model equations demonstrate good response prediction, enabling estimation of soaked CBR

10.3 CONTRIBUTION OF PRESENT INVESTIGATION TO THE EXISTING KNOWHOW IN LITERATURE

The present investigation significantly contributes to the existing body of knowledge on the use of waste materials, specifically tyre scrap, in civil engineering applications, particularly

in the stabilization of subgrade soils for flexible pavements. The key contributions are as follows:

- a) **Enhanced Understanding of Soil-Tyre Interaction:** This study provides a detailed analysis on influence of different sizes and proportions of tyre scrap on the mechanical properties of cohesive subgrade.
- b) **Validation through Field and Laboratory Studies:** By conducting both laboratory tests and field studies, the research bridges the gap between controlled experimental conditions and real-world applications. This dual approach validates the effectiveness of tyre scrap in improving subgrade performance.
- c) **Innovative Use of PLAXIS 3D for Subgrade Analysis:** The study introduces the use of PLAXIS 3D modelling to simulate and analyse the performance of tyre-modified subgrades under dynamic loading conditions. This application of advanced numerical methods enhances the predictive capabilities of pavement design and offers a novel approach for future research in geotechnical engineering.
- d) **Sustainable Engineering Practices:** The research advocates for sustainable construction practices by demonstrating the feasibility of repurposing waste materials in infrastructure projects. It provides a practical solution to the growing environmental issue of tyre waste, thus contributing to the development of more sustainable and eco-friendly civil engineering methodologies.
- e) **Comprehensive Comparative Analysis:** The research provides a strong foundation for assessing the advantages and drawbacks of utilizing tire waste in pavement construction through its comparative analysis of traditional and tyre-modified subgrades, which is backed by empirical data and regression analysis.

10.4 LIMITATION AND SCOPE OF THE FURTHER RESEARCH

10.4.1 Limitations of the Study

a) Cohesive Subgrade Focus: The study's applicability is limited to cohesive subgrades. This limitation implies that the findings may not be directly transferable to non-cohesive subgrades, such as sandy or gravelly soils, which behave differently under load due to their lack of cohesion.

b) Impulse Load Consideration: The research exclusively examines the effects of impulse loads. This focus excludes dynamic loads, such as those caused by moving vehicles, which can induce different stresses and deformations in road materials.

c) Long-Term Performance: The study primarily focuses on short-term performance improvements. However, the long-term durability and behavior of the modified subgrade, particularly under continuous traffic loading and environmental exposure, remain uncertain and require further investigation.

d) Single Road Stretch Analysis: The investigation was conducted on a singular stretch of road. Different road stretches, even within the same region, can have varying conditions such as soil type, traffic patterns, and maintenance history, which might influence the study's applicability to other contexts.

These limitations highlight the specific context in which the study's findings are valid and point towards areas for future research, such as expanding the scope to include non-cohesive subgrades, considering dynamic loads, and analysing multiple road stretches for broader applicability.

10.4.2 Scope of Future Research

a) The study may be extended for granular Subgrade.

b) The study may be extended for cyclic load simulating some traffic load with relevant soil properties under cyclic loading.

- c) the long-term durability and behaviour of the modified subgrade, particularly under continuous traffic loading and environmental exposure require further investigation
- d) The study may be extended with collection of real-life data for both cohesive and non-cohesive Subgrade and analysis by Artificial intelligence (AI) and Machine Learning (ML) for predicting performance in terms of variation of E of Subgrade with soil and scrapped tyre parameters.
- e) Design of a high-capacity batching plant and uniform mixer for efficient scrap tyre cutting and mixing, which may be done as interdisciplinary work with Mechanical Engineering.
- f) The investigation into subgrade performance with scrap tyre material through uniform mixing in different zones, such as the first 150 mm of the subgrade, the middle 150 mm, or the last 200 mm layer, will be conducted. The results from this type of mixing will be analysed, and the findings could prove to be economical.

REFERENCES:

1. Adigopula, V. K. (2022). A Simplified Empirical Approach for Prediction of Pavement Layer Moduli Values Using Lightweight Deflectometer Data. *International Journal of Pavement Research and Technology*, 15(3), 751–763. <https://doi.org/10.1007/s42947-021-00050-0>.
2. Akbarimehr, D., Aflaki, E., & Eslami, A. (2019). Experimental investigation of the densification properties of clay soil mixes with tire waste. *Civil Engineering Journal*, 5(2), 363–372.
3. Akshatha B A, Abhijith Jain, & Zaheer Ahmed. (2018). Stabilization Of Laterite Soil with Waste Tire Rubber. *International Journal of Engineering Sciences & Research Technology (A Peer Reviewed Online Journal) Impact*, 181–187. <https://doi.org/10.5281/zenodo.2294960>.
4. Alam*, Mohd., Nazim, M., & Singh, Dr. S. K. (2020). Deterioration Pattern of Flexible Pavement with the Help of Falling Weight Deflectometer. *International Journal of Innovative Technology and Exploring Engineering*, 9(8), 737–744. <https://doi.org/10.35940/ijitee.H6755.069820>.
5. Al-Neami, M. A. (2018). Stabilization of sandy soil using recycle waste tire chips. *International Journal of GEOMATE*, 15(48), 175–180. <https://doi.org/10.21660/2018.48.180228>.
6. Amin, H., Khan, B. J., Ahmad, M., Hakamy, A., Sikandar, M. A., Sabri, M. M. (2023). Evaluation of shear strength parameters of sustainable utilization of scrap tires derived geo-materials for civil engineering applications. *Frontiers in Earth Science*, 11. <https://doi.org/10.3389/feart.2023.1116169>.
7. Apriyono, A., Sumiyanto, Gusmawan, D. D. (2017). Application of woven tires waste as soft clay subgrade reinforcement for preventing highway structural failure. *AIP Conference Proceedings*, 1818. <https://doi.org/10.1063/1.4976868>
8. Bai, J., Zhang, Y., & Wu, S. (2020). Review Study of Physical and Mechanical Characteristics on Mixed Soil with Scrap Tire Rubber Particles. In *Jordan Journal of Mechanical and Industrial Engineering* (Vol. 14, Issue 1).
9. Bandyopadhyay, K., & Bhattacharjee, S. (2010). Comparative Study Between Laboratory and Field CBR by DCP and IS Method. *Indian Geotechnical Conference, IGS Mumbai Chapter*, 1011–1014.
10. Chai, G. W., Argadiba, S., Stephenson, G., Condric, I., Oh, E. Y., & Manoharan, S. P. (2013). Prediction of subgrade CBR using FWD for thin bituminous pavements. *International Journal of Pavement Research and Technology*, 6(4), 280–286. [https://doi.org/10.6135/ijprt.org.tw/2013.6\(4\).280](https://doi.org/10.6135/ijprt.org.tw/2013.6(4).280).

11. Chaudhary, P. M., Chaudhary, P. B., Desai, B. H., & Deshmukh, R. (2021). Design and Performance of Highway Pavement Reinforced with Geosynthetic. In S. Patel, C. H. Solanki, K. R. Reddy, & S. K. Shukla (Eds.), *Proceedings of the Indian Geotechnical Conference 2019* (pp. 351–363). Springer Singapore.
12. Coonse, J. (1999), Estimating California Bearing Ratio of COHESIVE piedmont Residual Soil using the Scala Dynamic Cone Penetrometer, Master's thesis, North Carolina State University, Raleigh, N
13. Dargay, J. (2007). Worldwide: 1960-2030 Article in *The Energy Journal*. Vehicle Ownership and Income Growth. <https://doi.org/10.2307/41323125>
14. Dhorajiya Pradip, Mayank Kanani, Yashwantsinh Zala. (2019). Utilization of Waste Rubber Tyre as Reinforcement in Flexible Pavement. *Journal of Emerging Technologies and Innovative Research (JETIR)*, 6(4). www.jetir.org
15. Díaz Flores, R., Aminbaghai, M., Eberhardsteiner, L., Blab, R., Buchta, M., & Pichler, B. L. A. (2023). Multi-directional Falling Weight Deflectometer (FWD) testing and quantification of the effective modulus of subgrade reaction for concrete roads. *International Journal of Pavement Engineering*, 24(1). <https://doi.org/10.1080/10298436.2021.2006651>
16. Ese, Dag, Myre, Jostein, Nos, Per Magne, and Vaernes, Einar. (1994), the Use of Dynamic Cone Penetrometer (DCP) for road strengthening design in Norway, *Proc., Int. Conf. on Bearing Capacity of Rd. and Airfield*. pp3-22
17. Farhana Tabasum, S. D., Laharipriya, M., Saranya, V., Jyothsna, Y., Dharani, D., Lakshmi, M. V. An Experimental Study on Stabilization of Soil by using Shredded Rubber Tyre. www.ijfmr.com
18. Fuentes, L., Taborda, K., Hu, X., Horak, E., Bai, T., & Walubita, L. F. (2022). A probabilistic approach to detect structural problems in flexible pavement sections at network level assessment. *International Journal of Pavement Engineering*, 23(6), 1867–1880. <https://doi.org/10.1080/10298436.2020.1828586>
19. Gabr, M. A., Hopkins, K., Coonse, J., & Hearne, T. (2000). DCP criteria for performance evaluation of pavement layers. *Journal of Performance of Constructed Facilities*, 14(4), 141–148.
20. Garga, V. K., & O'shaughnessy, V. (2000). Tire-reinforced earthfill. Part 1: Construction of a test fill, performance, and retaining wall design.
21. Goutami, K., Murthy, K., Sandhya Rani, D., Tech Student, M., & Guide, P. (2017). Flexible Pavement Design and Comparison of Alternative Pavements using IRC 37-2012 IITPAVE. In *IJSRD-International Journal for Scientific Research & Development* (Vol. 5). www.ijssrd.com
22. Government of India (2021), Union Budget, Ministry of Finance, New Delhi.
23. Hambleton, J. P., & Drescher, A. (2009). Modelling wheel-induced rutting in soils: Rolling. *Journal of Terra mechanics*, 46(2), 35–47.
24. Harish G. R. (2017). Analysis of Flexible Pavements using IIT Pave. *Imperial Journal of Interdisciplinary Research (IJIR)* Vol-3, Issue-6, 2017 ISSN: 2454-1362.
25. Harison, J. A. (1987). Correlation Between California Bearing Ratio and Dynamic Cone Penetrometer Strength Measurement of Soils. Technical Note 463. *Proceedings of the Institution of Civil Engineers*, 83(4), 833–844.

26. Horak E. (2008). Benchmarking the structural condition of flexible pavements with deflection bowl parameters. *Journal of the South African Institution of Civil Engineering*, 50(2), 2–9.
27. Howard, I. L., & Warren, K. A. (2009). Finite-element modelling of instrumented flexible pavements under stationary transient loading. *Journal of Transportation Engineering*, 135(2), 53–61.
28. HUANG, Y. H. (2004). *Pavement Analysis and Design*. America.
29. Hussainbhi Binginapalli, Sridhar K, Naidu V Mahalakshmi, & Mahalakshmi Naidu, V. (2021). An Analytical study on flexible pavement and rigid pavement design of a Road. *International Journal of Research in Engineering and Science (IJRES)* ISSN, 09(10), 81–88. www.ijres.org
30. Ibrahim, & Osinubi, K. J. (2022). Stabilization of Lateritic Soil with Scrap Tyre Crumb Rubber.
31. IRC: 37-2018 “Guidelines for the Design of Flexible Pavements”, New Delhi, 2018.
32. IRC 115. (2014). ‘Guidelines For Structural Evaluation and Strengthening of Flexible Road Pavements Using Falling Weight Deflectometer (Fwd.) Technique’, New Delhi.
33. IS 2720 (Part II) (1973): “Determination of water content”. Bureau of Indian Standards, New Delhi.
34. IS 2720 (Part III) (1980): “Determination of Specific gravity” Bureau of Indian Standards, New Delhi.
35. IS 2720 (Part IV) (1985): “Determination of Grain Size” Bureau of Indian Standards, New Delhi.
36. IS 2720 (Part V) (1985): “Determination of Liquid and Plastic limit” Bureau of Indian Standards, New Delhi.
37. IS 2720 (PART VIII) (1983): ‘Determination of water content-dry density relation using heavy compaction’ Bureau of Indian Standards, New Delhi.
38. IS 2720 (Part XI) (1993): ‘Determination of the shear strength parameters of a specimen tested in unconsolidated undrained triaxial compression without the measurement of pore water pressure’. Bureau of Indian Standards, New Delhi.
39. IS 2720 (Part XVI) (1987): “Determination of California Bearing Ratio “Bureau of Indian Standards, New Delhi.
40. Jastrzębska, M. (2019). Strength characteristics of clay-rubber waste mixtures in UU triaxial tests. *Geosciences* (Switzerland), 9(8). <https://doi.org/10.3390/geosciences9080352>
41. Johns, D., Deepakraja, T. G., & Karthiga Devi, M. (2017). Use Of Waste Tyre as Subgrade in Flexible Pavement. *International Research Journal of Engineering and Technology*.
42. Juliana, I., Fatin, A. R., Rozaini, R., Masyitah, M. N., Khairul, A. H., & Nur Shafieza, A. (2020). Effectiveness of crumb rubber for subgrade soil stabilization. *IOP Conference Series: Materials Science and Engineering*, 849(1). <https://doi.org/10.1088/1757-899X/849/1/012029>
43. Kleyn, E. G. (1975). The use of the dynamic cone penetrometer (DCP). Transvaal Provincial Administration.
44. Kleyn, E. G., & Savage, P. F. (1982). Application of the pavement DCP to determine the bearing properties and performance of road pavements.

45. Korolev, K. V. (2014). Intermediate bearing capacity of saturated bed of strip foundation. *Soil Mechanics and Foundation Engineering*, 51(1), 1–8.
46. Kumar Mohan A N, & Kumar Praveen P. (2020). Analysis of Flexible Pavement using IITPAVE Software and Economic Analysis of the Project using HDM-4 Software. *International Journal for Research in Applied Science and Engineering Technology*, 8(5), 2651–2657. <https://doi.org/10.22214/ijraset.2020.5443>.
47. Lee, J. S., Kim, S. Y., Hong, W. T., & Byun, Y. H. (2019). Assessing subgrade strength using an instrumented dynamic cone penetrometer. *Soils and Foundations*, 59(4), 930–941. <https://doi.org/10.1016/j.sandf.2019.03.005>.
48. Li, S., & Li, D. (2018). Mechanical Properties of Scrap Tire Crumbs-Clayey Soil Mixtures Determined by Laboratory Tests. *Advances in Materials Science and Engineering*, 2018. <https://doi.org/10.1155/2018/1742676>.
49. Livneh, M. (1987), the Use of Dynamic Cone Penetrometer in Determining the Strength of Existing Pavements and Subgrade, Proc. 9th Southeast Asia Geotechnical Conference, Bangkok, Thailand.
50. Livneh, M. (1989), Validation of Correlations between a number of Penetration Tests and in situ California Bearing Ratio Tests, *Transportation Research Record* 1219, pp56-67.
51. Livneh M, Ishai I, Livneh. (1994). Effect of vertical confinement on dynamic cone penetrometer strength values in pavement and subgrade evaluations. *Transportation Research Record* 1473, 1–8.
52. Loizos, A., Al-Qadi, I. L., & Scarpas, T. (n.d.). Bearing capacity of roads, railways and airfields: proceedings of the 10th International Conference on the Bearing Capacity of Roads, Railways and Airfields (BCRRA 2017), June 28-30, 2017, Athens, Greece.
53. Loizos, A., & Scarpas, A. (2005). Verification of falling weight deflectometer back analysis using a dynamic finite elements simulation. *International Journal of Pavement Engineering*, 6(2), 115–123. <https://doi.org/10.1080/10298430500141030>.
54. Mangi Naeem, & Sarki Faisal Ahmed. (2021). Improvement of subgrade soil by blending tyre driven aggregate (TDA). *International Journal of Emerging Trends in Engineering Research*, 9(6), 612–616. <https://doi.org/10.30534/ijeter/2021/01962021>.
55. Maree J. H., & Bellekens R. J. L. (1991). The effect of asphalt overlays on the resilient deflection bowl response of typical pavement structures. RP90/102. Chief Directorate National Roads, Pretoria, South Africa, 1991.
56. Maree J H, & Jooste F. (1999). Structural classification of pavements through the use of IDM deflection basin parameters. RDAC Report PR 91/325.
57. Marefat V, & Soltani-Jigheh H. (2011). Laboratory behavior of clay-tire mixtures. *World Applied Sciences Journal*, 13(5), 1035–1041.
58. Mashiri, M. S., Vinod, J. S., Sheikh, M. N., & Tsang, H. H. (2015). Shear strength and dilatancy behaviour of sand-tyre chip mixtures. *Soils and Foundations*, 55(3), 517–528. <https://doi.org/10.1016/j.sandf.2015.04.004>.
59. Mehta, A., Mishra, A., Nikumbh, K., Ponkshe, T., Graduate Student, U., Professor, A., & Shah, A. (2021). Design of Flexible Pavement as per IRC:37-2018 and using IIT-Pave Department of Civil Engineering. In *IJSRD-International Journal for Scientific Research & Development* (Vol. 9).

60. Momin, K. A., & Hamim, O. F. (2022). Pavement Management System Using Deflection Prediction Model of Flexible Pavements in Bangladesh. *Lecture Notes in Civil Engineering*, 184, 363–370. https://doi.org/10.1007/978-981-16-5547-0_34
61. Munnoli, P. M., Sheikh, S., Mir, T., Kesavan, V., & Jha, R. (2013). Utilization of rubber tyre waste in subgrade soil. *C2013 IEEE Global Humanitarian Technology Conference: South Asia Satellite, GHTC-SAS 2013*, 330–333. <https://doi.org/10.1109/GHTC-SAS.2013.6629940>
62. Murana, A. A., Uruaka, A. C. D., Chukwuma, O. (2019). in Axle Load Distribution and Failure Pattern on Highways in Nigeria: A Case Study of The Traffic Analysis on Jebba-Mokwa-Bokani Road in Niger State, Nigeria Axle Load Distribution and Failure Pattern on Highways in Nigeria: A Case Study of The Traffic Analysis on Jebba-Mokwa-Bokani Road in Niger State, Nigeria. In *International Journal of Advances in Mechanical and Civil Engineering* (Issue 6). <http://iraj>.
63. Nega, A., Nikraz, H., & Al-Qadi, I. L. (2016). Dynamic analysis of falling weight deflectometer. *Journal of Traffic and Transportation Engineering (English Edition)*, 3(5), 427–437. <https://doi.org/10.1016/j.jtte.2016.09.010>
64. Nwanya, A. C., & Okeke, O. C. (2018). Using Dynamic Cone Penetrometer Tester to Determine CBR and Bearing Pressures of Subsurface Soils in Parts of Owerri, Southeastern Nigeria. *European Journal of Engineering and Technology Research*, 3(12), 1–7.
65. Pai, R. R., Patel, S., & Bakare, M. D. (2020). Applicability of Utilizing Stabilized Native Soil as a Subbase Course in Flexible Pavement. *Indian Geotechnical Journal*, 50(2), 289–299. <https://doi.org/10.1007/s40098-020-00432-4>
66. Pandey, A., Vanshaj, K., Singh, G., Yadav, S., & Srivastav, J. B. (2022). Design of flexible pavement using experimental and software approach. *International Research Journal of Engineering and Technology*.
67. Peddaiah S, & Suresh K. (2017). Experimental Study on Effect of Tyre Chips and Lime in Improvement of Strength Properties of Expansive Soils. *International Journal of Civil Engineering and Technology (IJCIET)*, 8(10), 425–434.
68. Pradeep, A. (n.d.). Engineering Strength characteristics of soil partially replaced with waste paper sludge ash and scrap tyre rubber.
69. Promputthangkoon, P., & Karnchanachetane, B. (2013). Geomaterial Prepared from Waste Tyres, Soil and Cement. *Procedia - Social and Behavioral Sciences*, 91, 421–428. <https://doi.org/10.1016/j.sbspro.2013.08.439>
70. Rabbi, M. F., & Mishra, D. (2021). Using FWD deflection basin parameters for network-level assessment of flexible pavements. *International Journal of Pavement Engineering*, 22(2), 147–161. <https://doi.org/10.1080/10298436.2019.1580366>
71. Ravichandran, P. T., Prasad, A. S., Krishnan, K. D., & Rajkumar, P. R. K. (2016). Effect of Addition of Waste Tyre Crumb Rubber on Weak Soil Stabilisation. *Indian Journal of Science and Technology*, 9(5). <https://doi.org/10.17485/ijst/2016/v9i5/87259>
72. Razali, M., Mahmood, N. A. C., Hashim, K. A., Mansor, S., & Zainuddin, N. I. (2018). The falling weight deflectometer (FWD) for characterization bonding state of subgrade. *AIP Conference Proceedings*, 2020. <https://doi.org/10.1063/1.5062648>

73. Rokade S, & Azad, M. (2012). Use of Waste Plastic and Waste Rubber Tyres in Flexible Highway Pavements. International Conference on Future Environment and Energy (IPCBEE), 28.
74. Sahoo, P. K., & Reddy, K. S. (2009). Evaluation of subgrade soils using dynamic cone penetrometer. International Journal of Earth Sciences and Engineering, 2(4), 384–388.
75. Scala AJ. (1956). Simple method of flexible pavement design using cone penetrometers. 2nd Australian and New Zealand Conference on Soil Mechanics and Foundation Engineering, 73–83.
76. Singh Jagtar, & Sonthwal Vinod Kumar. (2017). Improvement of Engineering Properties of clayey soil using shredded rubber tyre. International Journal of Theoretical & Applied Sciences, 1–6. www.researchtrend.net
77. Singh, Y. K., Ray, D. S., & Student, P. G. (2019). Analysis of Vehicle Damage Factor in Overloading for Different Types of Loading. In International Journal of Engineering Science and Computing. <http://ijesc.org/>.
78. Skels, P., Zariņš, A., Bondars, K., Haritonovs, V. (2017). Analytical and numerical design approaches for stabilized road pavement base layers. <https://doi.org/10.1201/9781315100333-167>.
79. Smith, I. M., Griffiths, D. V., & Margetts, L. (2013). Programming the finite element method. John Wiley & Sons.
80. Solanki, U., Gundaliya, P., Barasara, M. (2016). Structural evaluation of flexible pavement using Falling Weight Deflectometer. In Multi-disciplinary Sustainable Engineering: Current and Future Trends (pp. 141–146). CRC Press. <https://doi.org/10.1201/b20013-23>.
81. Solanki, U., Gundaliya, P., & Barasara, M. (2019). A Study on FWD Deflection Bowl Parameters for Structural Evaluation of Flexible Pavement.
82. Solanki Ujjval J. Solanki, Gundalia Pradip J., Barasara Mansukh D. (2014). A Review on Structural Evaluation of Flexible Pavements using Falling Weight Deflectometer. STM Journal, 2(1), 1–10.
83. Sousa, F. D. B. de. (2017). Devulcanization of Elastomers and Applications. In N. Cankaya (Ed.), Elastomers (p. Ch. 10). IntechOpen. <https://doi.org/10.5772/intechopen.68585>
84. Tahami, S. A., Mirhosseini, A. F., Dessouky, S., Mork, H., & Kavussi, A. (2019). The use of high content of fine crumb rubber in asphalt mixes using dry process. Construction and Building Materials, 222, 643–653.
85. Talvik, O., & Aavik, A. (2009). Use of FWD deflection basin parameters (SCI, BDI, BCI) for pavement condition assessment. Baltic Journal of Road and Bridge Engineering, 4(4), 196–202. <https://doi.org/10.3846/1822-427X.2009.4.196-202>
86. Teja, S. S., & Sidhhartha, P. (2015). Stabilization of subgrade soil of highway pavement using waste tyre pieces. International Journal of Innovative Research in Science, Engineering Technology, 4(5), 3265–3272. <https://doi.org/10.15680/ijirset.2015.0405045>
87. The National Green Tribunal (NGT) SOUTHERN ZONE, CHENNAI September 19, 2019.
88. Vakili, A. H., Salimi, M., & Shamsi, M. (2021). Application of the dynamic cone penetrometer test for determining the geotechnical characteristics of marl soils treated by lime. Heliyon, 7(9).

89. Van Vuuren D. (1969). Rapid determination of CBR with the portable dynamic cone penetrometer.
90. Walubita, L. F., Das, G., Espinoza, E., Oh, J., Scullion, T., Lee, S. I., Garibay, J. L., Nazarian, S., & Abdallah, I. (2011). TEXAS FLEXIBLE PAVEMENTS AND OVERLAYS: YEAR 1 REPORT-TEST SECTIONS, DATA COLLECTION, ANALYSES, AND DATA STORAGE SYSTEM 5. Report Date Project 0-6658 13. Type of Report and Period Covered Project performed in cooperation with the Texas Department of Transportation and the Federal Highway Administration. Project Title: Collection of Materials and Performance Data for Texas Flexible Pavements and Overlays Unclassified.
91. Wangmo, P., Selden, D., Wangmo, R., Choki, S., Phuntsho, S., Tobgyel, T., Dema, S. (2020). IMPROVEMENT OF ROAD SUBGRADE USING WASTE TYRES. In Zorig Melong: A Technical Journal (Vol. 4).
92. Yang, Z., Zhang, Q., Shi, W., Lv, J., Lu, Z., & Ling, X. (2020). Advances in properties of rubber reinforced soil. In Advances in Civil Engineering (Vol. 2020). Hindawi Limited. <https://doi.org/10.1155/2020/6629757>.
93. Zain, N. H. M., Salim, N. A. M., Bahri, I. S. S., & Yusof, Z. M. (2022). Experimental study using recycled waste tyre as sustainable clay soil stabilisation. *International Journal of Integrated Engineering*, 14(5), 122–129.
94. Zornberg J.G, Costa, Y. D., & Vollenweider, B. (2004, January). Mechanical Performance of a Prototype Embankment Backfill Built with Tire Shreds and Cohesive Soil. 83rd Annual Meeting of the Transportation Research Board, Washington, D.C

ANNEXURE- I

**PERMISSION LETTER FROM PWD, GOVT.OF WEST
BENGAL**

GOVERNMENT OF WEST BENGAL
OFFICE OF THE EXECUTIVE ENGINEER
SOUTH 24 PARGANAS DIVISION
PUBLIC WORKS DIRECTORATE
76, DR. DEODAR RAHAMAN ROAD
(3RD FLOOR)
KOLKATA – 700 033
 Phone (Office): -
 2422-0365 & 2422-0366
E-mail:- eessdivn1@gmail.com



পশ্চিমবঙ্গ সরকার
 নির্বাহী বাতুলকার
 দক্ষিণ ২৪ পরগনা ভুক্তি, পূর্ত দপ্তর
 ৭৬, ড: দেওদার রহমান রোড, চতুর্থ তল
 কোলকাতা - ৭০০ ০৩৩

দুরাভাষ (কার্যালয় ও ফ্যাক্স)-
 (০৩৩) ২৪২২-০৩৬৫ এবং ২৪২২-০৩৬৬
 ই-মেল :- eessdivn1@gmail.com

Memo No.: 1274

Date, the Kolkata 06-06-2019

To
 Dr. Sumit Kumar Biswas
 Associate Professor
 Department of Civil Engineering
 Jadavpur University
 Kolkata – 700 032

Sub.: - Permission to use P.W.D. Road for Ph. D Thesis work.

Ref.: - Your Memo No. JUCE/SKB/19-20/09 Dated 03-06-2019.

Sir,


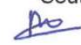
I am pleased to inform you that the road named – Jibantala to Taldi Bazar from Ch. 0.00 Kmp to 12.45 under South 24 Parganas Division, P.W.D., Government of West Bengal may be used for Ph. D. work of Mr. Sujoy Sarkar (Registration No. 1021703004 of 2017-2018) residing at 1 No. Bijoy Nagar, North 24 Parganas.

In this context Mr. Sarkar is permitted to do all the necessary job, related to Soil Test, Traffic Survey and allied works as per his requirement.

This is for your kind information and necessary action please.

Thanking you,




 Executive Engineer
 South 24 Parganas Division P.W. D.
 Executive Engineer, P.W.D.
 South 24 Parganas Division


ANNEXURE- II

LABORATORY TEST RESULTS FOR SCRAP TYRE, MIX SOIL AND TYRE MIX SOIL



OMEGA
Consultant Services

A Govt. Regd. Test House

www.omegaconsultantservices.com

Laboratory Accredited By :
NABL, A constituent Board of Quality
Council of India, Govt. of India
An ISO 9001-2015 Certified Company

HEAD OFFICE & LABORATORY
Campus - I

256A, M. G. Road, Purbasan, Thakurpukur, Kol.- 63
Phone : (033) 2497 1903, 2438 1677, M. 9830020628 / 9432219707
e-mail : omegalabinfo@gmail.com, omegalabinfo98@gmail.com

TEST REPORT

JOB ID No. TC- OCSK/19/04D - 0000025		Date: 18.04.2019	Page 1 of 1
Ref. No. : Jucon/OCS/PhD/testing/01 Date: 04.04.2019	Product : Nil		
Issued to : Mr. Sujoy Sarkar 1 No. Bijoy Nagar Boropukur Par, Naihati Dist- north 24 Parganas PIN-743165	Specification : Tabulated Below		
Description of sample(s) : 2nos. of Scrap Tyre sample for the following tests. Sub.: Testing of scrap tyre samples for research job (PhD)	Seal / Stamp / Mark : Marked (if any)		
Test Parameter : Density, Melting point, Specific gravity, Water absorption & Elastic Modulus	Sample received on : 04.04.2019 Sample tested on : 04.04.2019 to 18.04.2019		

This is to certify that the above sample (S) has/have been tested with the following results:

TEST RESULT

CHARACTERISTICS	FINDINGS		METHOD OF TEST
	Sample-1	Sample-2	
1. Density (gm/cc)	1.11	1.13	IS: 4511 (Part-2) 1986 Reaf. 2019
2. Melting Point ($^{\circ}$ C)	232	236	IS: 5762 - 1970
3. Specific Gravity	1.13	1.15	IS: 4511 (Part-2) 1986 Reaf. 2019
4. Water absorption (%)	Nil	Nil	IS: 13630 (Part-2) 2019
5. Elastic Modulus (Mpa)	1.01	1.03	IS: 16388 - 2013

Remarks: The above submitted samples were duly tested as per relevant specification.

[Signature]
Prepared by

For OMEGA CONSULTANT SERVICES

[Signature]
A. PATRA (IAS)
QUALITY MANAGER
(AUTHORISED SIGNATORY)

***** End of Report *****

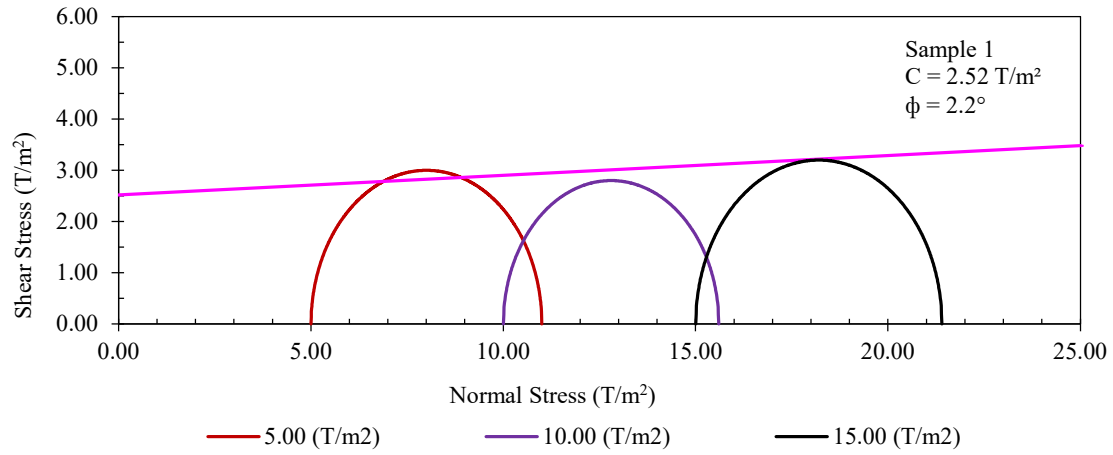
Note :

- ★ Analysed as on received basis and test results relate to the sample(s) only.
- ★ Liability for return of sample(s) ceases after fifteen days.
- ★ The reproduction of the report except in full is invalid without written approval of the laboratory.
- ★ The test results referred in certificate are based on observations & measurements under the stated environmental conditions.
- ★ The Test Report without EMBOSsing is Invalid.

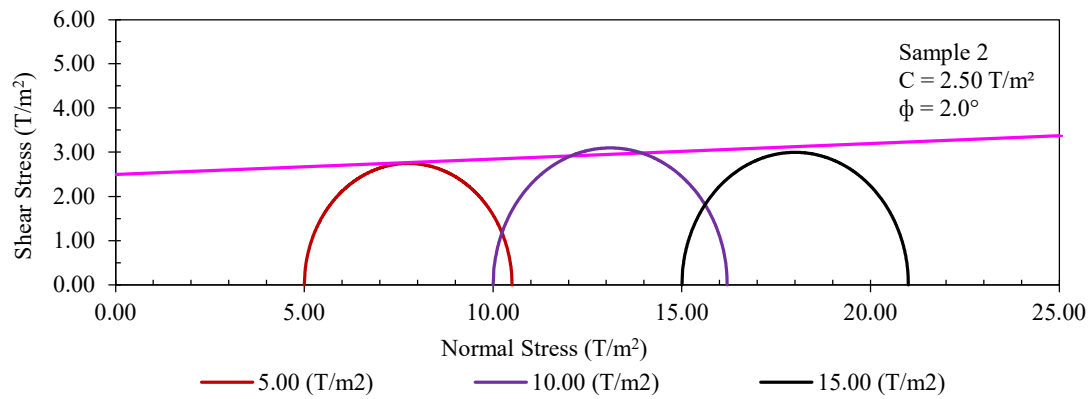
Campus - II : 996, M. G. Road, Purbasan, Thakurpukur, Kolkata - 700 063.

ANNEXURE- III

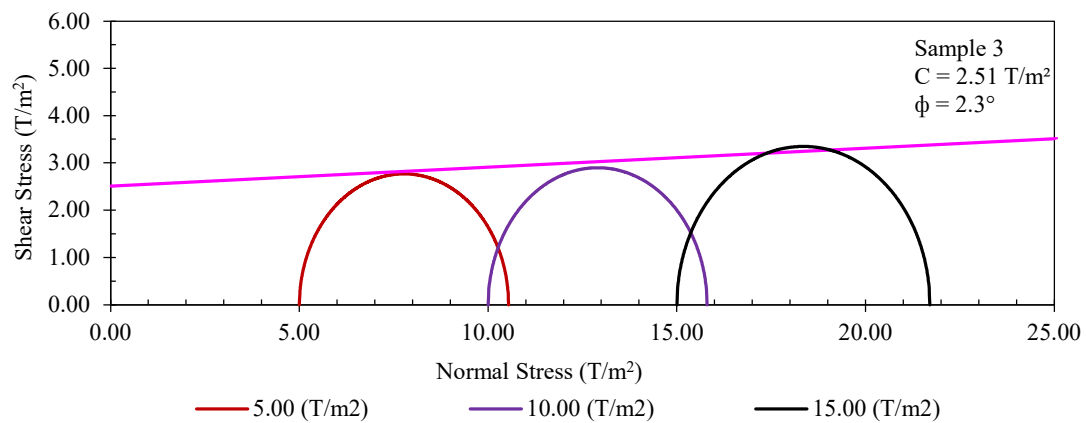
**LABORATORY TEST FOR MIX SOIL AND TYRE MIX
SOIL**



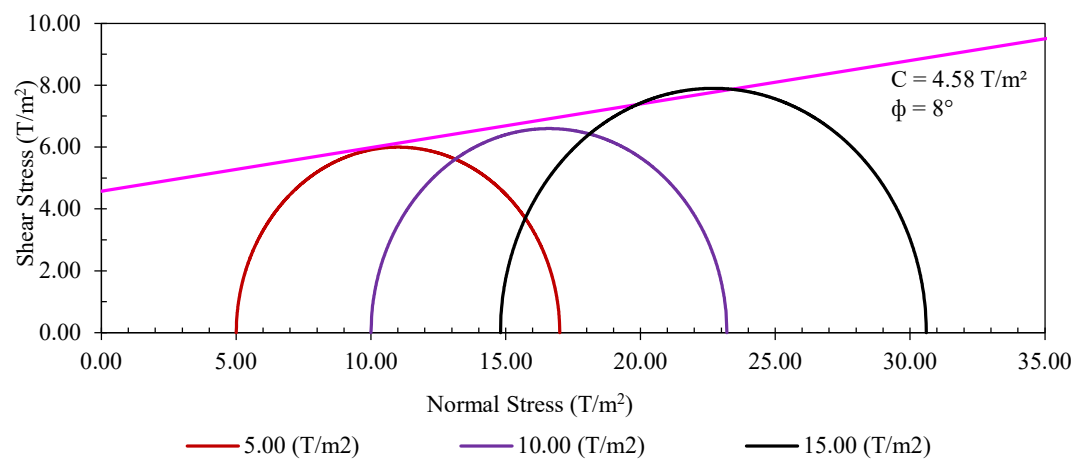
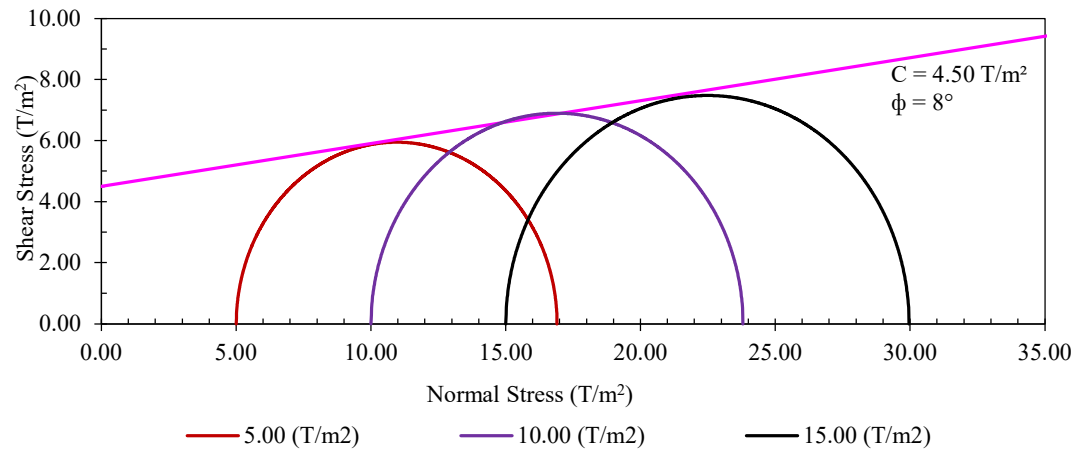
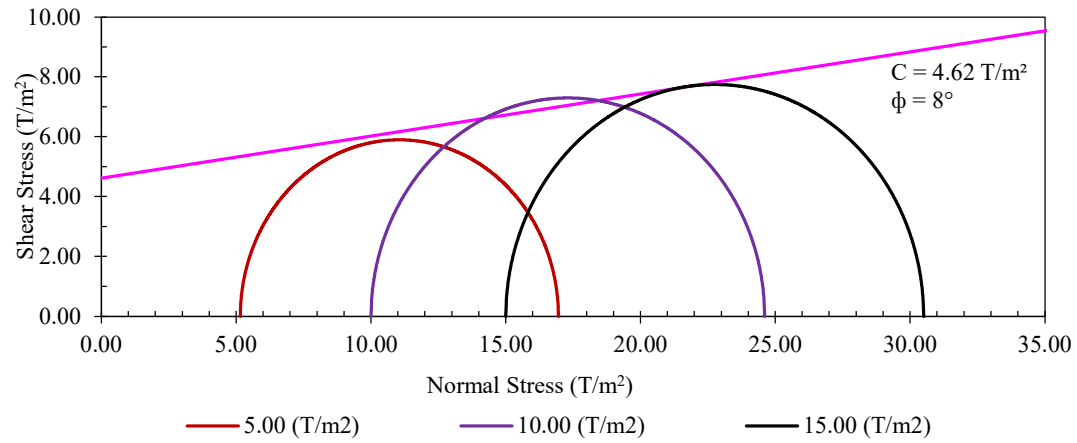
UU curve for sample 1 of mix soil.



UU curve for sample 2 of mix soil



UU curve for sample 3 of mix soil



ANNEXURE- IV

24/7 TRAFFIC STUDY DATA

Day-1

TRAFFIC DATA ANALYSIS
(Daily Sheet)

Road : Jibantala Bazar to Taldi bazar Road

Date of Work : 9-Jun-19 -to- 10-Jun-19

Chainage : 11+50 km

Location : Taldi

Day of Work :

Direction of Traffic :

Up	From: Jibantala	To: Taldi	Down	From: Taldi	To: Jibantala
-----------	-----------------	-----------	-------------	-------------	---------------

Time Period		Motorised Vehicle																								Non-motorised Vehicles												Total Hourly Vehicles			
		Fast Passenger												Fast Goods								Slow Goods				Total Motorised Vehicles		Animal / Hand Drawn		Cycle		Cycle Rickshaw		Others		Total Non-motorised Vehicles					
		Two-Wheeler		Auto Rickshaw		Car/Jee/v an/Taxi		Motorized Van		Bus		Truck				Agriculture Tractor		Agriculture Tractor with Trailer																							
From	To	Up	Down	Up	Down	Up	Down	Up	Down	Up	Down	Up	Down	Up	Down	Up	Down	Up	Down	Up	Down	Up	Down	Up	Down	Up	Down	Up	Down	Up	Down	Up	Down	Up	Down	Up+Dn					
8	9	8	25	0	0	0	0	0	0	0	0	0	0	0	0	1	1	0	0	0	0	0	0	1	1	10	27	0	0	6	8	0	0	0	0	6	8	16	35	51	
9	10	24	31	2	1	4	3	0	2	0	0	0	0	0	0	0	0	0	0	0	0	0	15	15	45	52	0	0	9	5	1	1	0	0	10	6	55	58	113		
10	11	33	11	1	2	2	6	1	1	0	0	0	0	0	0	1	1	0	0	0	0	0	1	2	39	23	0	0	8	5	1	1	0	0	9	6	48	29	77		
11	12	47	55	2	1	5	2	2	1	0	0	0	0	0	0	1	0	0	0	0	0	0	2	2	59	61	0	0	11	15	1	1	0	0	12	16	71	77	148		
12	13	53	30	2	1	20	22	0	0	0	0	0	0	2	1	0	3	0	0	0	0	1	3	1	2	79	62	0	0	18	16	1	2	0	0	19	18	98	80	178	
13	14	22	25	2	2	25	31	1	0	0	0	0	0	3	3	0	1	0	0	0	0	1	2	1	16	55	80	0	0	15	11	1	2	0	0	16	13	71	93	164	
14	15	25	25	2	1	20	30	0	1	0	0	0	0	6	6	2	1	2	0	0	0	1	0	2	3	60	67	0	0	10	12	2	1	0	0	12	13	72	80	152	
15	16	24	25	2	1	27	17	1	2	0	0	0	0	6	1	9	1	0	0	0	0	1	0	0	8	70	55	0	0	11	15	1	1	0	0	12	16	82	71	153	
16	17	24	22	1	1	21	20	0	0	0	0	0	0	3	2	8	3	0	0	0	0	1	3	10	60	59	0	0	12	10	1	1	0	0	13	11	73	70	143		
17	18	65	47	1	1	25	26	1	1	0	0	0	0	5	4	8	5	0	0	1	0	0	0	1	5	107	89	0	0	11	12	1	1	0	0	12	13	119	102	221	
18	19	36	52	1	2	31	31	1	1	0	0	0	0	4	1	1	9	0	0	0	0	1	0	1	2	76	98	0	0	10	11	1	1	0	0	11	12	87	110	197	
19	20	52	61	1	1	8	16	0	0	0	0	0	0	3	3	8	8	0	0	0	0	0	0	13	10	85	99	0	0	9	8	2	2	0	0	11	10	96	109	205	
20	21	22	23	1	1	16	25	0	0	0	0	0	0	3	5	3	9	0	0	0	0	1	0	3	3	49	65	0	0	8	7	0	0	0	0	8	7	57	72	129	
21	22	35	25	0	0	8	9	0	0	0	0	0	0	0	2	1	4	3	1	1	0	2	0	5	3	0	53	46	0	0	2	1	0	0	0	0	2	1	55	47	102
22	23	14	10	0	0	0	0	1	0	0	0	0	0	5	4	9	1	0	0	0	0	5	0	0	3	34	18	0	0	0	0	0	0	0	0	0	0	34	18	52	
23	0	0	0	0	0	0	0	0	0	0	0	0	0	9	3	8	2	1	9	0	0	5	5	1	1	24	20	0	0	0	0	0	0	0	0	0	0	24	20	44	
0	1	0	0	0	0	0	0	0	0	0	0	0	0	2	2	3	6	9	1	2	2	0	5	9	9	2	25	0	0	0	0	0	0	0	0	0	0	2	25	27	
1	2	0	0	0	0	0	0	0	0	0	0	0	0	0	1	6	3	0	0	0	0	0	5	3	2	9	11	0	0	0	0	0	0	0	0	0	0	9	11	20	
2	3	0	0	0	0	0	0	0	0	0	0	0	0	0	0	6	2	1	1	0	0	5	5	3	3	2	11	0	0	0	0	0	0	0	0	0	0	2	11	13	
3	4	0	0	0	0	0	0	0	0	0	0	0	0	0	0	9	9	8	9	2	2	5	6	3	3	27	29	0	0	0	0	0	0	0	0	0	0	27	29	56	
4	5	0	0	0	0	2	2	0	0	0	0	0	0	0	0	6	4	9	2	0	0	5	0	3	2	2	10	0	0	0	0	0	0	0	0	0	0	2	10	12	
5	6	9	8	2	1	8	8	2	2	0	0	0	0	0	0	2	6	1	3	0	2	5	0	3	20	32	50	0	0	0	0	0	0	0	0	0	0	32	50	82	
6	7	8	7	2	1	12	5	1	1	0	0	0	0	0	0	5	2	0	3	0	0	0	1	4	22	32	42	0	0	4	1	5	4	0	0	9	5	41	47	88	
7	8	6	3	3	2	15	9	1	2	0	0	0	0	0	0	3	1	3	0	0	0	0	1	2	1	33	19	0	0	4	5	6	6	0	0	10	11	43	30	73	
Daily Total		507	485	25	19	249	262	12	14	0	0	0	0	53	37	103	81	35	29	5	8	36	39	78	145	1044	1118	0	0	148	142	24	24	0	0	172	166	1216	1284	2500	
Total Vehicle (Up+Dn)		992		44		511		26		0		0		90		184		64		13		75		223		2162		0		290		48		0		338					
Equivalency Factor		0.5		1.0		1.0		1.0		1.5		3.0		1.5		3.0		3.0		4.5		1.5		4.5				6.0		0.5		2.0		4.5							
Daily PCU		254	243	25	19	249	262	12	14	0	0	0	0	80	56	309	243	105	87	23	36	54	59	351	653	1462	1672	0	0	74	71	48	48	0	0	122	119	1584	1791	3375	
Total PCU (Up+Down)		497		44		511		26		0		0		136		552		192		59		113		1004		3134		0		145		96		0		241					

Direction of Traffic :	Up	From: Jibantala	To: Taldi	Down	From: Taldi	To: Jibantala

209

Road : Jibantala Bazar to Taldi bazar Road

Date of Work : 11-Jun-19 -to- 12-Jun-19

Chainage: 11+50 km

Location : Taladi

Day of Work :

Direction of Traffic :

Up	From: Jibantala	To: Taldi
-----------	-----------------	-----------

Down

Down	From: Taldi	To: Jibantala
-------------	-------------	---------------

210

Road : Jibantala Bazar to Taldi bazar Road

Date of Work : 12-Jun-19 -to- 13-Jun-19

Chainage: 11+50 km

Location : Taldi

Day of Work :

Direction of Traffic :

Up	From: Jibantala	To: Taldi
-----------	-----------------	-----------

Down

Down	From: Taldi	To: Jibantala
-------------	-------------	---------------

Time Period		Motorised Vehicle																								Non-motorised Vehicles																Total Hourly Vehicles		
		Fast Passenger										Fast Goods										Slow Goods				Total Motorised Vehicles		Animal / Hand Drawn		Cycle		Cycle Rickshaw		Others		Total Non-motorised Vehicles								
		Two-Wheeler		Auto Rickshaw		Car / Jeep / Van		Motorized Van		Bus				Truck						Agriculture Tractor		Agriculture Tractor with Trailer																						
Mini / RTVs										Standard		LCV		2-Axle		3-Axle		MAV																										
From	To	Up	Down	Up	Down	Up	Down	Up	Down	Up	Down	Up	Down	Up	Down	Up	Down	Up	Down	Up	Down	Up	Down	Up	Down	Up	Down	Up	Down	Up	Down	Up	Down	Up	Down	Up+Dn								
8	9	16	24	0	1	7	13	0	0	0	0	0	0	3	1	3	5	1	0	0	0	0	0	1	2	31	46	0	0	4	7	1	0	0	0	5	7	36	53	89				
9	10	25	18	1	0	12	20	0	0	0	0	0	0	0	2	2	12	0	0	0	0	0	0	2	5	42	57	0	0	14	11	1	1	0	0	15	12	57	69	126				
10	11	45	49	0	0	17	11	0	1	0	0	0	0	0	0	4	6	0	0	0	0	0	0	3	1	69	68	0	0	5	12	2	2	0	0	7	14	76	82	158				
11	12	70	62	2	0	20	15	1	1	0	0	0	0	5	1	6	3	2	0	0	0	0	1	3	1	108	86	0	0	11	14	4	1	0	0	15	15	123	101	224				
12	13	45	44	0	1	17	11	0	2	0	0	0	0	1	2	6	0	0	0	0	0	2	0	1	1	72	61	0	0	15	10	3	3	0	0	18	13	90	74	164				
13	14	12	11	1	3	25	12	0	0	0	0	0	0	9	2	2	0	0	2	0	0	4	0	2	1	55	31	0	0	8	11	2	2	0	0	10	13	65	44	109				
14	15	61	52	1	1	34	22	1	1	0	0	0	0	4	0	5	3	0	0	0	0	2	0	0	8	108	87	0	0	9	15	3	1	0	0	12	16	120	103	223				
15	16	24	22	5	9	16	34	1	2	0	0	0	0	1	2	6	3	2	2	0	0	0	0	10	9	65	83	0	0	15	14	1	1	0	0	16	15	81	98	179				
16	17	71	22	2	0	31	18	0	0	0	0	0	0	1	6	1	2	1	0	0	0	1	0	2	8	110	56	0	0	11	13	0	0	0	0	11	13	121	69	190				
17	18	11	12	5	9	21	15	1	0	0	0	0	0	1	0	0	1	2	0	0	0	5	0	5	3	51	40	0	0	12	11	0	0	0	0	12	11	63	51	114				
18	19	24	51	7	1	10	34	2	0	0	0	0	0	5	0	0	0	0	0	0	0	0	0	6	9	54	95	0	0	10	12	0	0	0	0	10	12	64	107	171				
19	20	24	25	1	1	20	36	0	2	0	0	0	0	3	3	0	9	2	1	0	0	5	6	2	3	57	86	0	0	11	10	0	0	0	0	11	10	68	96	164				
20	21	22	25	4	9	23	19	3	1	0	0	0	0	5	3	0	3	0	0	0	2	1	0	3	8	61	61	0	0	9	9	0	0	0	0	9	9	70	70	140				
21	22	55	15	0	0	11	12	1	1	0	0	0	0	3	2	7	8	2	0	0	0	0	6	3	3	82	47	0	0	8	5	0	0	0	0	8	5	90	52	142				
22	23	14	11	0	0	9	7	1	0	0	0	0	0	2	5	3	9	1	2	2	2	5	0	10	9	47	45	0	0	4	1	0	0	0	0	4	1	51	46	97				
23	0	0	0	0	0	0	0	0	2	0	0	0	0	1	3	10	5	0	0	0	0	6	3	3	14	19	0	0	0	0	0	0	0	0	0	0	14	19	33					
0	1	0	0	0	0	0	0	0	0	0	0	0	0	0	0	5	1	0	1	0	0	5	0	0	3	10	5	0	0	0	0	0	0	0	0	0	0	10	5	15				
1	2	0	0	0	0	0	0	0	0	0	0	0	0	1	0	10	9	2	1	0	3	5	0	3	0	21	13	0	0	0	0	0	0	0	0	0	0	21	13	34				
2	3	0	0	0	0	0	0	0	0	0	0	0	0	2	1	10	9	2	0	0	0	5	0	10	3	29	13	0	0	0	0	0	0	0	0	0	29	13	42					
3	4	0	0	0	0	0	0	0	0	0	0	0	0	0	0	1	1	1	0	0	0	5	0	3	0	10	1	0	0	0	0	0	0	0	0	0	0	10	1	11				
4	5	0	0	0	0	0	0	0	0	0	0	0	0	0	0	10	9	3	1	0	0	0	6	3	3	16	19	0	0	0	0	0	0	0	0	0	0	16	19	35				
5	6	9	9	0	0	5	6	2	1	0	0	0	0	2	2	6	1	3	3	0	0	5	0	3	0	35	22	0	0	1	2	4	5	0	0	5	7	40	29	69				
6	7	1	2	0	0	8	7	1	2	0	0	0	0	2	1	10	0	0	3	0	0	0	2	1	1	23	18	0	0	4	3	2	5	0	0	6	8	29	26	55				
7	8	11	3	0	0	9	7	1	1	0	0	0	0	3	4	1	1	3	0	0	0	1	0	1	1	30	17	0	0	5	7	4	1	0	0	9	8	39	25	64				
Daily Total		540	457	29	35	295	299	15	17	0	0	0	0	54	40	108	100	27	16	2	7	52	29	78	85	1200	1076	0	0	156	167	27	22	0	0	183	189	1383	1265	2648				
Total Vehicle (Up+Dn)		997		64		594		32		0		0		94		208		43		9		81		163		2276		0		323		49		0		372								
Equivalency Factor		0.5		1.0		1.0		1.0		1.5		3.0		1.5		3.0		3.0		4.5		1.5		4.5				6.0		0.5		2.0		4.5										
Daily PCU		270	229	29	35	295	299	15	17	0	0	0	0	81	60	324	300	81	48	9	32	78	44	351	383	1533	1447	0	0	78	84	54	44	0	0	132	128	1665	1575	3240				
Total PCU (Up+Down)		499		64		594		32		0		0		141		624		129		41		122		734		2980		0		162		98		0		260								

Day-5

TRAFFIC DATA ANALYSIS

(Daily Sheet)

Road : Jibantala Bazar to Taldi bazar Road

Date of Work : 13-Jun-19 -to- 14-Jun-19

Chainage: 11+50 km

Location : Taldi

Day of Work :

Direction of Traffic :

Up	From: Jibantala	To: Taldi
----	-----------------	-----------

Down	From: Taldi	To: Jibantala
------	-------------	---------------

Time Period		Motorised Vehicle																								Non-motorized Vehicles												Total Hourly Vehicles		
		Fast Passenger												Fast Goods								Slow Goods				Total Motorised Vehicles		Animal / Hand Drawn		Cycle		Cycle Rickshaw		Others		Total Non-motorised Vehicles				
		Two-Wheeler		Auto Rickshaw		Car / Jeep / Van		Motorized Van		Bus		Truck				Agriculture Tractor		Agriculture Tractor with Trailer																						
From	To	Up	Down	Up	Down	Up	Down	Up	Down	Up	Down	Up	Down	Up	Down	Up	Down	Up	Down	Up	Down	Up	Down	Up	Down	Up	Down	Up	Down	Up	Down	Up	Down	Up	Down	Up+Dn				
8	9	11	21	2	2	6	8	0	0	0	0	0	0	1	3	2	4	0	0	0	0	0	0	1	2	23	40	0	0	11	15	2	3	0	0	13	18	36	58	94
9	10	15	22	1	2	15	11	2	1	0	0	0	0	1	2	5	3	0	0	0	0	0	0	2	5	41	46	0	0	12	11	2	2	0	0	14	13	55	59	114
10	11	31	51	2	1	17	13	1	1	0	0	0	0	2	1	2	2	0	0	0	0	2	0	7	0	64	69	0	0	22	27	2	2	0	0	24	29	88	98	186
11	12	32	51	5	0	19	19	3	0	0	0	0	0	2	2	3	2	1	0	0	0	1	2	8	8	74	84	0	0	17	20	2	1	0	0	19	21	93	105	198
12	13	12	21	1	1	15	17	3	2	0	0	0	0	2	2	5	5	0	0	0	0	1	0	9	9	48	57	0	0	12	10	1	3	0	0	13	13	61	70	131
13	14	22	21	1	1	12	22	2	0	0	0	0	0	6	5	4	1	0	0	0	0	2	0	5	5	54	55	0	0	11	11	2	2	0	0	13	13	67	68	135
14	15	68	61	1	1	21	12	2	2	0	0	0	0	2	3	1	0	0	0	0	2	0	10	6	107	85	0	0	10	10	2	2	0	0	12	12	119	97	216	
15	16	65	44	1	1	37	14	1	1	0	0	0	0	0	1	6	0	2	2	0	0	0	0	2	1	114	64	0	0	17	11	0	1	0	0	17	12	131	76	207
16	17	25	45	3	7	15	11	0	1	0	0	0	0	1	0	9	1	0	0	0	0	2	0	2	4	57	69	0	0	12	5	5	2	0	0	17	7	74	76	150
17	18	22	25	7	5	25	23	3	0	0	0	0	0	1	1	0	0	2	2	0	0	0	0	3	1	63	57	0	0	11	9	2	3	0	0	13	12	76	69	145
18	19	14	15	0	1	29	25	2	3	0	0	0	0	5	1	8	1	0	2	0	0	0	0	2	0	60	48	0	0	11	6	2	2	0	0	13	8	73	56	129
19	20	14	15	0	0	11	12	0	2	0	0	0	0	0	3	9	1	0	0	0	0	2	0	5	5	41	38	0	0	11	1	0	1	0	0	11	2	52	40	92
20	21	71	17	0	0	9	10	1	1	0	0	0	0	0	5	3	2	2	0	2	0	1	0	3	2	92	37	0	0	6	2	0	0	0	0	6	2	98	39	137
21	22	15	12	0	0	8	8	2	2	0	0	0	0	3	2	7	1	0	2	0	0	0	2	1	3	36	32	0	0	9	9	0	0	0	0	9	9	45	41	86
22	23	0	0	0	0	9	10	2	3	0	0	0	0	3	2	3	1	0	0	0	0	2	0	2	6	21	22	0	0	2	8	0	0	0	0	2	8	23	30	53
23	0	0	0	0	0	0	0	0	1	0	0	0	0	4	3	1	5	2	0	0	2	6	2	5	6	18	19	0	0	0	0	0	0	0	0	0	0	18	19	37
0	1	0	0	0	0	0	0	0	0	0	0	0	0	0	0	8	9	9	9	2	0	6	6	7	7	32	31	0	0	0	0	0	0	0	0	0	0	32	31	63
1	2	0	0	0	0	0	0	0	0	0	0	0	0	1	0	9	9	2	1	2	0	2	6	5	5	21	21	0	0	0	0	0	0	0	0	0	0	21	21	42
2	3	0	0	0	0	0	0	0	0	0	0	0	0	1	4	8	2	0	2	0	0	0	2	5	5	14	15	0	0	0	0	0	0	0	0	0	0	14	15	29
3	4	0	0	0	0	0	0	0	0	0	0	0	0	0	0	9	1	2	2	0	0	2	0	1	2	14	5	0	0	0	0	0	0	0	0	0	0	14	5	19
4	5	0	0	0	0	0	0	0	0	0	0	0	0	0	0	1	10	4	2	0	0	6	2	1	1	12	15	0	0	0	0	0	0	0	0	0	0	12	15	27
5	6	9	9	0	0	2	1	0	0	0	0	0	0	2	0	10	8	3	1	0	0	2	0	1	7	29	26	0	0	6	1	0	0	0	0	6	1	35	27	62
6	7	1	2	0	0	2	3	0	0	0	0	0	0	0	1	9	3	3	0	0	0	2	1	1	8	21	0	0	5	2	2	1	0	0	7	3	15	24	39	
7	8	10	5	0	0	4	8	1	0	0	0	0	0	1	1	5	2	3	2	0	0	1	0	10	1	35	19	0	0	1	2	1	2	0	0	2	4	37	23	60
Daily Total		437	437	24	22	256	227	25	20	0	0	0	0	38	42	119	79	35	30	6	2	40	24	98	92	1078	975	0	0	186	160	25	27	0	0	211	187	1289	1162	2451
Total Vehicle (Up+Dn)		874		46		483		45		0		0		80		198		65		8		64		190		2053		0		346		52		0		398				
Equivalency Factor		0.5		1.0		1.0		1.0		1.5		3.0		1.5		3.0		3.0		4.5		1.5		4.5				6.0		0.5		2.0		4.5						
Daily PCU		219	219	24	22	256	227	25	20	0	0	0	0	57	63	357	237	105	90	27	9	60	36	441	414	1571	1337	0	0	93	80	50	54	0	0	143	134	1714	1471	3185
Total PCU (Up+Down)		438		46		483		45		0		0		120		594		195		36		96		855		2908		0		173		104		0		277				

Road : Jibantala Bazar to Taldi bazar Road

Date of Work : 14-Jun-19 -to- 15-Jun-19

Chainage: 11+50 km

Location: Taldi

Day of Work :

Direction of Traffic:

Up	From: Jibantala	To: Taldi
-----------	-----------------	-----------

Down

Down	From: Taldi	To: Jibantala
------	-------------	---------------

213

Road : Jibantala Bazar to Taldi bazar Road

Date of Work : 15-Jun-19 -to- 16-Jun-19

Chainage: 11+50 km

Location: Taldi

Day of Work:

Direction of Traffic:

Up	From: Jibantala	To: Taldi
-----------	-----------------	-----------

Down

Down	From: Taldi	To: Jibantala
-------------	-------------	---------------

214

ANNEXURE- V

AXLE LOAD DATA COLLECTION

Axle Load Test Result

: LCV (Up & Down)

Sl. No.	TIME	Wheel Load [Ton]				Axle Load [KN]			Gross Vehicle Weight (Ton)	Damaging Effect		
		Front Axle	Rear Axle			Front Axle	Rear Axle			Front Axle	Rear Axle Group	Total
		Single Axle with Single Wheel (A1)	Single Axle with Single Wheel (A1)	Single Axle with Dual Wheel (A2)	Tandem Axle with Dual Wheel (A3)	Single Axle with Single Wheel (A1)	Single Axle with Single Wheel (A1)	Single Axle with Dual Wheel (A2)				
Direction: Up		From : JIBANTALA				To : TALDI						
1	6.25	1.54	4.50			30.21	88.26		12.08	0.0467	3.3994	3.4461
2	7.40	1.65	4.03			32.36	79.04		11.36	0.0614	2.1864	2.2478
3	8.24	1.81	4.52			35.50	88.66		12.66	0.089	3.4614	3.5504
4	9.17	1.75	3.99			34.32	78.26		11.48	0.0777	2.1014	2.1791
5	11.36	1.54	4.27			30.21	83.75		11.62	0.0467	2.756	2.8027
6	13.37	1.63	3.95			31.97	77.48		11.16	0.0585	2.0189	2.0774
7	15.21	1.72	3.78			33.74	74.14		11.00	0.0726	1.6926	1.7652
8	16.28	1.97	4.05			38.64	79.44		12.04	0.1249	2.231	2.3559
9	18.42	1.65	4.11			32.36	80.61		11.52	0.0614	2.3654	2.4268
10	20.12	1.87	4.01			36.68	78.69		11.76	0.1014	2.148	2.2494
										0.7403	24.3605	25.1008
Total Damaging Effect for LCV (Up)									25.1008			
Total No. of LCV (Up) :									10			
Vehicle Damage Facor (VDF) for LCV									2.510			

Road : JIBANTALA TALDI ROAD

Location : TALDI

Date :

09-06-2019 to 10-06-2019

Axle Load Test Result

: LCV (Up & Down)

Road : JIBANTALA TALDI ROAD

Location : TALDI

Date :

09-06-2019 to 10-06-2019

Sl. No.	TIME	Wheel Load [Ton]				Axle Load [KN]			Gross Vehicle Weight (Tonne)	Damaging Effect		
		Front Axle	Rear Axle			Front Axle	Rear Axle			Front Axle	Rear Axle Group	Total
		Single Axle with Single Wheel (A1)	Single Axle with Single Wheel (A1)	Single Axle with Dual Wheel (A2)	Tandem Axle with Dual Wheel (A3)	Single Axle with Single Wheel (A1)	Single Axle with Single Wheel (A1)	Single Axle with Dual Wheel (A2)				
Sl. No.	TIME	Wheel Load [Ton]				Axle Load [KN]			Gross Vehicle Weight (Ton)	Damaging Effect		
		Front Axle	Rear Axle			Front Axle	Rear Axle			Front Axle	Rear Axle Group	Total
		Single Axle with Single Wheel (A1)	Single Axle with Single Wheel (A1)	Single Axle with Dual Wheel (A2)	Tandem Axle with Dual Wheel (A3)	Single Axle with Single Wheel (A1)	Single Axle with Single Wheel (A1)	Single Axle with Dual Wheel (A2)				
Direction:		Down	From : TALDI				To : JIBANTALA					
1	6.32	1.45	3.93			28.44	77.08		10.76	0.0366	1.9775	2.0141
2	7.21	1.25	4.12			24.52	80.81		10.74	0.0203	2.3889	2.4092
3	9.42	1.39	4.54			27.26	89.05		11.86	0.0309	3.5228	3.5537
4	10.53	1.25	3.97			24.52	77.87		10.44	0.0203	2.0598	2.0801
5	11.23	1.53	4.32			30.01	84.73		11.70	0.0454	2.8873	2.9327
6	13.32	1.75	4.11			34.32	80.61		11.72	0.0777	2.3654	2.4431
7	14.11	1.49	3.87			29.22	75.91		10.72	0.0408	1.8601	1.9009
8	15.52	1.23	3.98			24.13	78.06		10.42	0.019	2.08	2.099
9	16.23	1.41	4.01			27.66	78.65		10.84	0.0328	2.1436	2.1764
10	17.15	1.35	4.19			26.48	82.11		11.07	0.0275	2.5464	2.5739
										0.3513	23.8318	24.1831
Total Damaging Effect for LCV (Down)										24.1831		
Total No. of LCV (down) :										10		
Vehicle Damage Factor (VDF) for LCV										2.418		

Axle Load Test Result: TRAILER (Up & Down)**Road : JIBANTALA TALDI ROAD****Location : TALDI****Date: 09-06-2019 to 10-06-2019**

Sl. No.	TIME	Wheel Load [Ton]				Axle Load [KN]			Gross Vehicle Weight (Tonne)	Damaging Effect			
		Front Axle	Rear Axle			Front Axle	Rear Axle			Front Axle	Rear Axle Group	Rear Axle Group	Total
		Single Axle with Single Wheel (A1)	Single Axle with Single Wheel (A1)	Single Axle with Single Wheel (A1)	Tandem Axle with Dual Wheel (A3)	Single Axle with Single Wheel (A1)	Single Axle with Single Wheel (A1)	Single Axle with Single Wheel (A1)					
Direction: Up		From : JIBANTALA				To : TALDI							
1	07:30	0.69	1.94	4.43		13.53	38.05	86.89	14.12	0.0019	0.1174	3.1932	3.3125
2	08:15	0.65	1.65	4.25		12.75	32.36	83.36	13.10	0.0015	0.0614	2.7051	2.768
3	16:20	0.78	1.73	3.67		15.30	33.93	71.98	12.36	0.0031	0.0742	1.5038	1.5811
4	17:30	0.35	1.78	4.33		6.86	34.91	84.93	12.92	0.0001	0.0832	2.9147	2.998
5	18:06	0.79	1.75	4.24		15.50	34.32	83.16	13.56	0.0032	0.0777	2.6792	2.7601
6	19:20	1.12	1.84	4.04		21.97	36.09	79.24	14.00	0.0131	0.095	2.2086	2.3167
7	19:30	0.85	1.68	3.43		16.67	32.95	67.28	11.92	0.0043	0.066	1.1479	1.2182
8	20:15	1.03	1.96	4.05		20.20	38.44	79.44	14.08	0.0093	0.1223	2.231	2.3626
9	20:20	0.78	1.77	4.67		15.30	34.72	91.60	14.44	0.0031	0.0814	3.9439	4.0284
10	20:30	0.74	1.81	3.33		14.51	35.50	65.31	11.76	0.0025	0.089	1.0192	1.1107
11	21:06	0.67	1.62	4.04		13.14	31.77	79.24	12.66	0.0017	0.0571	2.2086	2.2674
12	21:20	1.12	1.84	4.54		21.97	36.09	89.05	15.00	0.0131	0.095	3.5228	3.6309
13	21:30	0.49	1.75	3.95		9.61	34.32	77.42	12.37	0.0005	0.0777	2.0126	2.0908
14	22:06	0.74	1.92	4.60		14.51	37.66	90.22	14.52	0.0025	0.1127	3.7116	3.8268
15	22:20	0.96	1.71	4.30		18.83	33.54	84.34	13.94	0.007	0.0709	2.8345	2.9124
16	22:30	0.84	1.51	3.40		16.48	29.62	66.69	11.50	0.0041	0.0431	1.1081	1.1553
17	22:40	1.19	1.62	3.60		23.34	31.77	70.61	12.82	0.0166	0.0571	1.3926	1.4663
18	22:45	0.93	1.68	4.30		18.24	32.95	84.34	13.82	0.0062	0.066	2.8345	2.9067
19	22:55	1.02	1.65	4.30		20.01	32.36	84.34	13.94	0.009	0.0614	2.8345	2.9049
20	23:00	0.91	1.74	4.20		17.85	34.13	82.38	13.70	0.0057	0.076	2.5801	2.6618
										0.1085	1.5846	48.5865	50.2796
Total Damaging Effect for Trailer (Up):									50.2796				
Total No. of Trailer (Up) :									20				
Vehicle Damage Factor (VDF) for Trailer									2.514				

Axle Load Test Result: TRAILER (Up & Down)**Road : JIBANTALA TALDI ROAD****Location : TALDI****Date : 09-06-2019 to 10-06-2019**

Sl. No.	TIME	Wheel Load [Ton]				Axle Load [KN]			Gross Vehicle Weight (Tonne)	Damaging Effect			
		Front Axle	Rear Axle			Front Axle	Rear Axle			Front Axle	Rear Axle Group	Rear Axle Group	Total
		Single Axlewith Single Wheel (A1)	Single Axlewith Single Wheel (A1)	Single Axlewith Single Wheel (A1)	Tandem Axlewith Dual Wheel (A3)	Single Axlewith Single Wheel (A1)	Single Axlewith Single Wheel (A1)	Single Axlewith Single Wheel (A1)					
Sl. No.	TIME	Wheel Load [Ton]				Axle Load [KN]			Gross Vehicle Weight (Tonne)	Damaging Effect			
		Front Axle	Rear Axle			Front Axle	Rear Axle			Front Axle	Rear Axle Group	Rear Axle Group	Total
		Single Axlewith Single Wheel (A1)	Single Axlewith Single Wheel (A1)	Single Axlewith Single Wheel (A1)	Tandem Axlewith Dual Wheel (A3)	Single Axlewith Single Wheel (A1)	Single Axlewith Single Wheel (A1)	Single Axlewith Single Wheel (A1)					
Direction:		Down	From: TALDI				To: JIBANTALA						
1	03:16	0.71	1.52	3.37		34.00	29.81	66.10	11.20	0.0749	0.0442	1.0694	1.1885
2	04:12	0.98	1.98	3.65		19.28	38.84	71.59	13.23	0.0077	0.1275	1.4715	1.6067
3	05:31	0.91	1.67	3.14		17.85	32.76	61.59	47.14	0.0057	0.0645	0.8061	0.8763
4	06:55	0.87	1.27	3.78		17.06	24.91	74.14	11.84	0.0047	0.0216	1.6926	1.7189
5	07:20	0.58	1.12	3.45		11.38	21.97	67.67	10.30	0.0009	0.0131	1.1747	1.1887
6	08:16	0.89	1.56	3.36		34.00	30.60	65.90	11.62	0.0749	0.0491	1.0565	1.1805
7	08:22	0.81	1.58	3.64		15.89	30.99	71.39	12.06	0.0036	0.0517	1.4551	1.5104
8	08:31	0.92	1.45	3.15		18.04	28.44	61.78	47.12	0.0059	0.0366	0.8161	0.8586
9	08:55	1.02	1.27	3.79		20.01	24.91	74.34	12.16	0.009	0.0216	1.7109	1.7415
10	09:20	0.97	1.85	3.70		19.03	36.29	72.57	13.04	0.0073	0.0972	1.5537	1.6582
11	09:31	0.98	1.25	3.60		19.22	24.52	70.61	50.10	0.0076	0.0203	1.3926	1.4205
12	09:55	0.87	1.27	3.81		17.06	24.91	74.73	11.90	0.0047	0.0216	1.7471	1.7734
13	10:20	0.89	1.55	4.05		17.46	30.40	79.44	12.98	0.0052	0.0478	2.231	2.284
14	10:16	0.51	1.21	3.39		34.00	23.73	66.49	10.22	0.0749	0.0178	1.0949	1.1876
15	10:16	0.55	1.31	3.35		34.00	25.69	65.71	10.42	0.0749	0.0244	1.0444	1.1437
16	11:12	0.56	1.52	3.64		10.98	29.81	71.41	11.44	0.0008	0.0442	1.4567	1.5017
17	11:31	0.82	1.32	3.71		16.08	25.89	72.77	43.86	0.0037	0.0252	1.5709	1.5998
18	11:55	0.85	1.02	3.98		16.67	20.01	78.06	11.70	0.0043	0.009	2.08	2.0933
19	12:20	0.58	1.12	3.95		11.38	21.97	77.48	11.30	0.0009	0.0131	2.0189	2.0329
20	16:12	0.90	1.01	3.85		17.65	19.81	75.51	11.52	0.0054	0.0086	1.8212	1.8352
										0.377	0.7591	29.2643	30.4004
Total Damaging Effect for Trailer (Down)										30.4004			
Total No. of Trailer (Down) :										20			
Vehicle Damage Factor (VDF) for Trailer										1.520			

Axle Load Test Result: 2 - Axle Truck (Medium Truck) (Up & Down)

Road: JIBANTALA TALDI ROAD

Location: TALDI

Date:

09-06-2019 to 10-06-2019

Sl. No.	TIME	Wheel Load [Ton]					Axle Load [KN]					Gross Vehicle Weight (Ton)	Damaging Effect			
		Front Axle	Rear Axle				Front Axle	Rear Axle					Front Axle	Rear Axle Group	Total	
		Single Axlewith Single Wheel (A1)	Single Axlewith Single Wheel (A1)	Single Axlewith Dual Wheel (A2)	Tandem Axle withDual Wheel (A3)	Tridem Axle with Dual Wheel (A4)	Single Axlewith Single Wheel (A1)	Single Axlewith Single Wheel (A1)	Single Axlewith Dual Wheel (A2)	Tandem Axle with Dual Wheel (A3)	Tridem Axlewith Dual Wheel (A4)					
Direction: Up		From: JIBANTALA					To: TALDI									
1	13.32	3.89		5.26			76.30		103.17			18.30	1.8986	2.766	4.6646	
2	14.23	3.25		5.59			63.75		109.64			17.68	0.9253	3.5279	4.4532	
3	15.55	2.93		4.36			57.47		85.52			14.58	0.6111	1.3059	1.917	
4	16.22	2.68		4.08			52.57		80.03			13.52	0.4279	1.0015	1.4294	
5	16.53	2.23		4.02			43.74		78.85			12.50	0.2051	0.9437	1.1488	
6	17.02	4.14		6.23			81.20		122.20			20.74	2.4354	5.4441	7.8795	
7	17.35	5.32		7.63			104.35		149.65			25.90	6.6423	12.2447	18.887	
8	17.55	2.91		4.38			57.08		85.91			14.58	0.5947	1.3299	1.9246	
9	18.22	2.7		5.28			52.96		103.56			15.96	0.4407	2.8081	3.2488	
10	18.53	3.25		7.22			63.75		141.61			20.94	0.9253	9.8178	10.7431	
11	19.02	4.1		5.29			80.42		103.76			18.78	2.3432	2.8298	5.173	
12	19.32	5.08		7.06			99.64		138.47			24.28	5.5218	8.9756	14.4974	
13	19.58	4.06		5.76			79.63		112.98			19.64	2.2524	3.9778	6.2302	
14	16.22	2.06		4.28			40.40		83.95			12.68	0.1492	1.2126	1.3618	
15	16.53	2.3		4.72			45.11		92.58			14.04	0.232	1.7935	2.0255	
16	17.02	4.1		5.34			80.42		104.64			18.87	2.3432	2.9271	5.2703	
17	17.35	5.2		6.66			101.99		130.63			23.72	6.0615	7.1091	13.1706	
18	17.55	3.02		6.36			59.23		124.75			18.76	0.6895	5.9129	6.6024	
19	18.22	2.85		5.19			55.90		101.80			16.08	0.547	2.622	3.169	
20	18.53	5.23		7.89			102.58		154.75			26.24	6.2029	14.0011	20.204	
													41.4491	92.5511	134.0002	
Total Damaging Effect for 2-Axle (Up)												134.0002				
Total No. of 2-Axle (Up) :												20				
Vehicle Damage Factor (VDF) for 2-Axle												6.700				

Sl. No.	TIME	Wheel Load [Ton]					Axle Load [KN]					Gross Vehicle Weight (Tonne)	Damaging Effect			
		Front Axle	Rear Axle				Front Axle	Rear Axle					Front Axle	Rear Axle Group	Total	
		Single Axle with Single Wheel (A1)	Single Axle with Single Wheel (A1)	Single Axle with Dual Wheel (A2)	Tandem Axle with Dual Wheel (A3)	Tridem Axle with Dual Wheel (A4)	Single Axle with Single Wheel (A1)	Single Axle with Single Wheel (A1)	Single Axle with Dual Wheel (A2)	Tandem Axle with Dual Wheel (A3)	Tridem Axle with Dual Wheel (A4)					
Sl. No.	TIME	Wheel Load [Ton]					Axle Load [KN]					Gross Vehicle Weight (Ton)	Damaging Effect			
		Front Axle	Rear Axle				Front Axle	Rear Axle					Front Axle	Rear Axle Group	Total	
		Single Axle with Single Wheel (A1)	Single Axle with Single Wheel (A1)	Single Axle with Dual Wheel (A2)	Tandem Axle with Dual Wheel (A3)	Tridem Axle with Dual Wheel (A4)	Single Axle with Single Wheel (A1)	Single Axle with Single Wheel (A1)	Single Axle with Dual Wheel (A2)	Tandem Axle with Dual Wheel (A3)	Tridem Axle with Dual Wheel (A4)					
Direction:		Down	From: TALDI					To: JIBANTALA								
1	8.23	2.27		3.95			44.52		77.48			12.44	0.2201	0.8798	1.0999	
2	8.54	1.56		3.65			30.60		71.59			10.42	0.0491	0.6413	0.6904	
3	9.11	2.86		4.85			56.10		95.13			15.42	0.5549	1.9994	2.5543	
4	9.33	2.56		4.53			50.21		88.85			14.18	0.356	1.5215	1.8775	
5	11.56	4.26		7.58			83.56		148.67			23.68	2.7311	11.9271	14.6582	
6	13.37	3.87		5.56			75.91		109.05			18.86	1.8601	3.4526	5.3127	
7	14.15	2.98		4.89			58.45		95.91			15.74	0.6539	2.0658	2.7197	
8	14.49	3.84		6.96			75.32		136.51			21.60	1.803	8.4781	10.2811	
9	15.54	4.56		6.65			89.44		130.43			22.42	3.5849	7.0656	10.6505	
10	16.11	2.8		4.87			54.92		95.52			15.34	0.5096	2.0324	2.542	
11	16.33	2.5		5.12			49.04		100.42			15.24	0.324	2.4827	2.8067	
12	17.56	4.2		5.88			82.38		115.33			20.16	2.5801	4.3193	6.8994	
13	18.37	3.8		7.56			74.53		148.28			22.72	1.7285	11.8024	13.5309	
14	19.15	2.9		4.89			56.88		95.91			15.58	0.5864	2.0658	2.6522	
15	19.49	3.8		4.96			74.53		97.29			17.52	1.7285	2.1873	3.9158	
16	20.33	2.56		5.29			50.21		103.76			15.70	0.356	2.8298	3.1858	
17	21.56	4.2		5.58			82.38		109.45			19.56	2.5801	3.5035	6.0836	
18	22:00	3.75		4.56			73.55		89.44			16.62	1.6394	1.5623	3.2017	
19	22.15	2.28		4.99			44.72		97.87			14.54	0.2241	2.24	2.4641	
20	22.49	3.14		5.96			61.59		116.96			18.21	0.8061	4.5687	5.3748	
													24.8759	77.6254	102.5013	
Total Damaging Effect for 2-Axle (Down)												102.5013				
Total No. of 2-Axle (Down) :												20				
Vehicle Damage Factor (VDF) for 2-Axle												5.125				

Axle Load Test Result: 3 - Axle Truck (Up & Down)

Road: JIBANTALA TALDI ROAD

Location: TALDI

Date: 09-06-2019 to 10-06-2019

Sl. No.	TIME	Wheel Load [Ton]					Axle Load [KN]					Gross Vehicle Weight (Tonne)	Damaging Effect								
		Front Axle	Rear Axle				Front Axle	Rear Axle					Front Axle	Rear Axle Group	Rear Axle Group	Total					
		Single Axlewith Single Wheel (A1)	Single Axlewith Single Wheel (A1)	Single Axlewith Dual Wheel (A2)	Tandem Axle with Dual Wheel(A3)	Tridem Axle with Dual Wheel (A4)	Single Axlewith Single Wheel (A1)	Single Axlewith Single Wheel (A1)	Single Axlewith Dual Wheel (A2)	Tandem Axle with Dual Wheel	Tridem Axle with Dual Wheel (A4)										
Direction: Up												From: JIBANTALA					To: TALDI				
1	7.02	3.26			5.62	9.95		63.94		110.23	195.16		37.66	0.9363	3.6045	3.0235	7.5643				
2	8.43	3.45			5.25	9.75		67.67		102.97	191.24		36.90	1.1747	2.7446	2.7878	6.7071				
3	9.11	3.53			5.64	10.82		69.24		110.62	212.22		39.98	1.2876	3.6557	4.2276	9.1709				
4	19.15	3.85			5.42	10.75		75.51		106.31	210.85		40.04	1.8212	3.1184	4.1195	9.0591				
5	20.32	3.36			5.12	9.95		65.90		100.42	195.16		36.86	1.0565	2.4827	3.0235	6.5627				
6	21.23	3.29			5.02	10.85		64.53		98.46	212.81		38.32	0.9714	2.2945	4.2749	7.5408				
7	22.23	3.39			5.31	10.90		66.49		104.15	213.79		39.20	1.0949	2.8726	4.3541	8.3216				
8	23.23	3.99			5.1	10.76		78.26		100.03	210.95		39.69	2.1014	2.4443	4.1273	8.673				
													10.444	23.2173	29.9382	63.5995					
Total Damaging Effect for 3-Axle (Up)												63.5995									
Total No. of 3-Axle (Up):												8									
Vehicle Damage Factor (VDF) for 3-Axle												7.950									

Sl. No.	TIME	Wheel Load [Ton]					Axle Load [KN]					Gross Vehicle Weight (Ton)	Damaging Effect			
		Front Axle	Rear Axle				Front Axle	Rear Axle					Front Axle	Rear Axle Group	Rear Axle Group	Total
		Single Axle with Single Wheel (A1)	Single Axle with Single Wheel (A1)	Single Axle with Dual Wheel (A2)	Tandem Axle with Dual Wheel (A3)	Tridem Axle with Dual Wheel(A4)	Single Axle with Single Wheel (A1)	Single Axle with Single Wheel (A1)	Single Axle with Dual Wheel (A2)	Tandem Axle with Dual Wheel	Tridem Axle with Dual Wheel(A4)					
Sl. No.	TIME	Wheel Load [Ton]					Axle Load [KN]					Gross Vehicle Weight (Ton)	Damaging Effect			
		Front Axle	Rear Axle				Front Axle	Rear Axle					Front Axle	Rear Axle Group	Rear Axle Group	Total
		Single Axle with Single Wheel (A1)	Single Axle with Dual Wheel (A2)	Single Axle with Dual Wheel (A2)	Tandem Axle with Dual Wheel (A3)	Tridem Axle with Dual Wheel(A4)	Single Axle with Single Wheel (A1)	Single Axle with Dual Wheel (A2)	Single Axle with Dual Wheel (A2)	Tandem Axle with Dual Wheel	Tridem Axle with Dual Wheel(A4)					
Direction:	Down	From: TALDI					To: JIBANTALA									
1	6.44	3.56		5.25	10.10		69.83		102.97	198.10		37.82	1.332	2.7446	3.2099	7.2865
2	7.12	3.96		5.05	9.65		77.67		99.05	189.28		37.32	2.0387	2.3499	2.6753	7.0639
3	8.34	3.12		4.52	9.80		61.20		88.66	192.22		34.88	0.7859	1.5085	2.8454	5.1398
4	19.26	3.06		5.21	11.20		60.02		102.19	219.68		38.94	0.727	2.6624	4.8542	8.2436
5	20.23	3.64		5.62	9.60		71.39		110.23	188.29		37.72	1.4551	3.6045	2.6198	7.6794
6	21.54	3.68		5.23	9.23		72.18		102.58	181.10		36.29	1.5206	2.7033	2.242	6.4659
7	22.42	3.08		6.89	9.30		60.41		135.14	182.41		38.54	0.7461	8.1428	2.3075	11.1964
													8.6054	23.716	20.7541	53.0755
Total Damaging Effect for 3-Axle (Down)												53.0755				
Total No. of 3-Axle (Down) :												7				
Vehicle Damage Factor (VDF) for 3-Axle												7.582				

Axle Load Test Result: MAV (Up & Down)

Road: JIBANTALA TALDI ROAD

Location: TALDI

Date: 09-06-2019 to 10-06-2019

Sl. No.	TIME	Wheel Load [Ton]					Axle Load [KN]					Gross Vehicle Weight (Ton)	Damaging Effect			
		Front Axle	Rear Axle				Front Axle	Rear Axle					Front Axle	Rear Axle Group	Rear Axle Group	Total
		Single Axle with Single Wheel (A1)	Single Axle with Single Wheel (A1)	Single Axle with Dual Wheel (A2)	Tandem Axle with Dual Wheel (A3)	Tridem Axle with Dual Wheel	Single Axle with Single Wheel (A1)	Single Axle with Single Wheel (A1)	Single Axle with Dual Wheel (A2)	Tandem Axle with Dual Wheel	Tridem Axle with Dual Wheel (A4)					
Direction: Up		From: JIBANTALA					To: TALDI									
1	7.02	4.26		5.55	9.5	11.20	83.56		108.86	186.33	219.68	61.02	2.7311	5.941	0.9251	9.5972
2	8.43	3.45		5.42	9.8	12.10	67.67		106.31	192.22	237.33	61.54	1.1747	5.9638	1.2601	8.3986
3	9.11	3.53		6.51	8.5	12.80	69.24		127.63	166.72	251.06	62.67	1.2876	8.0885	1.578	10.9541
													5.1934	19.9933	3.7632	28.9499
Total Damaging Effect for MAV (Up)												28.9499				
Total No. of MAV (Up) :												3				
Vehicle Damage Factor (VDF) for MAV												9.650				

Sl. No.	TIME	Wheel Load [Ton]					Axle Load [KN]					Gross Vehicle Weight (Ton)	Damaging Effect			
		Front Axle	Rear Axle				Front Axle	Rear Axle					Front Axle	Rear Axle Group	Rear Axle Group	Total
		Single Axle with Single Wheel (A1)	Single Axle with Dual Wheel (A2)	Single Axle with Dual Wheel (A2)	Tandem Axle with Dual Wheel (A3)	Tridem Axle with Dual Wheel	Single Axle with Single Wheel (A1)	Single Axle with Dual Wheel (A2)	Single Axle with Dual Wheel (A2)	Tandem Axle with Dual Wheel	Tridem Axle with Dual Wheel (A4)					
Direction:		Down		From: TALDI			To: JIBANTALA									
1	6.44	3.56		6.8	9	11.20	69.83		133.38	176.53	219.68	61.12	1.332	9.751	0.9251	12.0081
4	7.15	3.84		5.6	8.7	11.50	75.26		109.84	170.64	225.56	59.27	1.7972	5.3209	1.0281	8.1462
2	8.12	3.26		4.2	9.5	11.30	63.94		82.38	186.33	221.64	56.52	0.9363	3.6368	0.9585	5.5316
													4.0655	18.7087	2.9117	25.6859
Total Damaging Effect for MAV (Down)												25.6859				
Total No. of MAV (Down) :												3				
Vehicle Damage Factor (VDF) for MAV												8.562				

ANNEXURE- VI

ESTIMATION

<u>1.COST OF PAKUR VARIETY STONE MATERIALS AT SITE THROUGH BALLYGUNGE RAILWAY SIDINGS Rs/m3</u>																		
	Distance from Ballygunge to site =	38.3 km		Middle distance of site =	6.225 km		<u>Total distance from Ballygunge Railway Yard=</u>									44.525 km	=	45 km
	Size Of Metals & Chips	Unit	Boulder 30/45 Kg	Grade -I	Grade -II	37.5 mm	26.5 mm	22.4mm	13.2mm	11.2mm	5.6mm	stone grit	stone dust mixed with grit	Screening Type-A	Screening Type-B	40 mm nominal size	20 mm nominal size	10 mm nominal size
1	Cost of Materials at Ballygunge Railway Siding (VP-225, Tab-2 of SOR 2018)	M ³	1201.00	1399.00	1421.00	1417.00	1476.00	1491.00	1514.00	1375.00	1122.00	1022.00	1008.00	1204.00	1010.00	1439.00	1430.00	1299.00
2	Cost of Road Transport for a lead of 45km.	M ³	517.00	517.00	517.00	517.00	517.00	517.00	517.00	517.00	517.00	517.00	517.00	517.00	517.00	517.00	517.00	517.00
3	Add Loading & Unloading without Stacking.75% of Rs83.00, 75% of Rs 77.00 & 75% of Rs 62.00	M ³	62.25	62.25	62.25	57.75	57.75	57.75	57.75	57.75	57.75	57.75	46.50	57.75	57.75	62.25	57.75	57.75
4	Cost Of Materials at Site for HMP works or Concrete works without stacking	M ³	1780.25	1978.25	2000.25	1991.75	2050.75	2065.75	2088.75	1949.75	1696.75	1596.75	1571.50	1778.75	1584.75	2018.25	2004.75	1873.75

2. COST OF LATERITE & MOORUM AT WORK SITE Rs/m3

Size Of Metals & Chips	Unit	Moorum	(Local)
Cost Of Materials at Quarry	M ³	117	
Add Loading Unloading	M ³	62	
Cost of Road Transport for a lead of 172Km from Sandhipur	M ³	1553.3	
Cost of Materials at work site for general works including stacking = 1+2+3	M ³	1732.3	

JIBANTALA BAZAR TO TALDI BAZAR ROAD FROM CH. 0.00 KMP TO 12.45 KMP – STRENGTHENING WORK UNDER SOUTH 24 PARGANAS DIVISION IN THE DISTRICT OF SOUTH 24 PARGANAS.				
Analysis Of Rate of Bitumen of Different Grades supplied by Contractor., of SOR 2018)				
A. Carriage of 60/70 Bulk Bitumen (VG-30) from Haldia to site = 168 Km				
C. Carriage of Bitumen Emulsion from Haldia to site = 168 km				
B. Carriage of 10/20 Packed Bitumen Emulsion from Dhulagarh to site = 90 km				
As per schedule of rate of PW(Roads) DEPT. Wef. 30.08.2018 & 9TH ADDENDA & CORRIGENDA				
ITEM DESCRIPTION		Bulk Bitumen 60/70 (VG-30) (From Haldia)	Packed Bitumen 10/20 (From Dhulagarh)	Bitumen Emulsion Bulk (from Haldia)
Carriage of Bulk Bitumen 60/70 grade from Haldia to Site		1014.90	0.00	0.00
Carriage of Bitumen Emulsion (bulk) from Haldia to Site		0.00	0.00	1014.90
Carriage of 10/20 Bitumen (Packed) from Dhulagarh to site.		0.00	787.00	0.00
Cost of Loading, Unloading		0.00	42.00	0.00
Total		1014.90	829.00	1014.90
<u>To arrive Cost of Bitumen at Site Supplied by Contractor (FORMAT-B)</u>				
		Bulk Bitumen 60/70 (VG-30) (From Haldia)	Packed Bitumen 10/20 (From Dhulagarh)	Bitumen Emulsion Bulk (from Haldia)
(A) Cost of materials including of all taxes at the nearest source of manufacturer.	Rs	26780.00	33400.00	22170.00
(B) Add overhead charges 5% of A	Rs	1339.00	1670.00	1108.50
(C) Add contractor profit 10% of (A+B)	Rs	2811.90	3507.00	2327.85
(D) Carriage from stackyard to site for	Rs	1014.90	829.00	1014.90
(E) Deduct Cost of container	Rs	0.00	1000.00	0.00
F. Rate of material at site (Rs Per MT)	Rs	31945.80	38406.00	26621.25
G. Rate of material at site (Rs Per Kg)	Rs	31.95	38.41	26.62

JIBANTALA BAZAR TO TALDI BAZAR ROAD FROM CH. 0.00 KMP TO 12.45 KMP – STRENGTHENING WORK UNDER SOUTH 24 PARGANAS DIVISION IN THE DISTRICT OF SOUTH 24 PARGANAS.										
QUANTITY OF ROAD WORKS										
Sl No	Description of Item	No	L (m)	B(m)	D(m)		Quantity	Unit	Rate (Rs./Unit)	Amount (Rs.)
1	Construction of granular sub-base by providing graded material, mixing in Wet Mix Plant at OMC, carriage of mixed material to work site, spreading in uniform layers with Motor grader on prepared surface in proper grade and camber, compacting with vibratory power roller to achieve the desired density, including lighting, guarding, barricading, including cost of all materials, machinery, tools and plants and cost of quality control complete as per Clause 401 of Specifications for Road & Bridge Works of MoRT&H (5th Revision).(v) Grading – V It No.-4.08 A (V) & Pg.- 246 (WBSOR, R&B VOL)									
	GSB	1	1000	5.5	0.200	=	1100.00	m ³		
					Total	=	1100.00	m ³	2649.11	Rs. 2914021.5896
2	Providing, laying, spreading and compacting graded stone aggregate to Wet Mix Macadam specification including screening of aggregates and granular materials, premixing the material with water at OMC in Wet Mix Plant, carriage of mixed material by tipper to site, laying in uniform layers with Paver in Sub- base / Base course on well-prepared surface and compacting with Vibratory Roller to achieve the desired density, including supply of all materials, machinery, fuel and lubricants, including incidental costs for lighting, guarding, barricading, making earthen bundh to protect the edges including cost of quality control complete as per Clause 406 of Specifications for Road & Bridge Works of MoRT&H (5th Revision).It No.-4.12 & Pg.- 249 (WBSOR, R&B VOL)									
	WMM	1	1000	5.50	0.25	=	1375.00	m ³		
					Total	=	1375.00	m ³	2779.36	Rs. 3821620
3	Providing and laying dense bituminous macadam with Hot Mix Plant producing an average output of 75 tonnes per hour using coarse aggregate, fine aggregate, filler and bituminous binder as per design Job Mix Formula conforming Marshall Method as per specification, including screening, cleaning of chips and preparing a uniform and quality mix in Hot Mix Plant and ensuring a homogeneous mix, in which all particles of the mineral aggregates are coated uniformly, transporting the hot mix to work site, laying the mixed materials at specified laying temperature with a hydrostatic paver finisher with sensor control to the required grade, level and alignment over prepared surface coated with tack coat, rolling with smooth wheeled, vibratory and tandem rollers for break down, inter-mediate and finished rolling to achieve the desired density of at least 98% of that of Laboratory Marshall specimen, hand packing and pinning to give an even surface including cost and carriage of bitumen, coarse and fine aggregates and filler materials and hire charges of machinery and equipment for construction and quality control, fuels and lubricants and wages of operational staff complete as per Clause 505 of Specifications for Road & Bridge Works of MoRT&H (5th Revision). B. For Grading 2(i) Using Batch Type HMP of minimum capacity 100-120 TPH. It No.-5.05(b) & Pg.- 252 (Vol-III)									
	DBM	1	1000	5.50	0.08	=	440.00	m ³		
					Total	=	440.00	m ³	7850.15	Rs. 3454066.36
4	Providing and laying bituminous concrete with Hot Mix Plant using coarse aggregates, fine aggregates, filler materials and bituminous binder of required specification including screening, cleaning of chips and preparing a uniform and quality mix in Hot Mix Plant and ensuring a homogeneous mix, in which all particles of the mineral aggregates are coated uniformly, transporting the hot mix to work site, laying the mixed materials at specified laying temperature with a hydrostatic paver finisher with sensor control to the required grade, level and alignment over prepared surface coated with tack coat, rolling with smooth wheeled, vibratory and tandem rollers for break down, inter-mediate and finished rolling to achieve the desired density of at least 98% of that of Laboratory Marshall specimen, including cost and carriage of bitumen, coarse and fine aggregates and filler materials and hire charges of machinery and equipment for construction and quality control, fuels and lubricants and wages of operational staff complete as per Clause 507 of Specifications for Road & Bridge Works of MoRT&H (5th Revision).B. For Grading 2 (13.2 mm nominal size, 30mm/40 mm thick.) (i) Using Batch Type HMP of minimum capacity 100-120 TPH. It No.-5.08b & Pg.- 255 (Vol-III)									
	BC	1	1000	5.50	0.040	=	220.00	m ³		
					Total	=	220.00	m ³	8585.88	Rs. 1888893.6

JIBANTALA BAZAR TO TALDI BAZAR ROAD FROM CH. 0.00 KMP TO 12.45 KMP – STRENGTHENING WORK UNDER SOUTH 24 PARGANAS DIVISION IN THE DISTRICT OF SOUTH 24 PARGANAS.										
QUANTITY OF ROAD WORKS										
Sl No	Description of Item	No	L (m)	B(m)	D(m)		Quantity	Unit	Rate (Rs. /Unit)	Amount (Rs.)
1	Construction of granular sub-base by providing graded material, mixing in Wet Mix Plant at OMC, carriage of mixed material to work site, spreading in uniform layers with Motor grader on prepared surface in proper grade and camber, compacting with vibratory power roller to achieve the desired density, including lighting, guarding, barricading, including cost of all materials, machinery, tools and plants and cost of quality control complete as per Clause 401 of Specifications for Road & Bridge Works of MoRT&H (5th Revision).(v) Grading – VI It No.-4.08 A (V) & Pg.- 246 (WBSOR, R&B VOL)									
	GSB	1	1000	5.5	0.150	=	825.00	m ³		
					Total	=	825.00	m ³	2649.11	Rs. 2185515.7896
2	Providing, laying, spreading and compacting graded stone aggregate to Wet Mix Macadam specification including screening of aggregates and granular materials, premixing the material with water at OMC in Wet Mix Plant, carriage of mixed material by tipper to site, laying in uniform layers with Paver in Sub- base / Base course on well-prepared surface and compacting with Vibratory Roller to achieve the desired density, including supply of all materials, machinery, fuel and lubricants, including incidental costs for lighting, guarding, barricading, making earthen bundh to protect the edges including cost of quality control complete as per Clause 406 of Specifications for Road & Bridge Works of MoRT&H (5th Revision).It No.-4.12 & Pg.- 249 (WBSOR, R&B VOL)									
	WMM	1	1000	5.50	0.25	=	1375.00	m ³		
					Total	=	1375.00	m ³	2779.36	Rs. 3821620
3	Providing and laying dense bituminous macadam with Hot Mix Plant producing an average output of 75 tonnes per hour using coarse aggregate, fine aggregate, filler and bituminous binder as per design Job Mix Formula conforming Marshall Method as per specification, including screening, cleaning of chips and preparing a uniform and quality mix in Hot Mix Plant and ensuring a homogeneous mix, in which all particles of the mineral aggregates are coated uniformly, transporting the hot mix to work site, laying the mixed materials at specified laying temperature with a hydrostatic paver finisher with sensor control to the required grade, level and alignment over prepared surface coated with tack coat, rolling with smooth wheeled, vibratory and tandem rollers for break down, inter-mediate and finished rolling to achieve the desired density of at least 98% of that of Laboratory Marshall specimen, hand packing and pinning to give an even surface including cost and carriage of bitumen, coarse and fine aggregates and filler materials and hire charges of machinery and equipment for construction and quality control, fuels and lubricants and wages of operational staff complete as per Clause 505 of Specifications for Road & Bridge Works of MoRT&H (5th Revision).B. For Grading 2 (i) Using Batch Type HMP of minimum capacity 100-120 TPH. It No.-5.05(b) & Pg.- 252 (Vol-III)									
	DBM	1	1000	5.50	0.05	=	275.00	m ³		
					Total	=	275.00	m ³	7850.15	Rs. 2158791.23
4	Providing and laying bituminous concrete with Hot Mix Plant using coarse aggregates, fine aggregates, filler materials and bituminous binder of required specification including screening, cleaning of chips and preparing a uniform and quality mix in Hot Mix Plant and ensuring a homogeneous mix, in which all particles of the mineral aggregates are coated uniformly, transporting the hot mix to work site, laying the mixed materials at specified laying temperature with a hydrostatic paver finisher with sensor control to the required grade, level and alignment over prepared surface coated with tack coat, rolling with smooth wheeled, vibratory and tandem rollers for break down, inter-mediate and finished rolling to achieve the desired density of at least 98% of that of Laboratory Marshall specimen, including cost and carriage of bitumen, coarse and fine aggregates and filler materials and hire charges of machinery and equipment for construction and quality control, fuels and lubricants and wages of operational staff complete as per Clause 507 of Specifications for Road & Bridge Works of MoRT&H (5th Revision).B. For Grading 2 (13.2 mm nominal size, 30mm/40 mm thick.) (i) Using Batch Type HMP of minimum capacity 100-120 TPH. It No.-5.08b & Pg.- 255 (Vol-III)									
	BC	1	1000	5.50	0.030	=	165.00	m ³		
					Total	=	165.00	m ³	8585.88	Rs. 1416670.2

ANALYSIS OF RATES									
JIBANTALA BAZAR TO TALDI BAZAR ROAD FROM CH. 0.00 KMP TO 12.45 KMP – STRENGTHENING WORK UNDER SOUTH 24 PARGANAS DIVISION IN THE DISTRICT OF SOUTH 24 PARGANAS.									
ROAD PORTION									
1.0	Rate of GSB: Grading - V (By Plant Mix Method:-)								
	Cost of 37.5 mm chips	0.2560	m3 @ Rs	1991.75		Rs	509.89		
	Cost of 22.4 mm chips	0.2560	m3 @ Rs	2065.75		Rs	528.83		
	Cost of 11.2 mm chips	0.1920	m3 @ Rs	1949.75		Rs	374.35		
	Cost of 5.6 mm chips	0.3200	m3 @ Rs	1696.75		Rs	542.96		
	Cost of Medium Sand	0.2560	m3 @ Rs	1180.00		Rs	302.08		
	Labour + T&P [P - 246 / It - 4.08 /a/v)]					Rs	391.00		
						Total	Rs	2649.11	
			Say Rs	2649.11	Per m³				
2.0	Rate of Wet Mix Macadam /M³ By Mechanised unit fully computerised (Pakur variety)								
	Cost of 26.5mm chips	0.3960	m3 @ Rs	2050.75		= Rs	812.10		
	Cost of 13.2mm chips	0.2640	m3 @ Rs	2088.75		= Rs	551.43		
	Cost of 5.6mm chips	0.3564	m3 @ Rs	1696.75		= Rs	604.72		
	Cost of S/dust	0.3036	m3 @ Rs	1571.50		= Rs	477.11		
	Labour + T&P [P- 249/It - 4.12]					= Rs	334.00		
						Total		2779.36	
		Say Rs	2779.36	Per M³					
3.0	Rate of Dense Bituminous Macadam, Grading 2,(50-75 mm thick.) .								
	Cost of 26.5 mm chips	0.2197	m3 @ Rs	2050.75		= Rs	450.55		
	Cost of 22.4mm	0.2197	m3 @ Rs	2065.75		= Rs	453.85		
	Cost of 11.2mm	0.3662	m3 @ Rs	1949.75		= Rs	714.00		
	Cost of 5.6mm	0.2197	m3 @ Rs	1696.75		= Rs	372.78		
	Cost of S/dust with grit	0.4394	m3 @ Rs	1571.50		= Rs	690.52		
	Cost of Lime	44	kg @ Rs	7.50		= Rs	330.00		
	Cost of Bitumen	111.00	kg @ Rs	31.95		= Rs	3546.45		
	Labours [P-253/It.-5.05(b(i))]						1292.00		
						= Rs	7850.15		
		Say Rs	7850.15	Per M³					
4.0	Rate of Bituminous Concrete using Viscosity grade Paving Bitumen. Using Batch Mix Type HMP								
	100-120 TPH								
	Cost of 13.2mm	0.2959	m3 @ Rs	2088.75		= Rs	618.06		
	Cost of 11.2mm	0.2959	m3 @ Rs	1949.75		= Rs	576.93		
	Cost of 5.6mm	0.2959	m3 @ Rs	1696.75		= Rs	502.07		
	Cost of S/dust with grit	0.5919	m3 @ Rs	1571.50		= Rs	930.17		
	Cost of Lime	45.00	kg @ Rs	7.50		= Rs	337.50		
	Cost of Bitumen	137.00	kg @ Rs	31.95		= Rs	4377.15		
	Labour +T & P [P - 255/It-5.08(B)/(i)]					= Rs	1244.00		
							8585.88		
		Say Rs	8585.88	Per M³					

1) Cost of carriage of Stone materials from Ballygunge Rail Yard to work site up to = $38.3 + 12.45/2 = 44.525$ km = 45 km (P-230, It-3 of SOR 2018)							
i) Upto 5.00 km per Cum.	=						Rs.124.00
ii) 5.00 km to 10.00km	=	5.00	@	Rs.10.90	/Cum.=		Rs.54.50
iii) 10.00 km to 20.00km	=	10.00	@	Rs.10.10	/Cum.=		Rs.101.00
iv) 20.00 km to 45.00km	=	25.00	@	Rs.9.50	/Cum.=		Rs.237.50
							Rs. 517.00
2) Cost of carriage of 60/70 Bulk Bitumen from Haldia to work site up to = $140 + 21.5 + 12.45/2 = 167.725$ km = 168 km (P-231, It-11 of SOR 2018)							
i) Upto 100.00 km per Cum.	=						Rs.654.50
ii) 100.00 km to 156.00km	=	68.00	@	Rs.5.30	/Cum.=		Rs.360.40
							Rs. 1,014.90
3) Cost of carriage of Bitumen Emulsion (Bulk) from Haldia to site up to = $140 + 21.5 + 12.45/2 = 167.725$ km = 168 km (P-230, It-4 of SOR 2018)							
i) Upto 5.00 km per Cum.	=						Rs.82.00
ii) 5.00 km to 10.00km	=	5.00	@	Rs.7.30	/Cum.=		Rs.36.50
iii) 10.00 km to 20.00km	=	10.00	@	Rs.6.70	/Cum.=		Rs.67.00
iv) 20.00 km to 50.00km	=	30.00	@	Rs.6.30	/Cum.=		Rs.189.00
v) 50.00 km to 100.00km	=	50.00	@	Rs.5.60	/Cum.=		Rs.280.00
vi) 100.00 km to 156.00km	=	68.00	@	Rs.5.30	/Cum.=		Rs.360.40
							Rs. 1,014.90
4) Cost of carriage of Penetration grade Bitumen (Packed) from Dhulagarh to site up to = $62 + 21.5 + 12.45/2 = 89.725$ km = 90 km (P-230, It-4 of SOR 2018)							
i) Upto 5.00 km per Cum.	=						Rs.82.00
ii) 5.00 km to 10.00km	=	5.00	@	Rs.7.30	/Cum.=		Rs.36.50
iii) 10.00 km to 20.00km	=	10.00	@	Rs.6.70	/Cum.=		Rs.67.00
iv) 20.00 km to 50.00km	=	30.00	@	Rs.6.30	/Cum.=		Rs.189.00
v) 50.00 km to 90.00km	=	40.00	@	Rs.5.60	/Cum.=		Rs.224.00
							Rs. 598.50
5) Cost of carriage of Moorum from Sandhipur to work site up to = 172.0 km. (P-230, It-1 of SOR 2018)							
i) Up to 5.00 km per Cum.	=						Rs.124.00
ii) 5.00 km to 10.00km	=	5.00	@	Rs.10.90	/Cum.=		Rs.54.50
iii) 10.00 km to 20.00km	=	10.00	@	Rs.10.10	/Cum.=		Rs.101.00
iv) 20.00 km to 50.00km	=	30.00	@	Rs.9.50	/Cum.=		Rs.285.00
v) 50.00 km to 100.00km	=	50.00	@	Rs.8.40	/Cum.=		Rs.420.00
vi) 100.00 km to 172.00km	=	72.00	@	Rs.7.90	/Cum.=		Rs.568.80
							Rs. 1,553.30
6) Cost of carriage of Steel Materials from Kolkata to work site up to = 55 km. (P-230, It-5 of SOR 2018)							
i) Up to 5.00 km per Cum.	=						Rs.82.00
ii) 5.00 km to 10.00km	=	5.00	@	Rs.7.30	/Cum.=		Rs.36.50
iii) 10.00 km to 20.00km	=	10.00	@	Rs.6.70	/Cum.=		Rs.67.00
iv) 20.00 km to 50.00km	=	30.00	@	Rs.6.30	/Cum.=		Rs.189.00
v) 50.00 km to 55.00km	=	5.00	@	Rs.5.60	/Cum.=		Rs.28.00
							Rs. 402.50

2. COST OF DIFFERENT MATERIALS AT WORK SITE Rs / m³

Sl No.	Ref.	Unit	Coarse sand	Medium sand	Fine sand	Silver sand	Brick Aggregates (40 mm down)	Jhama metal	Moorum	Lime stone dust	Hydrated Lime powder
1	Cost of Materials at Site (It. - 1, 2, 3, 4, 5 (e) (g), 7 & 10 Pg.- 222 of SOR/ R&B/ 2018	M ³	1430.00	1180.00	990.00	800.00	1176.00	1667.00	117.00	3.70	7.50
2	Add Loading, Unloading (I-1.03, P-224)	M ³	0.00	0.00	0.00	0.00	0.00	0.00	62.00	0.00	0.00
3	Cost of Road Transport 166.0 Km for Moorum (I-1, P-227)	M ³	0.00	0.00	0.00	0.00	0.00	0.00	1505.90	0.00	0.00
4	Cost of Materials at work site for = 1+2+3	M ³	1430.00	1180.00	990.00	800.00	1176.00	1667.00	1684.90	3.70	7.50

3. COST OF CEMENT AT WORK SITE Rs / MT

Sl No.	Ref.	Unit	PPC / PSC / OPC 33 / OPC 43	OPC 53
1	Cost of Materials at Site (It. - 1 & 2 (ii) (b) Pg.- 218 of SOR /R&B /2018	MT	5717.00	5873.00
2	Add Loading, Unloading (I-1.03, P-224 & 225)	MT	0.00	0.00
3	Cost of Road Transport 120.0 Km for HYSD bar (I-1, P-227)	MT	0.00	0.00
4	Cost of Materials at work site for = 1+2+3	MT	5717.00	5873.00

Sujit Samanta
18/04/2024

Smit Kr. Bhowmik
18/04/2024
Associate Professor
Department of Civil Engineering
Jadavpur University
Kolkata-700 032

Dr. Saibal Chakraborty
18-04-2024
Dr. Saibal Chakraborty
Head, Civil Engineering Department
Jnan Chandra Ghosh Polytechnic
Department of Technical Education,
Training & Skill development
Govt. of West Bengal